THE CONTRIBUTION OF KINETOPLAST DNA TO *LEISHMANIA MAJOR*
EXPERIMENTAL INFECTION AND EVALUATION OF LEISHMANIA
EXTRACELLULAR VESICLE BASED VACCINE AGAINST CUTANEOUS
LEISHMANIASIS IN BALB/C MICE

A THESIS SUBMITTED TO
THE GRADUATE SCHOOL OF NATURAL AND APPLIED SCIENCES
OF
MIDDLE EAST TECHNICAL UNIVERSITY

BY

İHSAN CİHAN AYANOĞLU

IN PARTIAL FULFILLMENT OF THE REQUIREMENTS
FOR
THE DEGREE OF DOCTOR OF PHILOSOPHY
IN
BIOLOGY

SEPTEMBER 2019

Approval of the thesis:

THE CONTRIBUTION OF KINETOPLAST DNA TO *LEISHMANIA MAJOR* EXPERIMENTAL INFECTION AND EVALUATION OF LEISHMANIA EXTRACELLULAR VESICLE BASED VACCINE AGAINST CUTANEOUS LEISHMANIASIS IN BALB/C MICE

submitted by **İHSAN CİHAN AYANOĞLU** in partial fulfillment of the requirements for the degree of **Doctor of Philosophy in Biology Department, Middle East Technical University** by,

Prof. Dr. Halil Kalıpçılar
Dean, Graduate School of **Natural and Applied Sciences**   _____

Prof. Dr. Ayşegül Çetin Gözen
Head of Department, **Biology**   _____

Prof. Dr. Mayda Gürsel
Supervisor, **Biology, METU**   _____

Examining Committee Members:

Prof. Dr. Kamil Can Akçalı
Biophysics, Ankara University   _____

Prof. Dr. Mayda Gürsel
Biology, METU   _____

Prof. Dr. Sreeparna Banerjee
Biological Sciences, METU   _____

Prof. Dr. Mesut Muyan
Biological Sciences, METU   _____

Assoc. Prof. Dr. Özlen Konu
Molecular Biology and Genetics, Bilkent University   _____

Date: 04.09.2019

I hereby declare that all information in this document has been obtained and presented in accordance with academic rules and ethical conduct. I also declare that, as required by these rules and conduct, I have fully cited and referenced all material and results that are not original to this work.

Name, Surname: İhsan Cihan Ayanoğlu

Signature:

ABSTRACT

THE CONTRIBUTION OF KINETOPLAST DNA TO *LEISHMANIA MAJOR* EXPERIMENTAL INFECTION AND EVALUATION OF LEISHMANIA EXTRACELLULAR VESICLE BASED VACCINE AGAINST CUTANEOUS LEISHMANIASIS IN BALB/C MICE

Ayanoğlu, İhsan Cihan
Doctor of Philosophy, Biology
Supervisor: Prof. Dr. Mayda Gürsel

September 2019, 193 pages

Cutaneous Leishmaniasis (CL) is a neglected vector borne parasitic infection that manifests as self-healing skin lesions or cause debilitating large chronic or recurring lesions. CL is endemic in Turkey and its incidence rate is on the rise due to immigration of refugees from affected regions.

Leishmania parasites harbor a unique mitochondrial DNA structure called kinetoplast DNA (kDNA), consisting of giant networks of catenated mini and maxi-circles. The role of kDNA in infection is poorly understood. In the first part of this thesis, we evaluated the possible contribution of kDNA to *Leishmania major* experimental infection. Herein we show that stimulation of immune cells with kDNA increases the parasite load *in vitro* and exacerbates disease progression in *L.major* induced BALB/c model of CL. Our results suggest that kDNA may have a role in facilitating parasite evasion from the immune system through induction of type-I interferon signaling pathways.

The absence of an available licensed vaccine coupled with the cost, toxicity and drug resistance associated with drugs used for treatment, necessitates the development of an effective preventive vaccine. In the second part of this thesis, we explored the

immunoprotective and immunotherapeutic potential of Leishmania antigen-rich extracellular vesicles (exosomes) in combination with CpG-ODN, cGAMP or glycolipid based (αGalCER) vaccine adjuvants. Our results demonstrated that chemically inactivated *L.major* exosomes exhibited immunotherapeutic effects when combined with D-ODN, resulting in reduction in parasite loads in infected BALB/c mice. Vaccination studies revealed that exosomes adjuvanted with αGalCER provided immunoprotection in *L.major* induced BALB/c model of CL.

Keywords: *Leishmania major,* Extracellular Vesicles, Kinetoplast DNA, Vaccine, Cutaneous Leishmaniasis

ÖZ

KİNETOPLAST DNANIN *LEISHMANIA MAJOR* DENEYSEL ENFEKSİYONU ÜZERİNE ETKİSİ VE KÜTANÖZ LEİSHMANİASİSE KARŞI LEISHMANIA HÜCRE DIŞI KESECİKLERİNE DAYALI AŞININ BALB/C FARELERDE DEĞERLENDİRİLMESİ

Ayanoğlu, İhsan Cihan
Doktora, Biyoloji
Tez Danışmanı: Prof. Dr. Mayda Gürsel

Eylül 2019, 193 sayfa

Kutanöz Leishmaniasis (KL) ihmal edilmiş, vektör aracılığıyla bulaşan parazitik bir enfeksiyondur. Oluşan lezyonlar kendiliğinden iyileştiğinde skartise neden olur veya kronik ve tekrarlayan lezyonlara dönüşebilirler. KL Türkiye'de endemik olmakla beraber son yıllarda ülkemizin hastalığın yüksek oranda görüldüğü bölgelerden göç alması KL'nin görülme sıklığını artırmıştır.

Leishmania parazitleri, kinetoplast DNA (kDNA) olarak adlandırılan iç içe geçmiş maksi ve mini halkalardan oluşan eşsiz bir DNA yapısına sahiptir. kDNA'nın, parazitin enfeksiyonu üzerine etkisi konusunda net bir bulgu yoktur. Bu çalışmanın ilk kısmında, kDNA'ın deneysel *Leishmania major* enfeksiyonuna muthemel katkısı değerlendirildi. Bu kısımda, immün hücrelerinin kDNA ile uyarılması ile hücre başına düşen parazit miktarının arttığını ve BALB/c KL fare modelinde hastalığın kötüleştiğini gösterdik. Elde edilen bulgular kDNA'nın tip-1 interferonlar aracılığıyla parazitin immün sistemden kaçınmasında rolü olabileceğini göstermektedir.

Şu ana kadar KL'ye karşı onaylanmış etkin bir aşı yoktur. Tedavi için kullanılan ilaçların toksik olmasının yanında, parazitlerin kullanılan ilaçlara direnç geliştirmesi etkili bir önleme yöntemi olarak aşı geliştirilmesi gerekliliğini işaret etmektedir. Tezin

ikinci kısmında, antijen açısından zengin Leishmania hücre dışı keseciklerinin (eksozomlar) CpG-ODN, cGAMP veya glikolipid bazlı (αGalCER) adjuvanlarla kombine edilmesiyle hazırlanmış formülasyonlarının immünoterapatik ve immunoprotektif potansiyelleri araştırılmıştır. Bulgular kimyasal yolla inaktive edilmiş *L. major* eksozomlarının D-ODN ile adjuvanlandığında immünoterapatik etki göstererek BALB/c farelerde parazit enfeksiyonunu azalttığını göstermektedir. Ayrıca aşılama çalışmalarında eksozomlar αGalCER ile kombine edildiğinde *L. major* parazitinin BALB/c farelerdeki KL modelinde immünoprotektif etkiler göstermiştir.

Anahtar Kelimeler: *Leishmania major*, Hücre Dışı Kesecikler, Kinetoplast DNA, Aşı, Kutanöz Leishmaniasis

To my beloved wife and son

ACKNOWLEDGEMENTS

TABLE OF CONTENTS

LIST OF TABLES

TABLES

LIST OF FIGURES

FIGURES

xxiii

xxiv

LIST OF ABBREVIATIONS

AFM: Atomic Force Microscopy

AP: Alkaline Phosphatase

APC: Allophycocyanin

BALB/c: Bagg Albino mouse strain

BMDM: Bone Marrow Derived Macrophages

BSA: Bovine Serum Albumin

CBA: Cytometric Bead Array

CFSE: Carboxyfluorescein Succinimidyl Ester

cGAMP: cyclic GMP-AMP

CL: Cutaneous Leishmaniasis

DAPI: 4',6-Diamidino-2-Phenylindole, Dihydrochloride

DMSO: Dimethyl Sulfoxide

DNA: Deoxyribonucleic Acid

DPBS: Dulbecco's Phosphate-Buffered Saline

EDTA: Ethylenediaminetetraacetic Acid

EGFP: Enhanced Green Flourescent Protein

ELISA: Enzyme Linked Immunosorbent Assay

Exo: Exosomes (Extra-cellular vesicles)

FBS: Fetal Bovine Serum

FSC: Forward Scatter

gDNA:	Genomic DNA
GO:	Gene Ontology
gp63:	Glycoprotein 63kDa
H_2O_2:	Hydrogen Peroxide
HCl:	Hydrochloric Acid
HEPES:	4-(2-hydroxyethyl)-1-piperazineethanesulfonic acid)
HK:	Heat-killed
IFN:	Interferon
Ig:	Immunoglobulin
IL:	Interleukin
i.p.:	Intraperitoneal
ISG:	Interferon Stimulated Genes
IVIS:	*in vivo* Imaging System
kDNA:	Kinetoplast DNA
log:	Logarithmic
LPG:	Lipophosphoglycan
LUC:	Firefly Luciferase
MCL:	Mucocutaneous Leishmaniasis
MCSF:	Macrophage Colony-Stimulating Factor
MEM:	Minimal Essential Medium
MFI:	Mean Fluorescent Intensity
MS:	Mass Spectrometry

MVBs: Multivesicular Bodies

NET: NaCl-EDTA-Tris

NKT: Natural Killer T-cells

ODN: Oligodeoxynucleotide

PE: Phycoerythrin

PKDL: Post-Kala-azar Dermal Leishmaniasis

PMA: Phorbol 12-myristate 13-acetate

PNPP: p-nitrophenyl Phosphate

RPMI 1640:   Roswell Park Memorial Institute 1640

RT: Room Temperature

s.c.:   Subcutaneous

SDS: Sodium Dodecyl Sulfate

SEAP: Secreted Embryonic Alkaline Phosphatase

SLA: Soluble Leishmania Antigen

SSC: Side Scatter

Th1:   T-helper cell type-1

Th2:   T-helper cell type-2

THP-1:   Tohoku Hospital Pediatrics-1

TNF: Tumor Necrosis Factor

VL: Visceral Leishmaniasis

WCL: Whole Cell Lysate

<center>**CHAPTER 1**</center>

<center>**INTRODUCTION**</center>

1.1. **Leishmaniasis: A Complex Parasitic Disease**

1.1.1. **The Parasite as the Causative Agent**

1.1.1.1. **General Characteristics and History of Leishmania Parasites**

Leishmania genus was named after the Scottish physician Sir William Bogg Leishman (1865-1926) discovered the parasite species that caused visceral leishmaniasis (named as *Leishmania donovani* later on). Sir Leishman reported his finding in his paper (Leishman, 1903) and eventually, the term 'Leishmania' was adopted by scientific authorities (Gibson, 1983).

Leishmania genus belongs to the Trypanosomatidae family under the order of Kinetoplastida (Hide et al., 2007). Leishmania species are flagellate protists and are obligate intracellular eukaryotic parasites (Lukeš, Skalický, Týč, Votýpka, & Yurchenko, 2014; A. G. B. Simpson, Stevens, & Lukeš, 2006). Leishmania genus is speculated to have evolved in the Mezosoic era (250-60 million years ago) (Momen & Cupolillo, 2000).

There are 52 identified Leishmania species. 30 of those species can infect mammals and at least 20 are pathogenic to humans (Alvar et al., 2012; Gramiccia & Gradoni, 2005). While some Leishmania species are zoonotic, and hence can be transmitted from animal reservoirs to human, others are anthroponotic capable of human to human transmission through a sand fly vector (Sundar & Chakravarty, 2012).

Humans can be infected with at least 20 different species of Leishmania that are often classified according to their region of origin as the new world and the old world Leishmania. The new world species occur in central and south America whereas the

<center>1</center>

old world species predominate in Asia, Europe and Africa (Iowa State University/College of Veterinary Medicine, 2009).

1.1.1.2. **The Kinetoplast: A Unique Mitochondrial Structure**

The order Kinetoplastida, which Leishmania genus belongs, is characterized by a specialized mitochondrial region called the kinetoplast. This specialized structure harbors one of the most unusual and complex mitochondrial DNA named as kinetoplast DNA (kDNA) which comprises 30% of cellular DNA (Larry Simpson & da Silva, 1971). Cellular structure of a typical trypanosome is given in Figure 1.1.
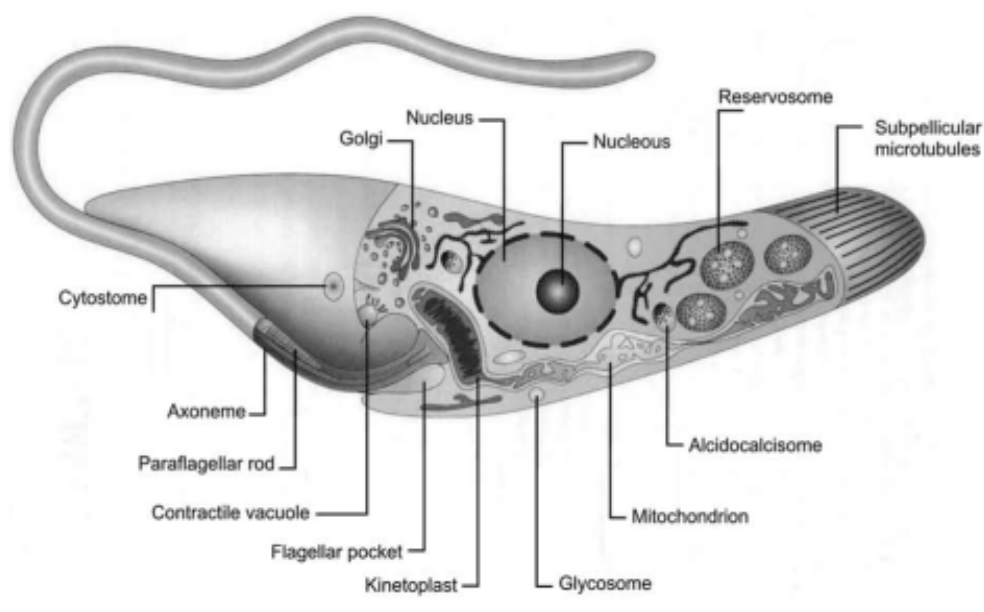
Figure 1.1. Schematic View of Main Cellular Structures of *T. cruzi* as Observed in Transmission Electron Microscope.

Adopted from (W. De Souza, 2008)

The kinetoplast was first described as a rod shaped structure, stained with basic dyes (Trager, 1965) and observed as an electron dense region by transmission electron

microscopy (Meyer, Musacchio, & Mendonça, 1958), located posterior to the basal body of the flagellum. Early studies suggested that this structure contained mitochondrial DNA but the beautiful and complex structure of kDNA was only understood later on through advances in the field of electron microscopy (Laurent & Steinert, 1970; Larry Simpson & da Silva, 1971).

kDNA is a single network of interlocked circular DNA composed of two different types of nucleic acids: minicircles and maxicircles. Size of minicircles vary between 0.5-2.5 kbp depending on the species and there are several thousands of them in a network. Maxicircles are 20-40 kbp in size and a network usually contains a few dozen. (Jensen & Englund, 2012; Shapiro, 1993). Electron micrograph of a kDNA network is presented in Figure 1.2.
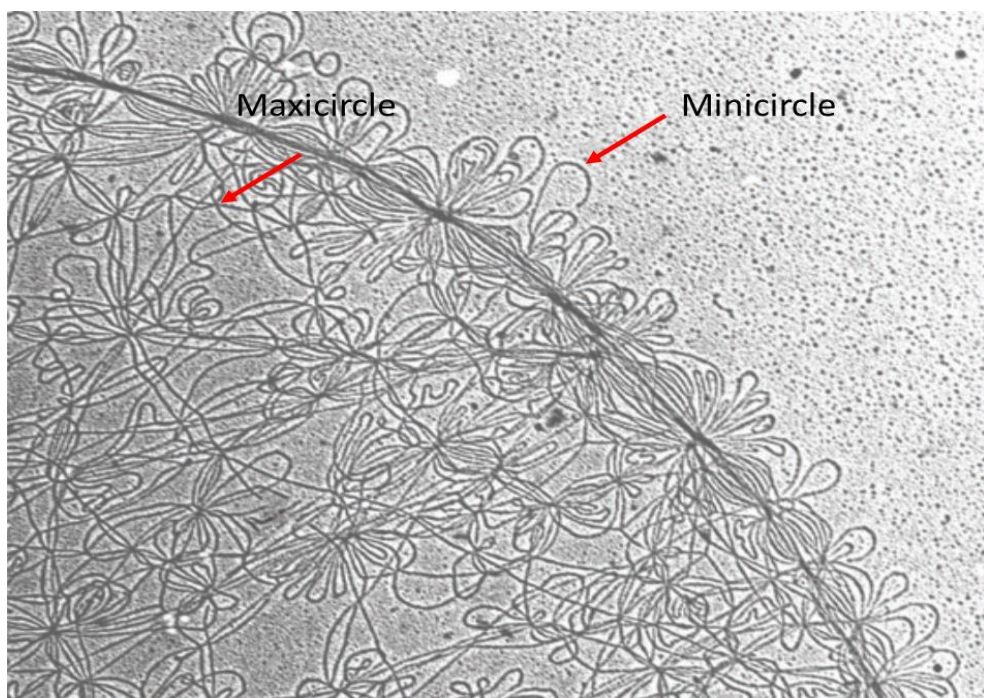
Figure 1.2. Electron Micrograph of kDNA Network

Adopted from (Jensen & Englund, 2012)

Maxicircles, which exist in multiple identical copies per network, encode ribosomal RNAs (rRNAs) and proteins such as NADPH dehydrogenase, ATP synthase and subunits of cytochrome oxidase, that are involved in oxidative phosphorylation. Thus, maxicircles are analogous to mitochondrial DNA of higher eukaryotes (L Simpson, 1987). Transcripts of maxicircles are edited extensively to form functional mRNA. During editing, uridylated residues are added and/or removed to generate an open reading frame, through a process known as 'RNA editing'. This is where minicircles come into play since minicircles encode for small guide RNAs to provide specificity to the editing process (Aphasizhev & Aphasizheva, 2014). It has been hypothesized that kDNA is a single network to maintain extensive interplay between minicircles and maxicircles to produce functional rRNAs and proteins. If they were not found in a single network, some minicircle classes would be lost by random segregation, which eventually results in incomplete editing of maxicircle transcripts, therefore, leading to death of the parasite (Borst, 1991). Furthermore, minicircles are more heterogeneous when compared to maxicircles, only bearing a small conserved region. This indicates that there may be other functions of minicircles besides RNA editing. In this context, evidence suggests that kDNA minicircles can be integrated into the host genome during infection with *Trypanosoma cruzi* (Teixeira, Hecht, Guimaro, Sousa, & Nitz, 2011). Whether such a phenomenon also occurs in the case of Leishmaniasis or how kDNA impacts the course of infection is still unknown.

Akin to its structure, replication of kDNA is highly unusual and complicated. Details of the replication process will not be discussed here but it is worth mentioning that minicircles do not replicate inside the networks. Instead, they are released from the network by Topoisomerase II and attached back to the network after replication. Each replicated minicircle has a nick until all minicircles are replicated. This mechanism ensures that each minicircle is only replicated once per generation and equally segregated to daughter cells to prevent loss of minicircle classes (Drewa & Englunda, 2001; Engel & Ray, 2002; Shlomai, 2005).

1.1.1.3. **The Life Cycle of the Parasite**

The life cycle of leishmania is digenetic, including an insect vector and a mammalian host. Insect vectors of Leishmania species, capable of infecting humans are the *Lutzomyia* of the new world and *Phlebotomes* of the old world species (Killick-Kendrick, 1999; Paul D. Ready, 2013).

Leishmania species alternate between two developmental stages: promastigote (vector form) and amastigote (host form). Amastigotes are small (2-4 µm) spherical and have no external flagella. In contrast, promastigotes are thin, elongated (5-15 µm in length, 1.5-3 µm in width) and flagellated (D. L. Sacks & Perkins, 1985; J. Sunter & Gull, 2018).

Female sand flies are always in need of blood meal to produce eggs (P. D. Ready, 1979). It has been reported that sand flies infected with Leishmania species feed more frequently than non-infected insects, thereby accelerating transmission (Rogers & Bates, 2007). Life cycle of Leishmania starts with the bite of and infected female sand fly. Female sand flies inject infective stage of promastigotes into the skin during a blood meal. Promastigotes within the wound are mainly phagocytosed by macrophages and transform into amastigotes inside phagolysosomes. Then, amastigotes replicate by simple cell division inside the host cell and infect other cells, either locally or disseminate distant tissues depending on the species of the parasite. When a sand-fly takes a blood meal from an infected host, it ingests parasitized cells of the host and become infected by Leishmania. Amastigotes transform into promastigotes and replicate in the gut of sand fly by binary fission. Following replication, they migrate to proboscis and are ready to infect a new host, thereby completing the Leishmania life cycle (Prevention, 2019; Reithinger et al., 2007). The life cycle of Leishmania is summarized in Figure 1.3.
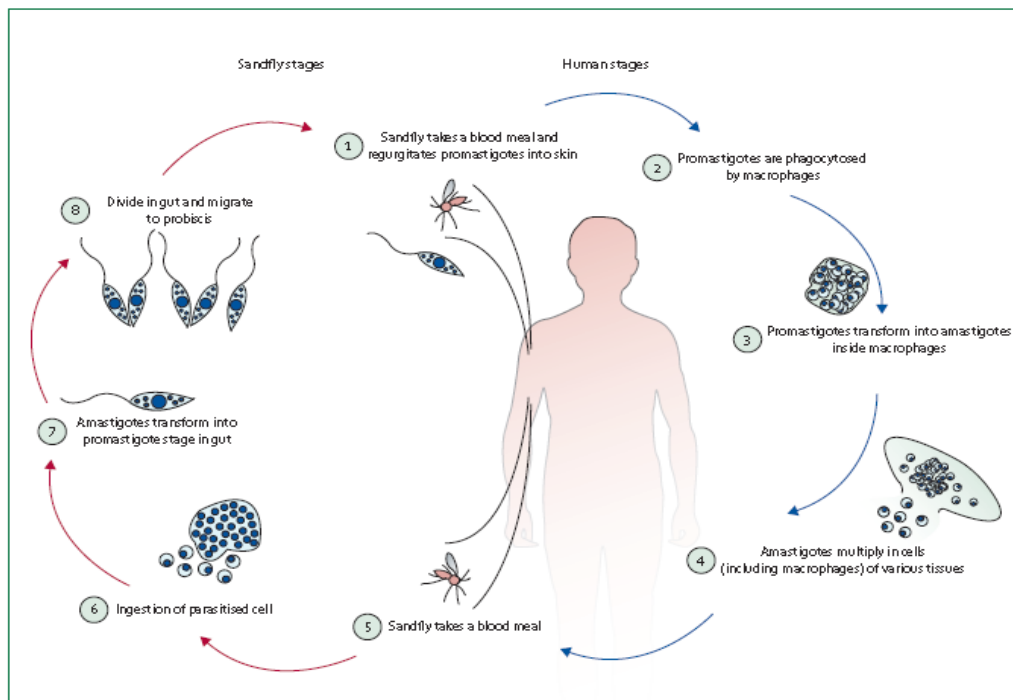
Figure 1.3. The Life Cycle of Leishmania

Adopted from (Reithinger et al., 2007)

1.1.2. **The Disease**

Leishmaniasis is a neglected tropical and subtropical vector-borne parasitic disease caused by protozoa of the Leishmania genus (Alvar et al., 2012). The disease is transmitted by the bite of female sand flies.

1.1.2.1. **Brief History of Leishmaniasis**

Leishmaniasis is a disease that caused significant suffering throughout human history. Descriptions of lesions, and disease progression have been reported in Pharaoh's Papyrology and ancient Egyptian medical documents. The disease was named as 'Nile Pimple' around 1885 BC (Oumeish, 1999; Steverding, 2017). In a paleoparasitological study, bone marrows of mummies derived from a tomb in the

Egyptian city West Thebes (2050-1650 BC), were examined for the presence of kDNA and 4 out 91 mummies were identified as Leishmania positive (Zink et al., 2006). This shows that presence of Leishmaniasis in the human population dates back to more than 4,000 years.

The first clinical report on cases of the Leishmaniasis from Aleppo, Syria was reported by Alexander Russell (1714-1768) (Alvar, Yactayo, & Bern, 2006).

Although Leishmaniasis was mentioned in countless documents for more than 4,000 years, the causative agent of the disease was described in the beginning of 20th century as previously explained in Section 1.1.1.1.

1.1.2.2. **Epidemiology**

Leishmaniasis is estimated to cause ninth largest disease burden among infectious diseases (Alvar et al., 2012; Hotez et al., 2004) and has been listed as the second most common parasitic infection worldwide by World Health Organization (WHO) (World Health Organization, 2010).

Leishmaniasis is endemic in 98 countries and 3 territories distributed to 5 continents, except Oceania. Approximately 270,000 Leishmania cases are officially reported annually. Considering that, only 2/3 of countries provide official reports to WHO that are sometimes underrepresented, the global estimate of occurrence of Leishmaniasis is 0.9-1.6 million each year (Alvar et al., 2012) causing approximately 70,000 deaths per year (Bravo & Sanchez, 2003; WHO, 2016). Over 1 billion people living in endemic areas are under risk of being infected (WHO, 2016).

Although the prevalence of Leishmaniasis is globally high, it is mainly ignored by authorities (Hotez et al., 2006) and classified as a neglected tropical disease (NTD).

1.1.2.3. **Types of Leishmaniasis**

Clinical manifestations of leishmaniasis range from small cutaneous lesions and mucosal tissue disruption to systemic destruction of viscera depending on Leishmania species and host immune response (Colmenares, Kar, Goldsmith-Pestana, & McMahon-Pratt, 2004; Copeland & Aronson, 2015). Main forms of the disease include Visceral Leishmaniasis (VL), Post-kala-azar dermal leishmaniasis (PKDL), Cutaneous Leishmaniasis (CL) and Mucocutaneous Leishmaniasis (MCL) (WHO, 2016). Clinical forms of the disease are depicted in Figure 1.4.

Figure 1.4. Different Clinical Forms of Leishmaniases

From left to right: Visceral Leishmaniasis (VL), Post-kala-azar dermal leishmaniasis (PKDL), Cutaneous Leishmaniasis (CL) and Mucocutaneous Leishmaniasis (MCL). (Adopted from: https://www.who.int/leishmaniasis/clinical_forms_leishmaniases)

Visceral leishmaniasis (VL), also known as kala-azar (meaning black fever in Hindi), caused by *L. infantum* and *L. donovani* infections is the fatal type of the disease. It is characterized by persistent fever, splenomegaly, weight loss and anemia. The disease is endemic in east Africa (Ethiopia, Sudan) and the Indian subcontinent (India, Bangladesh) (Desjeux, 2004; Guerin et al., 2002). Incubation period of VL is usually 3-8 months but symptoms may be observed only when an individual is immune suppressed such as when co-infected with Human Immunodeficiency Virus (HIV) (Paul D. Ready, 2014). If left untreated, disease is fatal within about 2 years due to

multi system failure, severe anemia and/or secondary bacterial infections (Blum et al., 2014; Sundar & Chakravarty, 2015).

Post-kala-azar dermal leishmaniasis (PKDL) is a post complication of VL caused by *L. donovani* and observed in 5%-15% of cases (Mondal et al., 2018; Zijlstra, Musa, Khalil, El Hassan, & El-Hassan, 2003). After healing from VL, parasites reside in the host and relapse when the host is immunocompromised (Stark, Pett, Marriott, & Harkness, 2006). As a result, PKDL lesions that resemble leprosy are formed. Patients do not feel ill and are not in search of treatment most of the time. PKDL should be treated systematically because lesions are reservoirs for Leishmania transmission (Aronson, 2017).

Cutaneous leishmaniasis (CL), also known as 'Aleppo sore', is limited to self-healing ulcerated skin lesions or debilitating large chronic or recurring lesions. Lesions appear at bite sites which mainly include exposed body parts such as face and forearms (Blum et al., 2014). Self-healing takes 2-15 months depending of Leishmania species but tend to leave permanent scars (Desjeux, 2004; Reithinger et al., 2007). Since the progression of the disease depends on the parasite species and host interaction, cutaneous leishmaniasis might show exacerbated manifestations such as mucocutaneous leishmaniasis and diffuse cutaneous leishmaniasis. These species are prevalent around the Mediterranean Basin and Middle East. While *L. tropica*, *L major*, *L. mexicana* species account for cutaneous leishmaniasis, *L. brazilensis* and *L. guyanensis* engenders mucocutaneous leishmaniasis, in which oronasopharyngeal mucosa and cartilage is destroyed (Davies et al., 2000; Goto & Lauletta Lindoso, 2012). CL caused by *L. tropica* infection may manifest a new scar after healing. This condition is called as leishmania recidivans and may lead to diffuse cutaneous leishmaniasis in immunocompromised individuals (Van Griensven, Carrillo, López-Vélez, Lynen, & Moreno, 2014).

Leishmania species capable of infecting humans and the clinical and epidemiological characteristics of leishmaniases are summarized in Table 1.1 (Lainson & Shaw, 1987; Roberts & Janovy, 2009).

Table 1.1. *Clinical and Epidemiological Characteristics of the Main Leishmania Species*

Species	Clinical Form	Regions and Countries with High Burden
Old World Species		
L. tropica	cutaneous leishmaniasis leishmania recidivans	Middle East, Eastern Mediterranean, Southern and Northeastern Africa
L. major	cutaneous leishmaniasis	Middle East, North Africa, Central Asia, Iran, Saudi Arabia, North India and Pakistan
L. donovani	visceral leishmaniasis post-kala-azar dermal leishmaniasis	Sudan, Ethiopia, Kenya, India, Bangladesh
L. infantum	visceral leishmaniasis cutaneous leishmaniasis	Middle East, China, Southern Europe, South America
L. aethiopica	cutaneous leishmaniasis	Ethiopia, Kenya
New World Species		
L. braziliensis	cutaneous leishmaniasis mucocutaneous leishmaniasis	South America
L. mexicana	cutaneous leishmaniasis	South America
L. guyanensis	cutaneous leishmaniasis mucocutaneous leishmaniasis	South America
L. amazonensis	cutaneous leishmaniasis	South America

1.1.2.4. **Leishmaniasis in Turkey**

Old world Leishmania species cause critical health issues in endemic countries such as Iran, Iraq, Syria and Turkey. Especially, Turkey is located at the crossroad of the continents with a subtropical climate that is highly favorable for sandflies to disseminate visceral and cutaneous leishmaniasis. During 1990-2010, more than 50,000 new cutaneous leishmaniasis (CL) cases caused by four different Leishmania

species have been reported in Turkey. Dominant Leishmania species in Turkey are reported as *L. tropica*, *L. major*, *L. infantum* and *L. donovani* (Özbilgin et al., 2016).

During the last decade, Turkey received more than 3 million Syrian refugees due to the civil war in Syria. CL is highly endemic in Syria and therefore, there is an expected increase in CL cases in Turkey (Özbilgin et al., 2017). An epidemiological study conducted in Gaziantep, examined 563 patients admitted to hospitals with the suspicion of CL. 263 of the cases were identified as Leishmania positive, where 174 of them (66.15%) were Syrians (Özkeklikçi, Karakuş, Özbel, & Töz, 2017). According to the World Health Organization (WHO) report on leishmaniasis, Turkey has the highest reported imported CL cases with 1089 cases in 2016. In contrast, this number is only 222 in Brazil (World Health Organization., 2018). Such increase in imported CL cases shows the severity of the situation, necessitating the development of urgent prevention/treatment strategies.

1.1.2.5. **Diagnosis**

Microscopic examination of Giemsa-Wright stained aspirates or biopsy smears is the most commonly used diagnosis tool for Leishmaniasis. This histopathological examination is inexpensive and relatively easy to perform (Durdu, Baba, & Seçkin, 2009; Escobar, Martinez, Smith, & Palma, 1992; Uzun et al., 2018)

Serological tests such as agglutination test and ELISA can be used for diagnosis of VL but rarely used for CL diagnosis due to unreliability and insensitivity. These tests require technical expertise, which is lacking in endemic areas. Furthermore, they are more expensive and time consuming than histopathological diagnosis (Kar, 1995).

Leishmania skin test (LST), also known as the Montenegro test, is a delayed hypersensitivity test where leishmania antigens are injected intradermally. LST is useful in VL but rarely used in CL cases (Weigle et al., 1987).

As an alternative to serological tests and LST, chemiluminescent ELISA technique was developed to measure antibodies against α-galactosyl which is shown to be increased 9 fold in patients infected with *L.tropica* or *L.major* compared to healthy individuals (Al-Salem et al., 2014).

Molecular methods based on amplification of kinetoplast or genomic DNA by PCR are highly sensitive in diagnosis. However, application of this technique requires laboratories equipped with special equipment which is not always available in endemic regions (Chappuis et al., 2007; Goto & Lindoso, 2010; Salam, Al-Shaqha, & Azzi, 2014).

1.1.2.6. **Treatment**

Since visceral leishmaniasis (VL) is fatal within two years of occurrence, treatment is a must (Paul D. Ready, 2014). For cutaneous leishmaniasis (CL), lesions usually selfheal within two years for most of the cases. For instance, in immunocompetent hosts 70% of *L. major* cases heal within 4 months (Morizot et al., 2013). As a conservative approach, non-systemic treatments can be applied to prevent dissemination or for cosmetic reasons (Reithinger et al., 2007). In addition, treatment is recommended for cases where there are multiple and/or persistent lesions that last more than 6 months (Hodiamont et al., 2014). In immunocompromised patients, systemic treatment for CL is strongly recommended to prevent dissemination and occurrence of mucocutaneous leishmaniasis (MCL) (Markle & Makhoul, 2004).

Pentavalent antimonials has been used for more than 70 years as first-line therapy in two different forms: sodium stibogluconate and meglumine antimoniate (Salam et al., 2014). These drugs can be administered intramuscularly, intravenously and intralesionally (Uzun et al., 2018). There are two major problems associated with pentavalent antimonial use for therapy. First, these drugs have severe side effects such as cardiotoxicity, renal failure and hepatotoxicity (Berman, 1997). Second, parasite strains develop resistance against the drugs. For instance, usage of pentavalent

antimonials are no longer recommended in the Indian subcontinent (Sundar et al., 2000). Currently, they are recommended for combination treatments with other drugs such as liposomal amphotericin B, which also has severe side effects such as myocarditis and nephrotoxicity (Sundar & Chakravarty, 2015; Wortmann et al., 2010).

As an alternative to drug treatment, thermotherapy is also used for treatment of CL. Since amastigotes are heat sensitive and cannot replicate at temperatures higher than 39 °C, heating up lesions up to 40-42 °C by using radiofrequency, results in healing of lesions. For instance, healing rate of thermotherapy is 89% for *L. major* and 94% for *L. tropica* cases (Sundar & Chakravarty, 2015). The main advantages of thermotherapy are being inexpensive and having no significant side effects (Valencia, Miller, Witzig, Boggild, & Llanos-Cuentas, 2013).

1.1.2.7. Control and Prevention

The most common method for personal protection from Leishmania infection is the use of insecticide sprayed nets to prevent sand fly bites. Indoor and outdoor spraying is also used for vector control (Croft & Coombs, 2003; Schubach et al., 2009).

Considering the serious side effects of drug treatment and developing resistance against drugs, protection through vaccination would be an ideal choice. Although several vaccine candidates have been tested in pre-clinical and clinical trials, currently, there is no registered vaccine against leishmaniasis (Alvar et al., 2013).

The oldest reported vaccination attempts involved delivering of live virulent parasites, also known as 'leishmanization'. This approach was abandoned due to formation of non-healing lesions, immunosuppressive effects and development of autoimmune disorders such as psoriasis (Modabber, 1989).

Following failure of leishmanization approach, use of killed parasites was adopted as the first generation vaccines. Inactivated polyvalent vaccine was tested in a vaccination trial conducted in Brazil between 1939 and 1940 and reported to be 80%

effective (Genaro et al., 1996). In 1970s, a clinical study conducted with a pentavalent vaccine showed that recipients were positive for the Montenegro test as an indicative of anti-leismanial immunity (Mayrink et al., 1978). However, heat-killed vaccine formulations tested in a double-blind study including a placebo control reported only 35% effectiveness (Antunes et al., 1986). Another clinical trial was conducted in Ecuador, where a trivalent vaccine combined with a BCG adjuvant was used. This formulation has been shown to be 73% effective in children aged 5.5 on average (Rodrigo X. Armijos, Weigel, Aviles, Maldonado, & Racines, 1998). A similar approach was used in Iran where *L. major* promastigotes were used with or without combination of BCG adjuvant. In this study, phase I and II clinical trials showed that use of BCG as an adjuvant improved anti-leishmanial response (Bahar et al., 1996; Dowlati, Ehsasi, Shidani, & Bahar, 1996). Although the first generation vaccines seem to be promising, they failed to provide clinical protection in Phase III trials (R. X. Armijos et al., 2004; Vélez et al., 2000).

Second generation vaccines are based on recombinant DNA technology. This approach relies on delivery of plasmids encoding Leishmania specific genes. Only one second-generation vaccine candidate has been tested in clinical trials. This vaccine candidate was tested solely for its immunogenicity and protection against the infection was not tested (Chakravarty et al., 2011). Second generation vaccines are still highly experimental and were shown to be insufficient for induction of protection especially in non-murine models (Kedzierski, 2010; Khan, 2013).

Considering that Leishmania life cycle is highly complex and involves expression of several different antigens/virulence factors, a successful vaccine should be produced polyvalently and should be combined with a well-developed adjuvant (Kedzierski, 2010).

1.1.3. **Immune Responses to Leishmania Infections**

In this section, immune responses to Leishmania infections and parasite immune evasion mechanisms will be discussed. Since this thesis is concerned with cutaneous leishmaniasis (CL) caused by *L. major*, this section will mainly concentrate on this sub-type of leishmaniasis.

As mentioned in previous sections, different leishmania species cause different clinical manifestations. Therefore, differences in host immune responses exist depending on the Leishmania species. All Leishmania species share a similar life cycle and are obligate cellular parasites. They have to locate and rapidly invade host cells, among which macrophages represent the primary target (Liu & Uzonna, 2012).

1.1.3.1. **Innate Immunity to Leishmania**

When infective promastigotes are injected into skin through the bite of an infected sand fly, parasites rapidly localize and invade the phagocytes. In this context, sand fly salivary proteins act as chemo-attractants and augment phagocyte recruitment to the bite site (Chagas et al., 2014).

The initial host defense that parasites encounter is complement proteins, yet parasites evade complement-mediated lysis mainly due to their thick Lipophosphoglycan (LPG) layer (Franco, Beverley, & Zamboni, 2012). It was also reported that gp63, the main Leishmania metalloprotease, is capable of cleaving complement proteins and provides protection against complement mediated-lysis (Brittingham et al., 1995). Furthermore, Leishmania benefits from complement activation by LPG, which promotes phagocytosis of parasites (Vinet, Fukuda, Turco, & Descoteaux, 2009).

When parasites infect macrophages, establishment of long-lasting infection occurs within phagolysosomes, the acidic sub-cellular compartment enriched in lytic enzymes (Chang & Dwyer, 1976). Production of reactive oxygen species (ROS) and reactive nitrogen species (RNS) represent the two main mechanisms through which

parasites are killed within the phagolysosomes (Fang, 2004; Iles & Forman, 2002). ROS production is activated through respiratory burst during phagocytosis, resulting in superoxide generation through NADPH oxidase 2 (NOX2) induction (Panday, Sahoo, Osorio, & Batra, 2015). RNS production is achieved through classical activation (M1) of macrophages, resulting in nitric oxide production (NO) by inducible nitric oxide synthase (iNOS) (Aktan, 2004).

Leishmania developed several strategies to evade ROS and RNS mediated killing. The thick LPG layer expressed on parasites not only shields parasites from ROS and RNS but also suppresses superoxide production by inhibiting NOX2 complex (Carneiro et al., 2018). Furthermore, parasites can secrete their own arginase inside macrophages and can induce macrophages to produce high levels of arginase in response to infection. Arginase competes with iNOS for arginine and thereby suppresses NO production, which results in alternatively activated (M2) macrophage differentiation characterized by their inability to kill intracellular parasites (Gaur et al., 2007). In addition, arginase convert arginine to nutrients essential for parasite survival. Another evasion mechanism from RNS and ROS is that gp63 can interfere with macrophage signaling pathways and downregulate expression of iNOS and NOX2 (Olivier, Atayde, Isnard, Hassani, & Shio, 2012). Moreover, Leishmanial antioxidants were shown to provide ROS resistance to parasites by reducing superoxide (Bose et al., 2012; Sansom et al., 2013).

One cell type that is rapidly recruited to infection site is the neutrophils, which play dual roles in Leishmania infection depending on the species and severity of the infection (Peters et al., 2008). Production of neutrophil extracellular traps (NETs), which are extracellular fibril networks containing DNA and antimicrobial peptides, is defined as neutrophil mediated pathogen killing mechanism and *L. amazonensis* promastigotes were reported to be killed by NETs (Guimarães-Costa et al., 2009; Rochael et al., 2015). However, sand fly salivary proteins (Chagas et al., 2014) and/or proteolytic activity of gp63 (Gabriel, McMaster, Girard, & Descoteaux, 2010) can protect parasites from NETs. Neutrophils can also interact with macrophages and

provide protection against *L. amazonensis and L. braziliensis* infections (de Souza Carmo, Katz, & Barbiéri, 2010; Novais et al., 2009). On the other hand, phagocytosis of apoptotic neutrophils following *L. major* infection can suppress activation of macrophages and dendritic cells (DCs), therefore resulting in parasite survival (Ribeiro-Gomes, Peters, Debrabant, & Sacks, 2012; van Zandbergen et al., 2004). In summary, tightly regulated neutrophil activities are required in Leishmania infections.

Production of chemokine C-C motif ligand2 (CCL2) through platelet activation recruits inflammatory monocytes and DCs to infection site (Goncalves, Zhang, Cohen, Debrabant, & Mosser, 2011). In early stages, some DCs and monocytes are infected with parasites (Lai et al., 2008; Ribeiro-Gomes et al., 2012). Parasite infection results in a strong respiratory burst in monocytes and is critical for early control, whereas activation of macrophages by IFN-γ is required for efficient killing of parasites (Goncalves et al., 2011). Importance of inflammatory monocytes were also shown in a murine model of CL, where $CCR2^{-/-}$ (CC-chemokine receptor 2) C57BL/6 mice, normally resistant to *L. major* infection, developed non-healing lesions upon *L. major* infection (Sato et al., 2000).

Innate immune cells are characterized by expression of pattern recognition receptors (PRRs), which are capable of recognizing pathogen associated conserved motifs such as peptidoglycans, lipopeptides, single and double stranded nucleic acids. All these conserved motifs collectively are named as pathogen-associated molecular patterns (PAMPs) (Kumar, Kawai, & Akira, 2011). Main PRR classes are toll-like receptors (TLRs), NOD-like receptors (NLRs), RIG-I like receptors (RLRs), C-type lectin receptors (CLRs) and cytosolic DNA sensors (CDSs). Collectively, these receptors are capable of recognizing a wide variety of PAMPs in various sub-cellular compartments of innate immune cells (cell membrane, endosomes and cytosol) depending on the nature of the infectious agent (Brubaker, Bonham, Zanoni, & Kagan, 2015; Kumar et al., 2011; N Barber, 2011). Herein, only the PRRs defined to play critical roles in Leishmania infection will be briefly discussed.

Leishmania express numerous ligands that can be recognized by TLRs, and this family of PRRs play a protective or counter-protective role (summarized in Figure 1.5.) in Leishmania infections depending on the ligands and the parasite species (Faria, Reis, & Lima, 2012; Tuon et al., 2008). Since studies on roles of PRRs other than TLRs in Leishmania infections are scarce and suggest controversial findings, the following text of this sub-section will concentrate in the contrasting roles of TLRs.
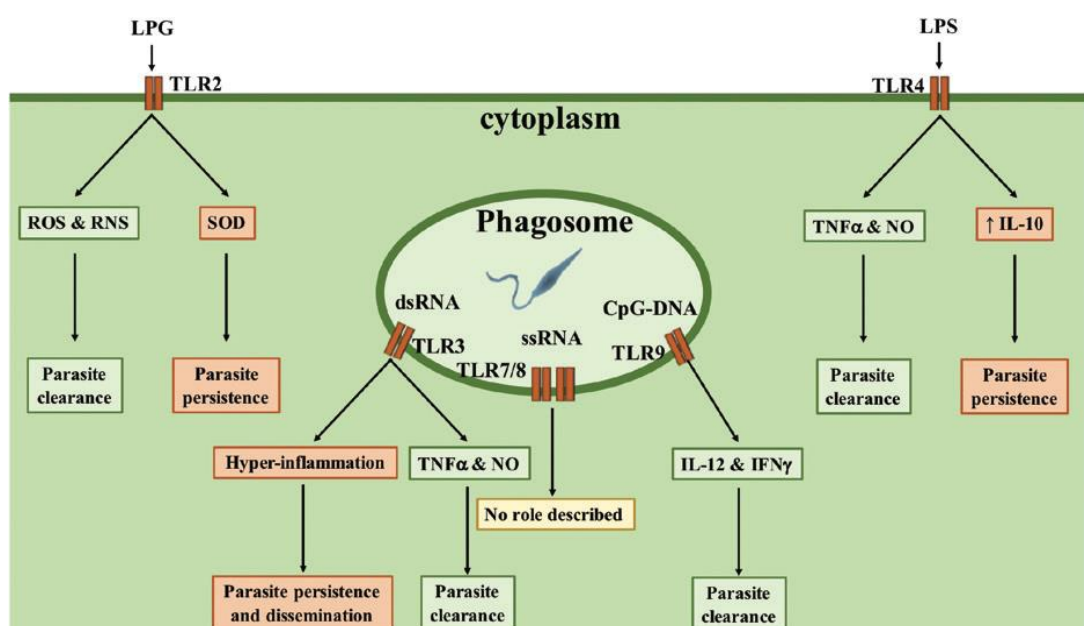
Figure 1.5. Contrasting Roles of TLRs in Leishmania Infections

Adopted from (Rossi & Fasel, 2018)

Induction of TLR2 by LPG stimulation promotes RNS and ROS production and results in clearance of *L. major*, *L. mexicana* and *L. aethiopica* infections (Becker et al., 2003; de Veer et al., 2003). In contrast, TLR2 stimulation in *L. amazonensis* and *L. braziliensis* were shown to upregulate superoxide dismutase-1 (SOD-1) in macrophages, thereby resulting in parasite persistence (Ilg, Stierhof, Wiese, Overath, & McConville, 1994; Kavoosi, Ardestani, & Kariminia, 2009). The paradoxical role

18

of TLR2 signaling suggests that undefined Leishmanial ligands may play a role in differential activation of TLR2 in a species dependent manner.

For *L. donovani* infection, TLR3 signaling was reported to be required for phagocytosis and subsequent TNF-α and NO production, leading to parasite clearance (Flandin, Chano, & Descoteaux, 2006). Conversely, recognition of viral dsRNA by TLR3 in infection by symbiotic Leishmania RNA virus (LRV) positive *L. guyanensis*, results in hyper inflammation and exacerbation of the disease (Ives et al., 2011).

Role of TLR4 in Leishmania infection depends on the time of stimulation. Stimulation before parasite infection results in parasite persistence through increased IL-10 production (Filardy et al., 2010), whereas simultaneous or subsequent stimulations lead to parasite elimination through TNF-α and NO production (Faria et al., 2011; Ribeiro-Gomes et al., 2007).

In contrast to divergent roles of other TLRs, role of TLR9 (recognizes unmethylated CpG-rich DNA) was clearly identified as providing parasite resistance to the host. This resistance is achieved through stimulation of IL-12 production from plasmacytoid dendritic cells (pDCs) and IFN-γ production from NK cells, which activates macrophages (M1) for effective killing of parasites (Hkima Abou Fakher, Rachinel, Klimczak, Louis, & Doyen, 2009; Li et al., 2004; Liese, Schleicher, & Bogdan, 2007; Schleicher et al., 2007).

1.1.3.2. **Adaptive Immunity to Leishmania**

Innate immune cells react to Leishmania infection by secreting of various cytokines which collectively mold the developing adaptive immunity and determine the fate of infection, either resulting in parasite clearance or persistence. Although adaptive immune cells are required for complete parasite clearance and providing memory response to re-infections, they have been also shown to contribute disease progression.(Scott & Novais, 2016).

Although several studies reported exacerbatory roles of B cells in *L. donovani* and *L. amazonensis* infections (Silva-Barrios et al., 2016; Smelt, Cotterell, Engwerda, & Kaye, 2000; Wanasen, Xin, & Soong, 2008), the role of B cells in Leishmania infections are thought to be negligible. Therefore, adaptive host response to leishmania infections are mainly established through T-cell mediated immunity.

The role of CD8^{+} cytotoxic T-lymphocytes (CTLs) in Leishmania infection depends on the parasite species and severity of the infection. In *L. major* induced murine model of CL, CTLs were reported to be involved parasite clearance through IFN-γ production in low-dose infections, whereas they were shown to be non-essential in high-dose infections (Stäger & Rafati, 2012). Conversly, CTLs were associated with increased disease severity and augmented metastasis of *L. braziliensis* in the murine model of CL (Novais et al., 2013).

Sub-types of T-helper cells (Th cells), also known as CD4^{+} T-cells, play divergent roles in Leishmania infection. In murine models of CL, balance of Th1/Th2 polarization was defined as the primary factor affecting the outcome of Leishmania infection. Th1 cell development mainly depends on IL-12 secreted from DCs, which initiate antigen specific immune responses (Sypek et al., 1993; Von Stebut, Belkaid, Jakob, Sacks, & Udey, 1998). Most DCs that prime naïve T-cells in draining lymph nodes are derived from inflammatory monocytes (also known as monocyte-derived DCs, mo-DCs), which are recruited to the infection site (León, López-Bravo, & Ardavín, 2007). Th1 cells are mainly characterized by secretion of their signature cytokines IFN-γ and TNF-α, which activates macrophages (M1) to enhance ROS and RNS mediated killing of parasites, thereby resulting in parasite clearance (Kima & Soong, 2013). NK cells in draining lymph nodes are the main producers of IFN-γ until Th1 cell development, providing early resistance to parasite infection (Scharton & Scott, 1993). In contrast, Th2 cells are characterized by IL-4, IL-10 and IL-13 secretion and support alternative macrophage activation (M2), thereby augmenting parasite persistence due to insufficient parasite killing capacity of M2 macrophages (Gordon & Martinez, 2010). In brief, Th1 dominated responses results in parasite

clearance, whereas Th2 dominated responses results in susceptibility to parasite infection and persistence. However, recent studies revealed that disease progression is not strictly depended on Th1/Th2 dominancy. For example, robust Th1 responses were reported to result in hyper-inflammation resulting in tissue damage and exacerbation of Leishmania infection (Silveira, Lainson, De Castro Gomes, Laurenti, & Corbett, 2009). Moreover, Th17 subset (characterized by IL-17 secretion) was reported to exert contrasting roles in Leishmania infection depending on the parasite species. Th17 responses are associated with healing lesions in *L. braziliensis* and *L. infantum* infections (Agallou, Margaroni, & Karagouni, 2011; Vargas-Inchaustegui, Xin, & Soong, 2008), whereas Th17 cells exacerbate *L. major* and *L. guyanensis* infections (Hartley et al., 2016; Lopez Kostka et al., 2009). These findings indicate that a delicate balance in Th1/Th2 and Th17 responses are required to establish a protective host immune response.

In summary, several innate mechanisms are involved in Leishmania infection and parasites developed various strategies to evade or alter these mechanisms. Well-orchestrated innate and adaptive immune responses are required for development of protective immunity to Leishmania; otherwise, immune responses may contribute to pathogenesis. Protective and pathological host immune responses to Leishmania infections are summarized in Figure 1.6.
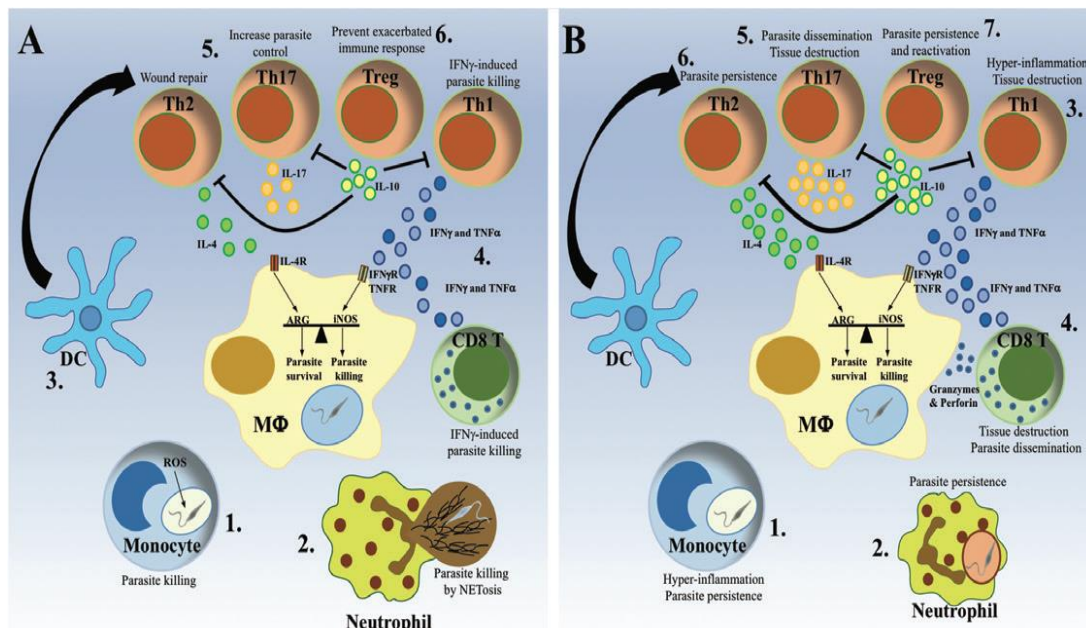
Figure 1.6. Protective (A) and Pathological (B) Host Immune Responses to Leishmania Infection

Adopted from (Rossi & Fasel, 2018)

1.2. Extracellular Vesicles and Adjuvants used in the Study

1.2.1. Extracellular Vesicles

Extracellular vesicles (EVs) are membranous structures that are secreted from cells in different types of organisms ranging from prokaryotes to highly evolved eukaryotes (Yáñez-Mó et al., 2015). EVs are classified as exosomes, microvesicles and apoptotic bodies with respect to their biological formation pathways (Bobrie, Colombo, Krumeich, Raposo, & Théry, 2012). Exosomes are formed through the fusion of multi-vesicular bodies with the early endosomes, whereas microvesicles are originated from outer cell membrane budding. As the name suggests, apoptotic bodies are released from the cells that are going through apoptosis (Colombo, Raposo, & Théry, 2014).

Extracellular vesicles are considered as critical contributors mediating inter and/or intra-cellular communication. Extracellular vesicle-mediated exchange of biological information may result either in immune activation or immune regulation, depending

on the EV source and the state of the recipient cell. In general, extracellular vesicles secreted from pathogenic organisms modify host cellular immunity and constitute a new type of immune evasion mechanism (Gomez et al., 2009).

1.2.1.1. **Leishmania Extracellular Vesicles**

As a eukaryotic unicellular organism, Leishmania secrete extracellular vesicles that are morphologically identical to mammalian exosomes sharing ~50% protein content similarity (Judith. M. Silverman et al., 2008; R. J. Simpson, Lim, Moritz, & Mathivanan, 2009). Leishmania extracellular vesicles are secreted through a mechanism that was first defined by Silverman *et al.* (2010). Various studies demonstrated that exosome secretion serves as the primary Leishmania-specific protein secretion pathway and the extruded vesicles interact with host cells in the infection microenvironment *in vivo* (Dong, Filho, & Olivier, 2019; Marshall et al., 2018; Pérez-Cabezas et al., 2019). Exosomes carry wide variety of macromolecules in their cargo, including proteins, small non-coding RNAs and tRNAs that might be contributing to host cell immunomodulation (Lambertz et al., 2012).

Since the exosome release is one of the factors that has been exploited by the parasite to evade immune activity, exosomes are highly enriched in virulence factors. During the initial phase of Leishmania infection, the parasites are exposed to heat shock (shift to 37°C) and acidic environment, both of which contribute to increased EV secretion (Hassani, Antoniak, Jardim, & Olivier, 2011). It has been suggested that this strategy may be used to isolate Leishmania exosomes from axenic cultures. The rich antigenic content of exosomes attract attention and open up new avenues for their application in vaccine development (Olivier & Fernandez-Prada, 2019).

1.2.2. **Adjuvants used in the Study**

Adjuvants combined with Leishmanial antigens in this thesis will be briefly introduced in this section.

Single stranded synthetic oligodeoxynucleotides containing unmethylated cytosine-phosphate-guanine dinucleotide motifs (CpG ODN) are synthetic TLR9 agonists that imitate the bacterial CpG-rich DNA are excellent immune activatiors (Dunne, Marshall, & Mills, 2011; Hanagata, 2017; Hennessy, Parker, & O'Neill, 2010; Klinman, Klaschik, Sato, & Tross, 2009; Klinman et al., 2002; Li et al., 2004; Takeshita et al., 2001; Vollmer & Krieg, 2009). CpG ODNs are classified according to their sequences, chemical bonds, 3D conformations and type of immune response they support in human peripheral blood mononuclear cells (Hanagata, 2012). Based on this classification, so far, four different classes of CpG ODN have been defined (Hanagata, 2012). Among these, K type CpG ODNs activate B cells and stimulate proinflammatory cytokine production in peripheral blood cells. In contrast, D-type CpG ODNs stimulate IFNα production from pDCs (M. Gursel, Gursel, Mostowski, & Klinman, 2006; M. Gursel, Verthelyi, & Klinman, 2002; Verthelyi, Ishii, Gursel, Takeshita, & Klinman, 2001). The differential activation of immune cells through K versus D ODN stimulation, lead to distinct immune responses and therefore these two classes might offer noncomplementary adjuvant activities in vaccines.

Cyclic guanosine monophosphate–adenosine monophosphate (cGAMP) is a newly identified intracellular second messenger, capable of directly activating an important immune sensor, stimulator of interferon genes (STING) (Wu et al., 2013). In a previous study from our laboratory, combination of K type CpG-ODN (characterized by its phosphorothioate backbone) and cGAMP (K-cGAMP) was shown to be a Th1 promoting adjuvant in a murine model of protective cancer vaccination (Yildiz et al., 2015). In addition, in another study from our laboratory, complexing K type CpG-ODN with HIV-derived cell-penetrating TAT peptide, resulted in formation of stable CpG ODN nanorings replicating IFN stimulating activity of D-ODN (Gungor et al.,

2014). Thus, combination of these adjuvants with the Leishmania-specific antigens could be a strategy for anti-leishmanial vaccine development and therefore these adjuvants and the D-ODN were tested in immunoprotection and/or immunotherapy experiments in this thesis.

Natural killer T-cells (NKT cells) play a significant role in supporting adaptive and innate immunity. Alpha-Galactosylceramide (αGalCer) is a synthetic glycolipid that can bind to non-classical MHC-I molecules (CD1d) expressed by antigen presenting cells (APCs) (Brennan, Brigl, & Brenner, 2013). αGalCer bound to CD1d is recognized by invariant natural killer cells (iNKT). αGalCer recognition in the context of CD1d, induces activation of iNKTs and lead to IFN-γ production, thereby promoting innate and adaptive immunity. (Borg et al., 2007; Kawano et al., 1997; Smyth et al., 2002). While αGalCer causes a steady and delayed immune response, CpG ODNs have fast-acting inflammatory effects especially in the mucosa (Lindqvist, Persson, Thörn, & Harandi, 2009). Therefore, use of a longer-acting and less inflammatory adjuvant might favor both parasite clearance and wound healing in Leishmania infections.

1.3. Aims of the Study

During 1990-2010, more than 50,000 new cutaneous leishmaniasis (CL) cases caused by four different Leishmania species, including *L. major*, have been reported in Turkey. During the last decade, Turkey received more than 3 million refugees due to the civil war in Syria, where CL is highly endemic and therefore, there is an expected increase in CL cases in Turkey (Özbilgin et al., 2017). Such increase in disease prevalence necessitates the development of urgent prevention/treatment strategies.

For these purposes, in this thesis we aimed to examine the possible contribution of the *L. major* kinetoplast DNA to disease progression and severity, which may consequently provide insights to develop new therapeutic agents against

leishmaniasis. Furthermore, we aimed to develop a potential *L. major* exosome based vaccine/immunotherapeutic against cutaneous leishmaniasis (CL).

Leishmania parasites harbor one of the most unusual DNA structures, the kinetoplast DNA (kDNA) consisting of giant networks of catenated mini and maxi-circles. Evidence suggests that kDNA minicircles can be integrated into the host genome during infection with *Trypanosoma cruzi* (Teixeira, Hecht, Guimaro, Sousa, & Nitz, 2011). Moreover, parasite kDNA persists in tissues of Chagas patients and presence of kDNA correlates with inflammatory cell infiltration (Zhang & Tarleton, 1999). Based on these, it is likely that kDNA-induced immune recognition might modulate the immune response against the parasite. Whether such phenomena also occurs in the case of Leishmaniasis or how kDNA impacts the course of infection is still unknown.

Therefore, in the first part of the study, we first aimed to isolate and characterize kDNA. Then, we intended to test whether Leishmania kDNA contributes to infection *in vitro* and disease progression *in vivo*.

It has been suggested that type I interferon responses induced by endogenous or exogenous viral RNA contributes to severity of MCL (Ives et al., 2011; Rossi et al., 2017). Based on these findings, we also endeavored to quantify type I interferons induced by kDNA in *in vitro* infections.

Considering the serious side effects of drug treatment and parasites developing resistance against drugs, protection through vaccination would be an ideal choice. Although several vaccine candidates have been tested in pre-clinical and clinical trials, currently, there is no registered vaccine against leishmaniasis (Alvar et al., 2013).

In the second part of the study, we wanted to test the utility of antigen-rich Leishmania extracellular vesicles (exosomes) with excellent antigen delivery properties as a source of Leishmania antigens in an attempt to develop a vaccine and/or immunotherapeutic. Moreover, we also aimed to determine the best adjuvant to be combined with exosomes by testing Th1 or NKT supporting adjuvants.

For these purposes, we sought to isolate and characterize *L. major* exosomes and intended to improve their immunogenic properties by chemical inactivation. Furthermore, we aimed to develop mouse isolated transgenic parasites to establish a murine CL model that would enable direct parasite load determination *in vivo*.

Finally, we aimed to determine correlates of anti-Leishmanial protective mechanism induced through vaccination based on Leishmania-specific humoral and cellular responses.

CHAPTER 2

MATERIALS & METHODS

2.1. **Materials**

Details of media recipes and media components are provided at Appendix A. Reagents and materials used throughout this thesis are listed in Table 2.1. according to the order of their appearance in this Chapter.

Table 2.1. *Identities and Suppliers of Chemicals, Reagents and Kits Used Throughout the Thesis*

Reagent	Company	Cat No:
Fixation Medium (Medium A)	Thermo Fisher Scientific, U.S.A.	GAS001S100
DPBS	Biological Industries, Israel	02-023-1A
Ficoll® 400	Sigma-Aldrich, Germany	F2637
Proteinase K, Tritirachium album	Merck, Germany	539480
N-Lauroylsarcosine sodium salt solution (Sarcosyl)	Sigma-Aldrich, Germany	L7414
Plasmid-Safe™ ATP-Dependent DNase	Epicentre, U.S.A.	E3101K
RNase A	Thermo Fisher Scientific, U.S.A.	EN0531
Phenol solution	Sigma-Aldrich, Germany	P4557
Chloroform	Sigma-Aldrich, Germany	288306
Ethanol, Absolute (200 Proof), Molecular Biology Grade	Fisher Scientific, USA	BP2818100
Ammonium acetate	Sigma-Aldrich, Germany	A1542
Ultra-pure water	Biological Industries, Israel	01-866-1B
Qubit™ Protein Assay Kit	Invitrogen, U.S.A	Q33211
Albumin (BSA) Fraction V (pH 7.0)	AppliChem, Germany	A1391
Methanol	Isolab, Germany	947.046
DAPI	Invitrogen, U.S.A	D1306
Zeocin	Invivogen, France	ant-zn-1
Normocin	Invivogen, France	ant-nr-1

Table 2.1 cont`d. *Identities and Suppliers of Chemicals, Reagents and Kits Used throughout the Thesis*

Reagent	Company	Cat No:
Phorbol myristate acetate (PMA)	Invivogen, France	tlrl-pma
Recombinant Mouse M-CSF	Tonbo, U.S.A.	21-8983
ZAP-OGLOBIN II Lytic Reagent	Beckman Coulter, U.S.A.	NC0098316
CellTrace™ CFSE	Invitrogen, U.S.A.	C34554
Opti-MEM Reduced Serum Media	Thermo Fisher Scientific, U.S.A.	31985070
Lipofectamine 2000 Transfection Reagent	Thermo Fisher Scientific, U.S.A.	11668019
QUANTI-Blue™	Invivogen, France	rep-qb2
Trypsin EDTA Solution C	Biological Industries, Israel	03-051-5B
SYTO® 16 green fluorescent nucleic acid stain	Life Technologies, U.S.A	S7578
SYTOX® Orange Nucleic Acid Stain	Life Technologies, U.S.A	S11368
pLEXSY-neo2.1	Jena Biosciences, Germany	EGE-273
SwaI Restriction Enzyme	New England Biolabs, U.S.A.	R0604
Gene Pulser Electroporation Cuvettes 0.2 cm gap	Biorad, U.S.A	165-2086
LEXSY Neo Antibiotic	Jena Biosciences, Germany	AB-105
XenoLight D-Luciferin	Perkin Elmer, U.S.A.	122799
Hydrogen peroxide solution 30% (w/w)	Sigma-Aldrich, Germany	H1009
Gelatin	Merck, Germany	104078
PageRuler™ Prestained Protein Ladder, 10 to 180 kDa	Thermo Fisher Scientific, U.S.A.	26616
Catalase from bovine liver	Sigma-Aldrich, Germany	C9322
Peroxide Assay Kit	Sigma-Aldrich, Germany	MAK311
PI Staining Solution	Tonbo, U.S.A.	13-6990
PNPP Substrate	Thermo Fisher Scientific, U.S.A.	34045
Collagenase from Clostridium histolyticum	Sigma-Aldrich, Germany	C5138
Hyaluronidase from bovine testes	Sigma-Aldrich, Germany	H3506
Deoxyribonuclease I	Sigma-Aldrich, Germany	D4263

Table 2.1 cont`d. *Identities and Suppliers of Chemicals, Reagents and Kits Used throughout the Thesis*

Reagent	Company	Cat No:
NNN Modified Medium	HiMedia, India	M681
Rabbit Blood Defibrinated	Rockland, U.S.A.	R109

Table 2.2. *Antibodies and Kits Used in ELISA and Flow Cytometer Experiments*

Reagent	Company	Cat No:
Anti-Leishmania Major Surface Protease (GP-63) Antibody-FITC	Cedarlane, Canada	CLP005F
Goat Anti-Mouse IgG1-AP	Southern Biotech, U.S.A.	1071-04
Goat Anti-Mouse IgG2a-AP	Southern Biotech, U.S.A.	1081-04
Cytometric Bead Array (CBA) Mouse Th1/Th2/Th17 Cytokine Kit	Becton, Dickinson, U.S.A.	560485

2.2. Methods

2.2.1. Parasite Culture and Maintenance

2.2.1.1. Parasites

Leishmania major parasites isolated from a cutaneous leishmaniasis patient`s lesion were kindly provided by Prof. Ahmet Özbilgin from Department of Molecular Parasitology, Celal Bayar University. The species of the isolated parasites were identified and validated by Seray Özensoy Töz from Department of Parasitology, Ege University.

2.2.1.2. Maintenance of Axenic Promastigote Culture

L. major parasites were maintained and cultured in leishmania growth medium (Table A.1., Appendix A). Parasite cultures were contained in plug sealed tissue culture flasks

(SPL, South Korea). Parasite culture flasks were incubated in vertical position at 26°C inside a standard incubator (Nüve, Turkey) without CO_2.

Required amount of leishmania fresh growth medium was added onto previous culture every 2-3 days to dilute parasite concentration from late-log to early-log phase (Leishmania growth curve will be explained in section 2.2.1.4).

2.2.1.3. **Quantification of Leishmania Promastigotes in Culture**

After parasite culture was mixed vigorously with a serological pipette, 20 µl sample was taken and fixed by adding 20 µl Fixation Medium (4% paraformaldehyde, Medium A, Invitrogen, U.S.A.) dropwise. Then, the sample was incubated for 10 minutes at room temperature. Fixed samples were diluted by adding 160 µl DPBS (10 fold dilution considering original volume). 20 µl of diluted fixed sample was analyzed on a Novocyte 2060R flow cytometer (ACEA Biosciences, U.S.A.).

Number of parasites within a defined FSC versus SSC gate were multiplied by 50 x 10 (dilution factor) to calculate 'parasite number/ml' in cultures.

2.2.1.4. **Construction of Parasite Growth Curve**

Parasites were seeded in 10 ml medium at a concentration of $2.5x10^6$ parasites/ml on day 0. Parasite growth was monitored by counting parasites every consecutive day as described in section 2.2.1.3 until parasite growth was terminated. Early, mid and late-log phases together with stationary phase were specified based on this curve for future experiments.

2.2.1.5. **Cryopreservation of Leishmania Promastigotes**

When parasites were first received, they were grown in leishmania growth medium for a short period to expand parasite numbers. Then, parasites at mid-log phase were centrifuged at 1,500g for 10 minutes. Pellet was washed with leishmania growth medium by repeating the same centrifugation. Washed pellet was re-suspended in null RPMI-1640 (with no extra additives).

500 µl of ice-cold Leishmania freezing medium (Table A.2., Appendix A) was added to 2 ml cryogenic vials (Corning, U.S.A.) and vials were kept on ice. 500 µl from final suspension of parasites was added slowly and dropwise into each vial containing freezing medium in order to obtain 20% FBS and 10% DMSO final concentration. The resulting mixture was mixed gently by pipetting and placed into Mr. Frosty™ freezing container (Thermo Fisher Scientific, U.S.A.) to achieve a cooling rate of approximately -1°C/minute in a -80°C freezer overnight, cryogenic vials were then transferred to a liquid nitrogen tank for long-term storage.

Cryopreservation procedure was applied to parasites, which were at most in their third passage. It has been reported that prolonged axenic culture of leishmania promastigotes results in loss of virulence (Moreira et al., 2012; Segovia, Artero, Mellado, & Chance, 1992). For this reason, stocks were prepared at their earliest possible passage.

In the same context, parasites were discarded after being passaged more than 20 times (55-60 days old) and were not used for any *in vivo* or *in vitro* experiments. After an old culture was discarded, a new culture from a frozen stock was propagated for further experiments.

2.2.1.6. **Preparation of Parasites for *in vitro* Infection and *in vivo* Challenge Experiments**

Cultured parasites are found in procyclic stage in log phase of growth. It has been reported that parasites which were maintained at stationary phase transform into a more infective metacyclic stage (David L. Sacks & Perkins, 1984).

For all *in vitro* infection and *in vivo* challenge experiments, 2-3 days old stationary phase parasites were used. In other words, parasites were maintained at stationary phase for 2-3 days instead of regular passaging.

2.2.1.7. **Enrichment of Metacyclic Parasites by Ficoll Density Gradient Centrifugation**

For infection experiments, 2-3 days old stationary phase parasites were enriched for metacyclic parasites as described by Späth & Beverley (Späth & Beverley, 2001) and depicted in Figure 2.1.

Briefly, 40% Ficoll solution was prepared by suspending powdered Ficoll 400 (Sigma-Aldrich, Germany) in dH_2O. Part of this solution was diluted to 10% by null RPMI 1640. 2 ml 40% Ficoll solution was added at the bottom of a 15 ml collection tube and 2ml 10% Ficoll solution was layered on top of 40% solution. 2 ml stationary phase parasite culture was added on top of these layers. The tube was centrifuged at 1,300g for 10 minutes at RT with no breaks. The opaque cloudy layer located on the top of Ficoll layers was collected and washed with DPBS at the same centrifugation conditions. Following a wash step, the pellet was re-suspended in Leishmania growth medium for *in vitro* experiments or in DPBS for *in vivo* challenge experiments.
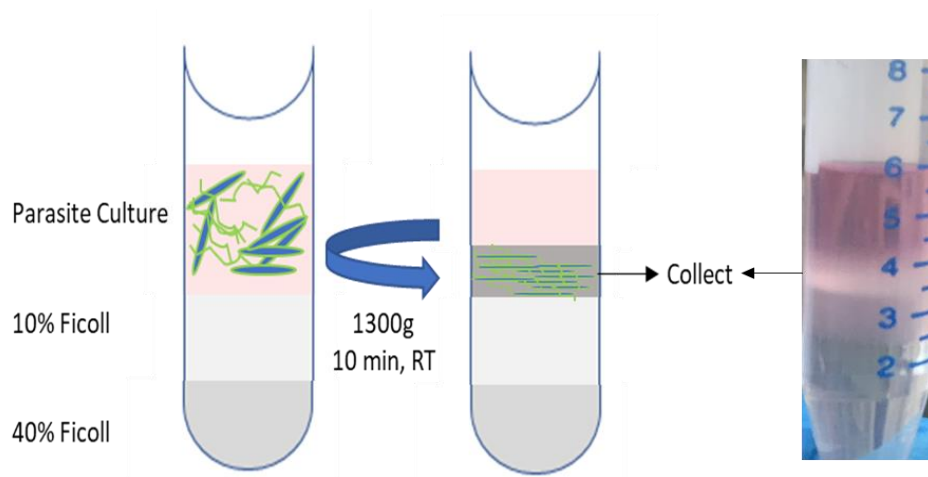
Figure 2.1. Schematic Presentation of Metacyclic Parasite Enrichment on a Ficoll Density Gradient

Enriched parasites were fixed as described in Section 2.2.1.3. Metacyclic parasites in the resulting culture were counted based on their morphology using FLoid Cell Imaging Station (Thermo Fisher Scientific, U.S.A.) to verify effectiveness of the enrichment.

2.2.2. **Isolation and Extraction of Various *L.major* Cellular Components**

2.2.2.1. **Isolation of Kinetoplast DNA (kDNA) and Genomic DNA (gDNA)**

Kinetoplast DNA (kDNA) and genomic DNA (gDNA) from *L.major* were isolated as previously described (Akman et al., 2000) with modifications.

Late-log phase parasites were counted as described in Section 2.2.1.3. 10^9 parasites were sedimented at 3,000g for 10 minutes at 4°C. The pellet was re-suspended in 6-8 ml NET buffer (Appendix B) and mixed vigorously by vortexing. The suspension was centrifuged once more. Pellet was re-suspended in 710 µl NET buffer. Subsequently, Proteinase K (Merck, Germany) and Sarcosyl (Sigma-Aldrich, Germany) were added into the solution at final concentrations of 100 µg/ml and 1% (v/v), respectively. After vortexing, the mixture was incubated over-night for cell lysis.

Following incubation, the lysate was centrifuged at 24,000g for 2 hours at 4°C to sediment the kDNA networks. The supernatant was transferred into a fresh micro-centrifuge tube to isolate the gDNA. Pellet was re-suspended in NET buffer and used to isolate kDNA. kDNA suspension was treated with Plasmid-Safe™ ATP-Dependent DNase (Epicentre, U.S.A.) and RNase A (Thermo Fisher Scientific, U.S.A.) according to the manufacturer`s instructions. These treatments were carried out to eliminate gDNA and RNA contaminants in the kDNA fraction.

For both of the samples (gDNA and kDNA) phenol:chloroform extraction method was applied for isolation. One volume (1x of the original volume) of phenol pH:7.9 (Sigma-Aldrich, Germany) was added onto solutions and mixed by inversions until an emulsion formed. The emulsion was centrifuged at 14,000g for 90 seconds at RT. Following centrifugation, aqueous phase was transferred to a new tube. One volume of chloroform (Sigma-Aldrich, Germany) was added onto the separated aqueous phase and the same mixing and centrifugation steps mentioned above were repeated.

1/3 volume of 5M ammonium acetate solution (Sigma-Aldrich, Germany) was added onto the collected aqueous phase and mixed by inversion. 2-3 volumes of molecular biology grade absolute ethanol (Fisher Scientific, USA) was added onto the sample and mixed by inversion. Samples were incubated at -20°C overnight.

After incubation, sample was centrifuged at maximum speed of standard tabletop centrifuge and supernatant was decanted. Precipitate was washed once more with 70% ethanol. After supernatant was decanted, precipitate was air-dried and dissolved in ultra-pure water (Biological Industries, Israel).

DNA concentrations of isolates were measured by using NanoDrop Microvolume Spectrophotometer (Thermo Fisher Scientific, U.S.A.). Furthermore, samples were run on a 0.7% (w/v) agarose gel for visual confirmation.

2.2.2.2. **Preparation of Heat-Killed (HK) Parasites**

Late-log parasites were sedimented at 1,500g for 10 minutes at RT. Pellet was washed with DPBS and re-suspended in DPBS. Resulting parasite suspension was incubated at 70°C for 60 minutes in a dry-block thermostat (Biosan, Latvia). After incubation, heat-killed parasites were centrifuged at 2,500g for 20 minutes at RT and re-suspended in DPBS.

HK parasites were used in immunization/challenge experiments and quantification was based on initial parasite number from which they were isolated.

2.2.2.3. **Preparation of Soluble Leishmania Antigen (SLA) and Whole Cell Lysate (WCL).**

Late-log phase parasites were centrifuged at 1,500g for 10 minutes at RT and washed with DPBS once. Pellet was dissolved in DPBS and suspension was subjected to rapid repeated freeze-thaw cycles for five times. Resulting solution was used as whole cell lysate (WCL). For isolation of soluble leishmania antigen (SLA), whole cell lysate was centrifuged at 5,000g for 20 minutes at 4°C and supernatant was collected as the soluble part. Protein contents of WCL and SLA were quantified by using Qubit™ Protein Assay Kit (Invitrogen, U.S.A.) following the instructions provided by the manufacturer.

Both isolates were stored at -20°C and fresh isolates were prepared for each experiment.

2.2.2.4. **Isolation of Leishmania Extracellular Vesicles (Exosomes)**

Leishmania growth medium was centrifuged at 100,000g for 3 hours at 4°C to sediment exosomes originating from FBS. Supernatant was collected as exosome-free medium.

Stationary phase parasites were centrifuged at 1,500g for 10 minutes at RT. Following DPBS wash, pellet was re-suspended and inoculated in acidic (pH: ~5.5) exosome collection medium (Table A.3., Appendix A) in the same volume of original culture. Parasites were incubated in acidic medium at 37°C with 5% CO_2 for 20 hours. Different from original parasite culture, parasites were contained in T-75 flasks with a ventilated cap (Sarstedt, Germany) to provide gas exchange.

Purpose of incubation at 37°C in acidic environment is to mimic the environment of phagolysosomes so that parasites start to transform from promastigotes to amastigotes. In addition to that, it has been reported that stress generated by low pH and high temperature results in higher rates of exosome secretion (Hassani, Antoniak, Jardim, & Olivier, 2011; Silverman et al., 2010).

After incubation, exosomes were isolated by serial differential centrifugation steps as summarized in Figure 2.2.
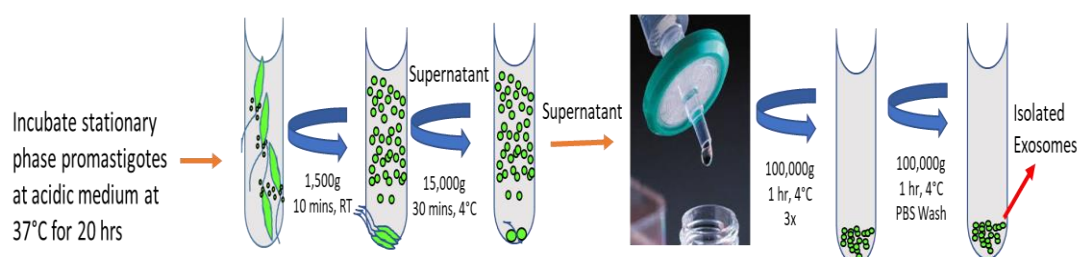
Figure 2.2. Leishmania Exosome Isolation by Differential Centrifugation

Briefly, parasites in acidic medium were centrifuged at 1,500g for 10 minutes at RT. Supernatant, which contains large vesicles and debris, was transferred to ultra-centrifuge tubes and centrifuged at 15,000g for 30 minutes at 4°C by using preparative ultra-centrifuge (Hitachi, Japan) to remove other small components except exosomes. After second centrifugation, supernatant was filtered through 0.22 μm syringe filters (Jet-Biofill, China) to further purify exosomes. Flow through was centrifuged at

100,000g for 1 hour at 4°C. This centrifugation step was repeated twice with different cultures in the same tube to increase the yield. Finally, exosome pellet was washed with DPBS at the same centrifugation conditions. Resulting pellet was re-suspended in DPBS.

Exosomes were quantified by their protein content using Qubit™ Protein Assay Kit (Invitrogen, U.S.A.) following the instructions provided by the manufacturer.

2.2.3. **Characterization of Kinetoplast DNA (kDNA) Isolated from *L.major***

2.2.3.1. **Fluorescence Microscopy of kDNA Networks**

5 μg isolated kDNA was mixed with 1% (w/v) BSA (AppliChem, Germany) in PBS solution. Mixture was spread on a sterile glass slide and immersed into cold methanol (Isolab, Germany) for 5 minutes for fixation. Fixed samples were air-dried and stained with DAPI (Thermo Fisher Scientific, U.S.A.) at a final concentration of 1μg/ml (~300nM). Stained slides were incubated for 5 minutes at RT. After incubation, excess stain was rinsed with DPBS several times. Rinsed samples were observed on the blue channel of FLoid Cell Imaging Station (Thermo Fisher Scientific, U.S.A.) to visualize kDNA networks.

2.2.3.2. **Conformational Analysis of kDNA by Atomic Force Microscopy (AFM)**

kDNA isolates were diluted in DNA attachment buffer (Appendix B) at a final concentration of 50 μg/ml. Since both DNA and mica surface are negatively charged, DNA adsorption is not possible at their natural states. Either DNA should be dissolved in a buffer containing divalent cations or mica should be pre-treated with metal cations (Pastré et al., 2003). We followed the former approach for DNA adsorption to mica surface.

Mica discs were immobilized on metal discs. Approximately 50 µl of kDNA in DNA attachment buffer was added onto freshly cleaved mica disc surface and incubated at RT for 5 minutes. Then, excess buffer was rinsed with ultra-pure water and sample was air-dried.

Air-dried samples were scanned on an Ambient AFM (Nanomagnetics Instruments, UK) following the manufacturer`s instructions. Briefly, whenever a new cantilever was inserted into the microscope, it was tuned based on its resonance. Laser and detector positions were arranged to obtain a total force of 3.0V with no lateral and nominal forces. Root mean square (RMS) value, which is an indicator of surface roughness, was set around 2-2.2. Oscillation amplitude was set to half of RMS value and samples were scanned at non-contact mode by using NMI SPM (v2.0.37) software.

Scanned images were plane-corrected and scaled by using the NMI Viewer (v1.4) software.

2.2.4. Characterization of Isolated Leishmania Exosomes

2.2.4.1. Analysis of gp63 Content of Leishmania Exosomes

Volume of isolated leishmania exosomes was completed to 200 µl by DPBS. Diluted exosomes were incubated with FITC conjugated anti-gp63 (1 µg/ml) antibody (Cedarlane, Canada) for 1 hour at RT. After incubation, samples were acquired on a Novocyte 2060R flow cytometer (ACEA Biosciences, U.S.A.).

Since exosomes are too small to be discriminated in flow cytometric analysis, DPBS was acquired to determine the background reading on FSC-H and SSC-H parameters. Exosome gate was determined based on this background reading. Unstained exosome sample was used to discriminate gp63 positive exosomes. Mean fluorescent intensities (MFIs) of both unstained and stained leishmania exosomes were recorded on the green BL-1 channel of the instrument.

2.2.4.2. **Proteomics Analysis of Leishmania Exosomes by Mass Spectrometry (MS)**

Mass Spectrometry (MS) analysis of two different leishmania exosome batches was kindly processed and analyzed by Ülkü Güler who is a post-doctoral fellow in Mass Spectrometry laboratory in Chemistry Department of Hacettepe University (Ankara, Turkey). Prof. Bekir Salih, head of Mass Spectrometry laboratory, supervised the process.

L.major reference proteome database was downloaded from UniProt database (https://www.uniprot.org/proteomes/UP000000542) in FASTA format. In order to analyze mass spectrometry results, reference database was uploaded to MASCOT server (http://www.matrixscience.com/server.html).

Most abundant proteins were determined by MASCOT score which is a statistical indicator of match between experimental and database sequences. Raw data output of MS analysis were run on PANTHER Protein Class GO Term Analysis (P. D. Thomas et al., 2003) by Volkan Yazar from Molecular Biology and Genetics Department of Bilkent University (Ankara, Turkey).

2.2.4.3. **Morphological Analysis of Leishmania Exosomes by Atomic Force Microscopy (AFM)**

Leishmania exosomes were diluted to 100-200 ng/ml concentration by ultra-pure water. 40-50 µl diluted exosome sample was distributed on a freshly cleaved mica layer. Sample was air-dried and scanned by using Atomic Force Microscopy (AFM) as described previously in Section 2.2.3.2.

2.2.5. **Cell Culture**

2.2.5.1. **Generation of PMA-Differentiated THP-1 Cells**

THP1-Blue™ ISG monocyte cell line (Invivogen,France) was maintained in 10% regular RPMI 1640 medium (Table A.4., Appendix A) supplemented with 100 µg/ml Zeocin (Invivogen, France) and 100 µg/ml Normocin (Invivogen, France) following the manufacturer`s instructions. Briefly, $5x10^5$ cells were inoculated at each sub-culturing process and it was repeated every three days before cells reached a concentration of $2x10^6$/ml.

THP1-Blue™ ISG cells were centrifuged at 250g for 10 minutes at RT. Pellet was re-suspended in 1 ml of 10% regular RPMI 1640 medium. 20 µl sample was taken from suspension and diluted 10 fold with 10% regular RPMI 1640 medium. 20 µl of diluted suspension was acquired on a Novocyte 2060R flow cytometer (ACEA Biosciences, U.S.A.). Number of alive THP-1 cells within a defined FSC-H/SSC-H gate was multiplied by 50 x 10 (initial dilution factor) to calculate cell concentration in terms of 'cells/ml'.

According to the calculated cell density, initial culture was diluted to a concentration of ~100,000 cells/180 µl. 180 µl of diluted cell suspension was distributed to each well of tissue culture treated flat bottom 96 well plates (Sarstedt, Germany). 20 µl phorbol myristate acetate (PMA) (Invivogen, France) was added into each well at a final concentration of 25 ng/ml and mixed by pipetting. Cells were incubated overnight at 37°C with 5% CO_2.

After incubation, cells were monitored under an inverted microscope (Olympus, Japan) for morphological changes. After confirming the presence of differentiated macrophage like PMA-differentiated THP-1 cells, medium was aspirated from each well. Wells were washed with wash medium (Table A.5., Appendix A) once and 200 µl fresh 10% regular RPMI 1640 medium was added onto cells. PMA-differentiated THP-1 cells were incubated at 37°C with 5% CO_2 up to three days for further experiments.

2.2.5.2. **Generation of Mouse Bone Marrow Derived Macrophages**

Femurs and tibias of sacrificed 6-10 weeks old BALB/c mice were collected. Bones were immersed into 70% (v/v) ethanol for sterilization. Ends of bones were cut with sterile scissors and marrow was flushed out of medullary cavity by applying wash medium with pressure from one side with the help of a sterile syringe. Collected marrow was passed through 40 μm cell strainer (Corning, USA). Cells were washed with wash medium at 300g for 10 minutes at RT. Pellet was re-suspended in ACK Lysis buffer (Appendix B) and incubated for 3 minutes at RT. Cells were washed once more as described above and counted as described at section 2.2.5.1. Cell concentration was adjusted to 600,000 cells/ml by adding required amount of 20% regular RPMI 1640 medium (Table A.5., Appendix A). 200 μl cell suspension was distributed to each well of tissue culture treated 48 well plates (Sarstedt, Germany). Recombinant mouse M-CSF (Tonbo, U.S.A.) was added onto cells at a final concentration of 20 ng/ml. Cells were incubated at 37°C with 5% CO_2 for 6-7 days. On day 3, 200 μl 20% regular RPMI medium containing M-CSF at a concentration of 20 ng/ml was added into each well for replenishment of M-CSF. Cells were observed under inverted microscope regularly to follow the differentiation process.

6-7 days after bone marrow isolation and cultivation, attached macrophages were used for infection and stimulation assays.

2.2.5.3. **Single Cell Suspension Preparation from Spleen**

After *in vivo* experiments were terminated, spleens from sacrificed mice were removed surgically. Each well of a tissue culture treated 6 well plate (Sarstedt, Germany) was filled with 2 ml of wash buffer and spleens were placed separately. Spleens were mashed gently by using the back of a sterile plunger with circular motions. Cells were washed with wash buffer twice at 300g for 10 minutes. Final cell pellet was re-suspended in 10% regular RPMI 1640 medium. 20 μl of final suspension was diluted to 10 ml with isotonic solution. 2-3 drops of ZAP-OGLOBIN II Lytic

Reagent (Beckman Coulter, U.S.A.) was added into solution for RBC lysis. 20 µl of diluted samples were acquired on an Accuri C6 Flow Cytometer (Becton, Dickinson, U.S.A.). Cell numbers within the defined splenocyte gate were multiplied by 50 x 500 (initial dilution factor) to calculate number of splenocytes/ml. Required number of cells was calculated and distributed to each well of tissue culture treated 96 well plate. Cells were allowed to rest for 2-3 hours. Then, splenocytes were used for stimulation experiments.

2.2.6. *In vitro* Infection Experiments with CFSE-Labelled *L.major*

2.2.6.1. **Generation of CFSE- Labelled Parasites**

Metacyclic parasites were re-suspended in DPBS at a final concentration of 5×10^6 cells/ml. Carboxyfluorescein Succinimidyl Ester (CFSE) (Invitrogen, U.S.A.) solution was added onto parasite suspension at a final concentration of 5µM. Solution was mixed by inversions and incubated in dark for 20 minutes at RT. After incubation, five times the original staining volume of wash buffer was added to quench the excess dye. Then, cells were centrifuged at 1500g for 10 minutes at RT and washed with DPBS once. Resulting pellet was re-suspended in Leishmania Infection Medium (Table A.6., Appendix A).

In addition to labelling metacyclic parasites, parasites at mid log-phase were stained with CFSE. In order to assess effects of CFSE staining on parasite proliferation, labelled parasites were monitored for five days by following the procedure described in Section 2.2.1.4.

2.2.6.2. **Preparation of DNA-Lipid Complexes for Transfection**

kDNA and gDNA isolates (described in Section 2.2.2.1) were diluted at desired concentrations in Opti-MEM reduced serum media (Thermo Fisher Scientific, U.S.A.). Lipofectamine 2000 Transfection Reagent (Thermo Fisher Scientific,

U.S.A.) was also diluted in Opti-MEM. Lipofectamine amount was determined according to the manufacturer`s recommendations: 1 µl Lipofectamine per 1 µg of DNA to be complexed.

DNA-lipid mixture was mixed well by pipetting and incubated for 15 minutes at RT for complexation to occur. After incubation, DNA-lipid complexes were added onto cells for DNA transfection.

2.2.6.3. **Infection of PMA-differentiated THP-1 Cells with CFSE Labelled Parasites in the Presence of kDNA and gDNA**

PMA-differentiated THP-1 cells were generated as described in Section 2.2.5.1 at a final concentration of 10^5 cells/well. Medium was aspirated and wells were washed gently with DPBS once. CFSE-labelled metacylic parasites were prepared as described in Section 2.2.6.1 at a concentration of 10^6 parasites/180 µl in Leishmania Infection Medium. 180 µl of labelled parasite suspension was added onto PMA-differentiated THP-1 cells to achieve a multiplicity of infection (MOI) of 1:10 (THP-1:parasites).

kDNA and gDNA complexed with Lipofectamine 2000 (Invitrogen, U.S.A) were prepared as described in Section 2.2.6.2 at DNA concentrations of 2.5 and 10 µg/ml for both. 20 µl of each DNA-lipid complex was added onto corresponding leishmania-THP-1 mixtures to reach final DNA concentrations of 0.25 and 1 µg/ml. Also 20 µl Leishmania Infection Medium was added onto cell-parasite mixtures as untreated controls. All wells were mixed gently by pipetting.

Samples were incubated at 37°C with 5% CO_2 for 24 hours for infection of THP-1 cells with parasites.

2.2.6.4. **Quantification of Interferon Induction by Quanti-Blue Assay**

THP1-Blue™ ISG cells (Invivogen, France) are genetically modified reporter cells. Upon activation of interferon signaling pathways, they produce secreted alkaline phosphatase (SEAP). Thus, interferon specific response of cells can be quantified by measuring IFN signaling induced SEAP activity. PMA-differentiated THP-1 cells were stimulated with different doses of IFNα to construct a standard curve for estimation of IFN concentration from SEAP activity assay.

PMA-differentiated THP-1 cells infected with parasites in the presence or absence of DNA stimulation were prepared as described in Section 2.2.6.3. After 24 hours incubation at 37°C, supernatants were collected from each well for Quanti-Blue Assay.

Quanti-Blue (Invivogen, France) SEAP activity assay was performed according to manufacturer`s instructions to measure IFN induction. Briefly, 180 µl pre-warmed (37°C) reconstituted Quanti-Blue solution was added into each well of sterile tissue culture treated 96 well plate. Then, 20 µl of collected supernatants from samples were added into corresponding wells. Plate was incubated at 37°C for 2-3 hours. After incubation, OD values were recorded at 640 nm wavelength using a Multiskan™ GO Microplate Spectrophotometer (Thermo Fisher Scientific, U.S.A.). Four-parametric logistic standard curve was constructed by using OD read-outs of IFNα stimulations (GraphPad Prism v.6). OD values of unknowns were fitted into the standard curve to estimate concentration of IFN production in infected cells.

2.2.6.5. **Assessment of Parasite Infection Rates of THP-1 Cells**

Following collection of supernatants for Quanti-Blue Assay (Section 2.2.6.4), infected PMA-differentiated THP-1 cells were washed with pre-warmed (37°C) null RPMI 1640 medium (with no additives) thrice. Washing was performed inside wells with gentle pipetting and aspiration. Then, 50 µl 1X Trypsin-EDTA solution (Biological

Industries, Israel) was added onto cells. Cells were incubated with Trpysin-EDTA solution for 10-15 minutes. After incubation, detached cells were collected and transferred to new micro-centrifuge tubes. 500 µl 10% Regular RPMI 1640 medium was added onto cells to inactivate trypsin. Samples were centrifuged at 1,500g for 5 minutes and pellets were re-suspended in 10% Regular RPMI 1640 Medium.

Re-suspended samples were acquired on Accuri C6 cytometer (Becton, Dickonson, U.S.A.). PMA-differentiated THP-1 cells were gated with respect to FSC-SSC parameters. Infection rates and MFI values were determined based on values on the green FL-1 channel.

2.2.6.6. **Fluorescence Microscopy Analysis of Leishmania Infected THP-1 Cells**

PMA-differentiated THP-1 cells were infected with unlabeled metacyclic parasites and stimulated as described in Section 2.2.6.3. After incubation, media were aspirated from wells. DPBS containing 1 µM SYTO® 16 Green fluorescent nucleic acid stain (Life Technologies, U.S.A) and 5 µM SYTOX® Orange nucleic acid stain (Life Technologies, U.S.A) were added into each well. While the former stain is cell membrane permeable and can stain both dead and alive cells, the latter is cell membrane impermeable and therefore can only stain dead cells. The purpose of double staining here is to observe parasites inside THP-1 cells and to discriminate dead versus live cells.

Cells were incubated at 37°C for 20 minutes with staining solution. After incubation, staining solution was aspirated and cells were washed inside wells by PBS once. 10% Regular RPMI 1640 Medium was added onto cells and infected cells were observed on green (for syto 16 green) and red (for sytox orange) channels of FLoid Cell Imaging Station (Thermo Fisher Scientific, U.S.A.). Merged images from each channel were taken from different regions of the wells.

2.2.7. Generation of EGFP-LUC Expressing Transgenic Parasites

2.2.7.1. Construction of Plasmid Vector

Backbone of pLEXSY-neo2.1 (Jena Biosciences, Germany) was used for designing the custom plasmid. Full sequence of vector backbone is available at manufacturer`s website (https://www.jenabioscience.com/images/103bb272b3/EGE-273.txt).

For expression of Enhanced Green Fluorescence Protein (EGFP) and Firefly Luciferase (LUC) fusion protein, EGFP-Luc sequence (Appendix C) was retrieved from pEGFPLuc vector (ClonTech, U.S.A, Cat No: 6169-1). Codon usage of EGFP-LUC sequence was checked by using Codon Usage Database of Kazusa DNA Research Institute, Japan specifically for *L.major* (http://www.kazusa.or.jp/codon/cgi-bin/showcodon.cgi?species=5664).
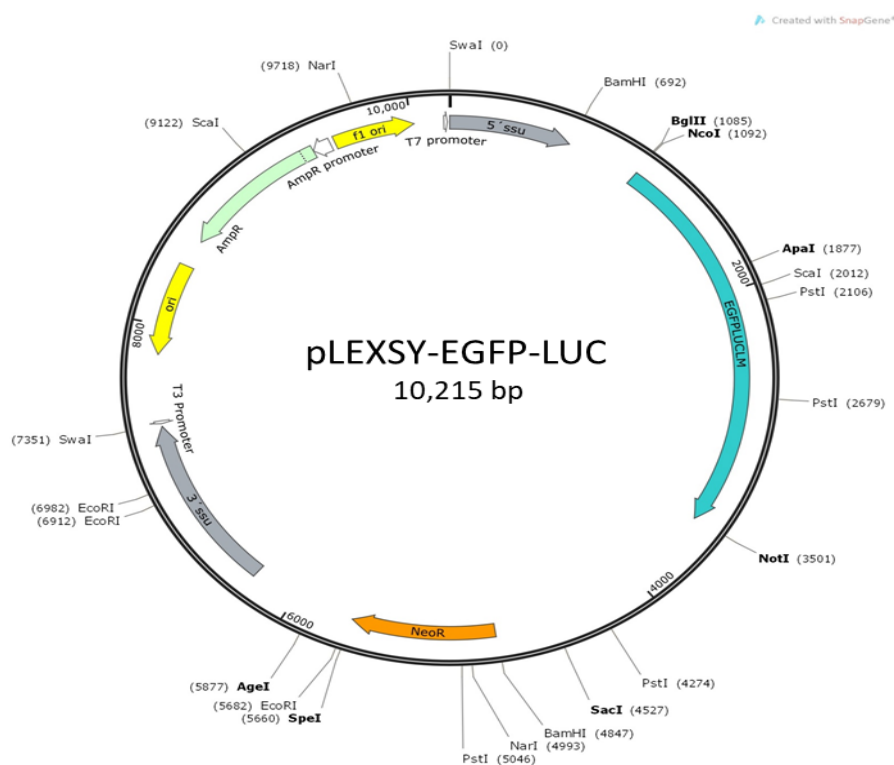
Figure 2.3. Map of Custom pLEXSY EGFP-LUC Plasmid

Synthesized custom vector was fully sequenced by Jena Biosciences, Germany. In addition, quality control test (Figure C.1., Appendix C) was performed for specific restriction enzymes before shipment.

2.2.7.2. Electroporation of Parasites for Transfection

10 μg of pLEXSY EGFP-LUC vector was digested with 10 units of SwaI (New England Biolabs, U.S.A.) at RT for 2 hours by following the manufacturer`s instructions. After incubation, samples were run on 0.8% (w/v) agarose gel for confirmation of successful digestion.

Parasites at log phase ($\sim15x10^6$ parasites/ml) were centrifuged at 1,500g for 10 minutes at RT. Pellet was re-suspended in DPBS and counted as described in Section 2.2.1.3. $4x10^7$ parasites were taken from suspension and washed once using the same centrifugation parameters. Then, final pellet was re-suspended in ice-cold 400 μl of electroporation buffer (Appendix B).

10 μg linearized expression plasmid was transferred onto parasites in electroporation buffer and mixture was kept on ice. DNA-parasite mixture was transferred to Gene Pulser electroporation cuvettes with 0.2 cm gap (Biorad, U.S.A.). Samples were pulsed for 30 seconds on the Gene Pulser® II Electroporation System (Biorad, U.S.A.) using the following parameters: 750 V (3750V/cm), 25 μF and 200 Ω. Pulsing was repeated twice using identical parameters and with 30 second breaks between pulses. Electroporated samples were incubated on ice for 10 minutes. After incubation, parasites were transferred to a T25 plug seal tissue culture flask filled with pre-warmed (25°C) 4 ml Leishmania growth medium. Parasites were allowed to rest for 24 hours.

Following a successful transfection, the linearized expression plasmid inserts itself into the 18S rRNA locus as depicted in Figure 2.4. This insertion enables constitutive expression of EGFP-LUC fusion protein.
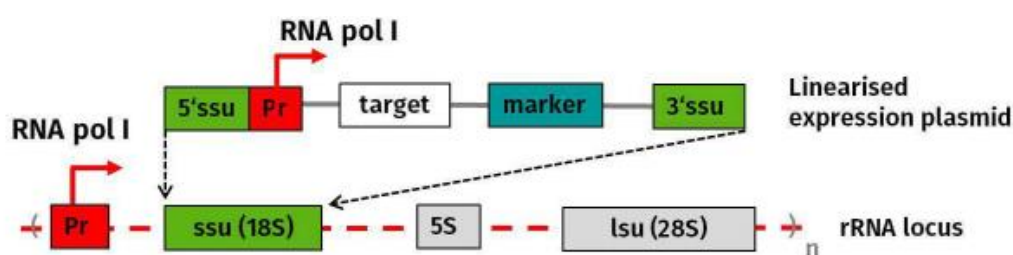
Figure 2.4. Schematic Depiction of Linearized Expression Plasmid Insertion Site

2.2.7.3. **Selection of Transgenic Parasites and Confirmation of EGFP Expression**

Following the 24 hours of recovery process, LEXSY-neo antibiotic (Jena Biosciences, Germany) was added into culture medium to select transgenic parasites at a final concentration of 50 µg/ml. Parasites were monitored microscopically on a daily basis. When significant amount of green fluorescent parasites were observed under a fluorescence microscope (~5-10 days), EGFP$^+$ parasites were counted as described in Section 2.2.1.3.

EGFP expression was confirmed by both fluorescence microscopic imaging and flow cytometry analysis as described in Section 2.2.6.6 and 2.2.1.3., respectively.

2.2.7.4. **Confirmation of Luciferase (LUC) Expression of Selected Transgenic Parasites**

1.9 ml of wash buffer was added into wells of 6 well plate. 100 µl solution containing 9×10^6 wild type parasites were added to one well as negative control. 100 µl suspensions containing 1×10^6, 3×10^6 and 9×10^6 transgenic parasites were added to separate wells. 10 µl D-Luciferin (30 mg/ml) (Perkin Elmer, U.S.A.) was added into each well (150 µg/ml final concentration). All wells were mixed by pipetting and the plate was incubated at RT for 10 minutes.

Transgenic parasites were scanned on IVIS Lumina III (Perkin Elmer, U.S.A.) following the manufacturer`s instructions. Briefly, field of view was set to 'A' and the plate was centered and zoomed. Then, luminescence signals were collected using 10 minutes exposure time for 30 minutes. Peak luminescence values were recorded.

2.2.7.5. Infection of Bone Marrow Derived Macrophages with Transgenic Parasites in the Presence of kDNA and gDNA

Bone marrow macrophages (BMDMs) were generated as described in Section 2.2.5.2. BMDMs were infected with transgenic parasites as previously described in Section 2.2.6.3. Differently, cells were stimulated with kDNA and gDNA at final concentrations of 0.5 µg/ml and 2 µg/ml. Infection rates of BMDMs were assessed as described in Section 2.2.6.5.

2.2.8. Chemical Inactivation of gp63 Metalloprotease

2.2.8.1. H_2O_2 Treatment of Parasites and Exosomes

Exosome samples (30 µg) and metacyclic parasites (60×10^6) were treated with molecular biology grade H_2O_2 solution (Sigma Aldrich, Germany) at final concentrations of 0.98M (3%) and 2.94M (9%), respectively. Samples were incubated at RT for 3 hours. H_2O_2 treated samples were used immediately for downstream experiments.

2.2.8.2. Assessment of Enzymatic Activity of gp63 by Gelatin Zymography

Separating gel (7.5% acrylamide) containing 7.5% gelatin (Merck, Germany) (Appendix B) and stacking gel (4% acrylamide) (Appendix B) were freshly prepared. Polyacrylamide gel was cast using 1.0 mm thick gel plates of Mini-PROTEAN II electrophoresis cell system (Biorad, Germany).

Whole cell lysates from H_2O_2 treated and untreated parasites were prepared as described in Section 2.2.2.3. All samples were mixed with 5X non-reducing sample buffer (Appendix B) before loading.

H_2O_2 treated and untreated samples with approximately 8 μg protein content were loaded to each well. PageRuler prestained protein ladder (Thermo Fisher Scientific, U.S.A.) was loaded to one of the wells for size determination. In addition, 8μg protein sample with no enzymatic activity was loaded to one of the wells as negative control. Loaded samples were run at 150 Volts until bands of the ladder is fully separated (2-3 hours).

Following completion of electrophoresis, the gel was incubated in washing solution (Appendix B) for 30 minutes. Wash step was repeated once more with fresh washing solution. Then, the gel was incubated in incubation buffer (Appendix B) for 5-10 minutes with constant agitation. Then, the gel was incubated in incubation buffer at 37°C for 24 hours for establishment of the gp63 enzymatic activity.

After 24 hours of incubation, the gel was incubated in staining solution (Appendix B) for 30-45 minutes at RT, and then rinsed with dH_2O to get rid of excess staining solution. Gel was incubated in destaining solution until white zones appeared at the expected gp63-associated location.

Since the gel contained gelatin, all gel is expected to be stained with a blue background. If gelatin was degraded by metalloproteases at specific sites, white zones appeared, attesting to the presence of active enzyme.

Following the completion of destaining, the gel was imaged by using the ChemiDoc™ Imaging System (Biorad, U.S.A.).

2.2.8.3. **Decomposition of H_2O_2 by Catalase Treatment**

Following inactivation of gp63 as described in Section 2.2.8.1., residual H_2O_2 in samples was decomposed by catalase (Sigma-Aldrich, Germany) treatment. For

decomposition, different amounts of catalase was added onto H_2O_2 treated samples: 9, 18 or 36 U. Samples were incubated for 1 hour at RT. During incubation, tube caps were placed loosely to enable gas outlet.

2.2.8.4. **Quantification of H_2O_2 concentration After Catalase Treatment**

Remaining H_2O_2 concentration in sample tubes were measured using colorimetric peroxide assay kit (Sigma-Aldrich, Germany) following instructions provided by the manufacturer. Briefly, eight standard samples were prepared between 0 and 30 µM H_2O_2 concentrations. Detection reagent was prepared by mixing reagent A and B at 1:100 ratio. 40 µl standard and unknown samples were distributed to a 96 well plate. 200 µl detection reagent was added onto each sample and mixed by pipetting. Plate was incubated for 30 minutes at RT. Following incubation, plate was read at 585 nm on a Multiskan™ GO Microplate Spectrophotometer (Thermo Fisher Scientific, U.S.A.). Background values obtained from assay blanks were subtracted from readings and four parametric logistic standard curve was constructed using the Skan It software (v.5.01). Concentration of unknown samples were determined based on this curve.

2.2.9. **Methods for *in vivo* Experiments**

2.2.9.1. **Animals**

6-10 weeks old, adult male or female BALB/c mice were used for *in vivo* experiments. All animals used in this study were maintained at Animal Facility of Molecular Biology and Genetics Department at Bilkent University (Ankara, Turkey) under controlled conditions. Animals were kept in special rooms where temperature was set to 22°C ± 2 and light/dark cycles were arranged as 12 hours. Animals were fed *ad libitum* and kept in filtered cages. Routine controls of mice were done by Gamze Aykut, DVM.

All animal protocols carried out in this study was approved by animal ethical committee of Bilkent University.

2.2.9.2. **Footpad Injection for Leishmania Challenge**

Metacyclic parasites were prepared at a concentration of 2×10^8 parasites/ml in DPBS as described in Section 2.2.1.6. and 2.2.1.7. In order to challenge mouse with *L.major*, 50 µl metacyclic parasite solution (10×10^6 parasites/mouse) was injected to of the left footpads of mice by using a 1 ml syringe with 26G needle (Ayset, Turkey). Injection process is illustrated in Figure 2.5.

Figure 2.5. Footpad Injection for Parasite Challenge

2.2.9.3. **Monitoring Lesion Size**

In order to monitor lesion size, footpads of mice were measured after parasite challenge by using a digital caliper. Two measurements were taken from each foot: width and depth of footpad. These two measurements were multiplied to approximate size of lesion. Measurements taken at first week with no lesion development and/or measurements of unchallenged feet were considered as baseline for comparisons. In

order to minimize human error, all measurements in the same experimental set were taken by the same person.

2.2.9.4. **Tail Bleeding for Sera Collection**

At designated time points, which will be specified for each experiment, blood of animals were collected by tail bleeding method. Animals were first put under a heating lamp for up to 5 minutes and constantly monitored during the process. Heating up leads to dilation of blood vessels so that they are observable during the process. Then, mice were placed into strainer where tail is exposed at the bottom. Tails were sterilized with 70% ethanol and location of tail vein was detected visually. Small cut was introduced at tail vein by using a sterile razor blade. 100 – 200 µl of blood from each animal was collected into sterile glass test tubes to enable coagulation.

Collected blood was incubated in glass test tubes at a slanted position for 2-3 hours. Sera were collected from top by pipetting gently. In order to eliminate small amount of cells from this collection, samples were centrifuged at 8,000g for 5 minutes. Following centrifugation, supernatants were transferred to 96 well plates. Sera were stored at -20°C until use.

2.2.9.5. **Detection of SLA Specific IgG1 and IgG2a Levels by ELISA**

Soluble Leishmania Antigen (SLA) specific IgG1 and IgG2a antibody levels in immunized mice were quantified by ELISA. 50 µl SLA (10 µg/ml) in Coating Buffer (Appendix B) was added to wells of Immulon 1B Plates (Thermo Fisher Scientific, U.S.A.). Plates were incubated overnight at 4°C for coating. After incubation, wells were emptied by flicking. 200 µl Blocking Buffer (Appendix B) was added into each well and plates were incubated at RT for 2-3 hours. Following blocking step, plates were flicked and soaked into Wash Buffer (Appendix B). Plates filled with wash buffer were incubated for 5 minutes at RT. Washing step was repeated 5 times. Plates

were rinsed with dH_2O thrice and dried. 100 µl collected sera (Section 2.2.9.4) 1:200 diluted in PBS were added to 'A' rows of plates and 50 µl PBS was added to other rows. Sera in 'A' row was serially diluted for up to row 'H' to obtain 8 different dilutions (1:200 - 1:25,600). Plates were incubated at 4°C overnight. After incubation, washing, rinsing and drying steps were repeated as previously mentioned. 50 µl 1:2000 diluted goat anti-mouse IgG1-AP or IgG2a-AP (Southern Biotech, U.S.A.) antibody solution was added into wells. Plates were incubated for 2 hours at RT and washing, rinsing and drying steps were repeated once more. 50 µl PNPP substrate solution was added into wells and plates were read at 405 nm on a Multiskan™ GO Microplate Spectrophotometer (Thermo Fisher Scientific, U.S.A.) every hour until saturation point was reached (2-8 hours).

Antibody titers were calculated by using analysis of dose-response curves package (Ritz, Baty, Streibig, & Gerhard, 2015) in 'R' (v.3.3.3) (Core Team, 2008). OD readings of unvaccinated groups was determined as background/undetectable level. Mean of all unvaccinated readings + 1.5 times standard deviation of all vaccinated readings was determined as threshold value. For every mouse, four parametric logistic regression curves were constructed for dilutions vs OD readings. Then, dilutions in which OD readings reached the threshold value were calculated by fitting threshold value into these curves. The dilutions calculated were recorded as antibody titers. To exemplify, if OD value of a mouse reached a threshold value at 1:1,250 dilution, it means that original sample contains 1,250 titer of antibody in arbitrary units.

2.2.9.6. **Detection of Th1/Th2/Th17 Cytokine Levels from SLA Pulsed Splenocytes**

When an *in vivo* experiment was terminated, spleens were collected from sacrificed animals and single cell suspensions were prepared as described in 2.2.5.3. 100 µl splenocyte suspension (10^7 cells/ml) was added into wells of a 96 well plate. SLA was diluted in 10% Regular RPMI Medium to a concentration of 100 µg/ml. 100 µl diluted

SLA sample was added onto cells for stimulation. In addition, 100 µl 10% Regular RPMI Medium was added onto replicates of identical samples as unstimulated controls. Plates were incubated at 37°C with 5% CO_2 for 48 hours. After incubation, plates were centrifuged at 300g for 10 minutes at RT. Resulting supernatants were collected and stored at -20°C for cytometric bead array (CBA) assay.

Cytokine responses of stimulated and unstimulated splenocytes were assessed using the mouse Th1/Th2/Th17 cytometric bead array (CBA) kit (Becton, Dickinson, U.S.A.) following the instructions provided by the manufacturer with modifications. There are seven different types of beads in the CBA assay with different far-red fluorescent intensities. These intensity differences are used to cluster beads in the far-red channel of the flow cytometer to form an array. Each of these populations are coated with unique antibodies specific to IL2, IL-4, IL-6, IFN-γ, TNF-α, IL-17A and IL-10. These cytokines were listed in the order from the brightest to the dimmest bead population based on their fluorescence on the far-red channel. Considering these specifications, CBA assay enables quantification of seven different cytokines from a small amount of sample at the same time. In other words, performing a CBA assay is equivalent to performing seven different ELISA assays. In addition, detection limit of CBA is much lower than ELISA.

To perform the assay, lyophilized cytokine standards were reconstituted at a concentration of 625 pg/ml and two fold serially diluted up to 1:256 dilution. Then, 10 µl capture beads for each cytokine was pooled and mixed well. 50 µl bead mixture was added into wells of 'U' bottom 96 well plate (Sarstedt, Germany). 50 µl standards or supernatants of splenocytes were added onto beads. At last, 50 µl PE detection reagent was added onto sample bead mixture. Plates were incubated at RT for 2 hours. Following incubation, 100 µl wash buffer was added and plates were centrifuged at 200g for 5 minutes at RT to sediment beads. Supernatant was discarded and wash step was repeated with 200 µl wash buffer. Final bead pellet was re-suspended in 200 µl wash buffer and acquired on a Novocyte 2060R flow cytometer (ACEA Biosciences, U.S.A.).

For analysis, flow cytometry readings were imported to FCAP Array software v.3 (Becton, Dickinson, U.S.A.). First beads were selected based on FSC and SSC parameters and bead library file that belonged to mouse Th1/Th2/Th17 kit was selected. Then, beads were clustered based on their intensities at APC (far-red) channel. PE channel was selected as reporter parameter and five parametric logistic regression curves were generated based on fluorescent intensities of each clustered bead population. Amount of each cytokine in samples was calculated by fitting readings of unknown samples to corresponding standard curves.

2.2.9.7. Assessment of Parasite Loads from Footpad and Lymph Nodes of Mice by using *in vivo* Imaging System (IVIS)

Before starting imaging, FOV24 lens attachment of device was installed and FOV setting was set to 'E' to extend field of view. Then, camera temperature was set to -90 °C and base temperature was set to 37 °C.

For footpad imaging, five mice were processed simultaneously. First, mice were anesthetized under Isoflurane Vaporizer (VetEquip, U.S.A.). Anesthetized mice were injected with D-Luciferin (0.75 mg/mouse) (Perkin Elmer, U.S.A.) intraperitoneally transferred to IVIS Lumina III (Perkin Elmer, U.S.A.) cabinet and kept under anesthesia during imaging via the integrated gas anesthesia unit.

Luminescence protocol was selected and a sequence was generated with 30 seconds exposure time for a total duration of 20 minutes (40 images in total). Region of interests (ROIs) were selected based on positions of parasite-infected feet and luminescence readings were recorded for each time point.

Then, animals were sacrificed and popliteal lymph nodes were collected for imaging at IVIS. An example of the inguinal lymph node collection process is illustrated in Figure 2.6. Lymph nodes were placed into wells of a black 96 well plate (Corning, U.S.A) and wells were filled with wash medium. D-Luciferin (150 µg/ml) was added

onto lymph nodes at the same time to start the reaction simultaneously for all of the samples. FOV24 lens attachment was detached from the device and plate was placed into IVIS Lumina III. FOV setting was adjusted to 'A' and luminesce readings were recorded as specified for footpad imaging by selecting each well as region of interests (ROIs).

Figure 2.6. Collected Lymph Node for IVIS Imaging

For each luminescence reading, an enzymatic curve was constructed and peak points where reactions reached their maximum rates were used to estimate parasite loads.

2.2.10. *In vivo* Passaging of *L.major* in Mice

2.2.10.1. Isolation of Amastigotes from Footpad Lesions

Metacyclic parasites (10×10^6 parasites/mouse) were injected to footpad of mice as described in Section 2.2.9.2. Lesion development was monitored visually on a weekly basis. When lesions developed at a significant size, animals were sacrificed and feet with lesions were cut at ankle position with sterile scissors.

Removed feet were first immersed into 70% ethanol for sterilization. Each lesion was removed from the base of feet by using a clean razor blade. Excised footpads were

placed into gentleMACS C tubes (Miltenyi Biotec, Germany). 2ml of RPMI containing Collagenase IV (4 mg/ml) (Sigma-Aldrich, Germany), Hyaluronidase (2 mg/ml) (Sigma-Aldrich, Germany) and DNase I (100 Unit/ml) (Sigma-Aldrich, Germany) was added into the tube. Footpad was gently minced by using sterile scissors and incubated at 37°C for 1 hour. After incubation, 2ml null RPMI medium was added into the tube. Tube was attached to the sleeve of gentleMACS Dissociator (Miltenyi Biotec, Germany) at upside down position. Program B was initiated on the device. When the process was completed, tube contents were transferred to gentleMACS M tubes (Miltenyi Biotec, Germany) and the tube was attached back to the device as before. Program B was run once more. Resulting suspension was passed through MACS Smart Strainer (Miltenyi Biotec, Germany) with a 70 μm mesh size. The strainer was washed with 5 ml DPBS twice and the resultant filtered cell suspension was used for amastigote culture.

2.2.10.2. **Amastigote Culture**

NNN Modified Medium (HiMedia, India) was used to culture amastigotes. This medium was composed of solid blood agar (Part 'A'), overlaid by a liquid part (Part 'B').

In order to prepare Part 'A', 31 grams of powdered Part 'A' was dissolved in 1 liters of boiling distilled water and autoclaved at 121 °C for 15 minutes. After sterilization, medium was cooled to 45-50 °C and 10% (v/v) defibrinated blood (Rockland U.S.A) was added aseptically. Medium was mixed well and 20-25 ml of it was transferred to plug capped T75 tissue culture flasks (SPL, South Korea) at vertical position. Medium was allowed to solidify at RT and stored at 4°C for long-term use.

In order to prepare Part 'B', 11.2 grams of powdered Part 'B' was dissolved in 1 liters of boiling distilled water and sterilized as mentioned before. After sterilization, it was cooled to RT and stored at 4 °C for long-term use.

Filtered amastigote cell suspension obtained as described in Section 2.2.10.1. was centrifuged at 3,000 g for 10 minutes at RT. Pellet was re-suspended in 10 ml pre-warmed (26 °C) Part 'B' of NNN medium. Suspension was added to pre-warmed (26 °C) flask containing Part 'A' of NNN medium. Resulting amastigote growth medium is depicted in Figure 2.7. Amastigote culture was incubated at 26 °C and monitored microscopically for transmission to promastigotes on a daily basis.
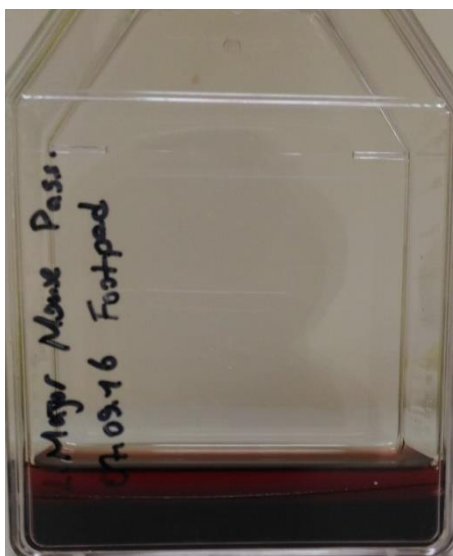
Figure 2.7. Amastigote Culture

When amastigotes transformed into promastigotes (4-7 days), liquid part of the medium was transferred to a 15 ml conical tube (SPL, South Korea) and centrifuged at 3,000g for 10 minutes at RT. Pellet was re-suspended in Leishmania growth medium for promastigote culture. After promastigotes proliferated, they were cryo-preserved for long-term storage as described in Section 2.2.1.5.

2.2.11. *In vivo* Immunization and Challenge Experiments

2.2.11.1. Challenge Experiment to Assess the Contribution of kDNA to Disease Progression

On day 0, metacylic parasites (10×10^6/mouse) were injected to footpad of 6-8 weeks old female BALB/c mice as described in Section 2.2.9.2. In addition, one group received kDNA (25 µg/mouse) intraperitoneally (ip). As a control group, PBS was injected intraperitoneally. PBS and kDNA injections were repeated twice on Days 3 and 6. Lesion development was monitored for 22 weeks to assess progression of infection as described in Section 2.2.9.3. Experimental schedule is given in Figure 2.8.
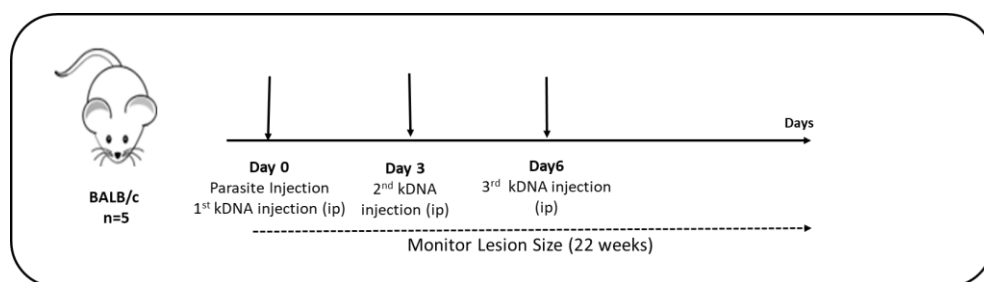
Figure 2.8. Experimental Schedule of Challenge Experiment to Assess the Contribution of kDNA to Disease Progression

2.2.11.2. Challenge Experiment for Confirmation of Virulence of *in vivo* Passaged Parasites

In order to confirm virulence of *in vivo* passaged *L.major* parasites, two BALB/c mice were challenged with the mouse isolate (*in vivo* passaged) or the human *L.major* isolate parasites. Mouse isolate parasites were obtained as described in Section 2.2.10. Metacyclic mouse isolate parasites (10×10^6/mouse) were injected to right footpad of mice as described in 2.2.9.2. Metacylic human isolate parasites (10×10^6/mouse) were injected to left footpad of the same mice. Lesion sizes were monitored for 5 weeks as described in Section 2.2.9.3.

2.2.11.3. **Vaccination Study and Challenge Experiments to Assess Adjuvant Activity of K type CpG-ODN and cGAMP**

In this study, Exosomes (Exo) and heat-killed parasites (HK) were used as such or combined with K-ODN+cGAMP as a vaccine adjuvant in immunization/vaccination. Experimental groups, antigen and adjuvant doses used in experiments are given in Table 2.3.

Table 2.3. *Experimental Groups with Doses of Antigens and Adjuvants* to Assess *the Adjuvant Activity of K-cGAMP*

Groups	Administrated Doses (per mouse)
PBS (Unvaccinated)	-
Exosomes	20 µg
Exosomes+K-ODN+cGAMP	20 µg + 15 µg + 15 µg
HK+ K-ODN+cGAMP	$5x10^6$+ 15 µg + 15 µg

6-8 weeks old, female BALB/c mice were injected subcutaneously with the formulations given in Table 2.3 on Days 0 and 14. Metacyclic mouse isolate parasites were injected to right footpad of mice as described in Section 2.2.9.2. Experimental schedule is given in Figure 2.9.
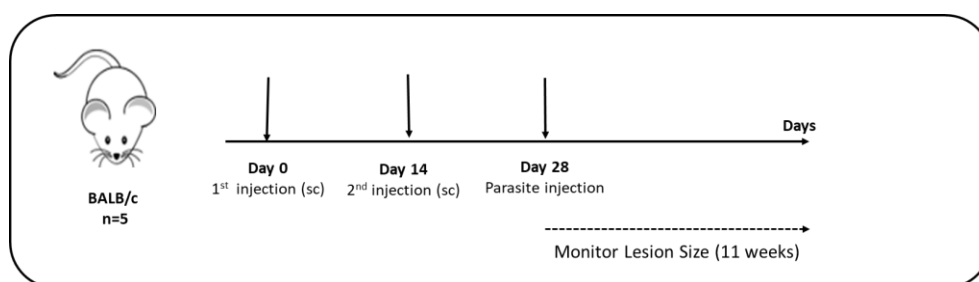
*Figure 2.9.*Experimental Schedule to Assess the Adjuvant Activity of K-cGAMP

2.2.11.4. **Immunization Experiment to Determine Potential Vaccination Formulation**

In this experiment, we have tested the potency of three different antigen sources as such or combined with three different adjuvants. All vaccination groups are listed in Table 2.4. together with the doses of corresponding antigen and/or adjuvant.

Table 2.4. *Experimental Groups with Doses to Assess the Optimal Antigen Adjuvant Combination*

Groups	Administrated Doses (per mouse)
PBS (Unvaccinated)	-
HK	$5x10^6$
HK + K-ODN	$5x10^6$ + 50 µg
HK + D-ODN	$5x10^6$ + 50 µg
HK + CpG Nano-ring (NR)	$5x10^6$ + (30 µg K-ODN+189 µg Tat peptide)
SLA	40 µg
SLA + K-ODN	40 µg + 50 µg
SLA + D-ODN	40 µg + 50 µg
SLA + NR	40 µg + (30 µg K-ODN+189 µg Tat peptide)
Exosomes	40 µg
Exosomes + K-ODN	40 µg + 50 µg
Exosomes + D-ODN	40 µg + 50 µg
Exosomes + NR	40 µg + (30 µg K-ODN+189 µg Tat peptide)

6-10 weeks old male BALB/c mice were injected subcutaneously with the vaccination formulations given in Table 2.4. on Days 0 and 14. On Day 21, blood was collected as described in Section 2.2.9.4 and SLA specific antibody levels were quantified as previously described in Section 2.2.9.5. After blood collection, animals were sacrificed and spleens were collected. Cytokine responses specific to SLA were measured as described in Section 2.2.9.6. Experimental schedule for the experiment is given in Figure 2.10.
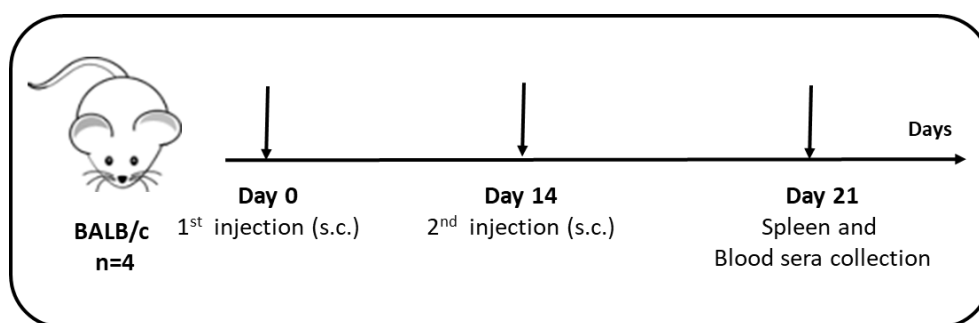
Figure 2.10. Experimental Schedule to Determinate Immunogenicity of the Vaccine Formulations

2.2.11.5. **Optimization of *in vivo* Imaging of EGFP-LUC Transgenic Leishmania Parasite in Live Mice**

Transgenic parasites were tested *in vivo* to assess whether they could be used in direct quantification of parasite loads, or not. For this, 1×10^6, 3×10^6 and 9×10^6 metacyclic transgenic parasites were injected to right footpads of 8 weeks old male BALB/c mice as described in 2.2.9.2. As a negative control, right footpad of one mouse was injected with non-transgenic metacyclic parasites. Mice were anesthetized and imaged using IVIS as previously described in Section 2.2.9.7. Device and assay parameters were optimized for future experiments. In addition, presence of correlation between injected parasite numbers vs luminescence signal was verified.

2.2.11.6. **Immunization and Challenge Experiment using Hydrogen Peroxide / Catalase Inactivated Vaccination Formulations**

For this experiment, some of vaccine antigens were inactivated with H_2O_2 as described in Section 2.2.8.1. and residual H_2O_2 was decomposed with catalase as described in 2.2.8.3. Vaccination groups, antigen and adjuvant doses are summarized in Table 2.5.

Table 2.5. *Experimental Groups, Antigen and Adjuvant Doses of Hydrogen Peroxide / Catalase Inactivated Vaccine Formulations*

Groups	Administered Doses (per mouse)
PBS (Unvaccinated)	-
Exosomes + D-ODN	40 µg + 50 µg
Exosomes-H_2O_2	40 µg inactivated with 0.98M H_2O_2
Exosomes-H_2O_2 + D-ODN	40 µg inactivated with 0.98M H_2O_2 + 50 µg
SLA-H_2O_2	40 µg inactivated with 0.98M H_2O_2
SLA-H_2O_2 + D-ODN	40 µg inactivated with 0.98M H_2O_2 + 50 µg

6-10 weeks old, female mice were injected subcutaneously with vaccination formulations given in Table 2.5. on Days 0 and 14. On Day 21, blood was collected as described in Section 2.2.9.4 and SLA specific antibody levels were quantified as previously described in Section 2.2.9.5. On Day 22, mice were challenged with transgenic metacyclic parasites ($9x10^6$/mouse) as explained in Section 2.2.9.2. Lesion sizes were monitored for 4 weeks as described in Section 2.2.9.3. On Day 50, parasite loads of infected feet were assessed by using *in vivo* Imaging System (IVIS) as described in Section 2.2.9.7. After IVIS procedure, animals were sacrificed and spleens were collected to measure cytokine responses specific to SLA as described in Section 2.2.9.6. In addition, IVIS procedure was performed for popliteal lymph nodes as described in Section 2.2.9.6. Experimental schedule is given in Figure 2.11.
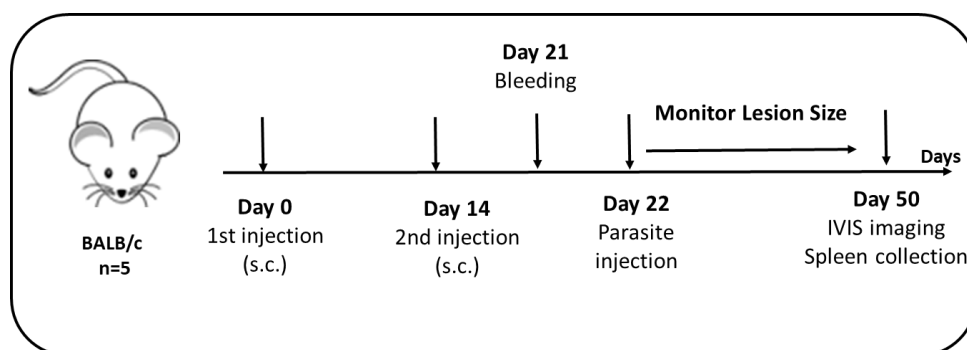
Figure 2.11. Experimental Schedule to Assess the Immunoprotective Activity of Hydrogen Peroxide / Catalase Inactivated Vaccine Formulations

2.2.11.7. **Immunotherapy Experiment with Hydrogen Peroxide / Lyophilization Inactivated Vaccine Formulations**

For this experiment, some of the immunotherapeutic formulations were inactivated with H_2O_2 as described in Section 2.2.8.1. Instead of catalase decomposition, all formulations were lyophilized to eliminate residual H_2O_2. Following H_2O_2 inactivation, formulations were snap-frozen in liquid nitrogen and lyophilized (freeze-dried) by using Virtis freeze-dryer (SP Scientific, U.S.A.) overnight.

Lyophilized formulations were re-hydrated just before injection. For groups where loading of adjuvant was aimed controlled hydration protocol was applied. Briefly, powdered material was re-suspended in 10-15% of original volume and mixed by vortexing. Following repeated mixing every 3 minutes for a total of 24 minutes, samples were incubated at RT for 30 minutes. After incubation, volumes were completed to their original volume by adding required amount of DPBS.

Experimental groups, antigen adjuvant doses are given in Table 2.6.

Table 2.6. *Experimental Groups, Antigen and Adjuvant Doses of Hydrogen Peroxide / Lyophilization Inactivated Immunotherapeutic Formulations*

Groups	Administered Doses (per mouse)
PBS (Unvaccinated)	-
Exosomes + D-ODN	40 µg + 50 µg
Exosomes-H_2O_2 + D-ODN	40 µg inactivated with 0.98M H_2O_2 + 50 µg
SLA-H_2O_2 + D-ODN	40 µg inactivated with 0.98M H_2O_2 + 50 µg

9×10^6 metacylic transgenic parasites were injected to right footpad of 6-8 weeks old female BALB/c mice as described in Section 2.2.9.2. Lesions size was monitored as described in Section 2.2.9.3. When significant lesion formation was observed (Day 20), footpads were imaged by IVIS as described in section 2.2.9.7. On Day 21, therapeutic formulations listed in Table 2.6. were injected subcutaneously. Therapeutic injection was repeated on Day 24. IVIS Imaging procedure was repeated

on Days 26 and 31 to follow the effect of immunotherapy on the progression of the disease. Experimental schedule is given in Figure 2.12.
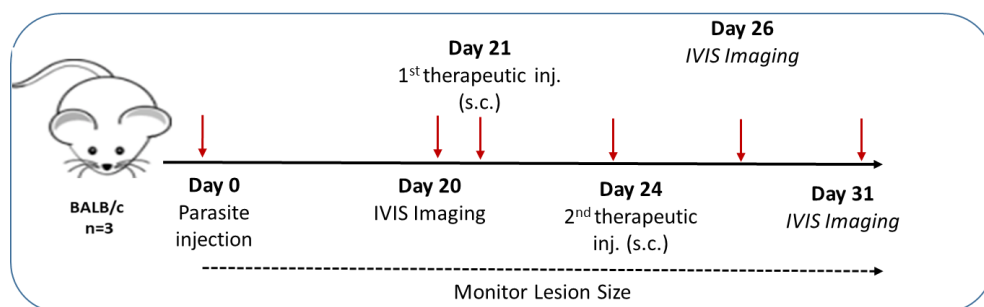
Figure 2.12. Experimental Schedule to Assess the Immunotherapeutic Activity of Hydrogen Peroxide / Lyophilization Inactivated Formulations

2.2.11.8. **Immunization and Challenge Experiment with Hydrogen Peroxide / Lyophilization Inactivated Vaccine Formulations**

In this experiment, some vaccination formulations were inactivated with H_2O_2 as described in Section 2.2.8.1. In order to eliminate residual H_2O_2 lyophilization method was used as described in Section 2.2.11.7. Independent from inactivation process, all vaccination groups were lyophilized and re-hydrated prior to injections for experimental consistency.

In order to check if there was any effect of lyophilization on parasites, H_2O_2 treated and untreated parasites were analyzed before and after lyophilization as following: For integrity of gp63, flow cytometric analysis was performed as described in Section 2.2.4.1, for enzymatic activity of gp63 gelatin zymography method was performed as described in Section 2.2.8.2.

Experimental group, antigens and adjuvant doses are given in Table 2.7.

68

Table 2.7. *Experimental Groups, Antigen and Adjuvant Doses of Hydrogen Peroxide / Lyophilization Inactivated Vaccine Formulations*

Groups	Administered Doses (per mouse)
PBS (Unvaccinated)	-
Lyophilized Parasites	5×10^6
H_2O_2 killed Parasites	5×10^6 inactivated with 2.94M H_2O_2
H_2O_2 killed Parasites + D35	5×10^6 inactivated with 2.94M H_2O_2 + 50 µg
Exosomes	30 µg
Exosomes + D-ODN	30 µg + 50 µg
Exosomes-H_2O_2	30 µg inactivated with 0.98M H_2O_2
Exosomes-H_2O_2 + D-ODN	30 µg inactivated with 0.98M H_2O_2 + 50 µg
SLA	30 µg
SLA-H_2O_2	30 µg inactivated with 0.98M H_2O_2
SLA-H_2O_2 + D-ODN	30 µg inactivated with 0.98M H_2O_2 + 50 µg
Exosomes + αGalCer	30 µg + 0.06 µg
Exosomes-H_2O_2 + αGalCer	30 µg inactivated with 0.98M H_2O_2 + 0.06 µg

6-10 weeks old, male mice were injected subcutaneously with vaccine formulations summarized in Table 2.7. on Days 0 and 14. On Day 21, blood was collected as described in Section 2.2.9.4 and SLA specific antibody levels were quantified as previously described in Section 2.2.9.5. On Day 25, mice were challenged with transgenic metacyclic parasites (9×10^6/mouse) as explained in Section 2.2.9.2. Lesion sizes were monitored for 5 weeks as described in Section 2.2.9.3 On Day 60 parasite loads of infected feet were assessed by using *in vivo* Imaging System (IVIS) as described in Section 2.2.9.7. After IVIS procedure, animals were sacrificed and spleens were collected to measure cytokine responses specific to SLA as described in Section 2.2.9.6. In addition, IVIS procedure was performed for popliteal lymph nodes as described in Section 2.2.9.6. Experimental schedule is summarized in Figure 2.13.
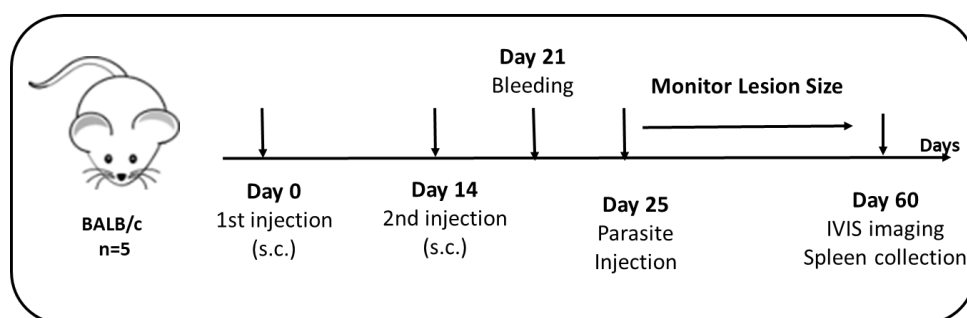
Figure 2.13. Experimental Schedule to Assess the Immunoprotective Activity of Hydrogen Peroxide / Lyophilization Inactivated Vaccine Formulations

2.2.12. **Statistical Analyses**

For comparison of two group means, Mann-Whitney Unpaired Test was applied. In order to compare multiple groups at once, Kruskal-Wallis test followed by Dunnet`s or Conover`s multiple comparison test was performed. For all statistical comparisons $p < 0.05$ was designated as significance level. In addition, exact p-values or ranges obtained for each test are specified in corresponding figure legends throughout the Chapter 3.

Graphical presentations and statistical tests were performed by using 'R' (v.3.3.3) (Core Team, 2008) and GraphPad Prism (v.6) (GraphPad, U.S.A.).

CHAPTER 3

RESULTS & DISCUSSION

3.1. Assessment of Growth Kinetics of *L. major* Parasites

Determination of *in vitro* growth phase of parasites is pivotal for infectivity and reproducibility of cellular component purifications. For isolation of cellular components of Leishmania, late-log parasites are used. For *in vitro* infection assays and *in vivo* challenge experiments, metacylic parasites are prepared through incubation in stationary phase for 1-2 days. Furthermore, determination of growth kinetic is important for maintenance and cryopreservation purposes.

To assess the time interval of entry into stationary phase, *L.major* parasites were inoculated at a concentration of 2.5×10^6 parasites/ml and parasite counts were recorded on a daily basis for a period of 10 days.
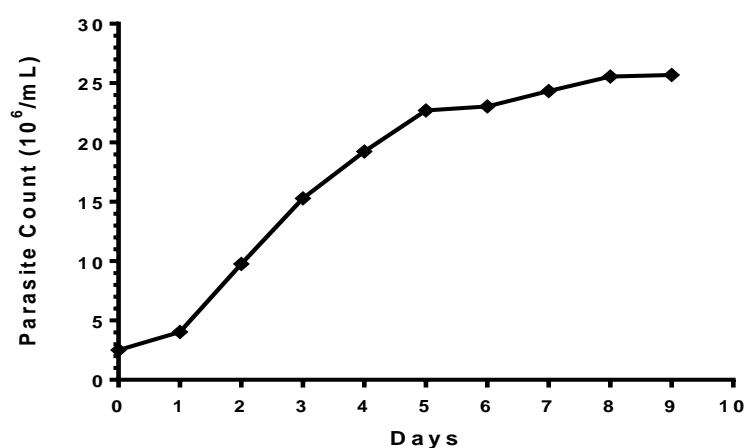
Figure 3.1. L.major Growth Curve

Parasite culture was grown at 26°C and was counted on a daily basis for 10 days in order to monitor the growth of parasites.

71

As can be inferred from Figure 3.1., parasites reached stationary phase (~25x10^6 parasites/ml) on day 6 of culture. Late-log phase was specified as parasite concentration of 20-25x10^6 parasites/ml and used as the reference point for soluble leishmania antigen and/or exosome isolation procedures. For cryopreservation, mid-log phase correspond to ~15x10^6 parasites/ml and stabilates were prepared using this cell density. For maintenance of *in vitro* cultures, parasites were diluted to 5-8x10^6 parasites/ml before entry into stationary phase and passaged every 3 days. Should the parasites reach stationary phase, they transform into metacylic promastigote form and cease replication (Gossage, Rogers, & Bates, 2003). For that reason, parasites were not allowed to reach stationary phase unless they were required for *in vitro* infection and/or *in vivo* challenge experiments, where metacyclic promastigotes were used. For infection/challenge experiments, required amount of parasites was maintained in a separate culture flask and was incubated at stationary phase for 1-2 days to obtain metacylic promastigotes.

3.2. Enrichment of Metacyclic Parasites

Metacylic promastigotes are more virulent than procyclic parasites. (David L. Sacks & Perkins, 1984). For this reason, metacylic parasites were used for all *in vitro* infection and challenge experiments in this study.

In *in vitro* cultures, parasites transform into metacyclic form when incubated in stationary phase but this transformation is not 100% efficient (David L. Sacks & Perkins, 1984). Metacyclic parasites in stationary phase cultures can be further enriched using peanut agglutinin (PNA). PNA can only bind to lipophosphoglycan (LPG) of procyclic parasites. The binding of PNA to metacyclic parasites is not possible due to structural changes in LPG. Using this LPG difference, metacylic parasites can be purified by negative selection (D. L. Sacks & Perkins, 1985). However, this method is not applicable to all Leishmania species. Furthermore, it is laborious and sometimes works with poor efficiency (Spath et al., 2000).

Instead of using PNA, metacyclic parasites were purified by Ficoll density gradient in this study. This method is much easier to perform and less expensive than PNA negative selection. Ficoll density gradient method relies on morphological changes in metacyclic parasites. Since metacyclic parasites are thin and elongated with a long flagellum more than twice the body size, they show different sedimentation rates (Späth & Beverley, 2001).

Parasites that were incubated at stationary phase for 2 days were subjected to Ficoll density gradient. Purified parasites were counted microscopically based on their morphology. In order to show the efficacy of the method, counting was also performed for non-purified stationary phase and log-phase parasites. Percent of metacylic parasites were calculated based on counts.
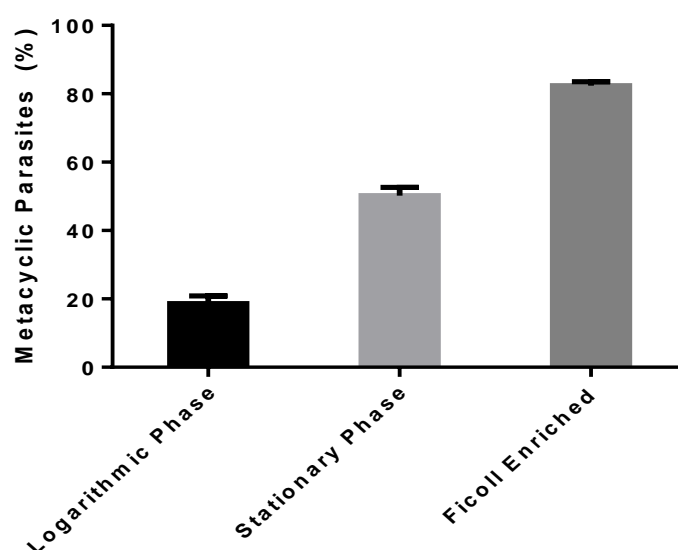
Figure 3.2. Enrichment of Metacyclic Parasites by Ficoll Density Gradient Centrifugation

Parasites incubated at stationary phase for 2 days were subjected to ficoll density gradient centrifugation. Metacyclic parasites from log-phase, stationary phase and ficoll enriched fraction was counted microscopically. Three independent counts from each group were used to the construct the graph.

As expected, only ~20% of log-phase parasites are metacyclic (Figure 3.2.). Percentage of metacyclics increased to around 50% when parasites were incubated at stationary phase. This percentage was further improved to more than 80% following Ficoll enrichment of parasites. This finding proves that the enrichment method was effective and therefore adopted for all *in vitro* and *in vivo* challenge experiments.

3.3. Evaluation of the Effect of Kinetoplast DNA (kDNA) on Leishmania Infection

3.3.1. kDNA Isolation from *L. major*

Detection of pathogen-derived nucleic acids through pattern recognition receptors of the innate immune cells evolved as an essential strategy for host innate immune defense. Evidence suggests that parasite kDNA persists in tissues of Chagas patients and presence of kDNA correlates with inflammatory cell infiltration (Zhang & Tarleton, 1999). Based on this observation, it is likely that kDNA-induced immune recognition might modulate the immune response against the parasite. Therefore, to assess whether Leishmania kDNA itself contributes to disease progression, we first isolated kDNA from the parasites. For this, kDNA was purified as described in Section 2.2.2.1.

Isolated *L. major* kDNA was analyzed for possible contaminations by genomic DNA (gDNA) and/or RNA using agarose gel electrophoresis. kDNA isolates were treated with DNase I and RNase A to determine which bands/smears correspond to DNA or RNA. Furthermore, one of the isolates were treated with plasmid safe DNase (Exonuclease V), which degrades linear but not circular DNA, to detect possible gDNA contamination. Following enzymatic treatment, samples were run on agarose gel to evaluate the effect of different treatments on kDNA isolates.

Since kDNA is a huge network, it was expected to remain in the wells of the gel. Possible gDNA contamination was expected to be observed as a sharp band more than

10 kbp in size and possible RNA contamination was expected be observed as a smear less than 1kbp in size.
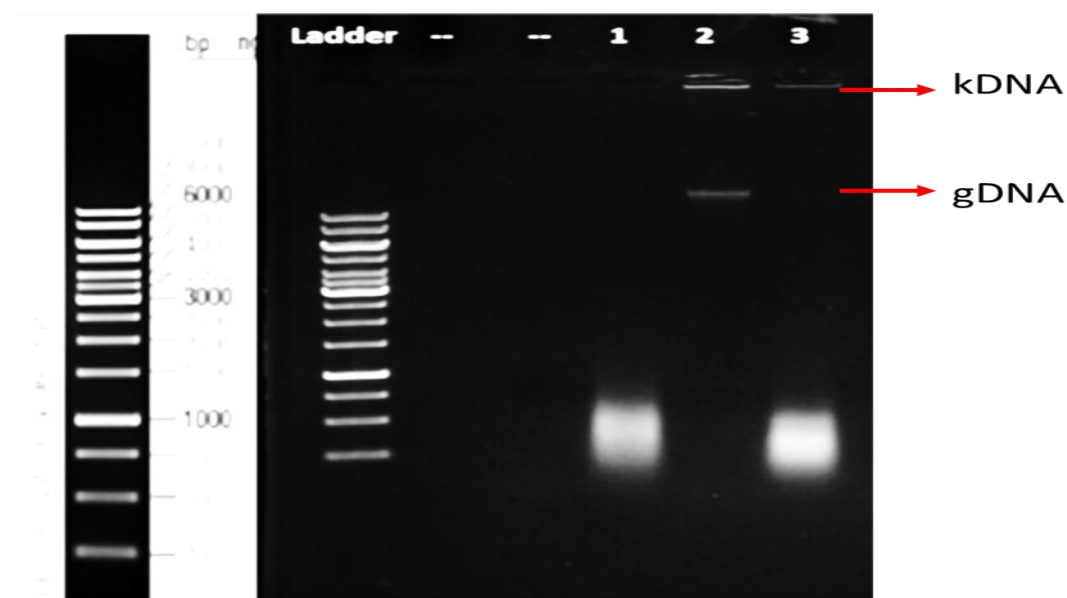
Figure 3.3. Effects of RNase and Plasmid Safe DNase Treatment on kDNA Isolates

kDNA isolates were treated with DNase I (1 Unit/10 µg kDNA), RNase A (1mg/ml) or Plasmid-safe DNase (10 Unit/Isolate). 5 µg of treated kDNA isolates were loaded to each well of 0.7% (w/v) agarose gel. The gel was run at 100 V for 90 minutes and visualized under UV light.

Lane 1: DNase I treated, Lane 2: RNase A treated, Lane 3: Plasmid-safe DNase treated kDNA isolates.

In kDNA isolates treated with DNase I (Lane 1), a smear below 1kbp was observed (Figure 3.3.). In RNase A treated samples, (Lane 2), this smear disappeared, leaving behind and two DNA- associated bands. One of these bands remained within the well, while the other one was located above the 10 kbp band of the DNA ladder, corresponding to kDNA and gDNA, respectively. Since these two bands were not observed in DNase treated sample, their identities were consistent with DNA. Furthermore, elimination of the smear at the second but not in the first well indicated RNA contamination of kDNA isolates.

Plasmid safe DNase treatment effectively removed DNA band corresponding to gDNA, leaving the kDNA inside the well, intact. This observation shows that, there was gDNA contamination in kDNA isolates which was eliminated with plasmid-safe DNase treatment.

Since there were both gDNA and RNA contamination in our kDNA isolates, RNase A and plasmid-safe DNase treatments were integrated into the kDNA isolation protocol to obtain highly purified kDNA. All experiments, which include kDNA in this study were conducted with such purified kDNA isolates.

3.3.2. **Structural Confirmation of Isolated kDNA networks**

Following enzymatic purification, isolated kDNA networks were analyzed using fluorescence and atomic force microscopic (AFM). For fluorescence microscopy analysis, isolates were stained with DAPI to observe clustered kDNA networks. Furthermore, purified kDNA networks were imaged using AFM for topological and conformational analysis.
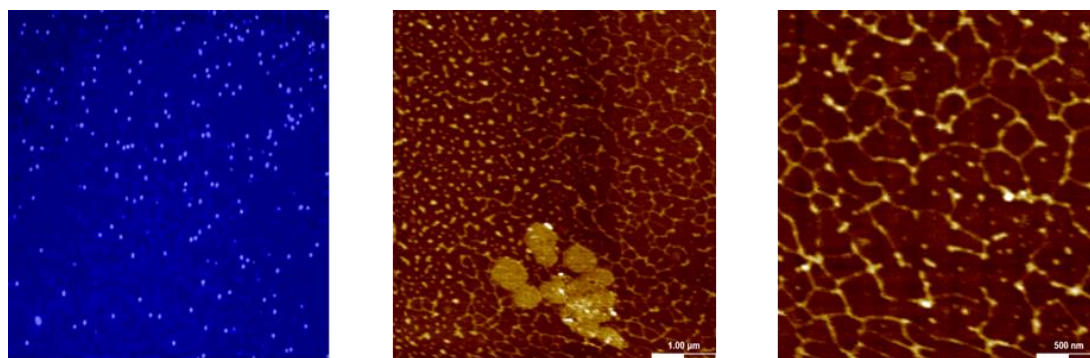
Figure 3.4. Fluorescence and Atomic Force Microscopy Images of the Purified kDNA Networks

Left: Fluorescence Microscopy Image of DAPI stained purified kDNA networks. Middle and Right: Atomic Force Microscopy Images of purified kDNA networks with scanning areas of 5x5 µm and 2.5x2.5 µm.

Uniformly distributed DAPI-stained DNA clusters were visible under the fluorescence microscope, suggesting that kDNA networks remained intact during the purification procedure (Figure 3.4, left panel). To further validate the structure of kDNA networks, purified isolates were scanned using AFM. Unique kDNA network structure composed of circular DNAs could be observed in 5x5 and 2.5x2.5 scans (Figure 3.4, middle and right panels). Breaks within kDNA networks were observed especially in the zoomed image. We hypothesized that shear forces during sample preparation protocol for AFM may have caused these breaks within the networks. In summary, our results demonstrate that it was possible to isolate highly purified kDNA network that could be employed in further studies.

3.3.3. *In vitro* Infection Assays

3.3.3.1. Effect of CFSE Labelling on Proliferation of Parasites

As mentioned in the previous section, to determine whether Leishmania kDNA contributes to infection and or parasite load, an in vitro infection model was established. For this, CFSE labelled parasites were used to quantify Leishmania infection of THP-1 cells in the absence or presence of kDNA *in vitro*. *In vitro* infection assays with CFSE labelled parasites were performed for *Trypanosoma cruzi*, *Leishmania infantum, Leishmania braziliensis* and *Leishmania chagasi* species in different studies (Gonçalves et al., 2005; P. E. A. Souza et al., 2007; Viana, Magalhães, Giunchetti, Dutra, & Gollob, 2018). Nevertheless, to test whether this method was also applicable to *L. major* species, CFSE labelled parasites were evaluated for their proliferative capacity to ensure that dye loading did not result in toxicity or anti-proliferative effects.

CFSE is a cytosolic stain that can be used to monitor cell proliferation by following dye dilution method. When a CFSE labelled cell replicates, cytosolic CFSE is equally distributed between daughter cells, leading to halving of fluorescence intensity, which can be followed on the green channel of a flow cytometer. In this context, parasites

were labelled with CFSE and inoculated into Leishmania growth medium at a density of 2.5×10^6 parasites/ml and monitored based on their CFSE fluorescence intensity on a daily basis for a period of 5 days.
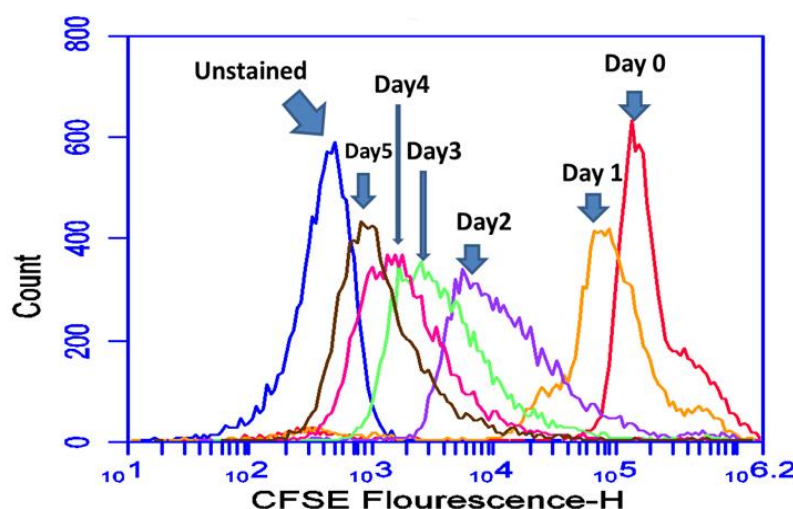
Figure 3.5. Proliferation Kinetic of CFSE-labelled *L. major* Parasites

CFSE labelled parasites were inoculated in Leishmania growth medium at a density of 2.5×10^6 parasite/ml. To assess proliferation, CFSE labelled parasite culture was monitored for a period of 5 days for dye dilution on green channel of flow cytometry.

CFSE fluorescence intensities of labelled parasites for consecutive days are presented as histogram overlays in comparison to unstained parasites in Figure 3.5. As can be inferred from the figure, successful labelling was achieved on Day 0 with a bright fluorescence intensity when compared to unstained samples. From Day 1 to 5 CFSE fluorescence intensity halved each day. This observation indicated that CFSE labelling did not interfere with proliferation and viability of parasites. Thus, CFSE labelled parasites were used for *in vitro* infection assays specifically for *L. major*.

78

3.3.3.2. **Infection of PMA-differentiated THP-1 Cells in the Presence or Absence of kDNA and gDNA**

Since there was no detrimental effect of CFSE labelling on *L. major* parasite growth, CFSE labelled *L. major* parasites were used in infection of PMA-differentiated THP-1 cells. For this, CFSE labelled parasites were co-incubated with PMA differentiated THP-1 cells in the presence or absence of kDNA or gDNA stimulation to assess the effects of different types of Leishmania derived nucleic acids on Leishmania infection.

As mentioned in previous sections, *in vitro* infection assays were designed to evaluate possible contribution of kDNA on Leishmania infection. gDNA was also used in these experiments to validate that any observed effect on Leishmania infection is specific to kDNA but not a generic response to any type of Leishmania derived nucleic acids.

Following co-incubation, cells were analyzed on the green channel of flow cytometer to determine percent of infected cells. Total parasite load was also evaluated based on the mean fluorescence intensities.
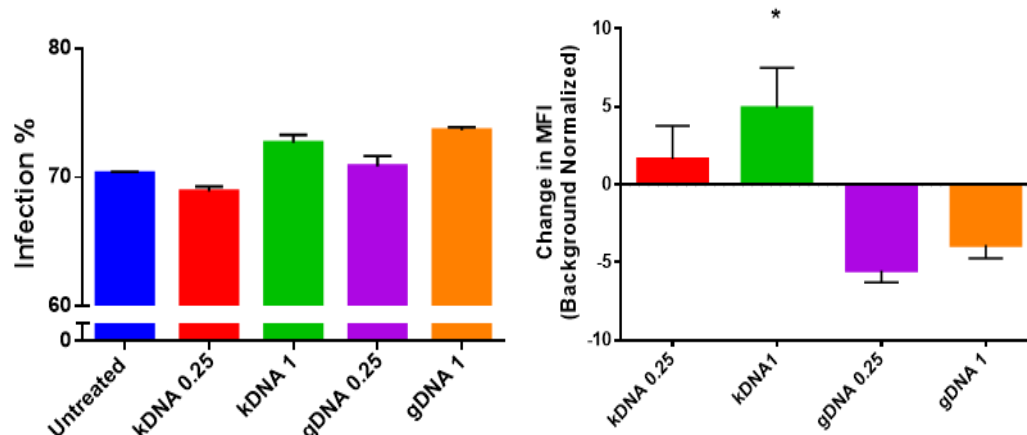
Figure 3.6. Assessment of Infection Rate and Parasite Loads of THP-1 Cells by Flow Cytometry

PMA-differentiated THP-1 cells ($5x10^5$ cells/ml) were co-incubated with CFSE labelled parasites ($5x10^6$ parasites/ml) for 24 hours in the presence or absence of kDNA and/or gDNA stimulation. Percentage of infected cells and total parasite loads (based on MFI) were evaluated on green channel of flow cytometer. Numbers on x-axis labels indicate concentration of corresponding nucleic acid in 'µg/ml'. Graphs were constructed based on two independent experiments.

All groups were compared statistically by using Kruskal-Wallis test followed by Dunnet`s multiple comparison test. *: p=0.0163 for pairwise comparison of kDNA 1 and gDNA 1 groups.

Results revealed that the percentage of infected THP-1 cells did not change significantly in the presence of kDNA or gDNA (Figure 3.5., left panel). In contrast, parasite load was significantly increased in kDNA but not gDNA treated samples (Figure 3.5, right panel).

Total parasite load calculations were based on the difference between the MFI of treated minus the untreated group. Since CFSE labeling efficiencies varied, this approach was necessary to normalize the differences observed in CFSE intensities of biological replicates. Thus, analysis of background normalized MFI values revealed that parasite loads of kDNA treated cells increased 1.6 and 4.9 folds (for 0.25 and 1 µg/ml, respectively), whereas gDNA treated cells had the opposite effect (Figure 3.5, right panel). Change in MFI value of cells treated with kDNA at 1µg/ml concentration was significantly higher than cells treated with gDNA at the same concentration.

These results suggest that kDNA treatment impacts on parasite survival but has no detectable effect on the percent of infected cells, indicating that innate immune recognition of kDNA might aggravate Leishmania infection

3.3.3.3. **Microscopic Analysis of Leishmania Infected PMA-differentiated THP-1 Cells**

In order to further investigate how kDNA influences *in vitro* infection of THP-1 cells, untreated or kDNA treated *L.major* infected THP-1 cells and uninfected cells were examined under a fluorescence microscope. For this purpose, THP-1 cells were stained with SYTO Green 16 (stains both dead and live cells) and SYTOX Orange (stains only dead cells) nucleic acid stains following the infection. Fluorescence microscopy images were taken in green channel for SYTO green 16 staining and in red channel for SYTOX Orange staining and consequently were merged in a single image for analysis. In these merged images, green cells were classified as live whereas double stained yellow/orange cells were specified as dead cells. Furthermore, Leishmania parasites and THP-1 cells can be discriminated based on the size of their nuclei. Considering all these parameters collectively, live THP-1 cells infected by Leishmania were discriminated from dead cells and/or uninfected cells to compare parasite loads in the presence and absence of kDNA qualitatively.
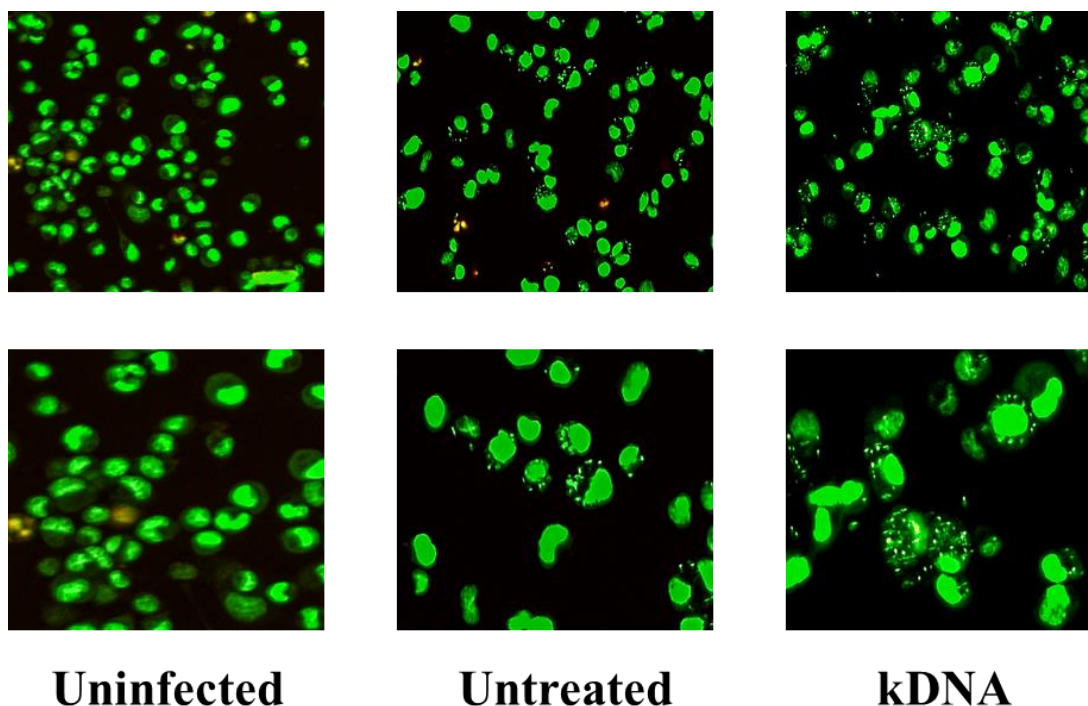
Figure 3.7. Fluorescence Microscopy Images of Uninfected and Infected THP-1 Cells Treated or not with kDNA

Following *in vitro* infection assay, infected and uninfected PMA-differentiated THP-1 cells were stained with SYTO Green 16 (1µM) and SYTOX Orange (5µM) nucleic acid stains. Images of stained cells were taken in green and red channels of fluorescence microscope and merged images are presented in the figure. Images in the bottom panel are zoomed versions of corresponding top panel images. Images are representatives of two independent experiments.

For all groups, the amount of dead THP-1 cells was negligible indicating that this model would be reliable in determination of parasite loads.

As expected, in uninfected THP-1 cells, only the cellular nuclei were stained (Figure 3.7, left panel). Absence of a signal from irrelevant subcellular structures provided evidence for the specificity of the employed dyes towards DNA. For both of the Leishmania infected groups small dots surrounding nuclei of THP-1 cells were visible (Figure 3.7, middle and right panels), corresponding to nuclear and kinetoplast DNA of Leishmania that had infected the cells.

No quantitative analysis was performed for infection rate but it could be inferred that in the kDNA treated sample, number of parasites per THP-1 cells was higher than the untreated group whereas, percent-infected THP-1 cells were not noticeably different. This observation further supports the conclusion made in the previous section and suggests that presence of kDNA contributes to parasite burden.

3.3.3.4. **Type-I Interferon Production from PMA-differentiated THP-1 Cells Infected in the Absence or Presence of kDNA or gDNA**

As discussed in previous sections, Leishmania infection was aggravated possibly through innate immune recognition of kDNA.

In mucocutaneous leishmaniasis (MCL) cases caused by Leishmania RNA virus (LRV) containing *L. guyanensis* (new world Leishmania species), upregulation of IFN-β through recognition of dsRNA of LRV exacerbates the disease (Ives et al., 2011). Furthermore, co-infections with IFN inducing viruses increase severity of MCL and also result in relapse of the disease (Rossi et al., 2017). These observations suggest that type I interferon responses induced by endogenous or exogenous viral RNA contributes to severity of MCL. Based on these findings, we hypothesized that, type I interferons induced through immune recognition of kDNA might be one of the contributing factors that aggravate *L. major* infection as observed in the case of Leishmania infections caused by new world species.

THP-1 cells used in *in vitro* infection assays are genetically engineered reporter cells that secrete alkaline phosphatase upon upregulation of interferon regulatory factors (IRFs) triggered by IFN signaling. To quantify type-I IFN production in PMA-differentiated THP-1 cells upon kDNA or gDNA stimulations, alkaline phosphatase activity in supernatants were measured by colorimetric Quanti-Blue assay. To construct a four parametric logistic standard curve for IFN concentration estimation, OD values obtained from supernatants of uninfected PMA-differentiated THP-1 cells stimulated with different concentrations (0.25-32 ng/ml) of recombinant IFN-α were

used. Using this standard curve, OD values obtained from supernatants of infected cells stimulated with kDNA or gDNA were used to calculate concentration of IFN produced by stimulated cells.
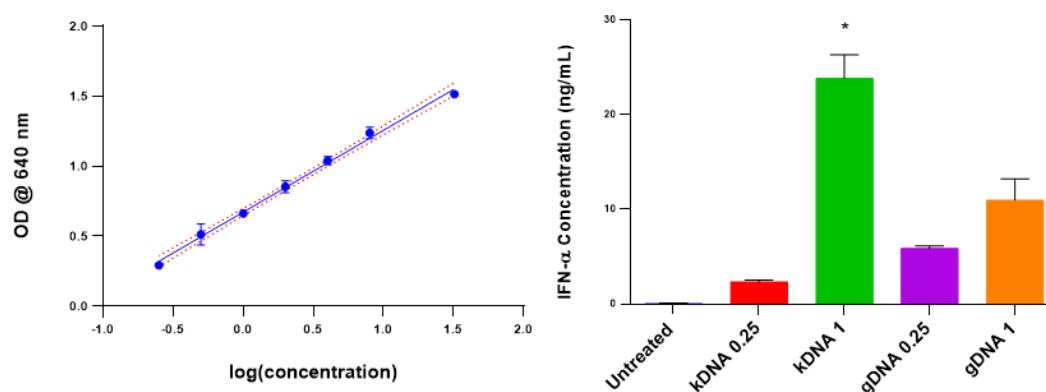
Figure 3.8. Quantification of IFN Production from Leishmania Infected THP-1 Stimulated with kDNA or gDNA

Following infection, supernatants of THP-1 cells were used to quantify soluble alkaline phosphatase activity. Left: Standard curve (R^2=0.9908) constructed using OD values of recombinant IFN-α (0.25-32 ng/ml) stimulated cells. Right: Estimated IFN concentrations of experimental groups based on the standard curve.

All groups were compared statistically by using Kruskal-Wallis test followed by Dunnet`s multiple comparison test. *****: p=0.033 for pairwise comparison of kDNA 1 and untreated groups.

The standard curve constructed for OD values and IFN concentrations fit to four-parametric logistic regression model (R^2=0.9908) with no significant deviations (p=0.4158) (Figure 3.8., left panel).

Infected PMA-differentiated THP-1 cells stimulated with kDNA at a concentration of 1µg/ml had significantly upregulated IFN production compared to untreated cells, whereas there was no significant increase in IFN production in gDNA stimulated infected cells (Figure 3.8., right panel). This result suggests that kDNA is a more potent stimulator of type I interferon production. Although the major cytosolic sensor

dedicated to recognition of DNA binds dsDNAs in a sequence-independent manner, it has been reported that it preferentially binds to U-turns or bent DNA. Such bent-DNA favor cGAS dimerization and facilitate nucleation of cGAS-DNA ladder formation (Andreeva et al., 2017). Interestingly, bent DNA was first discovered in the kinetoplast DNA minicircles (Marini, Levene, Crothers, & Englund, 1982). Therefore, it is highly likely that the affinity of cGAS towards optimally pre-structured kDNA would be much higher in magnitude when compared to gDNA. Our results demonstrate that kDNA-induced IFN production was ~2.5-fold higher than that triggered by an equivalent concentration of gDNA, supporting this view.

In summary, our results demonstrate that recognition of kDNA and/or ensuing IFN production, favorably contributes to parasite burden at least *in vitro*. It has been reported that nitric oxide production in *L.major* infected macrophages were reduced significantly when cells were co-treated with high levels of IFN α/β (Mattner et al., 2000), thereby, impairing parasiticidal activity of macrophages. In light of this observation, it is possible that high levels of type I interferons released from macrophages in response to immune recognition of kDNA might activate a similar mechanism and aid parasitaemia.

3.3.3.5. **Infection of Mouse Bone Marrow Derived Macrophages (BMDMs) in the Presence or Absence of kDNA or gDNA**

As discussed in previous sections, kDNA aggravated Leishmania infection in PMA-differentiated THP-1 cells. In order to test whether this phenomenon could be replicated in primary cells, mouse bone marrow derived progenitors were differentiated into macrophages and were then infected with enhanced green fluorescence protein (EGFP) and luciferase (LUC) expressing transgenic *L. major* parasites in absence or presence of kDNA or gDNA. These transgenic parasites were generated in the context of this thesis (see Section 3.4.4.) and mainly used for *in vivo* studies. Briefly, EGFP-LUC transgenic parasites constantly express green

fluorescence protein and hence offer an alternate to CFSE labelling (described in Section 3.3.3.2). The same experimental approach in Section 3.3.3.2. was followed for Leishmania infection assay using BMDMs to assess infection rate and parasite loads in the presence or absence of kDNA or gDNA. Differently, concentrations of kDNA and gDNA stimulations were increased by 2-fold (0.5 and 2 µg/ml instead of 0.25 and 1 µg/ml). The underlying reason was that stimulation with low dose (0.25 µg/ml) kDNA had no significant effect on parasite load and triggered very low levels of IFN production, indicating that this dose might have been sub-optimal.
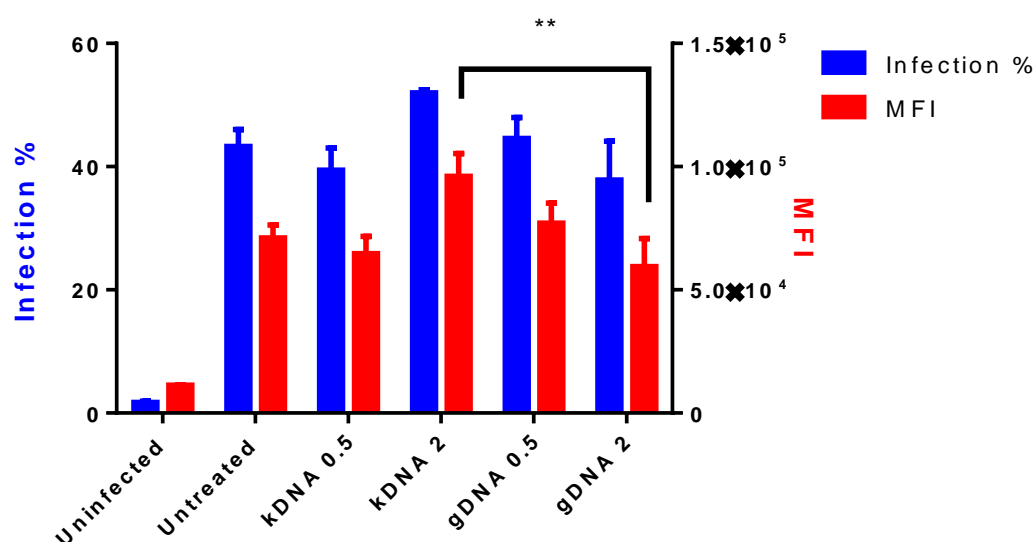
Figure 3.9. Assessment of Infection Rates and Parasite Loads of Mouse BMDMs by Flow Cytometry

Mouse bone marrow derived macrophages ($5x10^5$ cells/ml) were co-incubated with EGFP expressing parasites ($5x10^6$ parasites/ml) for 24 hours in the presence or absence of kDNA or gDNA stimulation. Percentage of infected cells and total parasite loads (based on MFI) were evaluated on green channel of a flow cytometer. Numbers on x-axis labels indicate the concentration of corresponding nucleic acid in 'µg/ml'.

All groups were compared statistically by using Kruskal-Wallis test followed by Dunnet`s multiple comparison test. **: p=0.0073 for pairwise comparison of kDNA 2 and gDNA 2 groups.

86

Consistent with previous results, Figure 3.9, presence of kDNA (2 μg/ml) or gDNA (2 μg/ml) had no significant effect on infection rate. However, parasite loads of BMDMs treated with kDNA at 2 μg/ml concentration were significantly higher than in cells treated with gDNA at the same concentration (~1.5 fold).

These results indicate that aggravation of Leishmania infection by immune recognition of kDNA is not unique to THP-1 cells, but also applicable to *in vitro* infection of primary murine macrophages.

3.3.4. **Effect of kDNA on Disease Progression in Murine Model of Cutaneous Leishmaniasis**

In vitro studies revealed that kDNA aggravated Leishmania infection in both human macrophage like cells and primary murine macrophages. In order to further investigate how kDNA affects disease progression *in vivo*, mice were infected with live parasites in the presence or absence of kDNA. For this purpose, metacylic *L. major* parasites were injected into footpads of BALB/c mice on Day 0. Either kDNA or PBS was administered systemically to mice by intraperitoneal injection on Days 0, 3 and 6. Lesion development was then followed in terms of area (width x height) to monitor disease progression.
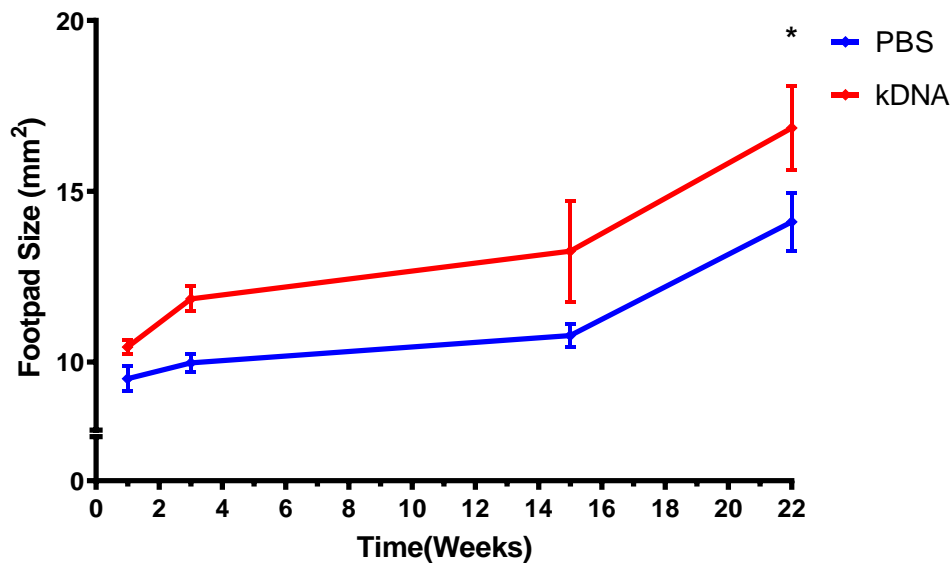
Figure 3.10. Progression of Disease in the Absence or Presence of kDNA

6-8 weeks old, BALB/c mice were challenged with metacylic *L.major* parasites (10×10^6 parasites/mouse) on Day 0. Mice were injected with PBS or kDNA (25 μg/mouse) on Days 0, 3 and 6 intraperitoneally. Lesion sizes (with x depth) were monitored for a period of 22 weeks to assess progression of disease.

Footpad sizes of groups were compared statistically within the same time point with Mann-Whitney Unpaired Test. *: $p=0.0317$ for pairwise comparison of kDNA and PBS groups on Week 22.

Consistent with *in vitro* findings, lesion size of kDNA treated group was larger than PBS treated mice that reached statistical significance on Week 22. Thus, this preliminary result indicate that kDNA might contribute to parasitaemia and impact disease progression *in vivo* (Figure 3.10).

3.4. **Development of a Potential Vaccine Formulation against Cutaneous Leishmaniasis based on Leishmania Extracellular Vesicles (Exosomes) Combined with CpG ODN and/or cGAMP Adjuvant Combinations**

In this part of the study, we aimed to develop a potential Leishmania exosome based vaccine against cutaneous leishmaniasis (CL). Leishmania extracellular vesicles

(exosomes) were shown to possess a very rich antigen content (Coakley, Maizels, & Buck, 2015; Schorey, Cheng, Singh, & Smith, 2015). However, they exhibit immunomodulatory activities when introduced simultaneously with live parasites (Atayde et al., 2016; Marshall et al., 2018). Based on their excellent antigen delivery property, herein we wanted to test the utility of Leishmania exosomes as a source of Leishmania antigens in an attempt to develop a vaccine.

Moreover, we also aimed to determine the best adjuvant candidate to be combined with the exosome-based vaccine. Since a Th1 dominated response is pivotal in protection against Leishmaniasis, adjuvants that supported Th1-type responses were tested.

In order to develop and test the best antigen-adjuvant combinations, immunization and parasite challenge experiments were conducted in BALB/c mice. This mouse strain was selected due to its susceptibility to *L.major* infection (D. Sacks & Noben-Trauth, 2002; Solbach & Laskay, 2000). This susceptibility can be attributed to several characteristics of the stain primarily, a lack of IL-12 responsiveness (Güler et al., 2006) and constant IL-4 production (Himmelrich, Parra-Lopez, Tacchini-Cottier, Louis, & Launois, 1998), lead to suppressed Th1 responses (Athie-Morales, Smits, Cantrell, & Hilkens, 2004; Lazarski, Ford, Katzman, Rosenberg, & Fowell, 2013) and render this mouse strain susceptible to Leishmania infections.

In the following sections, characterization of isolated *L.major* exosomes, optimization of a mouse model of CL, establishment of a protocol for determination of parasite loads and attempts to chemically modify Leishmania antigens will be discussed.

In order to evaluate the efficacy of candidate vaccine formulations, the following parameters were analyzed: Lesion sizes were estimated through footpad size measurements post-challenge by live parasite. Parasite loads were quantified during the course of experiments (except the first challenge experiment) using *in vivo* imaging system which was made possible through development of transgenic parasites expressing luciferase. Vaccine and/or post-challenge immune status was monitored

through measurement of Leishmania antigen specific humoral (IgG1 and IgG2a) and cellular responses (Th1, Th2 and Th17 specific cytokines).

3.4.1. Generation of Mouse Adapted *L.major* Parasites

A mouse model of cutaneous leishmaniasis was generated for *L. tropica* was established in previous studies in our laboratory, which required a duration of 10 months for development of significant lesions (Güngör, 2017). In this thesis, we switched to *L. major* as the infectious agent, a strain more aggressive than *L. tropica* (Remadi et al., 2017; Spotin, Rouhani, & Parvizi, 2014). Thus, lesions were expected to develop within 4-6 weeks of parasite challenge (Reiling et al., 2006; Rhee et al., 2002; Santiago et al., 1999).

The first *L.major* challenge experiment conducted in this thesis was to evaluate the effect of kDNA on disease progression (Section 3.3.4). In this model, lesion development took more than 5 months, which exceeded the expectation suggested by other studies published using CL model of *L.major*. The late-development of lesions in our experiment slowed the progression of our experiments and was inconvenient.

To circumvent this problem, the parasites were first *in vivo* passaged in mice to regain virulence that might have been caused by serial *in vitro* passages. This method has been shown to enhance infectivity of *L. donovoni* parasites (Katakura & Kobayashi, 1985), and also used for other species as well, including *L. major* (Eddaikra et al., 2016; Rafati, Baba, Bakhshayesh, & Vafa, 2000).

To test the success of *in vivo* passaging on recovery of *L. major* virulence, amastigotes were isolated from a lesion and transformed into promastigotes. Then, a small-scale challenge experiment was designed to compare the infectivity of mouse adapted and the human isolate parasites. For this purpose, right footpads of two BALB/c mice were injected with 10×10^6 mouse passaged metacyclic parasites whereas the left footpads of the same mice were injected with 10×10^6 human isolate metacyclic parasites.

Footpad sizes and lesion development were monitored for a period of 5 weeks, which is the average expected time for lesions to form.
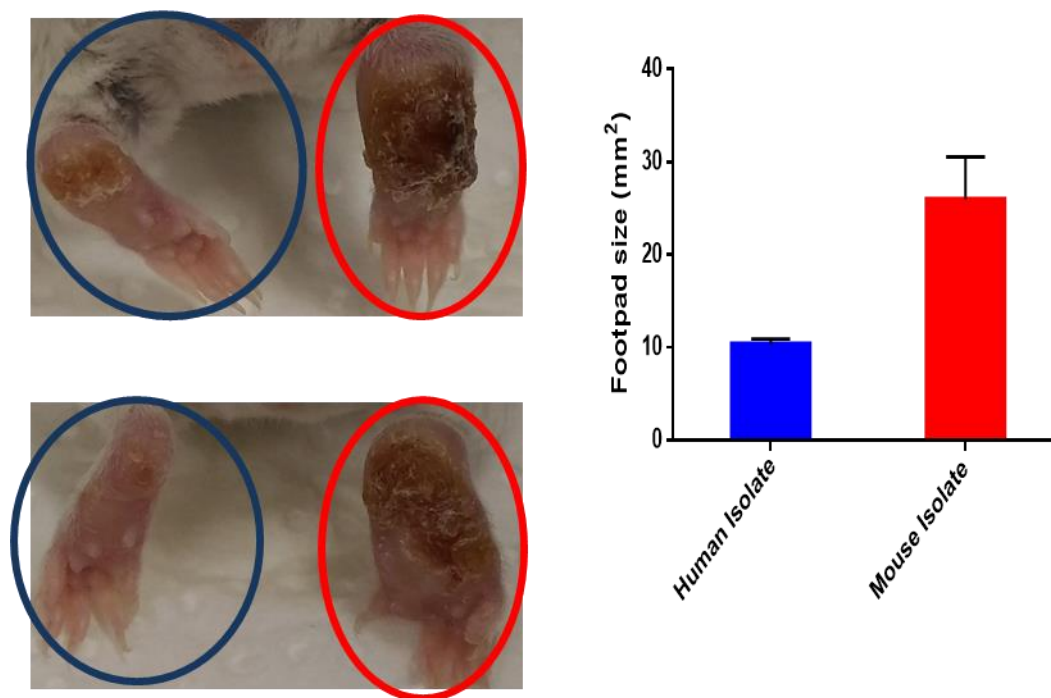
Figure 3.11. Comparison of *in vivo* Challenge Models using Human versus Mouse Isolates of *L. major* Parasites.

Right footpads (encircled with red on the left panels) of mice were injected with mouse isolate parasites (10×10^6/mouse), whereas left footpads (encircled with blue the on left panels) of the same mice were injected with human isolate parasites (10×10^6/mouse). Lesion sizes were monitored for a period of 5 weeks. Left: Photos of footpads, Right: Measurement of footpad sizes (width x depth). Photos and measurements were taken 5 weeks after the parasite challenge

Significant lesions developed in the right footpad of mice, where mouse isolate *L.major* was injected, 5 weeks after the challenge (Figure 3.11., left panels, red circles). In contrast, there was no noticeable lesion formation in left footpads, that received human isolate parasites (Figure 3.11., left panel, blue circles). Furthermore, lesion sizes of right footpads were ~2.5 fold higher than the left footpads 5 weeks after parasite challenge (Figure 3.11., right panel).

These results indicate that lesion development was accelerated when mouse isolate parasites were used in the CL infection model. Furthermore, timing of lesion development was consistent with published results (4-6 weeks). In light of this observation, use of mouse isolate *L. major* parasites was adopted for all experiments to increase consistency and reliability.

3.4.2. **Characterization of Isolated *L. major* Exosomes**

As mentioned previously Leishmania extracellular vesicles were selected as a source of Leishmania antigens for vaccination studies. For this purpose, Leishmania exosomes were first purified from stationary phase promastigotes and then characterized prior to their use in immunization/challenge experiments.

3.4.2.1. **Analysis of gp63 Content of *L.major* Exosomes**

gp63, also known as leishmanolysin, is a major metalloprotease found in all Leishmania species and is highly enriched in Leishmania exosomes. Therefore, gp63 was specified as a Leishmania exosome marker with immunogenic properties (Hassani, Shio, Martel, Faubert, & Olivier, 2014; Isnard, Shio, & Olivier, 2012; Olivier et al., 2012). Based on this, gp63 content of isolated exosomes were analyzed by flow cytometry to characterize exosomes and their antigen content.

Isolated exosomes were stained with FITC conjugated anti-gp63 antibody (1 µg/ml). Unstained and stained exosomes were analyzed on the green channel of a flow cytometer. Since exosomes are too small to be discriminated in flow cytometric analysis, PBS was acquired to determine the background reading on FSC and SSC parameters (Figure 3.12., top-left panel). Exosomes were defined as particles gated above this background noise in FSC/SSC plots (Figure 3.12, top-right panel). Unstained exosome sample (Figure 3.12, bottom-left panel) was used to discriminate gp63 positivity of exosomes.

92
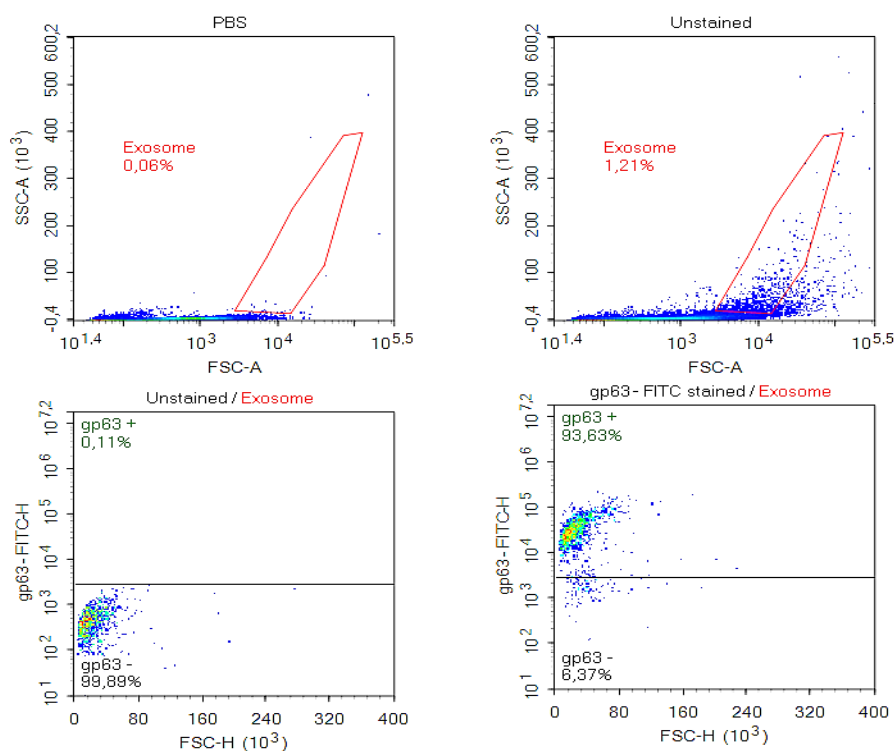
Figure 3.12. Analysis of gp63 Content of Exosomes by Flow Cytometry

Purified exosomes were stained with FITC conjugated anti-gp63 antibody (1 μg/ml) and analyzed on the green channel of flow cytometer in comparison to unstained exosomes. PBS alone was used for background noise determination to specify the exosome gating strategy based on FSC and SSC parameters.

Top-Left: PBS background reading, Top-Right: Gating strategy for exosomes based on FSC and SSC, Bottom-Left: Unstained samples, Bottom-Right: anti-gp63-FITC stained exosomes

Majority of isolated exosomes (93.63%) were positive for Leishmania exosome marker, gp63, based on anti-gp63-FITC staining (Figure 3.12, bottom-right panel). This observation indicates that isolated vesicles can be characterized as Leishmania exosomes, exhibiting rich gp63 antigen content.

3.4.2.2. Morphological Analysis of Leishmania Exosomes by Atomic Force Microscopy (AFM)

To further investigate Leishmania extracellular vesicles, their topological and morphological characteristics were analyzed by AFM. For this purpose, purified vesicles (100-200 ng/ml) were adsorbed onto mica surfaces and scanned at non-contact mode of an atomic force microscope. 2D images with a 10x10 µm (figure 3.13., top-left panel), 2x2 µm (figure 3.13., bottom-left panel) and 0.8x0.8 µm (figure 3.13., top-right panel) scan area are presented with representative size measurements. The 2x2 µm image was further processed to obtain a 3D image (figure 3.13., bottom-right panel).
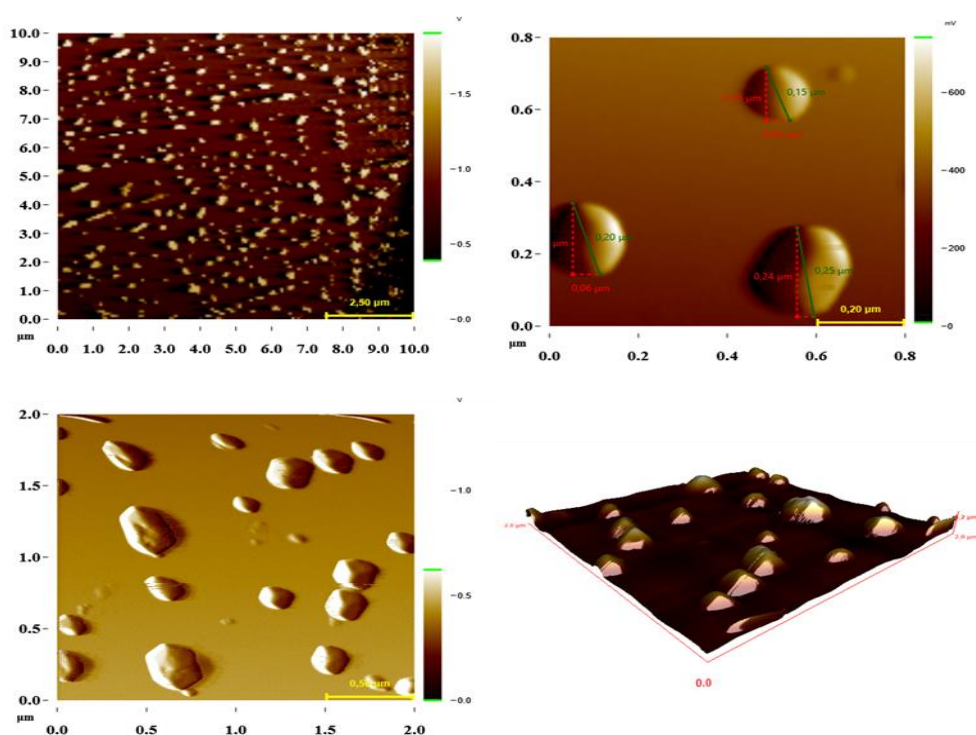
Figure 3.13. Atomic Force Microscopy Analysis of Purified Leishmania Exosomes

Purified vesicles (100-200 ng/ml) were scanned by AFM at non-contact mode. Images were taken from different scanning areas and a 3D image was constructed from Vz channel of the 2x2 µm image.

Representative images of 10x10 µm (top-left), 2x2 µm (bottom-left), 0.8x0.8 µm (top-right) scan areas are shown with corresponding scale bars. Bottom-right: 3D version of the 2x2 µm image.

Regularly dispersed vesicles were observed in the 10x10 μm image (figure 3.13., top-left panel) that were heterogeneous in size. Since the scale of this image was too large to determine individual vesicle sizes, 2x2 μm and 0.8x0.8 μm images were used to estimate size distribution of purified vesicles (figure 3.13., bottom-left and top- right panels). Leishmania extracellular vesicles ranged between 50-250 nm, corresponding to reported sizes of exosomes and micro-vesicles (Théry, Ostrowski, & Segura, 2009; Yáñez-Mó et al., 2015). Spherical shapes of purified vesicles were observed in 3D view of the 2x2 μm image (figure 3.13., bottom-right panel). AFM analysis indicated that Leishmania vesicles were purified in their natural form in terms of shape and size without any visible contamination.

3.4.2.3. **Proteomics Analysis of Purified Leishmania Exosomes by Mass Spectrometry**

To analyze protein content and specify exosome markers, mass spectrometry (MS) analysis was performed for two different Leishmania exosome batches. Peptide sequences obtained from MS were identified based on Gene Ontology (GO) terms and analyzed using Protein Analysis Through Evolutionary Relationships (PANTHER) tool (P. D. Thomas et al., 2003) to classify proteins found in exosomes.

As depicted in Figure 3.14., almost half of the identified exosomal proteins belonged to the hydrolase family according to PANTHER protein classification (PC00121). The majority of hydrolases found in purified exosomes were proteases (11 out 16), composed of cysteine proteases and metalloproteases. In addition to hydrolases, calcium binding/sensing proteins, tubulins and cell adhesion proteins were also present within the purified exosomes. General protein classes found in purified exosomes were consistent with published results (Atayde et al., 2015; Jones et al., 2018). The diversity of proteins found in purified Leishmania exosomes are in support of their utility as promising candidates of Leishmania antigen vaccine carriers.

PANTHER Protein Class	Leishmania major (REF) #	upload_1 (▽ Hierarchy NEW! ?)				
		#	expected	Fold Enrichment	+/-	P value
tubulin	8	4	.05	73.07	+	1.25E-04
cell adhesion molecule	9	4	.06	64.95	+	1.80E-04
annexin	20	6	.14	43.84	+	2.13E-06
↳calcium-binding protein	66	6	.45	13.29	+	1.14E-03
calmodulin	38	6	.26	23.08	+	5.95E-05
↳intracellular calcium-sensing protein	38	6	.26	23.08	+	5.95E-05
cysteine protease	72	6	.49	12.18	+	1.81E-03
↳protease	175	11	1.20	9.19	+	4.81E-06
↳hydrolase	426	16	2.91	5.49	+	2.73E-06
metalloprotease	65	5	.44	11.24	+	1.44E-02

Figure 3.14. Exosomal Proteins Classified by PANTHER Protein Class GO Term Analysis

Peptide sequences obtained from MS analysis were identified as GO terms and analyzed using PANTHER protein classification tool

Full list of proteins found in purified exosomes with a significant mascot score are given in Table C.1. (Appendix C). The most abundant proteins found in exosomes were listed in Table 3.1. In this table, mascot score represents statistical match between raw peptide sequences obtained from MS analysis and *L. major* reference sequences. Mascot scores presented in the table indicate significant matches where a higher mascot score implies higher significance. In addition to mascot scores, average number of matches were presented as an indicator of protein abundance in exosomes.

Table 3.1. *The Most Abundant Proteins in Leishmania Exosomes by MS Analysis*

Protein Name	Average Mascot Score	Average # of significant matches	Uniprot KB Accession Number
GP63, leishmanolysin	90.0	4	Q4QHH1
Putative heat-shock protein hsp70	87.0	3	Q4Q7Y4
Heat shock protein 83-1	102.0	3	Q4Q4I0
Tubulin beta chain	208.0	10	Q4Q4C4
Tubulin alpha chain	184.5	7	Q4QGC5
Thiol specific antioxidant	189	6.5	Q4QF68
Putative calpain-like cysteine peptidase (SMP-1)	222.5	5.5	Q5SDH5
Hypothetical protein LMJF_23_1020	378	4	Q4QB61

As mentioned previously (Section 3.4.2.1.), gp63 metalloprotease is an exosome marker and is found abundantly in our purified exosome samples based on MS analysis (Table 3.1.). In addition to gp63, two types of heat shock proteins were identified in purified exosomes, namely HSP70 and HSP83-1. These HSPs were also specified as exosomes markers (Atayde et al., 2015) and therefore, the presence of three distinct exosome markers in our purified samples provides strong evidence to specify them as *bona fide* Leishmania exosomes.

In addition to these well-defined Leishmania exosome markers, our study also revealed the presence of both subunits (α and β) of tubulin in the exosome proteome (Table 3.1.). Leishmania exosomes are secreted by formation of multivesicular bodies

(MVBs), a process that involves cytoskeletal dependent trafficking mechanism (Keller, Sanderson, Stoeck, & Altevogt, 2006). Therefore, presence of cytoskeletal proteins in our purified vesicles are in support of their exosomal nature (Jones et al., 2018).

Among the identified exosomal proteins that may be of interest for vaccine development and/or parasite biology was the thiol specific antioxidant, otherwise known as tryparedoxin peroxidase (Table 3.1.). This protein is capable of catalyzing reactive oxygen species such as hydroxyl radicals and thereby was reported to play a role in parasite survival and virulence (Iyer, Kaprakkaden, Choudhary, & Shaha, 2008; Lim et al., 1993).

Another protein identified in purified exosomes was putative calpain-like cysteine peptidase, also known as small myristoylated protein-1 (SMP-1) (Table 3.1.), which is found on flagellum membrane. In addition to conventional secretion of exosomes by MVBs, an alternative Leishmania exosome secretion from flagellar pockets was reported (Silverman et al., 2008). Thus, presence of a flagellar membrane protein in purified exosomes indicates that at least some of Leishmania exosomes were derived from this alternative pathway. Furthermore, SMP-1 is required for normal flagellum function (Tull et al., 2010) and has a role in entry of Leishmania into host cells (J. D. Sunter et al., 2019). Whether SMP-1 also plays a role in exosome delivery to host cells, remains to be determined.

In summary, presence of tubulins and SMP-1 in our purified exosomes are consistent with their secretion through two alternative pathways (MVBs and flagellar pockets), thereby contributing to the diversity of their antigenic content.

Most of the proteins specified in Table 3.1. were described as virulence and immunogenic factors. These include gp63 (Isnard et al., 2012), HSP70 (Rafati et al., 2007), tryparedoxin peroxidase (Iyer et al., 2008) and calpain-like cysteine peptidase (Mottram, Coombs, & Alexander, 2004). Presence of these proteins, which are critically important for parasite survival and virulence, suggests that exosomes possess

excellent antigenic diversity. Considering their high antigen delivery capacity and the diversity of their antigenic content, exosomes emerge as an ideal source of Leishmania antigens to be used in vaccine development.

It is noteworthy that, a hypothetical protein with unknown function (LMJF_23_1020) was detected with a high abundance in purified exosome samples (Table 3.1.). To gain insight into its conceivable biological function, sequence of this protein was ran on BLASTP (Altschul et al., 1997). BLASTP analysis (Figure C.2., Appendix C) showed that this protein is conserved among several Leishmania species including, *L. major*, *L. donovani*, *L. mexicana*, and *L. infantum* with unknown function. Interestingly, this unknown protein has a significant sequence similarity to a conserved *Plasmodium* (the causative agent of malaria) protein with unknown function. All of these findings indicate that this hypothetical protein may have an important role in parasitic infections. Thus, it emerges as a novel protein of interest for parasite biology, to be characterized in a separate study.

3.4.3. Immunization and Challenge Experiment to Assess Adjuvant Activity of K type CpG-ODN and cGAMP (K-cGAMP)

Following characterization of exosomes, we designed our first immunization and challenge experiment to test the antigenicity of *L. major* exosomes and the adjuvant activity of K-cGAMP. In a previous study from our laboratory, combination of K type CpG-ODN and cGAMP (K-cGAMP) was shown to be a Th1 promoting adjuvant combination in a murine model of protective cancer vaccination (Yildiz et al., 2015). Furthermore, this adjuvant combination was tested in mice vaccinated with *L. tropica* exosomes and exhibited Leishmania specific Th1 and Th17 responses (Güngör, 2017). Based on these preliminary findings, we wanted to test the protective effect of K-cGAMP adjuvant/*L. major* exosome combination in a mouse model of CL.

For this, BALB/c mice were immunized with Leishmania exosomes (Exo) or heat-killed parasites (HK) as such or combined with K-cGAMP on days 0 and 14 (see table

2.3 for administered doses). Next, immunized mice were challenged with metacylic *L.major* parasites (10×10^6 per mouse) on day 21. Lesion sizes were monitored for 11 weeks after parasite challenge based on footpad measurements. At the end of the experiment, photos of infected footpads were taken to demonstrate severity of lesions.

This experiment was the first experiment that mouse passaged parasites were used in this thesis. As can be seen in Figure 3.15, significant lesions developed within 7 weeks that reached peak levels within 11 weeks of parasite challenge, when the experiment was terminated. This observation indicates that mouse passaging of parasites reduced the time course of a challenge experiment more than half when compared to the first challenge experiment in this thesis (Section 3.3.4.), which took 22 weeks.
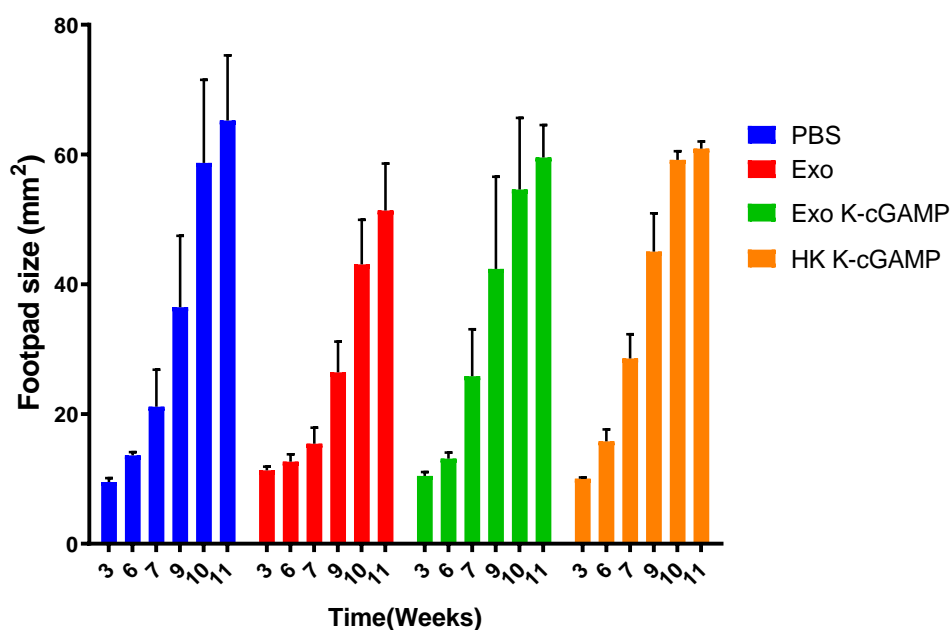
Figure 3.15. Progression of Disease in Mice Immunized with *L. major* Exosomes or HK Parasites in Combination with K-cGAMP as an Adjuvant

Mice were immunized with vaccine formulations (see Table 2.3. for doses) twice on Days 0 and 14. Immunized mice were challenged with *L. major* parasites (10×10^6 per mouse) on Day 21. Then, lesion sizes were monitored through footpad measurements for 11 weeks after challenge and presented as width x depth.

Lesion development in mice immunized with exosomes alone was delayed when compared to other groups but this difference was not statistically different from unvaccinated (PBS) group (Figure 3.15.). Disease progression of both experimental groups, where K-cGAMP was used as an adjuvant exhibited very similar pattern to unvaccinated group. These observations indicated that, exosomes alone had a vaccine potential but combination with K-cGAMP provided no additional benefit.

Representative photos of infected footpads showed that severe ulcerated lesions developed for all groups with no noticeable difference (Figure 3.16).

In light of these observations, use of K-cGAMP as an adjuvant was abandoned without evaluating any additional immunological parameters. To improve the possible antigenic potential of exosomes, the exosome dose in all other vaccination studies was increased from 20 µg to 40 µg per mouse.
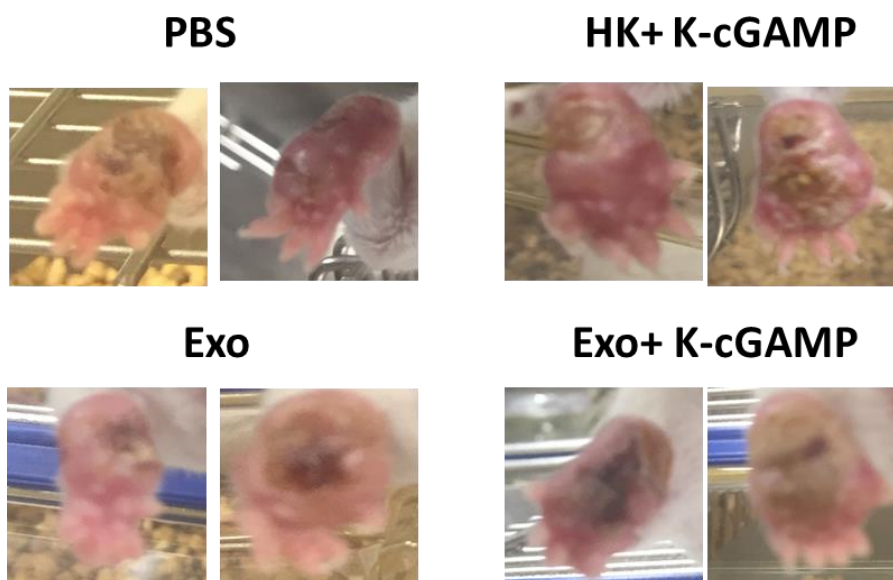
Figure 3.16. Representative Footpad Photos taken 11 weeks after Challenge

Lesion development was followed for 11 weeks and then photos of infected footpads were taken to demonstrate severity of lesions.

3.4.4. Integration of *in vivo* Imaging Method to Quantify Parasite Loads in Challenge Experiments

The challenge experiments presented in Section 3.3.4 and 3.4.3. involved lesion size estimation by footpad measurements as the only parameter used to follow disease progression. In murine cutaneous leishmaniasis model, lesion size and footpad swelling usually correlates with parasite load. However, when lesions starts to ulcerate, dimensions of infected tissue change drastically and may not significantly correlate with parasite load. Therefore, monitoring only lesions size to assess disease progression may be misleading especially for late stage lesions (Hill, North, & Collins, 1983; TITUS, MARCHAND, BOON, & LOUIS, 1985).

There are several additional methods used in parasite burden estimation to accompany lesion size measurement. One well-established protocol is the limiting dilution assay method, where amastigotes are isolated from infected tissues and grown *in vitro* with serial dilutions. However, this method is time consuming, requires previous knowledge of expected parasite density for adequate dilution estimation and is prone to bacterial and/or fungal contamination. Specifically, to precisely quantify parasite loads, cultures are prepared as 16 replicates that are then fitted to Poisson distribution for estimation of parasite counts (Taswell, 1981). Considering that, we have dealt with 65 animals in our last experiment, which will be discussed in the following sections, if we wanted to perform limiting dilution assay, we would have prepared 65x20x16= 20,800 cultures and examined them under a microscope. Handling of such a vast number of cultures is not feasible and would have been prone to errors.

Another alternative is to quantify kDNA or RNA isolated from tissue samples by PCR or qPCR (Abbasi et al., 2013; Nicolas, Prina, Lang, & Milon, 2002; Van Der Meide et al., 2008). However, evidence suggests that DNA released from dead parasites persist in tissues, resulting in inaccurate live parasite quantification and RNA is mostly applicable to experiments with short time course (Romero et al., 2010; Van den Bogaart, Schoone, Adams, & Schallig, 2014).

Both of these applied and established methods have their own disadvantages but the most important disadvantage, which is common in both, is that these methods can only be used for end-point quantification. In other words, the experiment has to be terminated to process infected tissues for parasite quantification.

The alternative method that we preferred to integrate into our *in vivo* studies was based on generating transgenic parasites for *in vivo* imaging. Enhanced green fluorescent protein (EGFP) and/or Luciferase (LUC) expressing transgenic parasites were generated in different studies for monitoring of parasites in live animals (Bolhassani et al., 2011; Goyard et al., 2014; Michel et al., 2011). In this method, anesthetized animals infected with transgenic parasites can be imaged in *in vivo* imaging systems (IVIS) based on fluorescence or luminescence readings for quantification at different time points during the course of the experiment.

Therefore, to take advantage of this system, we generated transgenic *L. major* parasites constitutively expressing EGFP-LUC fusion protein. *In vivo* imaging scans based on luminescence are more sensitive, and hence, LUC activity was chosen for this purpose. At the same time, EGFP expression was designed to replace CFSE labelling method for *in vitro* infection experiments.

In the following sub-sections, generation, confirmation and optimization experiments related to EGFP-LUC expressing transgenic parasites will be discussed.

3.4.4.1. **Generation and Selection of EGFP-LUC Expressing Transgenic *L. major***

To generate stable EGFP-LUC expressing transgenic *L. major* strain, a custom pLEXSY Leishmania expression vector containing EGFP-LUC sequence (Appendix C) was designed. Expression vector was digested with SwaI restriction enzyme (1 unit/1 μg plasmid) to obtain linearized expression vector (7,351 bp) (see Figure C.1., Appendix C). Mid-log phase parasites ($\sim15 \times 10^6$/ml) were electroporated in the presence of linearized expression vector (10μg). Following electroporation, transgenic

parasites were subjected to LEXSY-neo (resistance gene found in expression vector) antibiotic selection and monitored on green channel of a fluorescence microscope on a daily basis. Following observation of enriched EGFP expressing parasites, green fluorescence and white field merged images were taken on a fluorescence microscope (Figure 3.17, top panels).
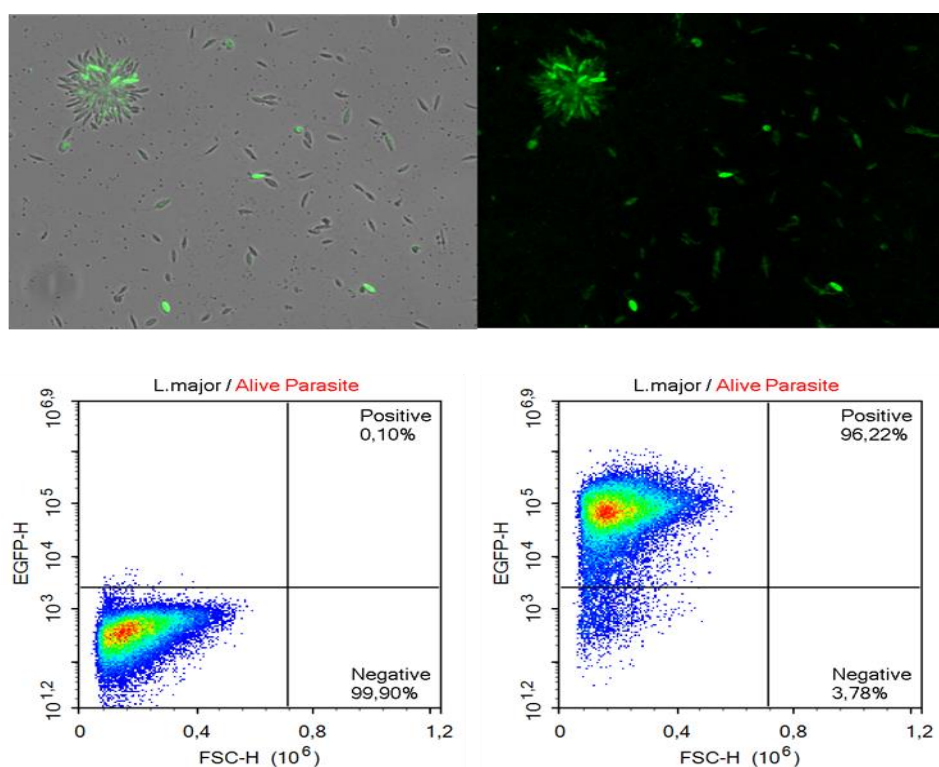
Figure 3.17. Confirmation of EGFP Expression in Transgenic Parasites by Fluorescence Microscopy and Flow Cytometry

Images of transgenic *L. major* parasites were taken on white and green channels of a fluorescence microscope after antibiotic selection. Wild type and transgenic parasites were analyzed on green channel of a flow cytometer.

Top Left: White field and green fluorescence merged image, Top Right: Image on green channel only. Flow cytometric analysis of EGFP expression in wild type (bottom-left) and transgenic parasites (bottom-right).

Results revealed that 96.22% of transgenic parasites were EGFP positive after antibiotic selection (Figure 3.17, bottom-right panel), confirming the efficiency of the transfection protocol.

3.4.4.2. **Confirmation of Luciferase (LUC) Expression in Transgenic Parasites**

As mentioned in the previous section, the vector was designed to generate transgenic parasites expressing EGFP-LUC fusion protein. To confirm that transgenic parasites were also expressing a functional LUC protein suitable for *in vivo* imaging, 9×10^6 wild type (EGFP-LUC$^-$) parasites and 1×10^6, 3×10^6 or 9×10^6 transgenic parasites (EGFP-LUC$^+$) were transferred to a 6-well plate. D-Luciferin (150 µg/ml) was added onto parasites as the substrate. Following incubation, the plate was scanned using IVIS in luminescence protocol and LUC activity of parasites were recorded in terms of radiance.
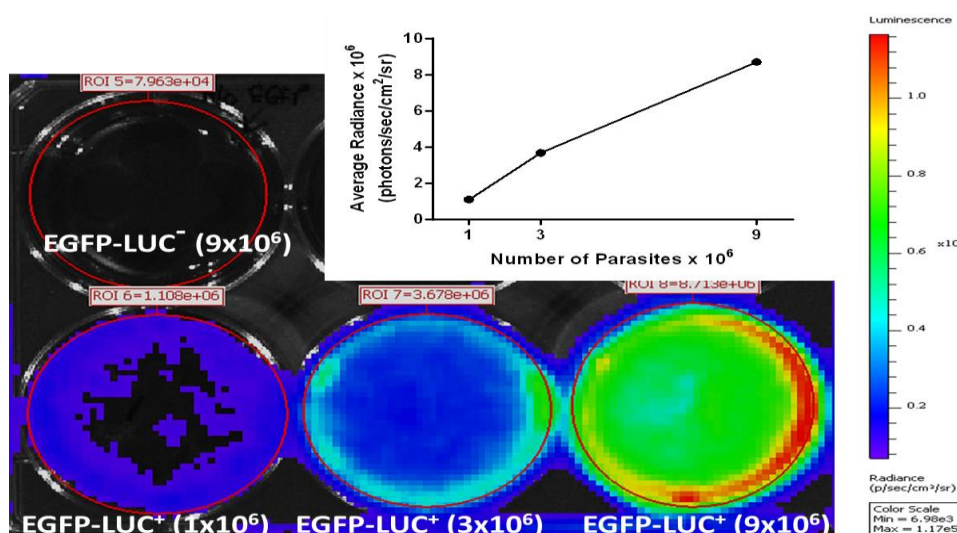
Figure 3.18. Confirmation of Luciferase Expression in Transgenic Parasites

Wild type (EGFP-LUC$^-$) parasites (9×10^6) and transgenic (EGFP-LUC$^+$) parasites (1×10^6, 3×10^6 and 9×10^6) were mixed with luciferin (150 µg/ml) in wells of a 6-well plate. Following 10 minutes incubation, plate was scanned using luminescence protocol of IVIS. Luciferase activity was recorded as radiance and images showing luminescence activity were taken. ROI: Region of Interest

As expected, EGFP-LUC- parasites did not generate luminescence signal (Figure 3.18). For EGFP-LUC$^+$ parasites, luminescence signal was recorded and its amplitude was correlated with increasing numbers of parasites (Figure 3.18.). This observation showed that, transgenic parasites were expressing a functional luciferase protein and luciferase activity measurement in IVIS could be used to quantify parasites at least *in vitro*.

3.4.4.3. **Optimization of *in vivo* Imaging System for Measurement of Parasite Load in Mice**

To confirm that transgenic parasites were suitable for parasite load estimation *in* vivo, right footpads of BALB/c mice were injected with 1×10^6, 3×10^6 and 9×10^6 metacyclic transgenic parasites (EGFP-LUC$^+$) or 9×10^6 wild type (EGFP-LUC$^-$) metacylic parasites. Immediately after challenge, animals were anesthetized and injected with D-Luciferin (0.75 mg/mouse) intraperitoneally. Then, footpads were imaged using the luminescence protocol on IVIS.

No significant luminescence signal was recorded in the footpad of mice that received EGFP-LUC$^-$ parasites (Figure 3.19.). Luminescence signal obtained from footpads of EGFP-LUC$^+$ parasite injected mice correlated with the number of injected parasites (Figure 3.19.), confirming that the use of EGFP-LUC$^+$ parasites was sufficiently sensitive for evaluation of parasite loads in immunization/challenge experiments. Furthermore, the scanning parameters such as exposure time (30 seconds) and duration of the scan for establishment of a kinetic curve (~20 minutes) were optimized in this trial.
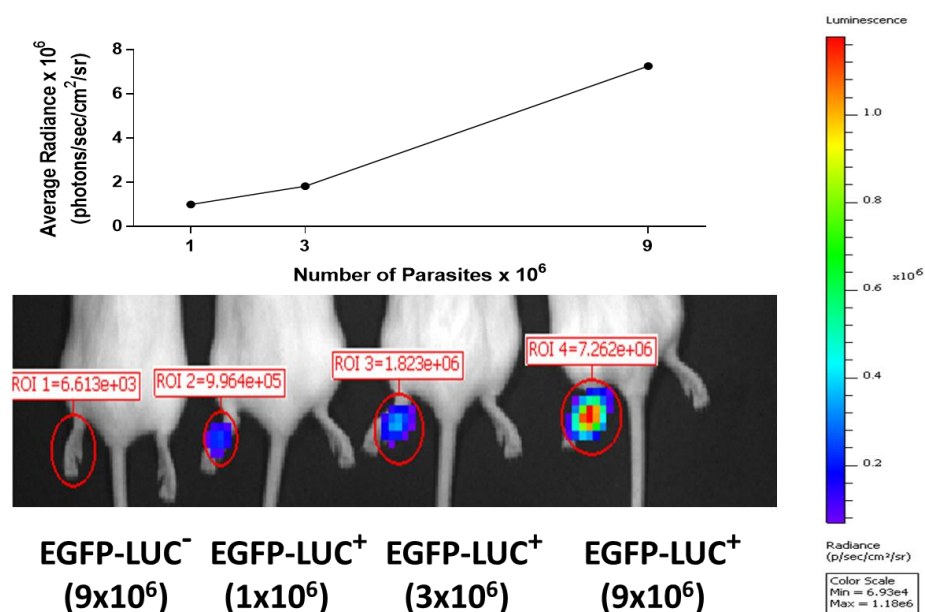
Figure 3.19. Optimization of *in vivo* Imaging of Transgenic Parasites in Footpads of Challenged Mice

$9x10^6$ metacyclic wild-type parasites (EGFP-LUC⁻), $1x10^6$, $3x10^6$ or $9x10^6$ metacyclic transgenic parasites (EGFP-LUC⁺) were injected into right footpads of BALB/c mice. Subsequent to challenge, anesthetized animals were injected with D-Luciferin (0.75 mg/mouse) intraperitoneally and were scanned using the luminescence protocol of IVIS. Luciferase activity was recorded as radiance and images representing luminescence activity were taken. ROI: Region of Interest

Since EGFP-LUC⁺ parasites were subjected to prolonged *in vitro* culturing for selection purposes, they were mouse passaged once more to regain virulence. For this purpose, mice injected with EGFP-LUC⁺ parasites in this trial experiment were monitored visually for lesion development for 8 weeks after IVIS protocol. Following formation of lesions, they were used to establish mouse passaged EGFP-LUC⁺ parasite strain as discussed previously. Stabilates were prepared and use of EGFP-LUC⁺ parasites were adopted for immunization/challenge experiments.

3.4.5. Determination of Immunogenicity of Leishmanial Antigen Formulations and Adjuvanticity of CpG ODN-based Immunostimulatory Agents

In the immunization/challenge experiment conducted to the test adjuvanticity of K-cGAMP (Section 3.4.3.), the TLR9/STING agonist combination failed to improve potential protective effects of Leishmania exosomes. Based on this finding, we designed an immunization experiment to determine the optimal antigen/adjuvant combination for subsequent challenge trials of cutaneous leishmaniasis. For this purpose, we used heat-killed parasites (HK), soluble Leishmania antigen (SLA) or Leishmania exosomes (Exo) as the source of antigen. These Leishmania antigens were used as such or combined with three different Th1 promoting adjuvants: K-type CpG ODN (K-ODN), D-type CpG ODN (D-ODN) (Hennessy et al., 2010; Ishii, Gursel, Gursel, & Klinman, 2004; Klinman et al., 2009, 2002; Vollmer & Krieg, 2009) or CpG nanorings (NRs) (Gungor et al., 2014).

To test the immunogenicity of antigen/adjuvant combinations, BALB/c mice were vaccinated with can didate formulations (see Table 2.4. for administered doses) on Days 0 and 14. Sera and spleens were collected from mice on Day 21.

To assess Leishmania antigen specific humoral responses, SLA-specific serum IgG1 and IgG2a levels were quantified by ELISA. Then, antibody titers were calculated based on background levels determined from the unvaccinated group (PBS). Furthermore, levels of cytokine production from Leishmania antigen stimulated splenocytes were quantified by using the Th1-Th2-Th17 cytometric bead array kit to evaluate Leishmania specific cellular responses induced by vaccination.

Th1 dominated responses (IFN-γ and TNF-α) were reported to provide protection against CL, whereas Th2 dominated responses (IL-4,IL-10 and IL-6) supports non-healing lesions (Castellano et al., 2009). The contribution of Th17 responses to anti-Leishmanial immunity is less clear, where Leishmania-specific IL-17 production was reported either as contributing to parasite clearance or exacerbating the disease (Banerjee et al., 2016). Based on these findings, successful antigen/adjuvant

combinations were defined based on their ability to generate Th1 dominated responses.
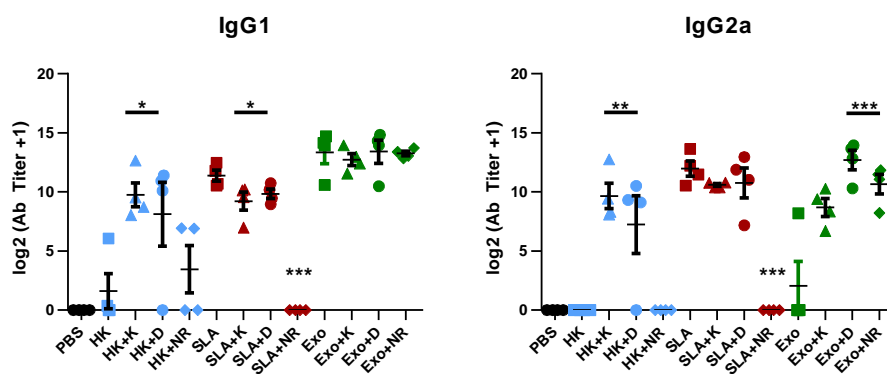
Figure 3.20. Leishmania Antigen Specific IgG1 and IgG2a Titers in Mice Immunized with Candidate Vaccine Formulations

Mice were immunized with the vaccine formulations (see Table 2.4. for doses) twice on Days 0 and 14. Sera were collected from animals on Day 21. Leishmania antigen specific IgG1 and IgG2a levels in collected sera were quantified by ELISA using SLA coated (10 μg/ml) plates. Antibody titers were calculated based on O.D. readings of unvaccinated group (PBS) and presented in log2 scale.

All antigen-adjuvant combinations were compared to their corresponding antigen alone groups statistically by Kruskal-Wallis test followed by Conover`s multiple comparison test (*: p<0.05, **:p<0.01, ***: p<0.001)

Figure 3.20. summarizes Leishmania specific IgG1 and IgG2a titers generated in vaccinated animals. IgG1 and IgG2a isotype switching are indicators of Th2 and Th1 dominated responses respectively, wherein the cytokines IL-4 and IFN-γ control the outcome of class switching (Finkelman et al., 1990; Snapper & Paul, 1987).

HK parasites alone stimulated very low levels of leishmania specific IgG1 but no IgG2a production, whereas, titers of these subclasses were considerably higher in SLA alone vaccinated groups. Furthermore, exosomes alone exhibited higher IgG1 titers than SLA but failed to induce Leishmania specific IgG2a production. These results indicate that the antigen content of SLA and exosomes but not HK parasites are

sufficiently enriched to generate Leishmania-specific antibody production and that SLA itself supports mixed Th1/Th2 whereas exosomes exhibit a Th2-dominated response.

Comparison of Leishmania antigen-specific IgG1 and IgG2a titers in K-, D-ODN or NR adjuvanted groups showed that nanorings were either ineffective or antagonized antibody production in HK and SLA vaccinated groups, respectively, whereas it modestly supported IgG2a production in the exosome vaccinated group. Based on this inconsistent adjuvanticity behavior of the nanorings, we decided to eliminate this immunostimulatory agent from our potential list of vaccine adjuvants. Use of K- or D-ODN enhanced antigen-specific IgG1 and IgG2a titers in HK vaccinated groups but decreased IgG1 titers in the SLA vaccinated groups. The highest IgG2a titers were generated in the Exosome/D-ODN immunized group.

In summary, based on the humoral responses generated in response to the antigen/adjuvant combinations tested, SLA and exosomes were considered as promising antigens whereas D-type ODN was considered as the optimal adjuvant..

Th1 (IFN-γ and TNF-α), Th2 (IL-4, IL-10 and IL-6) and Th17 (IL-17A) cytokine responses of SLA stimulated splenocytes of immunized mice are summarized in Figure 3.21.

Consistent with the humoral responses, HK parasites alone induced moderate levels of Th2 cytokine production (IL-4, IL-6, IL-10), however failed to induce Th1 and Th17 cytokines. All tested adjuvants suppressed IL-4 and IL-10 production induced by HK parasites and IL-6 production was significantly suppressed when combined with D-ODN or NRs. Furthermore, D-ODN significantly induced both Th1 cytokines. Also, K and D-ODNs lead to significantly increased IL-17 production.
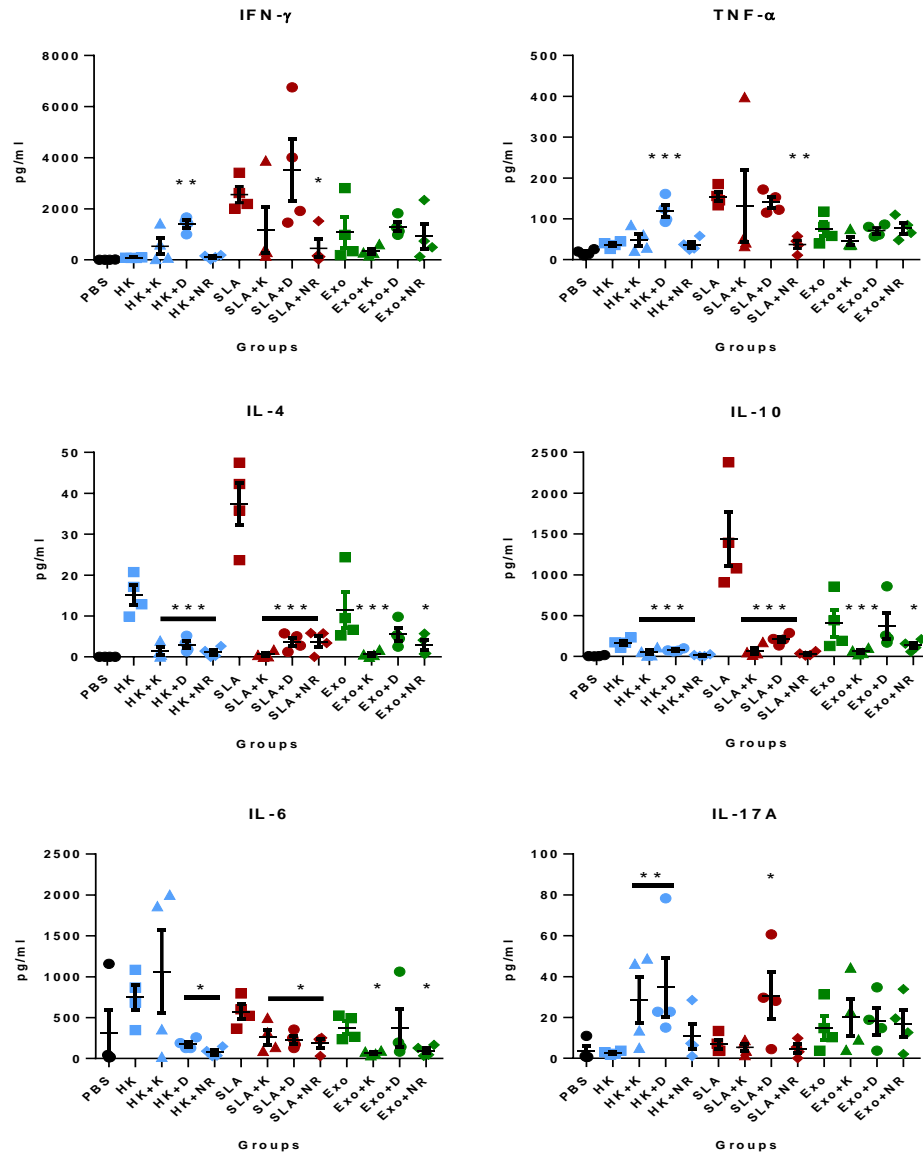
Figure 3.21. Leishmania Specific Th1-Th2-Th17 Cytokine Responses Generated in Mice Immunized
with Candidate Vaccine Formulations

Mice were immunized with the indicated vaccine formulations (see Table 2.4. for doses) twice on
Days 0 and 14. Spleens were collected from animals on Day 21 and splenocytes were prepared as
single cell suspensions. Th1-Th2-Th17 cytokine responses of SLA stimulated (10 μg/ml) splenocytes
were quantified using the cytometric bead array kit.

All antigen-adjuvant combinations were compared to their corresponding antigen alone groups
statistically by Kruskal-Wallis test followed by Conover`s multiple comparison test (*: p<0.05, **:
p<0.01, ***: p<0.001)

111

SLA alone induced high levels of IL-4 and IL-10 and moderate levels of IL-6, indicating a strong Th2 response, whereas moderate levels of Th1 cytokines and very low levels of IL17 were observed. Similar to the HK group, all adjuvants were able to suppress Th2 associated cytokine productions when combined with SLA. Although not significant, only the combination with D-ODN increased IFN-γ production, whereas K-ODN and NRs decreased both IFN-γ and TNF-α production. Moreover, only D-ODN was able to significantly increase IL17 production.

Exosomes alone induced low levels of cytokine production from all Th subsets. None of the adjuvants tested had an impact on IL17 production significantly. While K-ODN and NRs suppressed Th2 cytokines significantly, suppression caused by D-ODN was not significant. There was one outlier in each Th2 cytokines in Exo+D group, which makes it tempting to speculate that this individual error might be the cause of the non-significant outcome. When the levels of antigen specific Th1 cytokines were considered in exosome vaccinated groups, only D-ODN was able to moderately increase IFN-γ levels.

Although, all adjuvants successfully suppressed Th2 responses, only D-ODN was able to upregulate IFN-γ and IL17 production. Therefore, similar to the conclusion derived from measurement of humoral responses, the outcome of cellular responses also identified D-ODN as the most promising vaccine adjuvant.

Based on all observations collectively, SLA and exosomes were determined as potential antigen sources. However, although exosomes combined with D-ODN supported Th1 dominated IgG2a production, cellular responses remained weak. Based on this observation, we hypothesized that immunomodulatory proteins, which are enriched in exosomes, might be interfering with the immunogenicity of exosomes and/or adjuvanticity of D-ODN. In order to circumvent this problem, we proposed to chemically modify exosomes and SLA, which will be discussed in the following section.

3.4.6. Development of a Chemical Modification Protocol to Increase the Immunogenicity of Vaccine Formulations

Based on the results presented in Section 3.4.5., wherein the adjuvants only modestly augmented antigen-specific cytokine responses, we decided to inactivate the enzymatic activity of gp63, since it is abundantly expressed in both SLA and exosomes and exert immunomodulatory effects.

gp63 has been identified as an important virulence factor capable of subverting signaling in target cells. Proteolytic cleavage of anti-microbial peptides and histones by gp63 protects parasites against anti-microbial peptide induced apoptosis and neutrophil extracellular traps (NETs) mediated killing (Gabriel et al., 2010; Kulkarni et al., 2006). Furthermore, gp63 activity provides resistance against complement mediated lysis of parasites through modification of complement proteins (Brittingham et al., 1995). Effects of gp63 are not limited to extracellular milieu. It has been reported that gp63 can target mTOR and downregulate host protein translation in infected macrophages (Jaramillo et al., 2011). Furthermore, protein tyrosine phosphatases, SHP-1 and PTP1B, were reported to be activated upon gp63 cleavage and hence result in inhibition of JAK2 and IRAK1, which are central kinases in IFN-γ and TLR signaling pathways, respectively (Abu-Dayyeh et al., 2008; Blanchette, Racette, Faure, Siminovitch, & Olivier, 1999; Forget et al., 2005; Gomez et al., 2009). Inhibition of these pathways leads to inhibition of iNOS expression, nitric oxide, TNF-α and IL-12 production, therefore abolishing parasiticidal activity of infected macrophages (Forget, Gregory, Whitcombe, & Olivier, 2006; Nandan & Reiner, 1995). Considering the abovementioned data, we hypothesized that inactivation of the proteolytic activity of gp63 without interfering with its antigenic properties may improve the immunogenicity of our vaccine formulations.

Hydrogen peroxide (H_2O_2) can inactivate matrix metalloproteinases through modification of tryptophan and glycine residues located in the catalytical domain of

the enzyme (Fu, Kassim, Parks, & Heinecke, 2003). Furthermore, H_2O_2-inactivated viruses were tested for vaccine production and were found to be highly immunogenic, suggesting that this method preserves most antigenic structures. (Abd-Elghaffar, Ali, Boseila, & Amin, 2016; Amanna, Raué, & Slifka, 2012; Pinto et al., 2013; Poore et al., 2017). Based on its ability to inactivate metalloproteases and its minimal impact on antigenic epitopes, we hypothesized that inactivation of gp63 by H_2O_2 would diminish the immunomodulatory activities of exosomes without changing their antigenic properties.

In the following sub-sections, inactivation of gp63 by H_2O_2 treatment and decomposition of H_2O_2 in vaccine formulations will be discussed.

3.4.6.1. Assessment of gp63 Activity in H_2O_2 Inactivated Leishmania Lysates and Exosomes

To inactivate gp63, exosomes and metacyclic parasites were treated with H_2O_2 at final concentrations of 9% (2.94 M) or 3% (0.98 M). Following H_2O_2 treatment, gp63 activity was evaluated using gelatin zymography.

Gelatin zymography is a SDS-PAGE (sodium dodecyl sulphate - polyacrylamide gel electrophoresis) based method where the gel is supplemented with gelatin. Following completion of electrophoresis, the gel is incubated with zinc (cofactor for gp63) containing buffers and then, stained with coomassie blue. Since the gel contains gelatin, a blue background is formed after staining. Active proteases degrade gelatin and generate cleaved white bands against dark blue background in the area corresponding to size of the protein of interest. Therefore, appearance of the white bands in the gel indicate metalloprotease activity.

To assess gp63 activity, exosomes or whole parasites were treated with different concentrations of H_2O_2 or left untreated. Lysates were prepared from treated or untreated parasites. Sample were then loaded onto a gelatin gel. Ovalbumin (OVA)

protein was loaded to one of the wells as a negative control. Following electrophoresis, incubation, staining and destaining steps, the gel was imaged for evaluation of proteolytic activity.
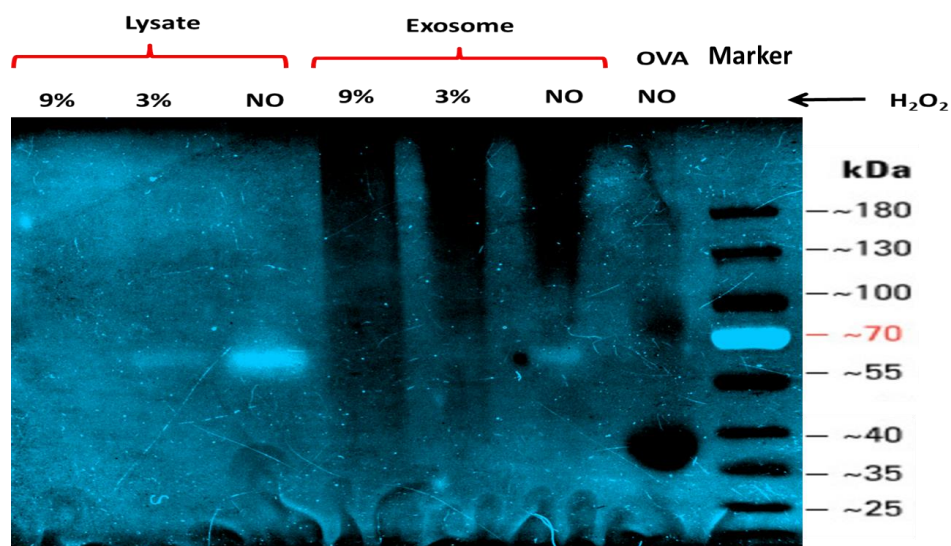
Figure 3.22. Assessment of gp63 Enzymatic Activity in H_2O_2 Untreated or Treated Samples by Gelatin Zymography

H_2O_2 treated (9% and 3%) and untreated samples (~8 μg each) were loaded into individual wells of gelatin containing 7.5% polyacrylamide gel. Ovalbumin (OVA) (~8 μg) was loaded to one well as negative control. Following electrophoresis (150V, ~2 hours), incubation (at 37°C, 24 hours), staining (30-45 minutes) and destaining (2-4 hours) steps, the gel was imaged for evaluation of proteolytic activity.

As expected, no white bands were formed in the lane, where OVA was loaded (Figure 3.22.). In untreated exosome or parasite lysate loaded wells, white bands appeared consistent with the molecular weight of gp63 (60-66 kDa). H_2O_2 treatment of exosomes or lysates resulted in suppression of proteolytic activity in a dose-dependent manner (Figure 3.22.). These results show that, gp63 was inactivated with 3% and 9% H_2O_2 treatments of exosome and lysate samples, respectively. Based on this, 3% (0.98 M) H_2O_2 concentration was used for exosome samples while 9% (2.94 M) H_2O_2

concentration was used for parasites and SLA to inactivate gp63 in the following immunization/challenge experiments.

3.4.6.2. **Decomposition of H_2O_2 by Catalase Treatment**

Following inactivation of gp63 by H_2O_2, residual peroxide remaining in the intended vaccine formulations was decomposed by catalase treatment to eliminate life-threatening ROS-mediated tissue damage.

For this, parasites treated with 9% (2.94M) H_2O_2 and exosomes treated with 3% H_2O_2 were incubated with 36, 18 or 9 Units of catalase to determine the optimal catalase concentration for H_2O_2 removal. Following catalase treatment, success of H_2O_2 decomposition was determined by colorimetric peroxide assay kit.
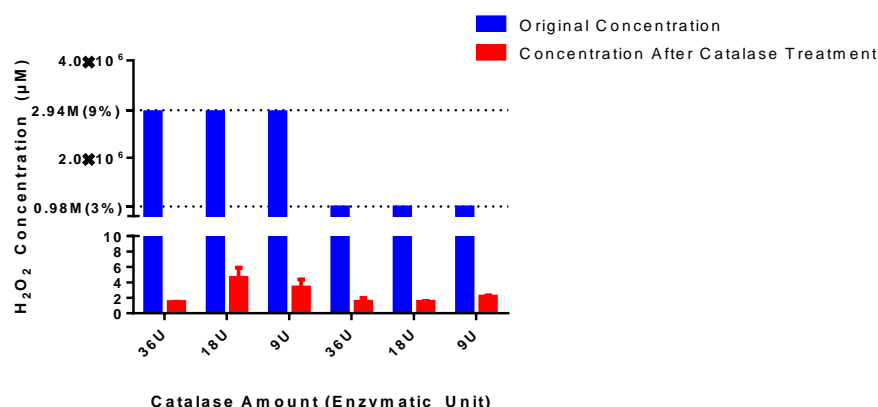
Figure 3.23. Validation of Catalase-Induced Decomposition of H_2O_2

Parasites treated with 9% (2.94M) H_2O_2 and exosomes treated with 3% (0.98M) H_2O_2 were subjected to catalase treatment (36, 18 or 9 Units). H_2O_2 concentrations before (original) and after catalase treatment were quantified by colorimetric peroxide assay kit.

H_2O_2 concentration was reduced to ~4 μM in 9% H2O2 treated parasites and to ~2 μM in 3% H_2O_2 treated exosomes, corresponding to ~7.3x10^5 and 4.9x10^5 fold

reduction (Figure 3.23.). This indicated that for all catalase treated samples, residual H_2O_2 concentrations were reduced to biologically tolerable levels.

To introduce the lowest possible amount of catalase (also a foreign protein) in our vaccine formulations, 9 Units of catalase was chosen for removal of residual H_2O_2 in the following immunization/challenge experiment.

3.4.6.3. **Assessment of gp63 Integrity of H_2O_2 Treated Samples**

As mentioned previously, gp63 inactivation by H_2O_2 was expected preserve on its antigenic properties as reported for viral vaccines. Should, H_2O_2 treatment resulted in gp63 denaturation or altered its confirmation significantly, that would have rendered this treatment inapplicable to vaccination experiments. To test whether the integrity of H_2O_2 treated gp63 was uncompromised, parasites treated with 3% or 9% H_2O_2 were stained with anti-gp63-FITC antibody (1 µg/ml) and analyzed on the green channel of a flow cytometer. This particular antibody recognizes only the intact protein but not the denatured or improperly folded gp63 (see the product data sheet). Thus, if H_2O_2 caused a significant change in the structure of gp63, there would be an observable reduction in percent gp63 positive parasites after treatment.

As can be seen in bottom panels of Figure 3.24., 99.55% and 99.89% of parasites were gp63 positive after 3% and 9% H_2O_2 treatment, respectively. This suggests that H_2O_2 treatment inactivated gp63 without altering its antigenic property. Therefore, H_2O_2 treated exosomes or SLA were used in the following immunization/challenge experiments.
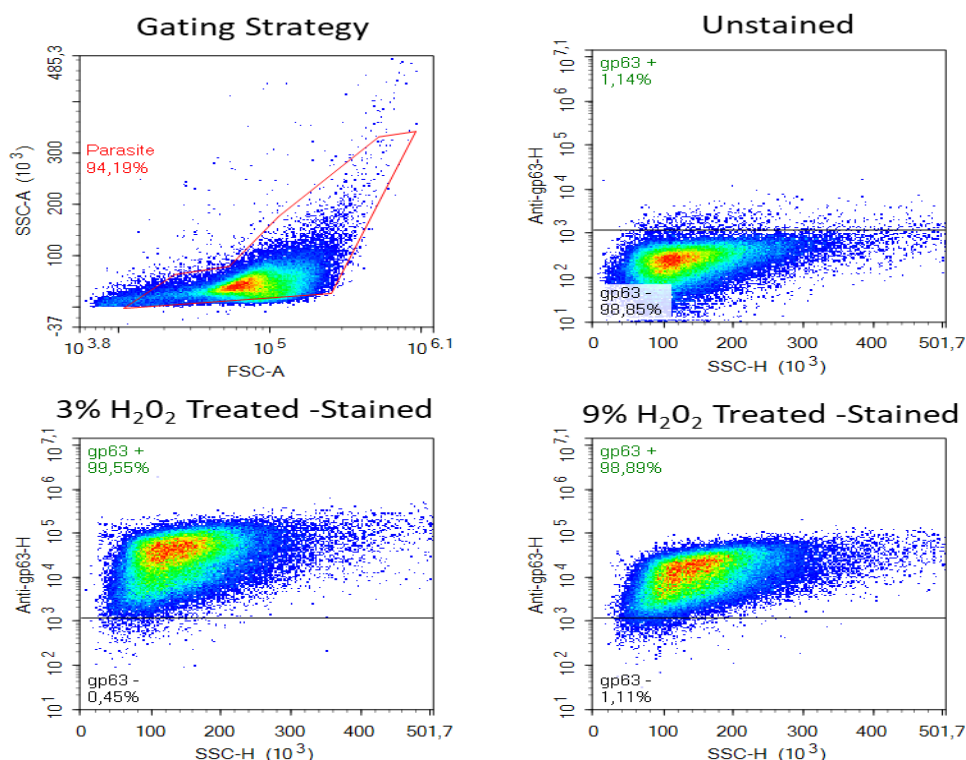
Figure 3.24. Flow Cytometry Analysis of gp63 Integrity following H_2O_2 treatment

Parasites treated with 3% or 9% H2O2 were stained with anti-gp63-FITC antibody (1 μg/ml) and analyzed on the green channel of a flow cytometer.

3.4.7. Evaluation of Immunoprotective Activity of gp63 Inactivated Vaccine Formulations in CL Model

As mentioned in Section 3.4.5. we hypothesized that inactivation of gp63 in vaccine formulations would enhance the immunostimulatory activity of the adjuvants employed in immunization experiments. To test whether this approach improved the immunoprotective activity of candidate antigen/adjuvant combinations, we designed an immunization/challenge experiment incorporating gp63 inactivated versus H_2O_2-untreated vaccine formulations. Furthermore, cellular and humoral responses generated in vaccinated/challenged mice were evaluated.

118

For this purpose, exosomes and SLA were used as source of antigens and D-ODN was used as adjuvant. BALB/c mice (5/group) either were sham treated (PBS) or immunized with exosome/D-ODN combination (Exo+D35) without H_2O_2 treatment. Furthermore, exosomes and SLA treated with H_2O_2 for gp63 inactivation were used as such (Exo-H_2O_2, SLA- H_2O_2) or combined with D-ODN (Exo-H_2O_2 +D35, SLA-H_2O_2 +D35). Mice were vaccinated with these formulations (see Table 2.5 for doses) twice on Days 0 and 14.

Sera of vaccinated mice were collected on Day 21 to assess Leishmania antigen specific humoral responses (IgG1 and Ig2a) using ELISA. Then, antibody titers were calculated based on background levels determined from the unvaccinated group (PBS).

Next, vaccinated mice were challenged with metacylic *L. major* (EGFP-LUC[+]) parasites ($9x10^6$/mouse) on Day 22 and disease progression was monitored by measuring footpads to estimate lesion sizes for 4 weeks. Parasite loads in footpads and lymph nodes (LN) were quantified using IVIS on Day 50.

Furthermore, spleens of vaccinated/challenged mice were collected on Day 50 and levels of cytokine production from Leishmania antigen stimulated splenocytes were quantified by using the Th1-Th2-Th17 cytometric bead array kit to evaluate Leishmania specific cellular responses induced by vaccination/challenge.

Results of *L. major* protection assays (footpad swelling and parasite loads) are summarized in Figure 3.25.
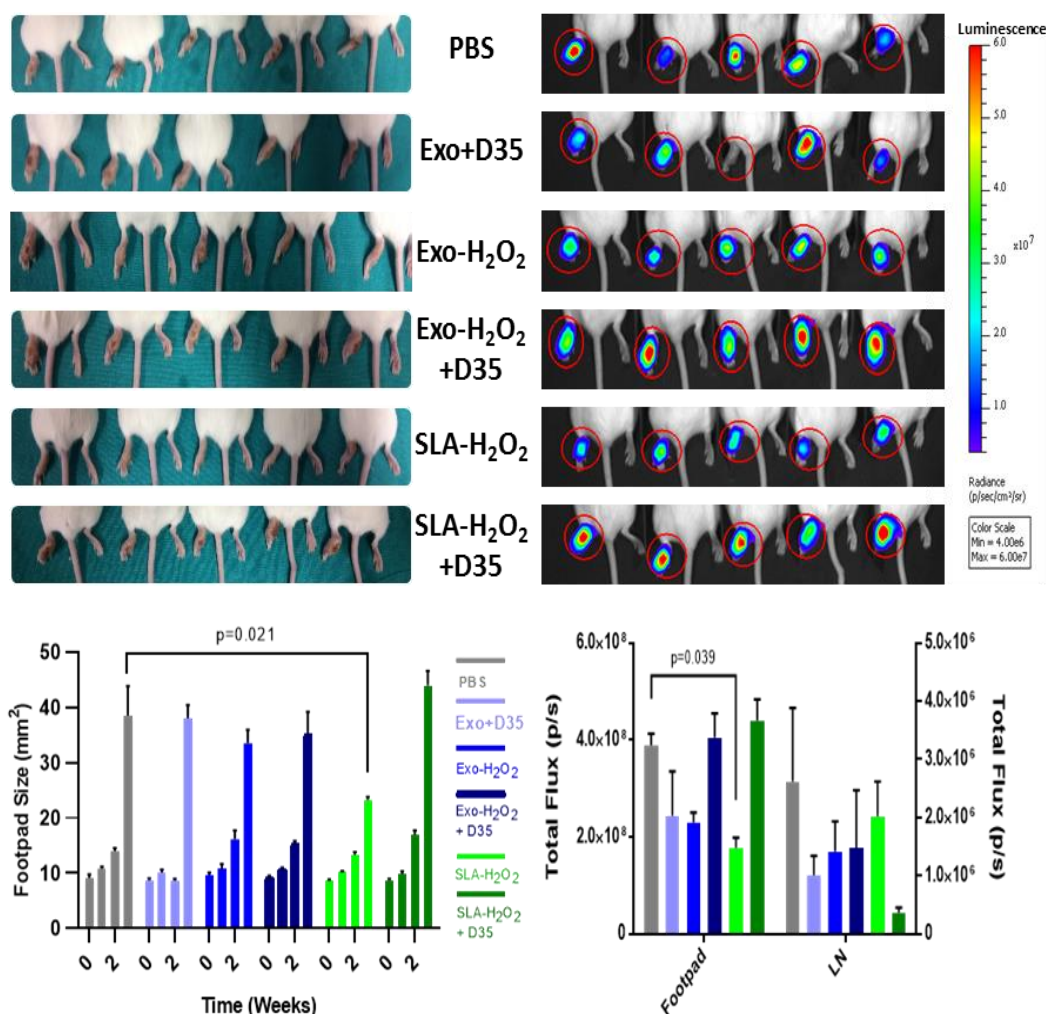
Figure 3.25. Progression of Footpad Swelling and Parasite Loads in Mice Immunized with Candidate Antigen/Adjuvant Combinations with or without gp63 Inactivation

Mice were immunized with the indicated vaccine formulations (see Table 2.5. for doses) twice on Days 0 and 14. Immunized mice were challenged with metacyclic *L. major* (EGFP-LUC[+]) parasites (9×10^6 per mouse) on Day 22. Then, lesion sizes were monitored through footpad measurements for 4 weeks after challenge and presented as width x depth (bottom-left panel). Photos were taken on Week 4 to demonstrate severity of lesions (top-left panels). Parasite loads in footpads and lymph nodes (LN) were quantified using IVIS following luciferin administration (0.75 mg/mouse, 150 µg/ml for LN). Images at the peak point of luminescence readings are presented (top-right panels). Parasite loads in footpads and LNs were quantified based on luminescence signal at peak points (bottom-right panel). For top panels, mice were positioned according to their tag numbers to enable pair-wise comparisons of footpad swelling versus parasite load images.

All antigen-adjuvant combinations were compared to the PBS administered group statistically by Kruskal-Wallis test followed by Dunnet`s multiple comparison test. ($p < 0.05$ considered as significant and significant p-values are stated on the graphs)

120

Based on footpad photos taken on Day 50 (Figure 3.25., top-left panels) severe lesions were observed in PBS (unvaccinated), Exo-H_2O_2 + D35 and SLA-H_2O_2 + D35 groups. Lesion development was delayed significantly only in the SLA- H_2O_2 immunized group. Visual inspection of lesions were consistent with lesion size measurements (Figure 3.25, bottom left panel) where footpad sizes of Exo-H_2O_2 + D35 and SLA-H_2O_2 + D35 groups were comparable to footpad sizes of PBS group, whereas lesion development in the SLA-H_2O_2 vaccinated mice was significantly hindered when compared to PBS group (p=0.021). In summary, based on lesion size measurements, only the SLA-H_2O_2 formulation demonstrated modest immunoprotective activity against *L. major* induced CL.

As discussed in previous sections, to improve assessment of disease severity and progression, parasite loads in footpads and lymph nodes (LNs) of vaccinated/challenged mice were determined by IVIS on Day 50. Images taken from peak luminescence readings were presented in Figure 3.25 (top-right panels). Mice were positioned from left to right in the same order in both footpad photos and IVIS images to enable matched comparison of these two panels (Figure 3.25., top-left and top-right panels). Comparison of these two panels revealed that, although there were some deviations, IVIS measurements generally were in agreement with footpad lesion severity. Consistent with lesion size measurements, quantitative comparison of luminescence signals obtained from infected footpads showed that parasite loads in SLA-H_2O_2 group were significantly (p=0.039) lower than the PBS group (Figure 3.25, bottom-right panel). Furthermore, parasite loads in Exo + D35 and Exo-H_2O_2 groups were moderately decreased when compared to unvaccinated mice (Figure 3.25, bottom-right panel), whereas no significant difference was detected for these groups in terms of lesion size measurements (Figure 3.25, bottom-left panel). These results showed that in general lesion size measurements correlated well with parasites loads when there were no ulcerated lesions (SLA-H_2O_2 group) but deviations were observed when there were ulcerated lesions (Exo + D35 and Exo-H_2O_2 groups), possibly stemming from masking of luminescence in necrotic/ulcerated footpads .

When parasite loads in inguinal lymph nodes were analyzed, among all tested vaccination formulations, only SLA-H_2O + D35 inhibited migration to the closest lymph node, suggestive of prevention of dissemination of parasites (Figure 3.25, bottom-right panel). However, the decrease in lymph node metastasis was not statistically significant, possibly due to the high variation in luminescence readings from LNs.

In summary, gp63 inactivation by H_2O_2 improved immunoprotective effects of SLA (SLA-H_2O_2), whereas metalloprotease inactivation diminished only the parasite loads in Exo-H_2O_2 vaccinated mice to level achieved with adjuvant combined exosomes (Exo + D35). Combination of D-ODN with exosomes as adjuvant (Exo + D35) reduced parasite loads moderately, however when D-ODN adjuvant was used in combination with H_2O_2 treated exosomes or SLA (Exo- H_2O_2 +D35, SLA-H_2O_2 +D35) no protective effect was observed in both parameters. These results indicated two main outcomes: H_2O_2 treatment possibly interfered with adjuvanticity of D-ODN or it did not significantly improve protective effects of exosomes.

Figure 3.26. summarizes Leishmania specific IgG1 and IgG2a titers generated in vaccinated animals.

SLA-H_2O_2, which provided the best protection against CL based on lesion size and parasite loads, stimulated significantly lower IgG1 titers than Exo- H_2O_2 group and failed to induce IgG2a production (Figure 3.26). Leishmania-specific IgG1 induction in the absence of specific IgG2a, is indicative of a Th2 dominant response, which should hypothetically support non-healing lesions. Yet, unexpectedly, results presented in Figure 3.25. indicated otherwise. When SLA-H_2O_2 was combined with D-ODN (SLA-H_2O_2 +D35) there was a modest increase in IgG1 titers and a significant increase in IgG2a titers, indicative of resumption of a balanced Th1/Th2 response (Figure 3.26). Nevertheless, SLA-H_2O_2 +D35 failed to delay on disease progression and had no impact on parasite loads. The discourse between disease progression and dominance of helper T cell responses based on Leishmania-specific antibody

122

subclasses remains a paradox, suggesting that mechanisms other than a Th1 dominated response might contribute to protection.

Figure 3.26. Leishmania Antigen Specific IgG1 and IgG2a Titers in Mice Immunized with Candidate Antigen/Adjuvant Combinations with or without gp63 Inactivation

Mice were immunized with the indicated vaccine formulations (see Table 2.5. for doses) twice on Days 0 and 14. Sera were collected from animals on Day 21. Leishmania antigen specific IgG1 and IgG2a levels in collected sera were quantified by ELISA using SLA coated (10 μg/ml) plates. Antibody titers were calculated based on O.D. readings of unvaccinated group (PBS) and presented in log2 scale.

All antigen-adjuvant combinations were compared with each other statistically by Kruskal-Wallis test followed by Dunnet`s multiple comparison test. ($p < 0.05$ considered as significant and significant p-values are stated on the graphs)

Consistent with results of the immunization experiment presented in Section 3.4.5., all exosome based groups induced high titers of Leishmania antigen specific IgG1 and IgG2a. However, H_2O_2 treated exosomes (Exo-H_2O_2) induced lower IgG2a titers, which was restored with D-ODN adjuvant but not higher than the Exo + D35 vaccinated group (Figure 3.26). Nonetheless, this slight shift towards Th2 dominancy in Exo-H_2O_2 surprisingly resulted in a moderate decrease in parasite load as discussed before (Figure 3.25, bottom-right panel).

In summary, the outcome of Leishmania-specific IgG1 and IgG2a responses induced by the vaccinate formulations contradict well-documented Th1 dominant protection dogma. However, it is conceivable that IgG antibodies may directly contribute to infectivity of Leishmania as suggested by a study where Leishmania-specific IgG correlated with an increase in interleukin IL-10 production in lesions, resulting in antibody-mediated disease exacerbation (Miles, Conrad, Alves, Jeronimo, & Mosser, 2005).

To gain insight into anti-Leishmanial protective mechanism, antigen-specific Th1 (IFN-γ and TNF-α), Th2 (IL-4, IL-10 and IL-6) and Th17 (IL-17A) cytokine responses from SLA stimulated splenocytes (collected on Day 50) of immunized mice were analyzed and the results were summarized in Figure 3.27.

Leishmania antigen specific IFN-γ production from splenocytes of mice vaccinated with Exo + D35 and SLA-H_2O_2 + D35 were significantly increased (p=0.0154 and p=0.0069, respectively) and moderately improved in mice immunized with Exo-H_2O_2 and Exo-H_2O_2 +D35. On the other hand, none of Th2 associated cytokines (IL-4, IL-10 and IL-6) were significantly different from PBS for these groups (Figure 3.27). Therefore, for the abovementioned groups, antigen specific Th1 but not Th2 responses were augmented. Nevertheless, among these groups only the Exo + D35 and Exo-H_2O_2 were able to moderately reduce parasite loads.

Excepting SLA-H_2O_2, all vaccine formulations generated a similar Th1/Th2 cytokine profile. A moderate decrease in IFN-γ and a significant decrease in TNF-α production (p=0.0033) from splenocytes of mice vaccinated with SLA-H_2O_2 were observed. Furthermore, IL-4 and IL-10 production was significantly suppressed (p<0.0001 and p=0.0378, respectively) in these mice (Figure 3.27.). These results indicate that this group had little impact on antigen-specific establishment of Th1/Th2 responses, yet was the most promising group in terms of providing protection against CL (Figure 3.25.).
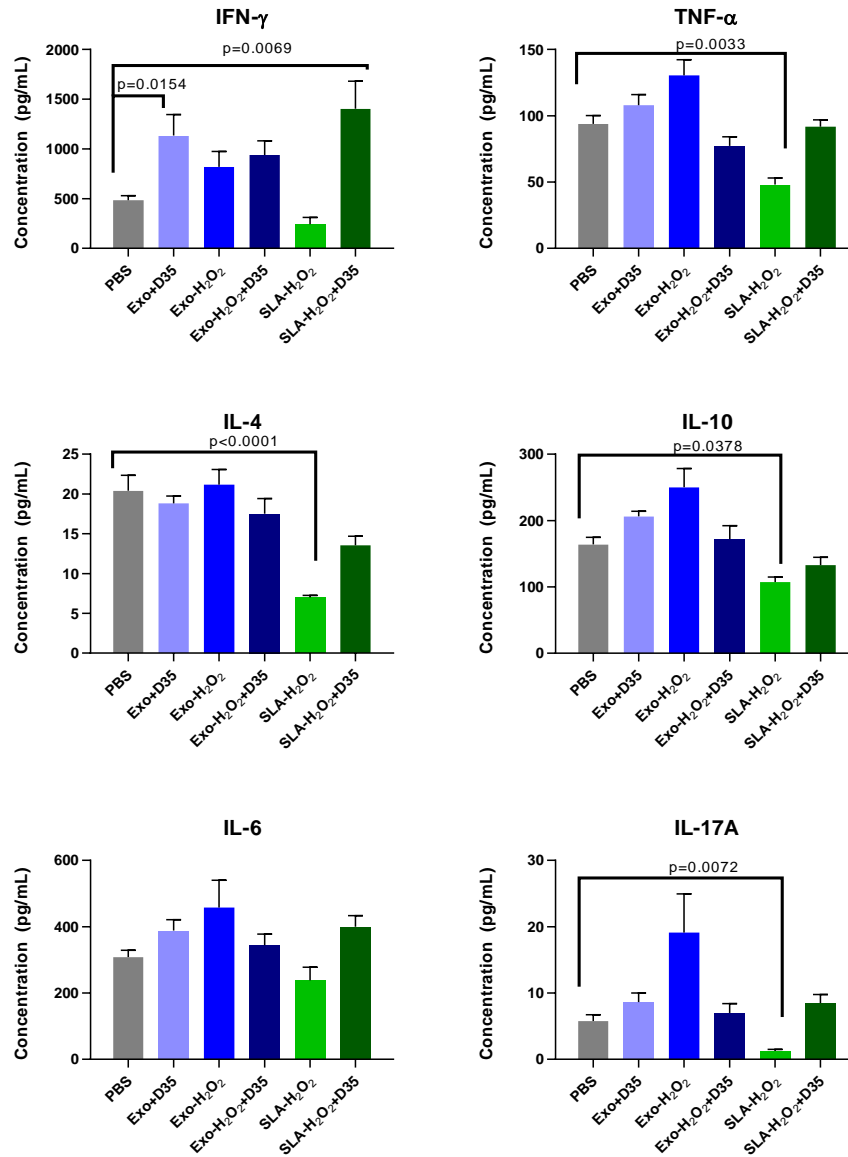
Figure 3.27. Leishmania Specific Th1-Th2-Th17 Cytokine Responses Generated in Mice Immunized
with Candidate Antigen/Adjuvant Combinations with or without gp63 Inactivation

Mice were immunized with the indicated vaccine formulations (see Table 2.5. for doses) twice on
Days 0 and 14. Immunized mice were challenged with metacyclic *L. major* (EGFP-LUC[+]) parasites
($9x10^6$ per mouse) on Day 22. Spleens of mice were collected from animals on Day 50 and
splenocytes were prepared as single cell suspensions. Th1-Th2-Th17 cytokine responses of SLA
stimulated (10 μg/ml) splenocytes were quantified using the cytometric bead array kit.

All antigen-adjuvant combinations were compared to the PBS administered group statistically by
Kruskal-Wallis test followed by Dunnet`s multiple comparison test. (p<0.05 considered as significant
and significant p-values are stated on the graphs)

These inconsistencies between Th1/Th2 responses and disease severity drew our attention to antigen specific Th17 cytokine responses. All tested groups other than the SLA-H_2O_2 formulation, induced moderately increased IL-17A production when compared to PBS whereas IL17-A production was almost non-existent in SLA-H_2O_2 immunized group (Figure 3.27). These observations suggested that in addition to Th1/Th2 dominancy, Th17 responses may play an important role in progression of CL.

Collectively, based on these results, we concluded that H_2O_2 treatment improved the protective ability of SLA but not exosomes. We hypothesized that exosomes may have shielded intraluminal H_2O_2 from catalase decomposition due to their lipid-based vesicular nature and may have resulted in inefficient elimination of H_2O_2 from exosome based formulations. Hence, catalase decomposition approach was abandoned and replaced with a lyophilization-based H_2O_2 removal technique in vaccine formulations, which will be discussed in detail in the following sections. Furthermore, we also envisioned that H_2O_2 treatment could have interfered with the adjuvanticity of D-ODN possibly through oxidation. To expand our arsenal of candidate adjuvants, we included a different glycolipid lipid based adjuvant in addition to D-ODN in the following immunization/challenge experiment.

3.4.8. **Evaluation of Immunotherapeutic Activity of gp63 Inactivated Lyophilized Formulations in CL Model**

As mentioned in Section 3.4.7., lyophilization-based H_2O_2 removal technique was adopted to replace catalase decomposition method in preparation of vaccine formulations. Incorporation of an irrelevant protein in an intended vaccine formulation is not desirable. Furthermore, catalase administration can result in suppression of inflammatory responses (Schalkwijk, Van Der Berg, & Van De Putte, 1985). Therefore, we aimed to eliminate the H_2O_2 contamination from the samples through freeze-drying, where the peroxide is removed in the vapor phase.

To assess the effect of lyophilization on gp63 inactivation, H_2O_2 treated and untreated parasites were freeze-dried, rehydrated and then, gp63 activity was evaluated by gelation zymography as discussed in Section 3.4.6.1. Results indicated that gp63 was inactive in H_2O_2 treated parasites only but lyophilization alone did not inactivate gp63 in H_2O_2 untreated samples, which otherwise would have rendered H_2O_2 treatment redundant (Figure D.1., Appendix D). Furthermore, to assess gp63 integrity in lyophilized samples, H_2O_2 treated and untreated parasites were processed through lyophilization. Following hydration, they were stained with anti-gp63-FITC antibody and analyzed by flow cytometry as previously discussed in Section 3.4.6.3. Results showed that 99.70% of untreated and 98.50% of H_2O_2 treated parasites were gp63 positive following lyophilization (Figure D.2., Appendix D). Based on these, gp63 inactivation and integrity following lyophilization was consistent with non-lyophilized formulations, which indicates that catalase decomposition method could be replaced with lyophilization-based technique to eliminate residual H_2O_2 without interfering with our previous findings.

Following adoption of the lyophilization technique, we designed a small-scale immunotherapy experiment to test the potential immunotherapeutic activities of the intact or chemically inactivated lyophilized/rehydrated vaccine formulations. As discussed in the previous section, gp63 inactivation and H_2O_2 removal through catalase treatment failed to improve the immunoprotective effects of exosomes and possibly interfered with adjuvanticity of D-ODN. To test whether exclusion of catalase improved the immunoprotection of D-ODN adjuvanted formulations, Exo+D35, Exo-H_2O_2 +D35 and SLA-H_2O_2 +D35, were selected.

To prepare lyophilized formulations, H_2O_2 treated antigen/adjuvant combinations were dehydrated using a freeze-dryer to evaporate residual H_2O_2. Next, dehydrated formulations were re-hydrated in a controlled manner to encapsulate D-ODNs with Leishmania exosomes (M. Gursel & Gursel, 2016) to improve uptake and immunostimulatory activities of D-ODN (Erikçi, Gursel, & Gürsel, 2011; I. Gursel,

Gursel, Ishii, & Klinman, 2001). H_2O_2 untreated formulations were also subjected to the same procedure for experimental consistency.

To test the immunotherapeutic effects of these formulations, BALB/c mice were first challenged with metacyclic *L. major* (EGFP-LUC[+]) parasites ($9x10^6$ per mouse) on Day 0. Challenged mice were monitored visually for lesion development and when noticeable lesions developed (Day 21), formulations were injected subcutaneously (see Table 2.6 for administered doses). This time point was demonstrated as 'Day 0' in Figure 3.28. to specify initiation of immunotherapy. The therapeutic injection was repeated on Day 24 (3 in the figure). Lesions sizes were monitored by footpad measurements on Days 20 (-1 in the figure), 24 (3 in the figure), 26 (5 in the figure), 28 (7 in in the figure) and 31 (10 in the figure). Furthermore, parasite loads in infected footpads were quantified on Days 20 (-1), 25 (5) and 31 (10) using IVIS.

Based on footpad photos taken on Day 31 (10 days after the first therapeutic injection) (Figure 3.28, top-left panels), significantly healed lesions were observed in mice treated with the Exo-H_2O_2 + D35 and SLA-H_2O_2 + D35 formulations. Lesion size measurements were consistent with these visual inspections. Although statistically not significant, lesion development in these groups were moderately delayed in response to therapeutic injections (Figure 3.28, bottom-left panel). This experiment was terminated on Day 31 (in our regular time course) but extending the duration of lesion size monitoring would have better reflect the delay in lesion development.
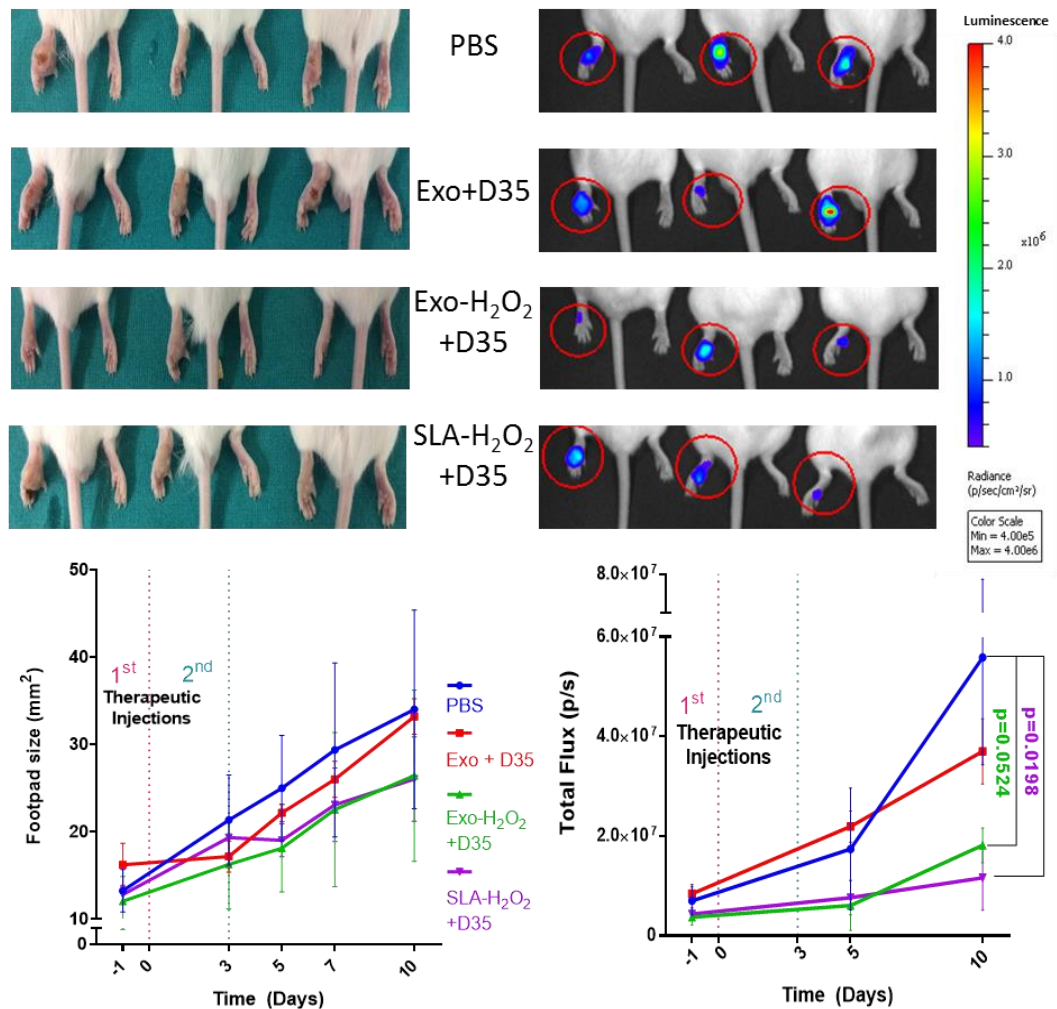
Figure 3.28. Assessment of Immunotherapeutic Activity of Chemically Inactivated Lyophilized Vaccine Formulations

Mice were challenged with metacyclic *L. major* (EGFP-LUC[+]) parasites (9×10^6 per mouse) on Day 0 and were injected with therapeutic formulations (s.c.) (see Table 2.6 for doses) on Day 21, (specified as Day '0'). Therapeutic injection was repeated on Day 24 (Day 3 in graphs). Then, lesion sizes were monitored through footpad measurements for 10 days after the first therapeutic application and presented as width x depth (bottom-left panel). Photos were taken 10 days after the first therapeutic injection on Day 31 (Day 10 in graphs) to demonstrate severity of lesions (top-left panels). Parasite loads in footpads were quantified using IVIS following luciferin administration (0.75 mg/mouse) on Days 20 (Day -1), 26 (Day 5) and 31 (Day 10). Images are representative of peak luminescence readings on Day31 (Day 10) (top-right panels). Parasite loads in footpads were quantified based on luminescence signal at peak points on Day 31(10) (bottom-right panel). For top panels, mice were positioned according to their tag numbers to enable pair-wise comparisons of footpad swelling versus parasite load images.

All therapeutic formulations were compared to the PBS administered (untreated) group statistically by Kruskal-Wallis test followed by Dunnet`s multiple comparison test. (p<0.05 considered as significant and significant p-values are stated on the graphs)

Images taken from peak luminescence readings on Day 31 (10) were presented in Figure 3.28 (top-right panels). Mice were positioned from left to right in the same order in both footpad photos and IVIS images to enable matched comparison of these two panels (Figure 3.28., top-left and top-right panels). As discussed in Section 3.4.7. (Figure 3.25), these two panels are consistent in general but there were striking differences between footpad swelling and parasite loads in some animals. For example, significant swelling was observable in the photo of footpad of first mouse of SLA-H_2O_2 + D35 treated mice (located at left in the corresponding photo, Figure 3.28, top-left panel), whereas luminescence reading (located at left in corresponding photo, Figure 3.28, top-right panel) indicated low parasite load in this footpad. Since healing of a lesion requires complex immunological processes and tissue re-modelling, elimination of parasites were not directly reflected to footpad swelling (Hill et al., 1983; Lima, Bleyenberg, & Titus, 1997). In the same context, parasites loads in footpads of Exo-H2O2 + D35 and SLA-H2O2 + D35 treated mice were significantly lower than footpads of untreated (PBS) mice (Figure 3.28, bottom right panel), whereas differences in lesion sizes of these groups were found to be statistically non-significant when compared to the untreated (PBS) group. The discord between the two-abovementioned methods support the idea that extended lesion size monitoring represents the therapeutic outcome in a delayed fashion, whereas parasite load measurements exemplify disease progression in real time. Therefore, these results suggested that parasite load determination by IVIS enabled more accurate and quicker assessment of severity of the disease than lesion size estimation.

As mentioned above, parasite loads in footpads of Exo-H2O2 + D35 and SLA-H2O2 + D35 treated mice were significantly lower than untreated (PBS) mice (p=0.0524 and p=0.0198, respectively), whereas lesion sizes are only moderately reduced in these groups. Footpads of Exo-D35 treated mice exhibited moderate decrease in parasite loads when compared to footpads of untreated mice and no difference was observed between these two groups in terms of lesion size.

Based on these findings, gp63 inactivation of exosomes and SLA combined with D-ODN adjuvant (Exo-H$_2$O$_2$ +D35 and SLA-H$_2$O$_2$ +D35) improved the immunotherapeutic effects of these formulations when prepared using the lyophilization-based technique. In contrast, these formulations were unable to provide immunoprotective effects in the previous immunization/challenge experiment (Section 3.4.7). In light of this promising outcome, lyophilized formulations were used in the following immunization experiment with extended antigen/adjuvant combinations.

3.4.9. Evaluation of Immunoprotective Activity of gp63 Inactivated Lyophilized Vaccine Formulations in CL Model

As mentioned in the previous section gp63 inactivation coupled with H$_2$O$_2$ removal through lyophilization improved the immunotherapeutic activities of the tested formulations. To examine whether lyophilization method also improved the immunoprotective activities of chemically inactivated vaccine formulations, we designed an immunization/challenge experiment where extended lyophilized/rehydrated antigen/adjuvant combinations were used.

As discussed in Section 3.4.7, chemical inactivation may have interfered with the adjuvanticity of D-ODN possibly through its oxidation or the Th1/Type I IFN inducing activity of D-ODN may have proved counterproductive in our CL model. To elucidate these possibilities and extend our efforts to identify the best adjuvant for inclusion in our protective vaccine. NKT promoting molecule alpha-Galactosylceramide (αGalCer, αGC) was also combined with the chemically inactivated or untreated exosomes as an alternative candidate. αGalCer is a synthetic glycolipid that can bind to non-classical MHC-I molecules (CD1d) expressed by antigen presenting cells (APCs) (Brennan, Brigl, & Brenner, 2013). αGalCer bound to CD1d is recognized by invariant natural killer cells (iNKT). αGalCer recognition in the context of CD1d, induces activation of iNKTs and lead to IFN-γ production,

131

thereby promoting innate and adaptive immunity (Borg et al., 2007; Kawano et al., 1997; Smyth et al., 2002).

In addition to αGalCer, to expand our antigen/adjuvant combinations, lyophilized/rehydrated whole parasites with or without chemical inactivation were also used as an alternative source of antigen to heat-killed parasites. Furthermore, chemically inactivated lyophilized parasites were combined with D-ODN to evaluate possible effects of H_2O_2 on adjuvanticity of D-ODN when combined with a different antigen source other than exosomes or SLA.

In this extended immunization/challenge experiment, lyophilized parasites, exosomes or SLA were used as source of antigens with or without chemical inactivation and combined with D-ODN or αGalCer as adjuvants. Full list of tested antigen/adjuvant combinations were specified in Table 2.7 and in the figures presented in this section (Figure 3.29.-31.).

To test the immunogenicity of lyophilized/rehydrated vaccine formulations, BALB/c mice were either sham treated (PBS) or immunized with the vaccine formulations (see Table 2.7 for doses) twice on Days 0 and 14.

Sera of vaccinated mice were collected on Day 21 to assess Leishmania antigen specific humoral responses (IgG1 and Ig2a) using ELISA. Then, antibody titers were calculated based on background levels determined from the unvaccinated group (PBS).

Next, vaccinated mice were challenged with metacylic *L. major* (EGFP-LUC[+]) parasites ($9x10^6$/mouse) on Day 25 and disease progression was monitored by footpad measurements to estimate lesion sizes for the duration of 5 weeks. Parasite loads in footpads were quantified using IVIS on Day 60. Furthermore, spleens of vaccinated/challenged mice were collected on Day 60 and levels of cytokine production from Leishmania antigen stimulated splenocytes were quantified by using the Th1-Th2-Th17 cytometric bead array kit to evaluate Leishmania specific cellular responses induced by vaccination/challenge.

132
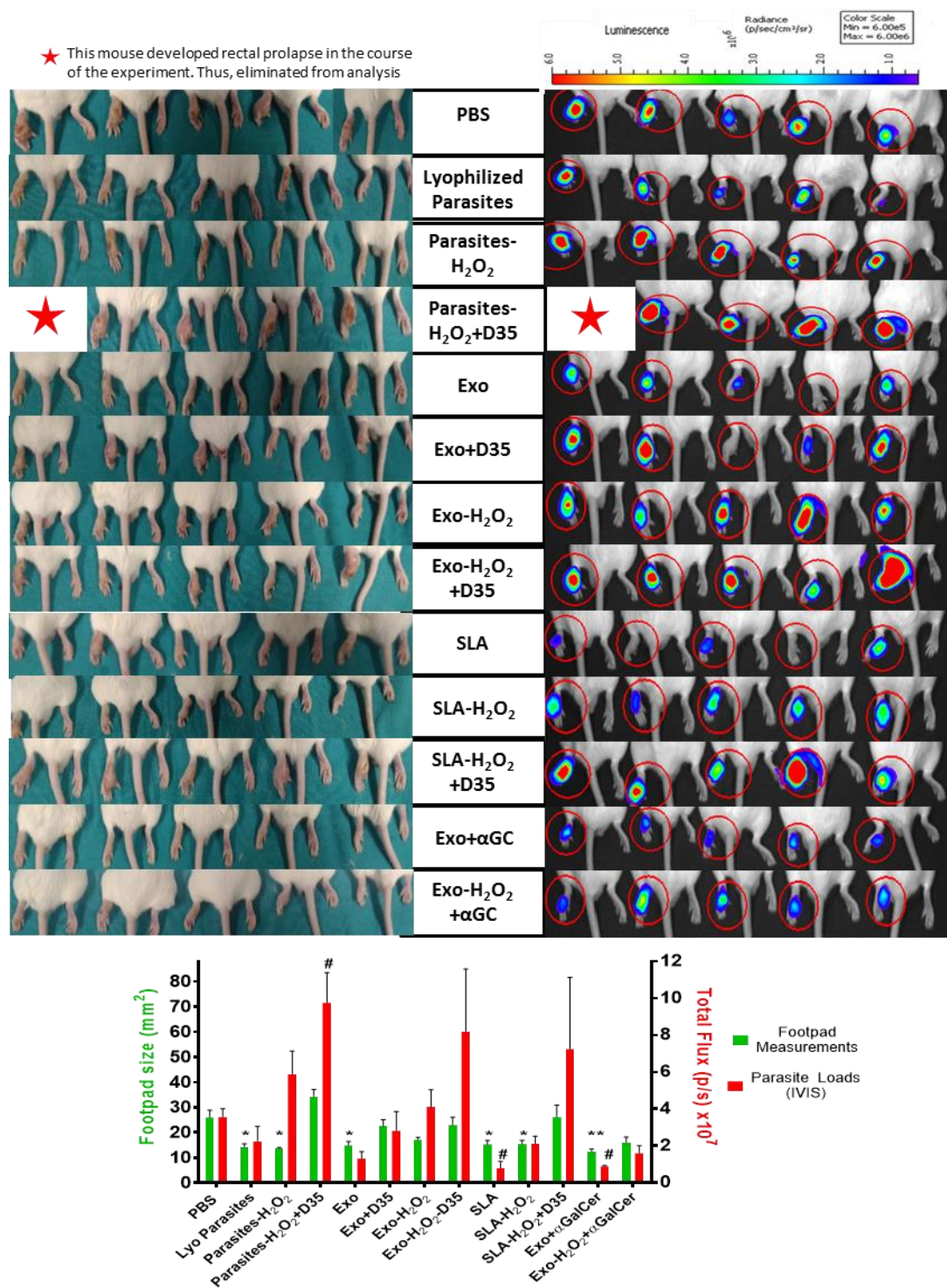
Figure 3.29. Progression of Footpad Swelling and Parasite Loads in Mice Immunized with Lyophilized Antigen/Adjuvant Combinations with or without gp63 Inactivation

133

Mice were immunized with the indicated vaccine formulations (see Table 2.7. for doses) twice on Days 0 and 14. Immunized mice were challenged with metacyclic *L. major* (EGFP-LUC$^+$) parasites (9×10^6 per mouse) on Day 25. Then, lesion sizes were monitored through footpad measurements for 5 weeks after challenge and presented as width x depth (bottom panel). Photos were taken on Week 5 to demonstrate severity of lesions (top-left panels). Parasite loads in footpads were quantified using IVIS following luciferin administration (0.75 mg/mouse). Images at the peak point of luminescence readings are presented (top-right panels). Parasite loads in footpads were quantified based on peak luminescence signals (bottom panel). For top panels, mice were positioned according to their tag numbers to enable pair-wise comparisons of footpad swelling versus parasite load images.

All antigen-adjuvant combinations were compared to the PBS administered group statistically by Kruskal-Wallis test followed by Dunnet`s multiple comparison test. (*: $p<0.05$, **: $p<0.01$ for lesion sizes, #: $p<0.05$ for parasite loads)

Results of parasite protection assays (footpad swelling and parasite loads) are summarized in Figure 3.29.

As expected, in unvaccinated (PBS) group severe footpad lesions were visible on Day 60 (Figure 3.29., top-left panels). Similarly, all mice in the parasites-H$_2$O$_2$+D35 immunized group and one mouse in each of the Exo-H$_2$O$_2$+D35 and SLA-H$_2$O$_2$+D35 groups (Mouse #5 and #4, respectively), exhibited severely ulcerated lesions (even worse than PBS). In other mice of the latter two groups, severity of developed lesions were comparable to the unvaccinated group. In general, for all groups where D-ODN was combined with chemically inactivated antigens (parasites-H$_2$O$_2$+D35, Exo-H$_2$O$_2$+D35, SLA-H$_2$O$_2$+D35) disease progression was exacerbated. Consistent with the visual inspections, lesion sizes of these groups were not significantly different from the unvaccinated group and even moderately increased in the parasites-H$_2$O$_2$+D35 group (Figure 3.29, bottom panel). Interestingly, lesion development was delayed noticeably in mice, which were vaccinated with antigen alone formulations (Lyo-parasites, Exo, SLA) (Figure 3.29., top-left panels). Furthermore, consistent with results of the previous vaccination/challenge experiment (Section 3.4.7), lesion development was delayed in mice vaccinated with chemically inactivated SLA (SLA-H$_2$O$_2$). Moreover, mice vaccinated with exosomes adjuvanted with αGalCer exhibited noticeably delayed lesion development (Exo-αGC). Visual inspection of footpads corroborated with lesions size measurements (Figure 3.29, bottom panel), where statistically significant reduction was observed in antigen alone groups (Lyo-parasites,

134

Exo, SLA), SLA-H$_2$O$_2$ and Exo-αGC groups with respect to PBS control. While αGalCer was able to improve immunoprotective effects of exosomes based on lesion sizes, D-ODN failed to do so.

Parasite loads quantified using IVIS on Day 60 were presented in Figure 3.29, top right panels. Mice were positioned from left to right in the same order in both footpad photos and IVIS images to enable matched comparison of these two panels. As discussed before, parasite loads in general were consistent with lesion size measurements. Parasite loads in mice vaccinated with antigen alone formulations or Exo-αGC were significantly lower than unvaccinated (PBS) mice. However, there was no significant improvement provided by D-ODN adjuvant or chemical inactivation of source of antigens when compared to untreated antigen alone formulations. As discussed previously, deviations between lesion sizes and parasite loads were observed especially in severely ulcerated footpads. Thus, parasite loads in mice, which were vaccinated with parasites-H$_2$O$_2$+D35, Exo-H$_2$O$_2$+D35, SLA-H$_2$O$_2$+D35 were higher than expectations based on lesion sizes. Parasite loads in parasites-H$_2$O$_2$+D35 group were significantly higher than unvaccinated (PBS) group and although statistically non-significant (due to outliers mentioned before), were moderately increased in Exo-H$_2$O$_2$+D35 and SLA-H$_2$O$_2$+D35 (Figure 3.29, bottom-panel). These observations in terms of parasite loads also supported the interpretation of exacerbation of disease when D-ODN was combined with chemically inactivated antigen sources.

In summary, based on lesion development and parasite loads, antigen alone formulations provided a significant immunoprotection and this protection was improved when αGalCer were combined with exosomes, at least. Use of D-ODN as adjuvant had no effect on immunoprotection provided by antigen alone groups and even exacerbated the disease when combined with chemically inactivated source of antigens. Although SLA-H$_2$O$_2$ formulation had immunoprotective effects, it was not significantly different from SLA alone formulation. In the same context, chemical inactivation did not improve protective effects of exosomes. These observations

showed that although chemical inactivation improved immunotherapeutic effects of lyophilized formulations (Section 3.4.8.), this was not the case in the immunoprotective vaccine trial. These results suggest that inactivation of gp63 might be of benefit in immunotherapy where live parasites and the therapeutic agents co-exist, but provide no additional advantage to the immunoprotective activity of the antigen formulations.

To gain insight to how humoral responses contributed to protection, Leishmania antigen specific IgG1 and IgG2a responses were analyzed (Figure 3.30).
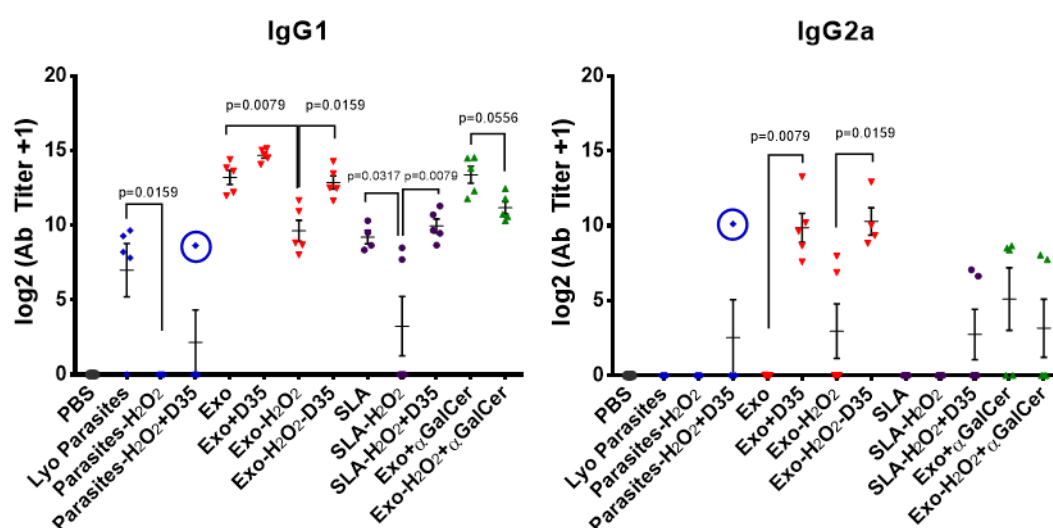
Figure 3.30. Leishmania Antigen Specific IgG1 and IgG2a Titers in Mice Immunized with Lyophilized Antigen/Adjuvant Combinations with or without gp63 Inactivation

Mice were immunized with the indicated vaccine formulations (see Table 2.7. for doses) twice on Days 0 and 14. Sera were collected from animals on Day 21. Leishmania antigen specific IgG1 and IgG2a levels in collected sera were quantified by ELISA using SLA coated (10 μg/ml) plates. Antibody titers were calculated based on O.D. readings of unvaccinated group (PBS) and presented in log2 scale. Blue circle was used to indicate the outlier in the corresponding group.

All antigen-adjuvant combinations were compared with each other statistically by Kruskal-Wallis test followed by Dunnet`s multiple comparison test. ($p < 0.05$ considered as significant and significant p-values are stated on the graphs)

There was an outlier observed in the parasites-H_2O_2+D35 group for both IgG subtypes (same mouse, Figure 3.30, encircled in blue). Therefore, this outlier was excluded from statistical analyses.

All exosome based formulations induced high levels of antigen-specific IgG1 production (Figure 3.30). The only formulations which were capable of inducing significant amount of specific IgG2a were Exo+D35 and Exo-H_2O_2+D35, indicating a shift towards Th1 response in the presence of D-ODN adjuvant (Figure 3.30). However, both of these formulations failed to provide significant immunoprotection against CL (Figure 3.29). Exo alone formulation induced no IgG2a production (indicative of absent Th1 response) yet, provided significant immunoprotection against CL. Similar to Exo alone formulation, other antigen alone formulations (Lyo-parasites, SLA), which were shown to provide significant immunoprotection also induced high levels of IgG1 production with no IgG2a induction (Figure 3.30). Other formulations that partially induced IgG2a were SLA-H_2O_2+D35, Exo+αGalCer and Exo-H_2O_2+αGalCer triggered high levels of IgG1 production, suggestive of a Th2 bias over Th1 (Figure 3.30). Although these groups induced similar levels of specific IgG2a/IgG1, SLA-H_2O_2+D35 failed to protect, whereas Exo-H_2O_2+αGalCer and especially Exo+αGalCer delayed lesion development and substantially lowered parasite loads (Figure 3.29). In brief, two formulations that induced significantly increased IgG2a production failed to provide immunoprotection. However, all formulations that were defined as immunoprotective based on lesion development and parasite loads induced high levels of IgG1 production with no IgG2a induction. These results suggest that although Th1 responses are required for parasite clearance, IgG2a itself might.

It has been reported that both IgG1 and IgG2a are capable of inducing IL-10 in macrophages *in vitro* and recognition of IgG1-*L. maxicana* complexes through FcγR (receptor for IgG) leads to secretion of high levels of IL-10 and suppression of IL-12 production , both of which contributes to disease progression *in vivo* (Chu, Thomas, Patel, & Buxbaum, 2010; Miles et al., 2005; B. N. Thomas & Buxbaum, 2008). These

findings raise the possibility that IgG subclasses may exert separate roles in CL caused by *L. major*. In this context, specific IgG2a production failed to provide immunoprotection, yet no IgG2a was induced in mice that developed the most severe lesions (parasites-H_2O_2+D35 group). These observations eliminate a possible pathogenic role of IgG2a in our model of CL. When disease severity and specific IgG1 levels were compared, high IgG1 production was observed in parasites-H_2O_2+D35 immunized mice that developed the most severe lesions and in Exo or Exo-αGalCer vaccinated animals that provided protection. Furthermore, another interesting observation was that although chemical inactivation of all antigen sources reduced specific IgG1 production significantly (Parasites-H_2O_2, Exo-H_2O_2 and Exo-H_2O_2) when compared to their corresponding antigen alone groups, this reduction was not correlated with better immunoprotection. These results suggest that specific IgG1 has no direct role in disease progression. In summary, conclusions based on IgG subclass responses and hence the dominance of Th2 versus Th1 dominated responses might over-simplify the mechanism(s) pivotal in providing immunity to Leishmania infections. Such a reductionist approach ignore the contribution of Th17 responses, as will be discussed, in results summarizing cellular responses.

To provide a better understanding of immunoprotection against CL, Leishmania antigen-specific Th1 (IFN-γ and TNF-α), Th2 (IL-4, IL-10 and IL-6) and Th17 (IL-17A) cytokine responses from SLA stimulated splenocytes (collected on Day 60) of immunized mice were analyzed and the results were summarized in Figure 3.31.

138
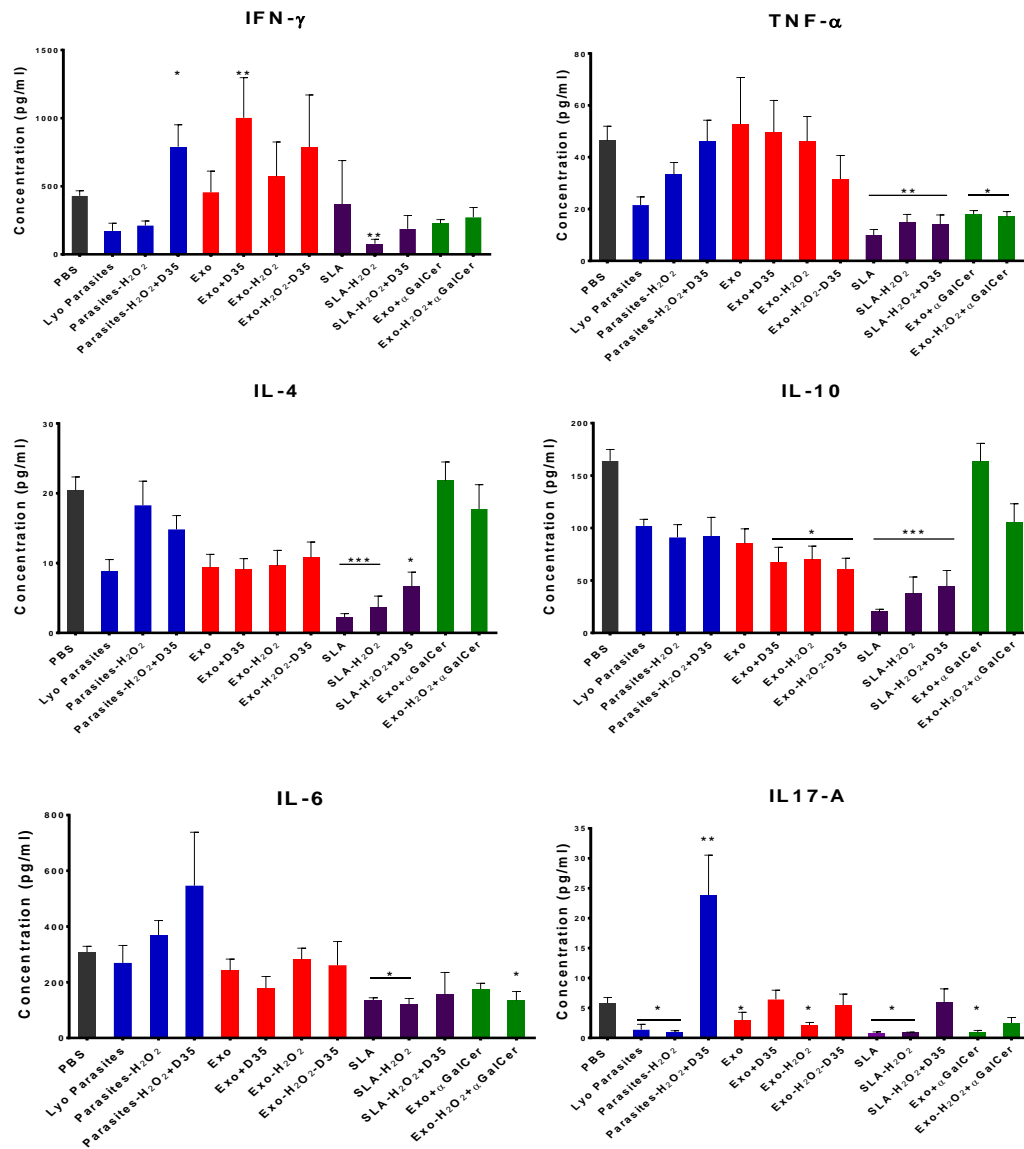
Figure 3.31. Leishmania Specific Th1-Th2-Th17 Cytokine Responses Generated in Mice Immunized with Lyophilized Antigen/Adjuvant Combinations with or without gp63 Inactivation

Mice were immunized with the indicated vaccine formulations (see Table 2.7 for doses) twice on Days 0 and 14. Immunized mice were challenged with metacyclic *L. major* (EGFP-LUC[+]) parasites (9×10^6 per mouse) on Day 25. Spleens of mice were collected from animals on Day 60 and splenocytes were prepared as single cell suspensions. Th1-Th2-Th17 cytokine responses of SLA stimulated (10 μg/ml) splenocytes were quantified using the cytometric bead array kit.

All antigen-adjuvant combinations were compared to the PBS administered group statistically by Kruskal-Wallis test followed by Dunnet`s multiple comparison test. (*: p<0.05, **: p<0.01, ***: p<0.001)

Leishmania antigen specific IFN-γ production from splenocytes of mice vaccinated with Exo + D35 was significantly increased when compared to unvaccinated (PBS) group. Exo-H_2O_2 + D35 vaccinated mice also displayed a modest increase. On the other hand, IL-10 production was significantly suppressed and moderate decrease in both groups in IL-4 and IL-6 was present. These results indicated that among all vaccine formulations, the most Th1 dominant Leishmania specific response was generated in these groups but both failed to provide immunoprotection against CL.

Mice vaccinated with parasites-H_2O_2-D35 formulation stimulated significantly increased IFN-γ production and moderately increased IL-6 production, exhibiting a balanced Leishmania specific Th1/Th2 response, which resulted in exacerbation of disease.

Vaccine formulations that provided significant immune protection (Lyo-parasites, Exo, SLA, SLA-H_2O_2, Exo+αGC) exhibited variable Th1/Th2 cytokine profiles. None of the Th1/Th2 cytokines significantly differed between the unvaccinated and Exo alone group, where levels correlated with balanced Th1/Th2 response. For lyo-parasites vaccinated mice, while Th2 cytokine levels were comparable to Exo alone vaccinated mice, Th1 cytokine levels were lower than Exo group, indicating a more Th2 dominant response at low levels. SLA and SLA-H_2O_2 formulations induced significantly suppressed production of both Th1 and Th2 cytokines, indicating balanced Th1/Th2 responses at low levels. On the other hand, Exo+αGC which provided significant immune protection, induced significantly low levels of Th1 cytokine production but generated significant IL-4 and IL-10 production, indicative of a Th2 dominant response. To summarize, vaccine formulations, which were evaluated as immunoprotective, exhibited either a balanced Th1/Th2 or a Th2 dominated response. These findings suggest that establishment of a Th1 dominant response may not be the sole factor providing immunoprotection against CL. Therefore, consistent with the results of previous vaccination/challenge experiment

(Section 3.4.7) Leishmania antigen specific Th17 responses (IL-17) were thought to be of critical importance and were evaluated.

Unlike Th1/Th2 dominancy, IL-17 production from splenocytes of vaccinated/challenged mice followed a pattern consistent with the outcome of immunoprotection. Mice vaccinated with parasites-H_2O_2-D35 formulation stimulated significantly increased IL-17 production when compared to the unvaccinated group and resulted in exacerbation of disease. Although mice vaccinated with Exo+D35 and Exo-H_2O_2+D35 formulations exhibited a Th1 dominated response, IL-17 production in these mice were not significantly different from unvaccinated group and these groups also failed to provide immunoprotection against CL. All vaccine formulations that provided significant immune protection (Lyo-parasites, Exo, SLA, SLA-H_2O_2, Exo+αGC) induced significantly lower IL-17 production than the unvaccinated control. These results indicate that Th17 responses promote parasitemia and contribute to progression of *L. major*-induced CL. It has been reported that IL-17 deficient BALB/c mice infected with *L. major* developed significantly smaller lesions when compared to wild type mice even though both exhibited a Th2 dominated response (Lopez Kostka et al., 2009). Although IL-17 can recruit neutrophils to the infection site and augment ROS production in macrophages to eliminate intracellular parasites, in the absence IL-10, this enhancement aggravates tissue injury and results in progression of CL (Gonçalves-de-Albuquerque et al., 2017; Gonzalez-Lombana et al., 2013). These findings are consistent with our data and explains the lack of immunoprotection in Th1 dominated responses when such a response is accompanied by increased Th17 responses.

Collectively, our data indicate that antigens adjuvanted with D-ODN induce Th1 dominated responses accompanied by Th17 responses, which failed to provide immunoprotection, and even exacerbated the disease. When D-ODN was combined with chemically inactivated antigens, Th17 responses were significantly elevated (parasites-H_2O_2+D35). Vaccine formulations, which provided immunoprotection against CL, induced Th1/Th2 balanced or Th2 dominated responses with significantly

suppressed Th17 responses. These observations indicate that instead of inducing strong Th1 responses accompanied with Th17 responses, a mild Th1 dominated response in the absence of IL-17 production may be the ideal anti-Leishmanial protection generating mechanism induced through vaccination.

CHAPTER 4

CONCLUSIONS AND FUTURE PERSPECTIVES

In our laboratory, early studies on Leishmania parasites involved *L. tropica* species, in which evaluation immunoprotective effects of potential vaccine formulations required a period of 10 months in the murine model of CL (Güngör, 2017). During these studies, *L. major* parasites isolated from a CL patient's lesion were kindly provided by our collaborator Prof. Ahmet Özbilgin. Similar to *L. tropica, L. major* species is among the dominant species in Turkey causing cutaneous leishmaniasis (CL) (Özbilgin et al., 2016). *L. major* is also more aggressive than *L. tropica* species and manifests as severely ulcerated lesions (Remadi et al., 2017; Spotin, Rouhani, & Parvizi, 2014). Considering these, we switched to *L. major* species as our infectious agent in this thesis. Throughout this thesis, we improved several experimental approaches, which explains occasional use of different methodologies for the same purpose.

The first thing that we determined was the *in vitro* growth curve of *L. major* parasites (Section 3.1.), which is pivotal for *in* vitro maintenance, long-term storage, purification of cellular components , establishing consistent *in vitro* infections and *in vivo* challenge experiments. To increase the consistency of *in vitro* and *in vivo* experiments, we successfully enriched highly infective metacyclic parasites using ficoll density gradient (Section 3.2.)

In the first part of the thesis, we dealt with the unusual kinetoplast DNA, unique to kinetoplastea order. It has been reported that kDNA of *Trypanosoma cruzi* may contribute to disease severity (Teixeira, Hecht, Guimaro, Sousa, & Nitz, 2011; Zhang & Tarleton, 1999). However, possible role of kDNA in Leishmania infections is still

unknown. Based on these observations for a closely related species, we wanted to evaluate the contribution of kDNA in Leishmania infections.

For this purpose, we first optimized and modified the kDNA purification method described by Akman *et al.* (2000) through elimination of gDNA and RNA contaminations (Section 3.3.1.). Then, we confirmed the success of kDNA purification using fluorescence and atomic force microscopy (Section 3.3.2.).

To assess the possible contribution of kDNA to *L. major* infection, we performed i*n vitro* infection assays with kDNA or gDNA stimulated immune cells. We showed that although percentage of infected cells did not differ significantly, parasite burden of kDNA stimulated THP-1 cells (~4 fold) and BMDMs (~1.5 fold) were significantly increased with respect to cells treated with equivalent concentration of gDNA (Section 3.3.3.). These results indicate that kDNA aggravates Leishmania infection *in vitro*. Furthermore, we demonstrated that kDNA exacerbated disease progression in preliminary *L. major* induced murine model of CL (Section 3.3.4). We intend to re-evaluate the effect of kDNA in the future using the murine model of CL with improvements achieved throughout this thesis in depth.

It has been suggested that type-I interferon responses induced by endogenous or exogenous viral RNA contributes to severity of mucocutaneous leishmaniasis (Ives et al., 2011; Rossi et al., 2017). Based on these findings, to elucidate one of the underlying mechanisms behind kDNA induced aggravation of *L. major* infection, we analyzed and demonstrated that kDNA-induced IFN production was ~2.5-fold higher than that triggered by an equivalent concentration of gDNA in *L. major* infected THP-1 cells (Section 3.3.3.). Our results suggest that kDNA may have a role in facilitating parasite evasion from the immune system through induction of type-I interferon signaling pathways.

It has been reported that cGAS preferentially binds to U-turns or bent DNA. Such bent-DNA favor cGAS dimerization and facilitate nucleation of cGAS-DNA ladder formation (Andreeva et al., 2017). Interestingly, bent DNA was first discovered in the

kinetoplast DNA minicircles (Marini et al., 1982). Therefore, it is highly likely that the affinity of cGAS towards optimally pre-structured kDNA would be much higher in magnitude when compared to gDNA. Furthermore, it has been reported that IRF3 (Interferon regulatory factor 3) activation through cGAS-STING-TBK1 pathway (results in induction of IFN production through recognition of cytosolic DNA) increases replication of *Toxoplasma gondii* (another protozoan parasite) both *in vitro* and *in vivo* (Majumdar et al., 2015). In light of these findings, we are currently conducting *in vitro L. major* infection experiments in cGAS or STING knockout THP-1 cells and evaluating the effects of TBK1 inhibitors on the Leishmania infection to test whether aggravation of *L. major* infection can be associated to recognition of kDNA through the cGAS-STING pathway.

Leishmania exosomes were shown to possess a very rich antigen content (Coakley, Maizels, & Buck, 2015; Schorey, Cheng, Singh, & Smith, 2015). Based on their excellent antigen delivery properties reported in other studies (Dong, Filho, & Olivier, 2019; Marshall et al., 2018; Pérez-Cabezas et al., 2019), in the second part of the thesis, we wanted to test the utility of Leishmania exosomes as a source of Leishmania antigens in an attempt to develop a vaccine/immunotherapeutic against *L. major* induced CL. Moreover, we also aimed to determine the best adjuvant candidate to be combined with the exosome-based vaccine through testing of several adjuvants that promotes Th1 or NKT responses.

For this purpose, we first generated mouse adapted *L. major* parasites and demonstrated that the use of mouse-adapted parasites increased the infectivity in our mouse our model of CL by shortening the time span required for lesion development (Section 3.4.1.).

To be able to conduct immunization/challenge experiments with exosome-based formulations, we purified Leishmania exosomes and characterized them based on expression of Leishmania exosome associated markers and their morphology (Section 3.4.2). Furthermore, we analyzed the protein content of purified exosomes by MS

analysis (Section 3.4.2.). MS analysis revealed the presence of several exosome markers in the purified vesicles and confirmed the presence of *bona fide* exosomes. In addition, we identified the presence of several immunomodulatory proteins in purified exosomes such as SMP-1, whose enzymatic activity can be potentially evaluated to improve immunogenic properties of purified exosomes. We also identified a conserved hypothetical protein in our purified exosomes as a novel protein of interest for parasite biology, to be characterized in a separate study.

In a previous study from our laboratory, combination of K type CpG-ODN and cGAMP (K-cGAMP) was shown to be a Th1 promoting adjuvant combination in a murine model of protective cancer vaccination (Yildiz et al., 2015). Therefore, this adjuvant combination was first evaluated in mice vaccinated with *L. tropica* exosomes and was shown to promote Leishmania-specific Th1 and Th17 responses (Güngör, 2017). Based on this finding, we tested the antigenicity of *L. major* exosomes and the adjuvant activity of K-cGAMP in BALB/c model of CL (Section 3.4.3.). We observed that exosomes alone had potential as a vaccine but combination with K-cGAMP provided no additional benefit. Based on outcome, we next tested the antigen/adjuvant properties of three different sources of Leishmanial antigens (HK, SLA, Exosomes) combined with three different Th1 promoting adjuvants (K-ODN, D-ODN and CpG nanorings) (Section 3.4.5.). We demonstrated that among the tested antigen/adjuvant combinations, exosomes or SLA combined with D-ODN induced Leishmania antigen specific Th1 dominated humoral and cellular responses and hence these formulations were determined as the most promising formulations to provide immunoprotection against CL in BALB/c model induced by *L. major*.

During this period we also successfully generated EGFP-LUC expressing transgenic *L. major* parasites (EGFP-LUC$^+$) for accurate quantification of parasite loads in BALB/c model of CL to better evaluate the immunoprotective and immunotherapeutic effects of our antigen/adjuvant combinations (Section 3.4.4.). For this purpose, we confirmed expression of EGFP and LUC in transgenic parasites and optimized their

use in *in vivo* imaging system (IVIS). We integrated parasite load determination using IVIS into our BALB/c model of CL in the following experiments.

gp63 has been identified as an important virulence factor (discussed in detail in Section 3.4.6.), which is abundantly expressed in exosomes and SLA. gp63 is also involved in the cleavage and degradation of various host kinases and transcription factors, thereby suppress signaling in target cells (Abu-Dayyeh et al., 2008; Blanchette, Racette, Faure, Siminovitch, & Olivier, 1999; Forget et al., 2005; Gomez et al., 2009). To eliminate this immunosuppressive activity, we chemically inactivated gp63 without altering its antigenic properties to improve the immunogenicity of exosomes and SLA (Section 3.4.6).

In our first immunization/challenge experiment with chemically inactivated formulations (Section 3.4.7.), we used catalase treatment to decompose residual H_2O_2. In this experiment, only chemically inactivated SLA formulation provided significant immunoprotection against CL. Since chemical inactivation was able improve immunogenic properties of SLA but not exosomes, we concluded that exosomes may have shielded intraluminal H_2O_2 from catalase decomposition due to their lipid-based vesicular nature and may have resulted in inefficient elimination of H_2O_2 from exosome-based formulations. To circumvent this problem we adopted lyophilization-based method to remove residual H_2O_2 in our formulations and we showed that lyophilization method did not interfere with chemical inactivation and integrity of gp63 (Appendix D, Section 3.4.8.). Furthermore, although formulations adjuvanted with D-ODN induced robust Th1 dominated Leishmania specific humoral and cellular immune responses, these formulations only moderately delayed disease progression (Section 3.4.7.). Based on this observation, we concluded that robust Th1 responses in D-ODN adjuvanted groups might have resulted in hyper-inflammation as reported for infection of other Leishmania species (Silveira, Lainson, De Castro Gomes, Laurenti, & Corbett, 2009) and hence failed to provide significant immunoprotection against CL. To elucidate this possibility, we included αGalCer as a NKT promoting glycolipid based adjuvant in the following immunization experiment (Section 3.4.9).

147

Following adaptation of lyophilization-based method, we showed that chemically inactivated formulations combined with D-ODN and prepared through lyophilization resulted in significant lesion healing when applied as immunotherapeutics (Section 3.4.8). In this experiment, we were not able to observe any significant changes in lesion sizes due to the short-time span of lesion monitoring. We intend to evaluate the immunotherapeutic activities of chemically inactivated formulations with extended adjuvant combinations prepared by lyophilization in an *in vivo* experiment by increasing the number of mice and duration of disease progression monitoring to gain better understanding of immunotherapeutic activities of our formulations.

In the last immunization experiment conducted with chemically inactivated formulations prepared by lyophilization (Section 3.4.9.), we demonstrated that all antigen alone formulations significantly delayed lesion development when compared to unvaccinated group. Although chemical inactivation failed to improve immunoprotective effects, the use of αGalCer as an adjuvant augmented the immunoprotective effects of exosomes. In contrast, antigens adjuvanted with D-ODN, failed to provide immunoprotection, and even exacerbated the disease.

We also showed that the use of D-ODN as adjuvant induced Leishmania specific Th1 dominated responses accompanied by elevated Th17 responses, whereas vaccine formulations which provided immunoprotection against CL, induced Th1/Th2 balanced or Th2 dominated responses with significantly suppressed Th17 responses (Section 3.4.9.).

It has been reported that IL-17 deficient BALB/c mice infected with L. major developed significantly smaller lesions when compared to wild type mice even though both exhibited a Th2 dominated response (Lopez Kostka et al., 2009). Although IL-17 can recruit neutrophils to the infection site and augment ROS production in macrophages to eliminate intracellular parasites, in the absence IL-10, this enhancement aggravates tissue injury and results in progression of CL (Gonçalves-de-Albuquerque et al., 2017; Gonzalez-Lombana et al., 2013). These findings are

consistent with our data and explains the lack of immunoprotection in the presence of Th1 dominated responses when such a response is accompanied by increased Th17 responses.

Based on these findings, we concluded that *L. major* exosomes combined with αGalCer provided the most striking immunoprotection against CL though suppressed Th17 responses even though it exhibited Th2 dominated responses over Th1. Furthermore, we concluded that robust Th1 dominated responses failed to provide immunoprotection. It is also possible that αGalCer acts on bystander cells and stimulate the secretion of cytokines, which subsequently activate anti-Leishmanial mechanisms in macrophages. In the future, we aim to improve the immunogenicity of exosomes-αGalCer combination by optimizing the dose and route of administration to develop a prototype vaccine against CL.

To summarize, in the first part of this thesis, we have shown that kDNA contributes to Leishmania infection *in vitro* and disease progression *in vivo*. Our preliminary data suggest that this effect depends on type-I interferon production through immune recognition of kDNA. We are continuing our efforts to associate this phenomenon with recognition of kDNA through the cGAS-STING pathway. In the second part, we have improved our murine model of CL to establish more consistent and accurate evaluation of disease progression. Furthermore, we have shown that chemically inactivated exosomes adjuvanted with D-ODN exhibited immunotherapeutic activities while exosomes adjuvanted with αGalCer provided significant immunoprotection against CL. We are designing extended immunization/challenge and immunotherapy experiments to improve both of these formulations.

REFERENCES

Abbasi, I., Aramin, S., Hailu, A., Shiferaw, W., Kassahun, A., Belay, S., … Warburg, A. (2013). Evaluation of PCR procedures for detecting and quantifying Leishmania donovani DNA in large numbers of dried human blood samples from a visceral leishmaniasis focus in Northern Ethiopia. *BMC Infectious Diseases*, *13*(1). https://doi.org/10.1186/1471-2334-13-153

Abd-Elghaffar, A. A., Ali, A. E., Boseila, A. A., & Amin, M. A. (2016). Inactivation of rabies virus by hydrogen peroxide. *Vaccine*, *34*(6), 798–802. https://doi.org/10.1016/j.vaccine.2015.12.041

Abu-Dayyeh, I., Shio, M. T., Sato, S., Akira, S., Cousineau, B., & Olivier, M. (2008). Leishmania-induced IRAK-1 inactivation is mediated by SHP-1 interacting with an evolutionarily conserved KTIM motif. *PLoS Neglected Tropical Diseases*, *2*(12). https://doi.org/10.1371/journal.pntd.0000305

Agallou, M., Margaroni, M., & Karagouni, E. (2011). Cellular vaccination with bone marrow-derived dendritic cells pulsed with a peptide of Leishmania infantum KMP-11 and CpG oligonucleotides induces protection in a murine model of visceral leishmaniasis. *Vaccine*, *29*(31), 5053–5064. https://doi.org/10.1016/j.vaccine.2011.04.089

Akman, L., Aksu, H. S. Z., Wang, R. Q., Ozensoy, S., Ozbel, Y., Alkan, Z., … Chang, K. P. (2000). Multi-site DNA polymorphism analyses of Leishmania isolates define their genotypes predicting clinical epidemiology of Leishmaniasis in a specific region. *Journal of Eukaryotic Microbiology*, *47*(6), 545–554. https://doi.org/10.1111/j.1550-7408.2000.tb00088.x

Aktan, F. (2004). iNOS-mediated nitric oxide production and its regulation. *Life Sciences*, *75*(6), 639–653. https://doi.org/10.1016/j.lfs.2003.10.042

Al-Salem, W. S., Ferreira, D. M., Dyer, N. A., Alyamani, E. J., Balghonaim, S. M., Al-Mehna, A. Y., … Acosta-Serrano, A. (2014). Detection of high levels of anti-α-galactosyl antibodies in sera of patients with Old World cutaneous leishmaniasis: A possible tool for diagnosis and biomarker for cure in an elimination setting. *Parasitology*, *141*(14), 1898–1903. https://doi.org/10.1017/S0031182014001607

Altschul, S. F., Madden, T. L., Schäffer, A. A., Zhang, J., Zhang, Z., Miller, W., & Lipman, D. J. (1997). Gapped BLAST and PSI-BLAST: A new generation of protein database search programs. *Nucleic Acids Research*, *25*(17), 3389–3402. https://doi.org/10.1093/nar/25.17.3389

Alvar, J., Croft, S. L., Kaye, P., Khamesipour, A., Sundar, S., & Reed, S. G. (2013).

Case study for a vaccine against leishmaniasis. *Vaccine*, *31*(SUPPL2). https://doi.org/10.1016/j.vaccine.2012.11.080

Alvar, J., Vélez, I. D., Bern, C., Herrero, M., Desjeux, P., Cano, J., … de Boer, M. (2012). Leishmaniasis worldwide and global estimates of its incidence. *PLoS ONE*, *7*(5), e35671. https://doi.org/10.1371/journal.pone.0035671

Alvar, J., Yactayo, S., & Bern, C. (2006). Leishmaniasis and poverty. *Trends in Parasitology*, *22*(12), 552–557. https://doi.org/10.1016/j.pt.2006.09.004

Amanna, I. J., Raué, H. P., & Slifka, M. K. (2012). Development of a new hydrogen peroxide-based vaccine platform. *Nature Medicine*, *18*(6), 974–979. https://doi.org/10.1038/nm.2763

Andreeva, L., Hiller, B., Kostrewa, D., Lässig, C., De Oliveira Mann, C. C., Jan Drexler, D., … Hopfner, K. P. (2017). CGAS senses long and HMGB/TFAM-bound U-turn DNA by forming protein-DNA ladders. *Nature*, *549*(7672), 394–398. https://doi.org/10.1038/nature23890

Antunes, C. M. F., Mayrink, W., Magalhaes, P. A., Costa, C. A., Melo, M. N., Dias, M., … Schettini, A. P. M. (1986). Controlled field trials of a vaccine against new world cutaneous leishmaniasis. *International Journal of Epidemiology*, *15*(4), 572–580. https://doi.org/10.1093/ije/15.4.572

Aphasizhev, R., & Aphasizheva, I. (2014). Mitochondrial RNA editing in trypanosomes: Small RNAs in control. *Biochimie*, *100*(1), 125–131. https://doi.org/10.1016/j.biochi.2014.01.003

Armijos, R. X., Weigel, M. M., Calvopina, M., Hidalgo, A., Cevallos, W., & Correa, J. (2004). Safety, immunogenecity, and efficacy of an autoclaved Leishmania amazonensis vaccine plus BCG adjuvant against New World cutaneous leishmaniasis. *Vaccine*, *22*(9–10), 1320–1326. https://doi.org/10.1016/j.vaccine.2003.06.002

Armijos, Rodrigo X., Weigel, M. M., Aviles, H., Maldonado, R., & Racines, J. (1998). Field Trial of a Vaccine against New World Cutaneous Leishmaniasis in an At-Risk Child Population: Safety, Immunogenicity, and Efficacy during the First 12 Months of Follow‐ Up. *The Journal of Infectious Diseases*, *177*(5), 1352–1357. https://doi.org/10.1086/515265

Aronson, N. E. (2017). Addressing a clinical challenge: Guidelines for the diagnosis and treatment of leishmaniasis. *BMC Medicine*, *15*(1). https://doi.org/10.1186/s12916-017-0843-3

Atayde, V. D., Aslan, H., Townsend, S., Hassani, K., Kamhawi, S., & Olivier, M. (2015). Exosome Secretion by the Parasitic Protozoan Leishmania within the Sand Fly Midgut. *Cell Reports*, *13*(5), 957–967. https://doi.org/10.1016/j.celrep.2015.09.058

Atayde, V. D., Hassani, K., da Silva Lira Filho, A., Borges, A. R., Adhikari, A., Martel, C., & Olivier, M. (2016). Leishmania exosomes and other virulence factors: Impact on innate immune response and macrophage functions. *Cellular Immunology*, Vol. 309, pp. 7–18. https://doi.org/10.1016/j.cellimm.2016.07.013

Athie-Morales, V., Smits, H. H., Cantrell, D. A., & Hilkens, C. M. U. (2004). Sustained IL-12 Signaling Is Required for Th1 Development. *The Journal of Immunology*, *172*(1), 61–69. https://doi.org/10.4049/jimmunol.172.1.61

Bahar, K., Dowlati, Y., Shidani, B., Alimohammadian, M. H., Khamesipour, A., Ehsasi, S., … Modabber, F. (1996). Comparative safety and immunogenicity trial of two killed Leishmania major vaccines with or without BCG in human volunteers. *Clinics in Dermatology*, *14*(5), 489–495. https://doi.org/10.1016/0738-081X(96)00071-5

Banerjee, A., Bhattacharya, P., Joshi, A. B., Ismail, N., Dey, R., & Nakhasi, H. L. (2016). Role of pro-inflammatory cytokine IL-17 in Leishmania pathogenesis and in protective immunity by Leishmania vaccines. *Cellular Immunology*, *309*, 37–41. https://doi.org/10.1016/j.cellimm.2016.07.004

Becker, I., Salaiza, N., Aguirre, M., Delgado, J., Carrillo-Carrasco, N., Kobeh, L. G., … Isibasi, A. (2003). Leishmania lipophosphoglycan (LPG) activates NK cells through toll-like receptor-2. *Molecular and Biochemical Parasitology*. https://doi.org/10.1016/S0166-6851(03)00160-9

Berman, J. D. (1997). Human leishmaniasis: Clinical, diagnostic, and chemotherapeutic developments in the last 10 years. *Clinical Infectious Diseases*, *24*(4), 684–703. https://doi.org/10.1093/clind/24.4.684

Blanchette, J., Racette, N., Faure, R., Siminovitch, K. A., & Olivier, M. (1999). Leishmania-induced increases in activation of macrophage SHP-1 tyrosine phosphatase are associated with impaired IFN-γ-triggered JAK2 activation. *European Journal of Immunology*. https://doi.org/10.1002/(SICI)1521-4141(199911)29:11<3737::AID-IMMU3737>3.0.CO;2-S

Blum, J., Buffet, P., Visser, L., Harms, G., Bailey, M. S., Caumes, E., … Lockwood, D. N. J. (2014). LeishMan recommendations for treatment of cutaneous and mucosal leishmaniasis in travelers, 2014. *Journal of Travel Medicine*, *21*(2), 116–129. https://doi.org/10.1111/jtm.12089

Bobrie, A., Colombo, M., Krumeich, S., Raposo, G., & Théry, C. (2012). Diverse subpopulations of vesicles secreted by different intracellular mechanisms are present in exosome preparations obtained by differential ultracentrifugation. *Journal of Extracellular Vesicles*, *1*(1). https://doi.org/10.3402/jev.v1i0.18397

Bolhassani, A., Taheri, T., Taslimi, Y., Zamanilui, S., Zahedifard, F., Seyed, N., … Rafati, S. (2011). Fluorescent Leishmania species: Development of stable GFP expression and its application for in vitro and in vivo studies. *Experimental*

Parasitology, 127(3), 637–645. https://doi.org/10.1016/j.exppara.2010.12.006

Borg, N. A., Wun, K. S., Kjer-Nielsen, L., Wilce, M. C. J., Pellicci, D. G., Koh, R., … Rossjohn, J. (2007). CD1d-lipid-antigen recognition by the semi-invariant NKT T-cell receptor. *Nature*, *448*(7149), 44–49. https://doi.org/10.1038/nature05907

Borst, P. (1991). Why kinetoplast DNA networks? *Trends in Genetics*, *7*(5), 139–141. https://doi.org/10.1016/0168-9525(91)90374-Y

Bose, M., Saha, R., Sen Santara, S., Mukherjee, S., Roy, J., & Adak, S. (2012). Protection against peroxynitrite by pseudoperoxidase from Leishmania major. *Free Radical Biology and Medicine*, *53*(10), 1819–1828. https://doi.org/10.1016/j.freeradbiomed.2012.08.583

Bravo, F., & Sanchez, M. R. (2003). New and re-emerging cutaneous infectious diseases in Latin America and other geographic areas. *Dermatologic Clinics*, *21*(4), 655–668. https://doi.org/10.1016/S0733-8635(03)00090-1

Brennan, P. J., Brigl, M., & Brenner, M. B. (2013). Invariant natural killer T cells: An innate activation scheme linked to diverse effector functions. *Nature Reviews Immunology*, *13*(2), 101–117. https://doi.org/10.1038/nri3369

Brittingham, A., Morrison, C. J., McMaster, W. R., McGwire, B. S., Chang, K.-P., & Mosser, D. M. (1995). Role of the Leishmania surface protease gp63 in complement fixation, cell adhesion, and resistance to complement-mediated lysis. *Parasitology Today*, *11*(12), 445–446. https://doi.org/10.1016/0169-4758(95)80054-9

Brubaker, S. W., Bonham, K. S., Zanoni, I., & Kagan, J. C. (2015). Innate Immune Pattern Recognition: A Cell Biological Perspective. *Annual Review of Immunology*, *33*(1), 257–290. https://doi.org/10.1146/annurev-immunol-032414-112240

Carneiro, M. B. H., Roma, E. H., Ranson, A. J., Doria, N. A., Debrabant, A., Sacks, D. L., … Peters, N. C. (2018). NOX2-Derived Reactive Oxygen Species Control Inflammation during Leishmania amazonensis Infection by Mediating Infection-Induced Neutrophil Apoptosis . *The Journal of Immunology*, *200*(1), 196–208. https://doi.org/10.4049/jimmunol.1700899

Castellano, L. R., Filho, D. C., Argiro, L., Dessein, H., Prata, A., Dessein, A., & Rodrigues, V. (2009). Th1/Th2 immune responses are associated with active cutaneous leishmaniasis and clinical cure is associated with strong interferon-γ production. *Human Immunology*, *70*(6), 383–390. https://doi.org/10.1016/j.humimm.2009.01.007

Chagas, A. C., Oliveira, F., Debrabant, A., Valenzuela, J. G., Ribeiro, J. M. C., & Calvo, E. (2014). Lundep, a Sand Fly Salivary Endonuclease Increases

Leishmania Parasite Survival in Neutrophils and Inhibits XIIa Contact Activation in Human Plasma. *PLoS Pathogens*, *10*(2). https://doi.org/10.1371/journal.ppat.1003923

Chakravarty, J., Kumar, S., Trivedi, S., Rai, V. K., Singh, A., Ashman, J. A., … Piazza, F. M. (2011). A clinical trial to evaluate the safety and immunogenicity of the LEISH-F1+MPL-SE vaccine for use in the prevention of visceral leishmaniasis. *Vaccine*, *29*(19), 3531–3537. https://doi.org/10.1016/j.vaccine.2011.02.096

Chang, K. P., & Dwyer, D. M. (1976). Multiplication of a human parasite (Leishmania donovani) in phagolysosomes of hamster macrophages in vitro. *Science*, *193*(4254), 678–680. https://doi.org/10.1126/science.948742

Chappuis, F., Sundar, S., Hailu, A., Ghalib, H., Rijal, S., Peeling, R. W., … Boelaert, M. (2007). Visceral leishmaniasis: What are the needs for diagnosis, treatment and control? *Nature Reviews Microbiology*, *5*(11), 873–882. https://doi.org/10.1038/nrmicro1748

Chu, N., Thomas, B. N., Patel, S. R., & Buxbaum, L. U. (2010). IgG1 Is Pathogenic in Leishmania mexicana Infection . *The Journal of Immunology*, *185*(11), 6939–6946. https://doi.org/10.4049/jimmunol.1002484

Coakley, G., Maizels, R. M., & Buck, A. H. (2015). Exosomes and Other Extracellular Vesicles: The New Communicators in Parasite Infections. *Trends in Parasitology*, *31*(10), 477–489. https://doi.org/10.1016/j.pt.2015.06.009

Colmenares, M., Kar, S., Goldsmith-Pestana, K., & McMahon-Pratt, D. (2004). Mechanisms of pathogenesis: differences amongst Leishmania species. *Transactions of the Royal Society of Tropical Medicine and Hygiene*, *96*, S3–S7. https://doi.org/10.1016/s0035-9203(02)90044-1

Colombo, M., Raposo, G., & Théry, C. (2014). Biogenesis, Secretion, and Intercellular Interactions of Exosomes and Other Extracellular Vesicles. *Annual Review of Cell and Developmental Biology*, *30*(1), 255–289. https://doi.org/10.1146/annurev-cellbio-101512-122326

Copeland, N. K., & Aronson, N. E. (2015). Leishmaniasis: Treatment updates and clinical practice guidelines review. *Current Opinion in Infectious Diseases*, *28*(5), 426–437. https://doi.org/10.1097/QCO.0000000000000194

Core Team, R. (2008). Computational Many-Particle Physics. *R Foundation for Statistical Computing*, Vol. 739. https://doi.org/10.1007/978-3-540-74686-7

Croft, S. L., & Coombs, G. H. (2003). Leishmaniasis - Current chemotherapy and recent advances in the search for novel drugs. *Trends in Parasitology*, *19*(11), 502–508. https://doi.org/10.1016/j.pt.2003.09.008

Davies, C. R., Reithinger, R., Campbell-Lendrum, D., Feliciangeli, D., Borges, R., &

Rodriguez, N. (2000). The epidemiology and control of leishmaniasis in Andean countries. *Cadernos de Saúde Pública / Ministério Da Saúde, Fundação Oswaldo Cruz, Escola Nacional de Saúde Pública*, *16*(4), 925–950. https://doi.org/10.1590/S0102-311X2000000400013

de Souza Carmo, É. V., Katz, S., & Barbiéri, C. L. (2010). Neutrophils reduce the parasite burden in Leishmania (Leishmania) amazonensis-infected macrophages. *PLoS ONE*, *5*(11). https://doi.org/10.1371/journal.pone.0013815

de Veer, M. J., Curtis, J. M., Baldwin, T. M., DiDonato, J. A., Sexton, A., McConville, M. J., … Schofield, L. (2003). MyD88 is essential for clearance of Leishmania major: Possible role for lipophosphoglycan and Toll-like receptor 2 signaling. *European Journal of Immunology*. https://doi.org/10.1002/eji.200324128

Desjeux, P. (2004). Leishmaniasis: Current situation and new perspectives. *Comparative Immunology, Microbiology and Infectious Diseases*, *27*(5), 305–318. https://doi.org/10.1016/j.cimid.2004.03.004

Dong, G., Filho, A. L., & Olivier, M. (2019). Modulation of host-pathogen communication by extracellular vesicles (EVs) of the protozoan parasite Leishmania. *Frontiers in Cellular and Infection Microbiology*, *9*(APR). https://doi.org/10.3389/fcimb.2019.00100

Dowlati, Y., Ehsasi, S., Shidani, B., & Bahar, K. (1996). Stepwise safety trial of a killed Leishmania vaccine in Iran. *Clinics in Dermatology*, *14*(5), 497–502. https://doi.org/10.1016/0738-081X(96)00072-7

Drewa, M. E., & Englunda, P. T. (2001). Intramitochondrial location and dynamics of Crithidia fasciculata kinetoplast minicircle replication intermediates. *Journal of Cell Biology*, *153*(4), 735–743. https://doi.org/10.1083/jcb.153.4.735

Dunne, A., Marshall, N. A., & Mills, K. H. G. (2011). TLR based therapeutics. *Current Opinion in Pharmacology*, *11*(4), 404–411. https://doi.org/10.1016/j.coph.2011.03.004

Durdu, M., Baba, M., & Seçkin, D. (2009). More experiences with the Tzanck smear test: Cytologic findings in cutaneous granulomatous disorders. *Journal of the American Academy of Dermatology*, *61*(3), 441–450. https://doi.org/10.1016/j.jaad.2009.02.050

Eddaikra, N., Kherachi Djenad, I., Benbetka, S., Benikhlef, R., Aït-Oudhia, K., Moulti-Mati, F., … Harrat, Z. (2016). Development of a Murine Infection Model with Leishmania killicki, Responsible for Cutaneous Leishmaniosis in Algeria: Application in Pharmacology. *BioMed Research International*, *2016*. https://doi.org/10.1155/2016/7985104

Engel, M. L., & Ray, D. S. (2002). The kinetoplast structure-specific endonuclease I is related to the 5' exo/endonuclease domain of bacterial DNA polymerase I and

colocalizes with the kinetoplast topoisomerase II and DNA polymerase during replication. *Proceedings of the National Academy of Sciences*, *96*(15), 8455–8460. https://doi.org/10.1073/pnas.96.15.8455

Erikçi, E., Gursel, M., & Gürsel, I. (2011). Differential immune activation following encapsulation of immunostimulatory CpG oligodeoxynucleotide in nanoliposomes. *Biomaterials*, *32*(6), 1715–1723. https://doi.org/10.1016/j.biomaterials.2010.10.054

Escobar, M. A., Martinez, F., Smith, D. S., & Palma, G. i. (1992). American Cutaneous and Mucocutaneous Leishmaniasis (Tegumentary): A Diagnostic Challenge. *Tropical Doctor*, *22*, 69–78. https://doi.org/10.1177/00494755920220S110

Fang, F. C. (2004). Antimicrobial reactive oxygen and nitrogen species: Concepts and controversies. *Nature Reviews Microbiology*, *2*(10), 820–832. https://doi.org/10.1038/nrmicro1004

Faria, M. S., Reis, F. C. G., Azevedo-Pereira, R. L., Morrison, L. S., Mottram, J. C., & Lima, A. P. C. A. (2011). Leishmania Inhibitor of Serine Peptidase 2 Prevents TLR4 Activation by Neutrophil Elastase Promoting Parasite Survival in Murine Macrophages . *The Journal of Immunology*, *186*(1), 411–422. https://doi.org/10.4049/jimmunol.1002175

Faria, M. S., Reis, F. C. G., & Lima, A. P. C. A. (2012). Toll-like receptors in Leishmania infections: Guardians or promoters? *Journal of Parasitology Research*, *2012*. https://doi.org/10.1155/2012/930257

Filardy, A. A., Pires, D. R., Nunes, M. P., Takiya, C. M., Freire-de-Lima, C. G., Ribeiro-Gomes, F. L., & DosReis, G. A. (2010). Proinflammatory Clearance of Apoptotic Neutrophils Induces an IL-12 low IL-10 high Regulatory Phenotype in Macrophages . *The Journal of Immunology*, *185*(4), 2044–2050. https://doi.org/10.4049/jimmunol.1000017

Finkelman, F. D., Holmes, J., Katona, I. M., Urban, J. F., Beckmann, M. P., Park, L. S., … Paul, W. E. (1990). Lymphokine Control of In Vivo Immunoglobulin Isotype Selection. *Annual Review of Immunology*, *8*(1), 303–333. https://doi.org/10.1146/annurev.iy.08.040190.001511

Flandin, J. F., Chano, F., & Descoteaux, A. (2006). RNA interference reveals a role for TLR2 and TLR3 in the recognition of Leishmania donovani promastigotes by interferon-γ-primed macrophages. *European Journal of Immunology*, *36*(2), 411–420. https://doi.org/10.1002/eji.200535079

Forget, G., Gregory, D. J., Whitcombe, L. A., & Olivier, M. (2006). Role of host protein tyrosine phosphatase SHP-1 in Leishmania donovani-induced inhibition of nitric oxide production. *Infection and Immunity*, *74*(11), 6272–6279. https://doi.org/10.1128/IAI.00853-05

Forget, G., Matte, C., Siminovitch, K. A., Rivest, S., Pouliot, P., & Olivier, M. (2005). Regulation of the Leishmania-induced innate inflammatory response by the protein tyrosine phosphatase SHP-1. *European Journal of Immunology*, *35*(6), 1906–1917. https://doi.org/10.1002/eji.200526037

Franco, L. H., Beverley, S. M., & Zamboni, D. S. (2012). Innate immune activation and subversion of mammalian functions by Leishmania lipophosphoglycan. *Journal of Parasitology Research*, Vol. 2012. https://doi.org/10.1155/2012/165126

Fu, X., Kassim, S. Y., Parks, W. C., & Heinecke, J. W. (2003). Hypochlorous Acid Generated by Myeloperoxidase Modifies Adjacent Tryptophan and Glycine Residues in the Catalytic Domain of Matrix Metalloproteinase-7 (Matrilysin). *Journal of Biological Chemistry*, *278*(31), 28403–28409. https://doi.org/10.1074/jbc.m304739200

Gabriel, C., McMaster, W. R., Girard, D., & Descoteaux, A. (2010). Leishmania donovani Promastigotes Evade the Antimicrobial Activity of Neutrophil Extracellular Traps . *The Journal of Immunology*, *185*(7), 4319–4327. https://doi.org/10.4049/jimmunol.1000893

Gaur, U., Roberts, S. C., Dalvi, R. P., Corraliza, I., Ullman, B., & Wilson, M. E. (2007). An Effect of Parasite-Encoded Arginase on the Outcome of Murine Cutaneous Leishmaniasis. *The Journal of Immunology*, *179*(12), 8446–8453. https://doi.org/10.4049/jimmunol.179.12.8446

Genaro, O., De Toledo, V. P. C. P., Da Costa, C. A., Hermeto, M. V., Afonso, L. C. C., & Mayrink, W. (1996). Vaccine for prophylaxis and immunotherapy, Brazil. *Clinics in Dermatology*, *14*(5), 503–512. https://doi.org/10.1016/0738-081X(96)00040-5

Gibson, M. E. (1983). The identification of kala azar and the discovery of leishmania donovani. *Medical History*, *27*(2), 203–213. https://doi.org/10.1017/S0025727300042691

Gomez, M. A., Contreras, I., Hallé, M., Tremblay, M. L., McMaster, R. W., & Olivier, M. (2009). Leishmania GP63 alters host signaling through cleavage-activated protein tyrosine phosphatases. *Science Signaling*, *2*(90). https://doi.org/10.1126/scisignal.2000213

Gonçalves-de-Albuquerque, S. da C., Pessoa-e-Silva, R., Trajano-Silva, L. A. M., de Goes, T. C., de Morais, R. C. S., Oliveira, C. N. d. C., … de Paiva-Cavalcanti, M. (2017). The equivocal role of Th17 cells and neutrophils on immunopathogenesis of leishmaniasis. *Frontiers in Immunology*, *8*(OCT). https://doi.org/10.3389/fimmu.2017.01437

Gonçalves, R., Vieira, E. R., Melo, M. N., Gollob, K. J., Mosser, D. M., & Tafuri, W. L. (2005). A sensitive flow cytometric methodology for studying the binding of

L. chagasi to canine peritoneal macrophages. *BMC Infectious Diseases*, *5*. https://doi.org/10.1186/1471-2334-5-39

Goncalves, R., Zhang, X., Cohen, H., Debrabant, A., & Mosser, D. M. (2011). Platelet activation attracts a subpopulation of effector monocytes to sites of Leishmania major infection. *Journal of Experimental Medicine*, *208*(6), 1253–1265. https://doi.org/10.1084/jem.20101751

Gonzalez-Lombana, C., Gimblet, C., Bacellar, O., Oliveira, W. W., Passos, S., Carvalho, L. P., … Scott, P. (2013). IL-17 Mediates Immunopathology in the Absence of IL-10 Following Leishmania major Infection. *PLoS Pathogens*, *9*(3). https://doi.org/10.1371/journal.ppat.1003243

Gordon, S., & Martinez, F. O. (2010). Alternative activation of macrophages: Mechanism and functions. *Immunity*, *32*(5), 593–604. https://doi.org/10.1016/j.immuni.2010.05.007

Gossage, S. M., Rogers, M. E., & Bates, P. A. (2003). Two separate growth phases during the development of Leishmania in sand flies: Implications for understanding the life cycle. *International Journal for Parasitology*, *33*(10), 1027–1034. https://doi.org/10.1016/S0020-7519(03)00142-5

Goto, H., & Lauletta Lindoso, J. A. (2012). Cutaneous and Mucocutaneous Leishmaniasis. *Infectious Disease Clinics of North America*, *26*(2), 293–307. https://doi.org/10.1016/j.idc.2012.03.001

Goto, H., & Lindoso, J. A. L. (2010). Current diagnosis and treatment of cutaneous and mucocutaneous leishmaniasis. *Expert Review of Anti-Infective Therapy*, *8*(4), 419–433. https://doi.org/10.1586/eri.10.19

Goyard, S., Dutra, P. L., Deolindo, P., Autheman, D., D'Archivio, S., & Minoprio, P. (2014). In vivo imaging of trypanosomes for a better assessment of host-parasite relationships and drug efficacy. *Parasitology International*, *63*(1), 260–268. https://doi.org/10.1016/j.parint.2013.07.011

Gramiccia, M., & Gradoni, L. (2005). The current status of zoonotic leishmaniases and approaches to disease control. *International Journal for Parasitology*, *35*(11–12), 1169–1180. https://doi.org/10.1016/j.ijpara.2005.07.001

Guerin, P. J., Olliaro, P., Sundar, S., Boelaert, M., Croft, S. L., Desjeux, P., … Bryceson, A. D. M. (2002). Visceral leishmaniasis: Current status of control, diagnosis, and treatment, and a proposed research and development agenda. *Lancet Infectious Diseases*, *2*(8), 494–501. https://doi.org/10.1016/S1473-3099(02)00347-X

Guimarães-Costa, A. B., Nascimento, M. T. C., Froment, G. S., Soares, R. P. P., Morgado, F. N., Conceição-Silva, F., & Saraiva, E. M. (2009). Leishmania amazonensis promastigotes induce and are killed by neutrophil extracellular

traps. *Proceedings of the National Academy of Sciences of the United States of America*, *106*(16), 6748–6753. https://doi.org/10.1073/pnas.0900226106

Güler, M. L., Gorham, J. D., Hsieh, C.-S., Mackey, A. J., Steen, R. G., Dietrich, W. F., & Murphy, K. M. (2006). Genetic Susceptibility to Leishmania: IL-12 Responsiveness in TH1 Cell Development. *Science*, *271*(5251), 984–987. https://doi.org/10.1126/science.271.5251.984

Güngör, B. (2017). *VACCINE ADJUVANT APPLICATIONS OF CPG ODN NANORINGS AND DEVELOPMENT OF LEISHMANIA EXTRACELLULAR VESICLE BASED CUTANEOUS LEISHMANIASIS VACCINE* (Middle East Technical University). Retrieved from http://0-eds.b.ebscohost.com.library.metu.edu.tr/eds/detail/detail?vid=1&sid=792f859e-5be9-4d65-8788-203d51b156e4%40sessionmgr103&bdata=JkF1dGhUeXBlPWlwJnNpdGU9ZWRzLWxpdmU%3D#AN=metu.b2206085&db=cat06966a

Gungor, B., Yagci, F. C., Tincer, G., Bayyurt, B., Alpdundar, E., Yildiz, S., … Gursel, M. (2014). CpG ODN nanorings induce IFNα from plasmacytoid dendritic cells and demonstrate potent vaccine adjuvant activity. *Science Translational Medicine*, *6*(235). https://doi.org/10.1126/scitranslmed.3007909

Gursel, I., Gursel, M., Ishii, K. J., & Klinman, D. M. (2001). Sterically Stabilized Cationic Liposomes Improve the Uptake and Immunostimulatory Activity of CpG Oligonucleotides. *The Journal of Immunology*, *167*(6), 3324–3328. https://doi.org/10.4049/jimmunol.167.6.3324

Gursel, M., & Gursel, I. (2016). Development of CpG ODN based vaccine adjuvant formulations. In *Methods in Molecular Biology* (Vol. 1404, pp. 289–298). https://doi.org/10.1007/978-1-4939-3389-1_20

Gursel, M., Gursel, I., Mostowski, H. S., & Klinman, D. M. (2006). CXCL16 influences the nature and specificity of CpG-induced immune activation. *Journal of Immunology (Baltimore, Md. : 1950)*, *177*(3), 1575–1580. Retrieved from http://www.ncbi.nlm.nih.gov/pubmed/16849465

Gursel, M., Verthelyi, D., & Klinman, D. M. (2002). CpG oligodeoxynucleotides induce human monocytes to mature into functional dendritic cells. *European Journal of Immunology*, *32*(9), 2617–2622. https://doi.org/10.1002/1521-4141(200209)32:9<2617::AID-IMMU2617>3.0.CO;2-F

Hanagata, N. (2012). Structure-dependent immunostimulatory effect of CpG oligodeoxynucleotides and their delivery system. *International Journal of Nanomedicine*, *7*, 2181–2195. https://doi.org/10.2147/IJN.S30197

Hanagata, N. (2017). CpG oligodeoxynucleotide nanomedicines for the prophylaxis or treatment of cancers, infectious diseases, and allergies. *International Journal of Nanomedicine*, *12*, 515–531. https://doi.org/10.2147/IJN.S114477

Hartley, M. A., Bourreau, E., Rossi, M., Castiglioni, P., Eren, R. O., Prevel, F., … Fasel, N. (2016). Leishmaniavirus-Dependent Metastatic Leishmaniasis Is Prevented by Blocking IL-17A. *PLoS Pathogens*, *12*(9). https://doi.org/10.1371/journal.ppat.1005852

Hassani, K., Antoniak, E., Jardim, A., & Olivier, M. (2011). Temperature-induced protein secretion by leishmania mexicana modulates macrophage signalling and function. *PLoS ONE*, *6*(5). https://doi.org/10.1371/journal.pone.0018724

Hassani, K., Shio, M. T., Martel, C., Faubert, D., & Olivier, M. (2014). Absence of metalloprotease GP63 alters the protein content of leishmania exosomes. *PLoS ONE*, *9*(4). https://doi.org/10.1371/journal.pone.0095007

Hennessy, E. J., Parker, A. E., & O'Neill, L. A. J. (2010). Targeting Toll-like receptors: emerging therapeutics? *Nature Reviews Drug Discovery*, *9*(4), 293–307. https://doi.org/10.1038/nrd3203

Hide, M., Bucheton, B., Kamhawi, S., Bras-Gonalves, R., Sundar, S., Lemesre, J.-L., & Bauls, A.-L. (2007). Understanding Human Leishmaniasis:The Need for an Integrated Approach. In *Encyclopedia of Infectious Diseases* (pp. 87–123). https://doi.org/10.1002/9780470114209.ch6

Hill, J. O., North, R. J., & Collins, F. M. (1983). Advantages of measuring changes in the number of viable parasites in murine models of experimental cutaneous leishmaniasis. *Infection and Immunity*, *39*(3), 1087–1094.

Himmelrich, H., Parra-Lopez, C., Tacchini-Cottier, F., Louis, J. A., & Launois, P. (1998). The IL-4 rapidly produced in BALB/c mice after infection with leishmania major down-regulates IL-12 receptor β2-chain expression on CD4+ T cells resulting in a state of unresponsiveness to IL-12. *Journal of Immunology*, *161*(11), 6156–6163.

Hkima Abou Fakher, F., Rachinel, N., Klimczak, M., Louis, J., & Doyen, N. (2009). TLR9-Dependent Activation of Dendritic Cells by DNA from Leishmania major Favors Th1 Cell Development and the Resolution of Lesions . *The Journal of Immunology*, *182*(3), 1386–1396. https://doi.org/10.4049/jimmunol.182.3.1386

Hodiamont, C. J., Kager, P. A., Bart, A., de Vries, H. J. C., van Thiel, P. P. A. M., Leenstra, T., … van Gool, T. (2014). Species-Directed Therapy for Leishmaniasis in Returning Travellers: A Comprehensive Guide. *PLoS Neglected Tropical Diseases*, *8*(5). https://doi.org/10.1371/journal.pntd.0002832

Hotez, P. J., Molyneux, D. H., Fenwick, A., Ottesen, E., Sachs, S. E., & Sachs, J. D. (2006). Incorporating a rapid-impact package for neglected tropical diseases with programs for HIV/AIDS, tuberculosis, and malaria: A comprehensive pro-poor health policy and strategy for the developing world. *PLoS Medicine*, Vol. 3, pp. 576–584. https://doi.org/10.1371/journal.pmed.0030102

Hotez, P. J., Remme, J. H. F., Buss, P., Alleyne, G., Morel, C., & Breman, J. G. (2004). Combating Tropical Infectious Diseases: Report of the Disease Control Priorities in Developing Countries Project. *Clinical Infectious Diseases*, *38*(6), 871–878. https://doi.org/10.1086/382077

Iles, K. E., & Forman, H. J. (2002). Macrophage signaling and respiratory burst. *Immunologic Research*, (26), 95–105.

Ilg, T., Stierhof, Y. D., Wiese, M., Overath, P., & McConville, M. J. (1994). Characterization of phosphoglycan-containing secretory products of Leishmania. *Parasitology*, *108*(S1), S63–S71. https://doi.org/10.1017/S0031182000075739

Iowa State University/College of Veterinary Medicine. (2009). Leishmaniasis (Cutaneous and Visceral). In *Iowa State University*.

Ishii, K. J., Gursel, I., Gursel, M., & Klinman, D. M. (2004). Immunotherapeutic utility of stimulatory and suppressive oligodeoxynucleotides. *Curr Opin Mol Ther*, *6*(2), 166–174.

Isnard, A., Shio, M. T., & Olivier, M. (2012). Impact of Leishmania metalloprotease GP63 on macrophage signaling. *Frontiers in Cellular and Infection Microbiology*, *2*. https://doi.org/10.3389/fcimb.2012.00072

Ives, A., Ronet, C., Prevel, F., Ruzzante, G., Fuertes-Marraco, S., Schutz, F., … Masina, S. (2011). Leishmania RNA virus controls the severity of mucocutaneous leishmaniasis. *Science*, *331*(6018), 775–778. https://doi.org/10.1126/science.1199326

Iyer, J. P., Kaprakkaden, A., Choudhary, M. L., & Shaha, C. (2008). Crucial role of cytosolic tryparedoxin peroxidase in Leishmania donovani survival, drug response and virulence. *Molecular Microbiology*, *68*(2), 372–391. https://doi.org/10.1111/j.1365-2958.2008.06154.x

Jaramillo, M., Gomez, M. A., Larsson, O., Shio, M. T., Topisirovic, I., Contreras, I., … Sonenberg, N. (2011). Leishmania repression of host translation through mTOR cleavage is required for parasite survival and infection. *Cell Host and Microbe*, *9*(4), 331–341. https://doi.org/10.1016/j.chom.2011.03.008

Jensen, R. E., & Englund, P. T. (2012). Network News: The Replication of Kinetoplast DNA. *Annual Review of Microbiology*, *66*(1), 473–491. https://doi.org/10.1146/annurev-micro-092611-150057

Jones, L., Bell, C., Bibb, K., Gu, L., Coats, M., & Matthews, Q. (2018). Pathogens and Their Effect on Exosome Biogenesis and Composition. *Biomedicines*, *6*(3), 79. https://doi.org/10.3390/biomedicines6030079

Kar, K. (1995). Serodiagnosis of Leishmaniasis. *Critical Reviews in Microbiology*, *21*(2), 123–152. https://doi.org/10.3109/10408419509113537

Katakura, K., & Kobayashi, A. (1985). Enhancement of Infectivity of Leishmania donovani Promastigotes by Serial Mouse Passages. *The Journal of Parasitology*, *71*(3), 393. https://doi.org/10.2307/3282033

Kavoosi, G., Ardestani, S. K., & Kariminia, A. (2009). The involvement of TLR2 in cytokine and reactive oxygen species (ROS) production by PBMCs in response to Leishmania major phosphoglycans (PGs). *Parasitology*, *136*(10), 1193–1199. https://doi.org/10.1017/S0031182009990473

Kawano, T., Cui, J., Koezuka, Y., Toura, I., Kaneko, Y., Motoki, K., … Taniguchi, M. (1997). CD1d-restricted and TCR-mediated activation of V(α)14 NKT cells by glycosylceramides. *Science*, *278*(5343), 1626–1629. https://doi.org/10.1126/science.278.5343.1626

Kedzierski, L. (2010). Leishmaniasis vaccine: Where are we today? *Journal of Global Infectious Diseases*, *2*(2), 177. https://doi.org/10.4103/0974-777X.62881

Keller, S., Sanderson, M. P., Stoeck, A., & Altevogt, P. (2006). Exosomes: From biogenesis and secretion to biological function. *Immunology Letters*, *107*(2), 102–108. https://doi.org/10.1016/j.imlet.2006.09.005

Khan, K. H. (2013). DNA vaccines: Roles against diseases. *Germs*, *3*(1), 26–35. https://doi.org/10.11599/germs.2013.1034

Killick-Kendrick, R. (1999). The biology and control of Phlebotomine sand flies. *Clinics in Dermatology*, *17*(3), 279–289. https://doi.org/10.1016/S0738-081X(99)00046-2

Kima, P. E., & Soong, L. (2013). Interferon gamma in leishmaniasis. *Frontiers in Immunology*, *4*(JUN). https://doi.org/10.3389/fimmu.2013.00156

Klinman, D. M., Klaschik, S., Sato, T., & Tross, D. (2009). CpG oligonucleotides as adjuvants for vaccines targeting infectious diseases. *Advanced Drug Delivery Reviews*, *61*(3), 248–255. https://doi.org/10.1016/j.addr.2008.12.012

Klinman, D. M., Takeshita, F., Gursel, I., Leifer, C., Ishii, K. J., Verthelyi, D., & Gursel, M. (2002). CpG DNA: Recognition by and activation of monocytes. *Microbes and Infection*, *4*(9), 897–901. https://doi.org/10.1016/S1286-4579(02)01614-3

Kulkarni, M. M., McMaster, W. R., Kamysz, E., Kamysz, W., Engman, D. M., & McGwire, B. S. (2006). The major surface-metalloprotease of the parasitic protozoan, Leishmania, protects against antimicrobial peptide-induced apoptotic killing. *Molecular Microbiology*, *62*(5), 1484–1497. https://doi.org/10.1111/j.1365-2958.2006.05459.x

Kumar, H., Kawai, T., & Akira, S. (2011). Pathogen recognition by the innate immune system. *International Reviews of Immunology*, *30*(1), 16–34. https://doi.org/10.3109/08830185.2010.529976

Lai, G. N., Hsu, A., Mandell, M. A., Roediger, B., Hoeller, C., Mrass, P., … Weninger, W. (2008). Migratory dermal dendritic cells act as rapid sensors of protozoan parasites. *PLoS Pathogens*, *4*(11). https://doi.org/10.1371/journal.ppat.1000222

Lainson, R., & Shaw, J. J. (1987). Evolution, classification and geographical distribution. In *The leishmaniases in biology and medicine. Volume I. Biology and epidemiology* (pp. 1–120).

Lambertz, U., Silverman, J. M., Nandan, D., McMaster, W. R., Clos, J., Foster, L. J., & Reiner, N. E. (2012). Secreted virulence factors and immune evasion in visceral leishmaniasis. *Journal of Leukocyte Biology*, *91*(6), 887–899. https://doi.org/10.1189/jlb.0611326

Laurent, M., & Steinert, M. (1970). Electron Microscopy of Kinetoplastic DNA from Trypanosoma mega. *Proceedings of the National Academy of Sciences*, *66*(2), 419–424. https://doi.org/10.1073/pnas.66.2.419

Lazarski, C. A., Ford, J., Katzman, S. D., Rosenberg, A. F., & Fowell, D. J. (2013). IL-4 Attenuates Th1-Associated Chemokine Expression and Th1 Trafficking to Inflamed Tissues and Limits Pathogen Clearance. *PLoS ONE*, *8*(8). https://doi.org/10.1371/journal.pone.0071949

Leishman, W. B. (1903). On the possibility of the occurrence of trypanosomiasis in india. *British Medical Journal*, *2*(2238), 1376–1377. https://doi.org/10.1136/bmj.2.2238.1376-a

León, B., López-Bravo, M., & Ardavín, C. (2007). Monocyte-Derived Dendritic Cells Formed at the Infection Site Control the Induction of Protective T Helper 1 Responses against Leishmania. *Immunity*, *26*(4), 519–531. https://doi.org/10.1016/j.immuni.2007.01.017

Li, Y., Ishii, K., Hisaeda, H., Hamano, S., Zhang, M., Nakanishi, K., … Himeno, K. (2004). IL-18 gene therapy develops Th1-type immune responses in Leishmania major-infected BALB/c mice: Is the effect mediated by the CpG signaling TLR9? *Gene Therapy*, *11*(11), 941–948. https://doi.org/10.1038/sj.gt.3302240

Liese, J., Schleicher, U., & Bogdan, C. (2007). TLR9 signaling is essential for the innate NK cell response in murine cutaneous leishmaniasis. *European Journal of Immunology*, *37*(12), 3424–3434. https://doi.org/10.1002/eji.200737182

Lim, Y. S., Cha, M. K., Kim, H. K., Uhm, T. B., Park, J. W., Kim, K., & Kim, I. H. (1993). Removals of hydrogen peroxide and hydroxyl radical by thiol-specific antioxidant protein as a possible role in vivo. *Biochemical and Biophysical Research Communications*, *192*(1), 273–280. https://doi.org/10.1006/bbrc.1993.1410

Lima, H. C., Bleyenberg, J. A., & Titus, R. G. (1997). A simple method for quantifying Leishmania in tissues of infected animals. *Parasitology Today*, *13*(2), 80–82.

https://doi.org/10.1016/S0169-4758(96)40010-2

Lindqvist, M., Persson, J., Thörn, K., & Harandi, A. M. (2009). The Mucosal Adjuvant Effect of α-Galactosylceramide for Induction of Protective Immunity to Sexually Transmitted Viral Infection. *The Journal of Immunology*, *182*(10), 6435–6443. https://doi.org/10.4049/jimmunol.0900136

Liu, D., & Uzonna, J. E. (2012). The early interaction of Leishmania with macrophages and dendritic cells and its influence on the host immune response. *Frontiers in Cellular and Infection Microbiology*, *2*, 83.

Lopez Kostka, S., Dinges, S., Griewank, K., Iwakura, Y., Udey, M. C., & von Stebut, E. (2009). IL-17 Promotes Progression of Cutaneous Leishmaniasis in Susceptible Mice. *The Journal of Immunology*, *182*(5), 3039–3046. https://doi.org/10.4049/jimmunol.0713598

Lukeš, J., Skalický, T., Týč, J., Votýpka, J., & Yurchenko, V. (2014). Evolution of parasitism in kinetoplastid flagellates. *Molecular and Biochemical Parasitology*, *195*(2), 115–122. https://doi.org/10.1016/j.molbiopara.2014.05.007

Majumdar, T., Chattopadhyay, S., Ozhegov, E., Dhar, J., Goswami, R., Sen, G. C., & Barik, S. (2015). Induction of Interferon-Stimulated Genes by IRF3 Promotes Replication of Toxoplasma gondii. *PLoS Pathogens*, *11*(3), 1–22. https://doi.org/10.1371/journal.ppat.1004779

Marini, J. C., Levene, S. D., Crothers, D. M., & Englund, P. T. (1982). Bent helical structure in kinetoplast DNA. *Proceedings of the National Academy of Sciences*, *79*(24), 7664–7668. https://doi.org/10.1073/pnas.79.24.7664

Markle, W. H., & Makhoul, K. (2004). Cutaneous Leishmaniasis: Recognition and Treatment. *American Family Physician*.

Marshall, S., Kelly, P. H., Singh, B. K., Pope, R. M., Kim, P., Zhanbolat, B., … Yao, C. (2018). Extracellular release of virulence factor major surface protease via exosomes in Leishmania infantum promastigotes. *Parasites and Vectors*, *11*(1). https://doi.org/10.1186/s13071-018-2937-y

Mattner, J., Schindler, H., Diefenbach, A., Röllinghoff, M., Gresser, I., & Bogdan, C. (2000). Regulation of type 2 nitric oxide synthase by type 1 interferons in macrophages infected withLeishmania major. *European Journal of Immunology*, *30*(8), 2257–2267. https://doi.org/10.1002/1521-4141(2000)30:8<2257::aid-immu2257>3.0.co;2-u

Mayrink, W., Magalhães, P. A., Dias, M., da Costa, C. A., Melo, M. N., & Lima, A. O. (1978). Responses to Montenegro antigen after immunization with killed Leishmania promastigotes. *Transactions of the Royal Society of Tropical Medicine and Hygiene*, *72*(6), 676. https://doi.org/10.1016/0035-9203(78)90041-X

Meyer, H., Musacchio, M. O., & Mendonça, I. A. (1958). Electron microscopic study of Trypanosoma cruzi in thin sections of infected tissue cultures and of blood-agar forms. *Parasitology*, *48*(1–2), 1–8. https://doi.org/10.1017/S0031182000021028

Michel, G., Ferrua, B., Lang, T., Maddugoda, M. P., Munro, P., Pomares, C., … Marty, P. (2011). Luciferase-expressing Leishmania infantum allows the monitoring of amastigote population size, in vivo, ex vivo and in vitro. *PLoS Neglected Tropical Diseases*, *5*(9). https://doi.org/10.1371/journal.pntd.0001323

Miles, S. A., Conrad, S. M., Alves, R. G., Jeronimo, S. M. B., & Mosser, D. M. (2005). A role for IgG immune complexes during infection with the intracellular pathogen Leishmania . *The Journal of Experimental Medicine*, *201*(5), 747–754. https://doi.org/10.1084/jem.20041470

Modabber, F. (1989). Experiences with vaccines against cutaneous leishmaniasis: Of men and mice. *Parasitology*, *98*(S1), S49–S60. https://doi.org/10.1017/S0031182000072243

Momen, H., & Cupolillo, E. (2000). Speculations on the Origin and Evolution of the Genus Leishmania. *Memorias Do Instituto Oswaldo Cruz*, *95*(4), 583–588. https://doi.org/10.1590/S0074-02762000000400023

Mondal, D., Bern, C., Ghosh, D., Rashid, M., Molina, R., Chowdhury, R., … Alvar, J. (2018). Quantifying the Infectiousness of Post-Kala-Azar Dermal Leishmaniasis Toward Sand Flies. *Clinical Infectious Diseases*. https://doi.org/10.1093/cid/ciy891

Moreira, D., Santarém, N., Loureiro, I., Tavares, J., Silva, A. M., Amorim, A. M., … Silvestre, R. (2012). Impact of continuous axenic cultivation in Leishmania infantum virulence. *PLoS Neglected Tropical Diseases*, *6*(1). https://doi.org/10.1371/journal.pntd.0001469

Morizot, G., Kendjo, E., Mouri, O., Thellier, M., Pérignon, A., Foulet, F., … Rebauder, S. (2013). Travelers with cutaneous leishmaniasis cured without systemic therapy. *Clinical Infectious Diseases*, *57*(3), 370–380. https://doi.org/10.1093/cid/cit269

Mottram, J. C., Coombs, G. H., & Alexander, J. (2004). Cysteine peptidases as virulence factors of Leishmania. *Current Opinion in Microbiology*, *7*(4), 375–381. https://doi.org/10.1016/j.mib.2004.06.010

N Barber, G. (2011). Innate immune DNA sensing pathways: STING, AIMII and the regulation of interferon production and inflammatory responses. *Current Opinion in Immunology*, *23*(1), 10–20. Retrieved from http://www.mendeley.com/catalog/innate-immune-dna-sensing-pathways-sting-aimii-regulation-interferon-production-inflammatory-responses/

Nandan, D., & Reiner, N. E. (1995). Attenuation of gamma interferon-induced tyrosine phosphorylation in mononuclear phagocytes infected with Leishmania donovani: Selective inhibition of signaling through Janus kinases and Stat1. *Infection and Immunity*, *63*(11), 4495–4500.

Nicolas, L., Prina, E., Lang, T., & Milon, G. (2002). Real-time PCR for detection and quantitation of Leishmania in mouse tissues. *Journal of Clinical Microbiology*, *40*(5), 1666–1669. https://doi.org/10.1128/JCM.40.5.1666-1669.2002

Novais, F. O., Carvalho, L. P., Graff, J. W., Beiting, D. P., Ruthel, G., Roos, D. S., … Scott, P. (2013). Cytotoxic T Cells Mediate Pathology and Metastasis in Cutaneous Leishmaniasis. *PLoS Pathogens*, *9*(7). https://doi.org/10.1371/journal.ppat.1003504

Novais, F. O., Santiago, R. C., Báfica, A., Khouri, R., Afonso, L., Borges, V. M., … de Oliveira, C. I. (2009). Neutrophils and Macrophages Cooperate in Host Resistance against Leishmania braziliensis Infection . *The Journal of Immunology*, *183*(12), 8088–8098. https://doi.org/10.4049/jimmunol.0803720

Olivier, M., Atayde, V. D., Isnard, A., Hassani, K., & Shio, M. T. (2012). Leishmania virulence factors: Focus on the metalloprotease GP63. *Microbes and Infection*, *14*(15), 1377–1389. https://doi.org/10.1016/j.micinf.2012.05.014

Olivier, M., & Fernandez-Prada, C. (2019). Leishmania and its exosomal pathway: A novel direction for vaccine development. *Future Microbiology*, *14*(7), 559–561. https://doi.org/10.2217/fmb-2019-0087

Oumeish, O. Y. (1999). Cutaneous leishmaniasis: A historical perspective. *Clinics in Dermatology*, *17*(3), 249–254. https://doi.org/10.1016/S0738-081X(99)00041-3

Özbilgin, A., Çulha, G., Uzun, S., Harman, M., Topal, S. G., Okudan, F., … Özbel, Y. (2016). Leishmaniasis in Turkey: First clinical isolation of Leishmania major from 18 autochthonous cases of cutaneous leishmaniasis in four geographical regions. *Tropical Medicine and International Health*, *21*(6), 783–791. https://doi.org/10.1111/tmi.12698

Özbilgin, A., Harman, M., Karakuş, M., Bart, A., Töz, S., Kurt, Ö., … Özbel, Y. (2017). Leishmaniasis in Turkey: Visceral and cutaneous leishmaniasis caused by Leishmania donovani in Turkey. *Acta Tropica*, *173*, 90–96. https://doi.org/10.1016/j.actatropica.2017.05.032

Özkeklikçi, A., Karakuş, M., Özbel, Y., & Töz, S. (2017). The new situation of cutaneous leishmaniasis after Syrian civil war in Gaziantep city, Southeastern region of Turkey. *Acta Tropica*, *166*, 35–38. https://doi.org/10.1016/j.actatropica.2016.10.019

Panday, A., Sahoo, M. K., Osorio, D., & Batra, S. (2015). NADPH oxidases: An overview from structure to innate immunity-associated pathologies. *Cellular and*

Molecular Immunology, *12*(1), 5–23. https://doi.org/10.1038/cmi.2014.89

Pastré, D., Piétrement, O., Fusil, S., Landousy, F., Jeusset, J., David, M. O., … Zozime, A. (2003). Adsorption of DNA to mica mediated by divalent counterions: A theoretical and experimental study. *Biophysical Journal*, *85*(4), 2507–2518. https://doi.org/10.1016/S0006-3495(03)74673-6

Pérez-Cabezas, B., Santarém, N., Cecílio, P., Silva, C., Silvestre, R., A. M. Catita, J., & Cordeiro da Silva, A. (2019). More than just exosomes: distinct Leishmania infantum extracellular products potentiate the establishment of infection. *Journal of Extracellular Vesicles*, *8*(1). https://doi.org/10.1080/20013078.2018.1541708

Peters, N. C., Egen, J. G., Secundino, N., Debrabant, A., Kimblin, N., Kamhawi, S., … Sacks, D. (2008). In vivo imaging reveals an essential role for neutrophils in leishmaniasis transmitted by sand flies. *Science*, *321*(5891), 970–974. https://doi.org/10.1126/science.1159194

Pinto, A. K., Richner, J. M., Poore, E. A., Patil, P. P., Amanna, I. J., Slifka, M. K., & Diamond, M. S. (2013). A Hydrogen Peroxide-Inactivated Virus Vaccine Elicits Humoral and Cellular Immunity and Protects against Lethal West Nile Virus Infection in Aged Mice. *Journal of Virology*, *87*(4), 1926–1936. https://doi.org/10.1128/jvi.02903-12

Poore, E. A., Slifka, D. K., Raué, H. P., Thomas, A., Hammarlund, E., Quintel, B. K., … Amanna, I. J. (2017). Pre-clinical development of a hydrogen peroxide-inactivated West Nile virus vaccine. *Vaccine*, *35*(2), 283–292. https://doi.org/10.1016/j.vaccine.2016.11.080

Prevention, C.-C. for D. C. and. (2019). CDC - Leishmaniasis - Biology. Retrieved July 30, 2019, from https://www.cdc.gov/parasites/leishmaniasis/biology.html

Rafati, S., Baba, A. A., Bakhshayesh, M., & Vafa, M. (2000). Vaccination of BALB/c mice with Leishmania major amastigote-specific cysteine proteinase. *Clinical and Experimental Immunology*, *120*(1), 134–138. https://doi.org/10.1046/j.1365-2249.2000.01160.x

Rafati, S., Gholami, E., Hassani, N., Ghaemimanesh, F., Taslimi, Y., Taheri, T., & Soong, L. (2007). Leishmania major heat shock protein 70 (HSP70) is not protective in murine models of cutaneous leishmaniasis and stimulates strong humoral responses in cutaneous and visceral leishmaniasis patients. *Vaccine*, *25*(21), 4159–4169. https://doi.org/10.1016/j.vaccine.2007.03.006

Ready, P. D. (1979). Factors affecting egg production of laboratory-bred Lutzomyia longipalpis (Diptera: Psychodidae). *Journal of Medical Entomology*, *16*(5), 413–423. https://doi.org/10.1093/jmedent/16.5.413

Ready, Paul D. (2013). Biology of Phlebotomine Sand Flies as Vectors of Disease Agents. *Annual Review of Entomology*, *58*(1), 227–250.

https://doi.org/10.1146/annurev-ento-120811-153557

Ready, Paul D. (2014). Epidemiology of visceral leishmaniasis. *Clinical Epidemiology*, *6*(1), 147–154. https://doi.org/10.2147/CLEP.S44267

Reiling, L., Jacobs, T., Kroemer, M., Gaworski, I., Graefe, S., & Clos, J. (2006). Spontaneous recovery of pathogenicity by Leishmania major hsp100 -/- alters the immune response in mice. *Infection and Immunity*, *74*(11), 6027–6036. https://doi.org/10.1128/IAI.00773-05

Reithinger, R., Dujardin, J.-C., Louzir, H., Pirmez, C., Alexander, B., & Brooker, S. (2007). Cutaneous leishmaniasis. *The Lancet Infectious Diseases*, *7*(9), 581–596. https://doi.org/10.1016/S1473-3099(07)70209-8

Remadi, L., Haouas, N., Chaara, D., Slama, D., Chargui, N., Dabghi, R., … Babba, H. (2017). Clinical Presentation of Cutaneous Leishmaniasis caused by Leishmania major. *Dermatology*, *232*(6), 752–759. https://doi.org/10.1159/000456543

Rhee, E. G., Mendez, S., Shah, J. A., Wu, C., Kirman, J. R., Turon, T. N., … Seder, R. A. (2002). Vaccination with Heat-killed Leishmania Antigen or Recombinant Leishmanial Protein and CpG Oligodeoxynucleotides Induces Long-Term Memory CD4 + and CD8 + T Cell Responses and Protection Against Leishmania major Infection . *The Journal of Experimental Medicine*, *195*(12), 1565–1573. https://doi.org/10.1084/jem.20020147

Ribeiro-Gomes, F. L., Moniz-de-Souza, M. C. A., Alexandre-Moreira, M. S., Dias, W. B., Lopes, M. F., Nunes, M. P., … DosReis, G. A. (2007). Neutrophils Activate Macrophages for Intracellular Killing of Leishmania major through Recruitment of TLR4 by Neutrophil Elastase . *The Journal of Immunology*, *179*(6), 3988–3994. https://doi.org/10.4049/jimmunol.179.6.3988

Ribeiro-Gomes, F. L., Peters, N. C., Debrabant, A., & Sacks, D. L. (2012). Efficient capture of infected neutrophils by dendritic cells in the skin inhibits the early anti-leishmania response. *PLoS Pathogens*, *8*(2). https://doi.org/10.1371/journal.ppat.1002536

Ritz, C., Baty, F., Streibig, J. C., & Gerhard, D. (2015). Dose-response analysis using R. *PLoS ONE*, *10*(12). https://doi.org/10.1371/journal.pone.0146021

Roberts, L., & Janovy, J. (2009). Foundations Of Parasitology 8th Ed. In *Society*. https://doi.org/10.1016/0169-4758(90)90219-T

Rochael, N. C., Guimarães-Costa, A. B., Nascimento, M. T. C., Desouza-Vieira, T. S., Oliveira, M. P., Garciae Souza, L. F., … Saraiva, E. M. (2015). Classical ROS-dependent and early/rapid ROS-independent release of Neutrophil Extracellular Traps triggered by Leishmania parasites. *Scientific Reports*, *5*. https://doi.org/10.1038/srep18302

Rogers, M. E., & Bates, P. A. (2007). Leishmania manipulation of sand fly feeding behavior results in enhanced transmission. *PLoS Pathogens*, *3*(6), 0818–0825. https://doi.org/10.1371/journal.ppat.0030091

Romero, I., Téllez, J., Suárez, Y., Cardona, M., Figueroa, R., Zelazny, A., & Saravia, N. G. (2010). Viability and burden of Leishmania in extralesional sites during human dermal leishmaniasis. *PLoS Neglected Tropical Diseases*, *4*(9). https://doi.org/10.1371/journal.pntd.0000819

Rossi, M., Castiglioni, P., Hartley, M.-A., Eren, R. O., Prével, F., Desponds, C., … Fasel, N. (2017). Type I interferons induced by endogenous or exogenous viral infections promote metastasis and relapse of leishmaniasis. *Proceedings of the National Academy of Sciences*, *114*(19), 4987–4992. https://doi.org/10.1073/pnas.1621447114

Rossi, M., & Fasel, N. (2018). How to master the host immune system? Leishmania parasites have the solutions! *International Immunology*. https://doi.org/10.1093/intimm/dxx075

Sacks, D. L., & Perkins, P. V. (1985). Development of infective stage Leishmania promastigotes within phlebotomine sand flies. *American Journal of Tropical Medicine and Hygiene*, *34*(3), 456–459. https://doi.org/10.4269/ajtmh.1985.34.456

Sacks, D., & Noben-Trauth, N. (2002). The immunology of susceptibility and resistance to Leishmania major in mice. *Nature Reviews Immunology*, *2*(11), 845–858. https://doi.org/10.1038/nri933

Sacks, David L., & Perkins, P. V. (1984). Identification of an infective stage of Leishmania promastigotes. *Science*, *223*(4643), 1417–1419. https://doi.org/10.1126/science.6701528

Salam, N., Al-Shaqha, W. M., & Azzi, A. (2014). Leishmaniasis in the Middle East: Incidence and Epidemiology. *PLoS Neglected Tropical Diseases*, *8*(10). https://doi.org/10.1371/journal.pntd.0003208

Sansom, F. M., Tang, L., Ralton, J. E., Saunders, E. C., Naderer, T., & McConville, M. J. (2013). Leishmania major Methionine Sulfoxide Reductase A Is Required for Resistance to Oxidative Stress and Efficient Replication in Macrophages. *PLoS ONE*, *8*(2). https://doi.org/10.1371/journal.pone.0056064

Santiago, H. C., Oliveira, M. A. P., Bambirra, E. A., Faria, A. M. C., Afonso, L. C. C., Vieira, L. Q., & Gazzinelli, R. T. (1999). Coinfection with Toxoplasma gondii inhibits antigen-specific Th2 immune responses, tissue inflammation, and parasitism in BALB/c mice infected with Leishmania major. *Infection and Immunity*, *67*(9), 4939–4944.

Sato, N., Ahuja, S. K., Quinones, M., Kostecki, V., Reddick, R. L., Melby, P. C., …

Ahuja, S. S. (2000). CC chemokine receptor (CCR)2 is required for langerhans cell migration and localization of T helper cell type 1 (Th1)-inducing dendritic cells: Absence of CCR2 shifts the Leishmania major - Resistant phenotype to a susceptible state dominated by Th2 cytok. *Journal of Experimental Medicine*. https://doi.org/10.1084/jem.192.2.205

Schalkwijk, J., Van Der Berg, W. B., & Van De Putte, L. B. A. (1985). Cationization of catalase, peroxidase, and superoxide dismutase: Effect of improved intraarticular retention on experimental arthritis in mice. *Journal of Clinical Investigation*, *76*(1), 198–205. https://doi.org/10.1172/JCI111946

Scharton, T. M., & Scott, P. (1993). Natural killer cells are a source of interferon γ that drives differentiation of CD4+ T cell subsets and induces early resistance to leishmania major in mice. *Journal of Experimental Medicine*, *178*(2), 567–578. https://doi.org/10.1084/jem.178.2.567

Schleicher, U., Liese, J., Knippertz, I., Kurzmann, C., Hesse, A., Heit, A., … Bogdan, C. (2007). NK cell activation in visceral leishmaniasis requires TLR9, myeloid DCs, and IL-12, but is independent of plasmacytoid DCs. *Journal of Experimental Medicine*, *204*(4), 893–906. https://doi.org/10.1084/jem.20061293

Schorey, J. S., Cheng, Y., Singh, P. P., & Smith, V. L. (2015). Exosomes and other extracellular vesicles in host-pathogen interactions. *EMBO Reports*, *16*(1), 24–43. https://doi.org/10.15252/embr.201439363

Schubach, A., Haddad, F., Neto, M. P., Degrave, W., Pirmez, C., Grimaldi, Jr., G., & Fernandes, O. (2009). Detection of Leishmania DNA by Polymerase Chain Reaction in Scars of Treated Human Patients . *The Journal of Infectious Diseases*, *178*(3), 911–914. https://doi.org/10.1086/515355

Scott, P., & Novais, F. O. (2016). Cutaneous leishmaniasis: Immune responses in protection and pathogenesis. *Nature Reviews Immunology*, *16*(9), 581–592. https://doi.org/10.1038/nri.2016.72

Segovia, M., Artero, J. M., Mellado, E., & Chance, M. L. (1992). Effects of long-term in vitro cultivation on the virulence of cloned lines of Leishmania major promastigotes. *Annals of Tropical Medicine and Parasitology*, *86*(4), 347–354. https://doi.org/10.1080/00034983.1992.11812677

Shapiro, T. A. (1993). Kinetoplast DNA maxicircles: networks within networks. *Proceedings of the National Academy of Sciences*, *90*(16), 7809–7813. https://doi.org/10.1073/pnas.90.16.7809

Shlomai, J. (2005). The Structure and Replication of Kinetoplast DNA. *Current Molecular Medicine*, *4*(6), 623–647. https://doi.org/10.2174/1566524043360096

Silva-Barrios, S., Smans, M., Duerr, C. U., Qureshi, S. T., Fritz, J. H., Descoteaux, A., & Stäger, S. (2016). Innate Immune B Cell Activation by Leishmania

donovani Exacerbates Disease and Mediates Hypergammaglobulinemia. *Cell Reports*, *15*(11), 2427–2437. https://doi.org/10.1016/j.celrep.2016.05.028

Silveira, F. T., Lainson, R., De Castro Gomes, C. M., Laurenti, M. D., & Corbett, C. E. P. (2009). Immunopathogenic competences of Leishmania (V.) braziliensis and L. (L.) amazonensis in American cutaneous leishmaniasis. *Parasite Immunology*, *31*(8), 423–431. https://doi.org/10.1111/j.1365-3024.2009.01116.x

Silverman, Judith. M., Chan, S. K., Robinson, D. P., Dwyer, D. M., Nandan, D., Foster, L. J., & Reiner, N. E. (2008). Proteomic analysis of the secretome of Leishmania donovani. *Genome Biology*, *9*(2). https://doi.org/10.1186/gb-2008-9-2-r35

Silverman, Judith Maxwell, Clos, J., de'Oliveira, C. C., Shirvani, O., Fang, Y., Wang, C., … Reiner, N. E. (2010). An exosome-based secretion pathway is responsible for protein export from Leishmania and communication with macrophages . *Journal of Cell Science*, *123*(6), 842–852. https://doi.org/10.1242/jcs.056465

Simpson, A. G. B., Stevens, J. R., & Lukeš, J. (2006). The evolution and diversity of kinetoplastid flagellates. *Trends in Parasitology*, Vol. 22, pp. 168–174. https://doi.org/10.1016/j.pt.2006.02.006

Simpson, L. (1987). The Mitochondrial Genome Of Kinetoplastid Protozoa: Genomic Organization, Transcription, Replication, And Evolution. *Annual Review of Microbiology*, *41*(1), 363–382. https://doi.org/10.1146/annurev.micro.41.1.363

Simpson, Larry, & da Silva, A. (1971). Isolation and characterization of kinetoplast DNA from Leishmania tarentolae. *Journal of Molecular Biology*, *56*(3). https://doi.org/10.1016/0022-2836(71)90394-9

Simpson, R. J., Lim, J. W. E., Moritz, R. L., & Mathivanan, S. (2009). Exosomes: Proteomic insights and diagnostic potential. *Expert Review of Proteomics*, *6*(3), 267–283. https://doi.org/10.1586/epr.09.17

Smelt, S. C., Cotterell, S. E. J., Engwerda, C. R., & Kaye, P. M. (2000). B Cell-Deficient Mice Are Highly Resistant to Leishmania donovani Infection, but Develop Neutrophil-Mediated Tissue Pathology . *The Journal of Immunology*, *164*(7), 3681–3688. https://doi.org/10.4049/jimmunol.164.7.3681

Smyth, M. J., Crowe, N. Y., Pellicci, D. G., Kyparissoudis, K., Kelly, J. M., Takeda, K., … Godfrey, D. I. (2002). Sequential production of interferon-γ by NK1.1+ T cells and natural killer cells is essential for the antimetastatic effect of α-galactosylceramide. *Blood*, *99*(4), 1259–1266. https://doi.org/10.1182/blood.V99.4.1259

Snapper, C. M., & Paul, W. E. (1987). Interferon-γ and B cell stimulatory factor-1 reciprocally regulate Ig isotype production. *Science*, *236*(4804), 944–947. https://doi.org/10.1126/science.3107127

Solbach, W., & Laskay, T. (2000). The host response to Leishmania infection. *Advances in Immunology*, *74*, 275–317.

Souza, W. De. (2008). Electron microscopy of trypanosomes--a historical view. *Memorias Do Instituto Oswaldo Cruz*, *103*(4), 313–325. https://doi.org/10.1590/S0074-02762008000400001

Souza, P. E. A., Rocha, M. O. C., Menezes, C. A. S., Coelho, J. S., Chaves, A. C. L., Gollob, K. J., & Dutra, W. O. (2007). Trypanosoma cruzi infection induces differential modulation of costimulatory molecules and cytokines by monocytes and T cells from patients with indeterminate and cardiac Chagas' disease. *Infection and Immunity*, *75*(4), 1886–1894. https://doi.org/10.1128/IAI.01931-06

Späth, G. F., & Beverley, S. M. (2001). A lipophosphoglycan-independent method for isolation of infective Leishmania metacyclic promastigotes by density gradient centrifugation. *Experimental Parasitology*, *99*(2), 97–103. https://doi.org/10.1006/expr.2001.4656

Spath, G. F., Epstein, L., Leader, B., Singer, S. M., Avila, H. A., Turco, S. J., & Beverley, S. M. (2000). Lipophosphoglycan is a virulence factor distinct from related glycoconjugates in the protozoan parasite Leishmania major. *Proceedings of the National Academy of Sciences*, *97*(16), 9258–9263. https://doi.org/10.1073/pnas.160257897

Spotin, A., Rouhani, S., & Parvizi, P. (2014). The Associations of Leishmania major and Leishmania tropica Aspects by Focusing Their Morphological and Molecular Features on Clinical Appearances in Khuzestan Province, Iran. *BioMed Research International*, *2014*. https://doi.org/10.1155/2014/913510

Stäger, S., & Rafati, S. (2012). CD8+ T cells in Leishmania infections: Friends or foes? *Frontiers in Immunology*, Vol. 3. https://doi.org/10.3389/fimmu.2012.00005

Stark, D., Pett, S., Marriott, D., & Harkness, J. (2006). Post-kala-azar dermal leishmaniasis due to Leishmania infantum in a human immunodeficiency virus type 1-infected patient. *Journal of Clinical Microbiology*, *44*(3), 1178–1180. https://doi.org/10.1128/JCM.44.3.1178-1180.2006

Steverding, D. (2017). The history of leishmaniasis. *Parasites and Vectors*, *10*(1), 1–10. https://doi.org/10.1186/s13071-017-2028-5

Sundar, S., & Chakravarty, J. (2012). Leishmaniasis: an update of current pharmacotherapy. *Expert Opinion on Pharmacotherapy*, *14*(1), 53–63. https://doi.org/10.1517/14656566.2013.755515

Sundar, S., & Chakravarty, J. (2015). An update on pharmacotherapy for leishmaniasis. *Expert Opinion on Pharmacotherapy*, *16*(2), 237–252. https://doi.org/10.1517/14656566.2015.973850

Sundar, S., More, D. K., Singh, M. K., Singh, V. P., Sharma, S., Makharia, A., … Murray, H. W. (2000). Failure of Pentavalent Antimony in Visceral Leishmaniasis in India: Report from the Center of the Indian Epidemic. *Clinical Infectious Diseases*, *31*(4), 1104–1107. https://doi.org/10.1086/318121

Sunter, J. D., Yanase, R., Wang, Z., Catta-Preta, C. M. C., Moreira-Leite, F., Myskova, J., … Gull, K. (2019). Leishmania flagellum attachment zone is critical for flagellar pocket shape, development in the sand fly, and pathogenicity in the host . *Proceedings of the National Academy of Sciences*, *116*(13), 6351–6360. https://doi.org/10.1073/pnas.1812462116

Sunter, J., & Gull, K. (2018). Correction to: Shape, form, function and Leishmania pathogenicity: From textbook descriptions to biological understanding (Open Biology (2017) 7 (170165) DOI: 10.1098/rsob.170165). *Open Biology*, *8*(8). https://doi.org/10.1098/rsob.180134

Sypek, J. P., Chung, C. L., Mayor, S. E. H., Subramanyam, J. M., Goldman, S. J., Sieburth, D. S., … Schaub, R. G. (1993). Resolution of cutaneous leishmaniasis: Interleukin 12 initiates a protective T helper type 1 immune response. *Journal of Experimental Medicine*, *177*(6), 1797–1802. https://doi.org/10.1084/jem.177.6.1797

Takeshita, F., Leifer, C. A., Gursel, I., Ishii, K. J., Takeshita, S., Gursel, M., & Klinman, D. M. (2001). Cutting Edge: Role of Toll-Like Receptor 9 in CpG DNA-Induced Activation of Human Cells. *The Journal of Immunology*, *167*(7), 3555–3558. https://doi.org/10.4049/jimmunol.167.7.3555

Taswell, C. (1981). Limiting dilution assays for the determination of immunocompetent cell frequencies. I. Data analysis. *Journal of Immunology (Baltimore, Md. : 1950)*, *126*(4), 1614–1619. Retrieved from http://www.ncbi.nlm.nih.gov/pubmed/7009746

Teixeira, A. R. L., Hecht, M. M., Guimaro, M. C., Sousa, A. O., & Nitz, N. (2011). Pathogenesis of chagas' disease: Parasite persistence and autoimmunity. *Clinical Microbiology Reviews*, *24*(3), 592–630. https://doi.org/10.1128/CMR.00063-10

Théry, C., Ostrowski, M., & Segura, E. (2009). Membrane vesicles as conveyors of immune responses. *Nature Reviews Immunology*, *9*(8), 581–593. https://doi.org/10.1038/nri2567

Thomas, B. N., & Buxbaum, L. U. (2008). FcγRIII mediates immunoglobulin G-induced interleukin-10 and is required for chronic Leishmania mexicana lesions. *Infection and Immunity*, *76*(2), 623–631. https://doi.org/10.1128/IAI.00316-07

Thomas, P. D., Campbell, M. J., Kejariwal, A., Mi, H., Karlak, B., Daverman, R., … Narechania, A. (2003). PANTHER: A library of protein families and subfamilies indexed by function. *Genome Research*, *13*(9), 2129–2141. https://doi.org/10.1101/gr.772403

174

TITUS, R. G., MARCHAND, M., BOON, T., & LOUIS, J. A. (1985). A limiting dilution assay for quantifying Leishmania major in tissues of infected mice. *Parasite Immunology*, *7*(5), 545–555. https://doi.org/10.1111/j.1365-3024.1985.tb00098.x

Trager, W. (1965). The Kinetoplast and Differentiation in Certain Parasitic Protozoa. *The American Naturalist*, *99*(907), 255–266. https://doi.org/10.1086/282371

Tull, D., Naderer, T., Spurck, T., Mertens, H. D. T., Heng, J., McFadden, G. I., … McConville, M. J. (2010). Membrane protein SMP-1 is required for normal flagellum function in Leishmania. *Journal of Cell Science*, *123*(4), 544–554. https://doi.org/10.1242/jcs.059097

Tuon, F. F., Amato, V. S., Bacha, H. A., AlMusawi, T., Duarte, M. I., & Neto, V. A. (2008). Toll-like receptors and leishmaniasis. *Infection and Immunity*, Vol. 76, pp. 866–872. https://doi.org/10.1128/IAI.01090-07

Uzun, S., Gürel, M. S., Durdu, M., Akyol, M., Fettahlıoğlu Karaman, B., Aksoy, M., … Harman, M. (2018). Clinical practice guidelines for the diagnosis and treatment of cutaneous leishmaniasis in Turkey. *International Journal of Dermatology*, *57*(8), 973–982. https://doi.org/10.1111/ijd.14002

Valencia, B. M., Miller, D., Witzig, R. S., Boggild, A. K., & Llanos-Cuentas, A. (2013). Novel Low-Cost Thermotherapy for Cutaneous Leishmaniasis in Peru. *PLoS Neglected Tropical Diseases*, *7*(5). https://doi.org/10.1371/journal.pntd.0002196

Van den Bogaart, E., Schoone, G. J., Adams, E. R., & Schallig, H. D. F. H. (2014). Duplex quantitative Reverse-Transcriptase PCR for simultaneous assessment of drug activity against Leishmania intracellular amastigotes and their host cells. *International Journal for Parasitology: Drugs and Drug Resistance*, *4*(1), 14–19. https://doi.org/10.1016/j.ijpddr.2013.11.001

Van Der Meide, W., Guerra, J., Schoone, G., Farenhorst, M., Coelho, L., Faber, W., … Schallig, H. (2008). Comparison between quantitative nucleic acid sequence-based amplification, real-time reverse transcriptase PCR, and real-time PCR for quantification of Leishmania parasites. *Journal of Clinical Microbiology*, *46*(1), 73–78. https://doi.org/10.1128/JCM.01416-07

Van Griensven, J., Carrillo, E., López-Vélez, R., Lynen, L., & Moreno, J. (2014). Leishmaniasis in immunosuppressed individuals. *Clinical Microbiology and Infection*, *20*(4), 286–299. https://doi.org/10.1111/1469-0691.12556

van Zandbergen, G., Klinger, M., Mueller, A., Dannenberg, S., Gebert, A., Solbach, W., & Laskay, T. (2004). Cutting Edge: Neutrophil Granulocyte Serves as a Vector for Leishmania Entry into Macrophages . *The Journal of Immunology*, *173*(11), 6521–6525. https://doi.org/10.4049/jimmunol.173.11.6521

Vargas-Inchaustegui, D. A., Xin, L., & Soong, L. (2008). Leishmania braziliensis Infection Induces Dendritic Cell Activation, ISG15 Transcription, and the Generation of Protective Immune Responses . *The Journal of Immunology*, *180*(11), 7537–7545. https://doi.org/10.4049/jimmunol.180.11.7537

Vélez, I. D., Del Pilar Agudelo, S., Arbelaez, M. P., Gilchrist, K., Robledo, S. M., Puerta, J. A., … Modabber, F. (2000). Safety and immunogenicity of a killed Leishmania (L.) amazonensis vaccine against cutaneous leishmaniasis in Colombia: Arandomized controlled trial. *Transactions of the Royal Society of Tropical Medicine and Hygiene*, *94*(6), 698–703. https://doi.org/10.1016/S0035-9203(00)90239-6

Verthelyi, D., Ishii, K. J., Gursel, M., Takeshita, F., & Klinman, D. M. (2001). Human Peripheral Blood Cells Differentially Recognize and Respond to Two Distinct CpG Motifs. *The Journal of Immunology*, *166*(4), 2372–2377. https://doi.org/10.4049/jimmunol.166.4.2372

Viana, A. G., Magalhães, L. M. D., Giunchetti, R. C., Dutra, W. O., & Gollob, K. J. (2018). Infection of human monocytes with Leishmania infantum strains induces a downmodulated response when compared with infection with Leishmania braziliensis. *Frontiers in Immunology*, *8*(DEC). https://doi.org/10.3389/fimmu.2017.01896

Vinet, A. F., Fukuda, M., Turco, S. J., & Descoteaux, A. (2009). The Leishmania donovani lipophosphoglycan excludes the vesicular proton-ATPase from phagosomes by impairing the recruitment of Synaptotagmin V. *PLoS Pathogens*, *5*(10). https://doi.org/10.1371/journal.ppat.1000628

Vollmer, J., & Krieg, A. M. (2009). Immunotherapeutic applications of CpG oligodeoxynucleotide TLR9 agonists. *Advanced Drug Delivery Reviews*, *61*(3), 195–204. https://doi.org/10.1016/j.addr.2008.12.008

Von Stebut, E., Belkaid, Y., Jakob, T., Sacks, D. L., & Udey, M. C. (1998). Uptake of Leishmania major amastigotes results in activation and interleukin 12 release from murine skin-derived dendritic cells: Implications for the initiation of anti-Leishmania immunity. *Journal of Experimental Medicine*, *188*(8), 1547–1552. https://doi.org/10.1084/jem.188.8.1547

Wanasen, N., Xin, L., & Soong, L. (2008). Pathogenic role of B cells and antibodies in murine Leishmania amazonensis infection. *International Journal for Parasitology*, *38*(3–4), 417–429. https://doi.org/10.1016/j.ijpara.2007.08.010

Weigle, K. A., de Davalos, M., Heredia, P., Molineros, R., Saravia, N. G., & D'Alessandro, A. (1987). Diagnosis of cutaneous and mucocutaneous leishmaniasis in Colombia: A comparison of seven methods. *American Journal of Tropical Medicine and Hygiene*, *36*(3), 489–496. https://doi.org/10.4269/ajtmh.1987.36.489

WHO. (2016). Leishmaniasis in high-burden countries: an epidemiological update based on data reported in 2014. *Weekly Epidemiological Record*, *91*, 287–296. https://doi.org/10.1186/1750-9378-2-15.Voir

World Health Organization. (2018). Global leishmaniasis surveillance update, 1998-2016. *Weekly Epidemiological Record Relevé Épidémiologique Hebdomadaire*, *40*, 521–540. https://doi.org/10.1186/1750-9378-2-15.Voir

World Health Organization. (2010). Control of the leishmaniases: Report of a meeting of the WHO Expert Committee on the Control of Leishmaniases,Geneva, 22–26 March 2010. In *World Health Organization Technical Report Series*.

Wortmann, G., Zapor, M., Ressner, R., Fraser, S., Hartzell, J., Pierson, J., … Magill, A. (2010). Lipsosomal amphotericin B for treatment of cutaneous leishmaniasis. *American Journal of Tropical Medicine and Hygiene*, *83*(5), 1028–1033. https://doi.org/10.4269/ajtmh.2010.10-0171

Wu, J., Sun, L., Chen, X., Du, F., Shi, H., Chen, C., & Chen, Z. J. (2013). Cyclic GMP-AMP is an endogenous second messenger in innate immune signaling by cytosolic DNA. *Science*. https://doi.org/10.1126/science.1229963

Yáñez-Mó, M., Siljander, P. R.-M., Andreu, Z., Zavec, A. B., Borràs, F. E., Buzas, E. I., … De Wever, O. (2015). Biological properties of extracellular vesicles and their physiological functions. *Journal of Extracellular Vesicles*, *4*, 27066. https://doi.org/10.3402/jev.v4.27066

Yildiz, S., Alpdundar, E., Gungor, B., Kahraman, T., Bayyurt, B., Gursel, I., & Gursel, M. (2015). Enhanced immunostimulatory activity of cyclic dinucleotides on mouse cells when complexed with a cell-penetrating peptide or combined with CpG. *European Journal of Immunology*, *45*(4), 1170–1179. https://doi.org/10.1002/eji.201445133

Zhang, L., & Tarleton, R. L. (1999). Parasite Persistence Correlates with Disease Severity and Localization in Chronic Chagas' Disease. *The Journal of Infectious Diseases*, *180*(2), 480–486. https://doi.org/10.1086/314889

Zijlstra, E. E., Musa, A. M., Khalil, E. A. G., El Hassan, I. M., & El-Hassan, A. M. (2003). Post-kala-azar dermal leishmaniasis. *Lancet Infectious Diseases*, Vol. 3, pp. 87–98. https://doi.org/10.1016/S1473-3099(03)00517-6

Zink, A. R., Spigelman, M., Schraut, B., Greenblatt, C. L., Nerlich, A. G., & Donoghue, H. D. (2006). Leishmaniasis in ancient Egypt and Upper Nubia [10]. *Emerging Infectious Diseases*, *12*(10), 1616–1617. https://doi.org/10.3201/eid1210.060169

APPENDICES

A. Recipes for Media

Table A.1. Leishmania Growth Medium

Ingredient	Volume (ml)	Final Concentration	Company	Cat No:
Heat Inactivated FBS	130	20 %	Biological Industries, Israel	04-127-1A
HEPES buffer 1M	13	20 mM	Biological Industries, Israel	03-025-1B
Penicillin/Streptomycin (Pen/Strep) Solution	6.5	Pen: 100 units/ml Strep: 100 µg/ml	Biological Industries, Israel	03-031-1B
RPMI 1640 Medium with L-glutamine and Phenol Red	500	-	Biological Industries, Israel	01-100-1A
TOTAL	649.5			

Table A.2. Leishmania Freezing Medium

Ingredient	Volume (ml)	Final Concentration	Company	Cat No:
Heat Inactivated FBS	4	40 %	Biological Industries, Israel	04-127-1A
Dimethyl Sulfoxide (DMSO)	2	20%	Merck, Germany	D8418
RPMI 1640 Medium with L-glutamine and Phenol Red	4	-	Biological Industries, Israel	01-100-1A
TOTAL	10			

Table A.3. Acidic Exosome Collection Medium (pH: ~5.5)

Ingredient	Volume (ml)	Final Concentration	Company	Cat No:
Exosome-Free Leishmania Growth Medium	31	--	--	--
MES Buffer (250mM)	3.5	25mM	Sigma-Aldrich, Germany	M1317
HCl (1N)	0.56	0.016N	Merck, Germany	1003171000
TOTAL	35			

Note: After acidic exosome isolation media were prepared, approximate pH of media was checked by using pH test strips (Macherey Nagel, Germany).

Table A.4. 20% and 10% Regular RPMI 1640 Medium

Ingredient	Volume (ml)	Final Concentration	Company	Cat No:
Heat Inactivated FBS	100,50	10 %, 20%	Biological Industries, Israel	04-127-1A
HEPES buffer 1M	10	20 mM	Biological Industries, Israel	03-025-1B
Penicillin/Streptomycin (Pen/Strep) Solution	5	Pen: 100 units/ml Strep: 100 µg/ml	Biological Industries, Israel	03-031-1B
MEM Non-Essential Amino Acids Solution (100X)	5	1X (100nm of each amino acid)	Biological Industries, Israel	01-340-1B
Sodium Pyruvate Solution	5	0.11 mg/ml	Biological Industries, Israel	03-042-1B
RPMI 1640 Medium with L-glutamine and Phenol Red	375,425	-	Biological Industries, Israel	01-100-1A
TOTAL	500			

Table A.5. Wash Medium

Ingredient	Volume (ml)	Final Concentration	Company	Cat No:
Heat Inactivated FBS	10	2 %	Biological Industries, Israel	04-127-1A
HEPES buffer 1M	10	20 mM	Biological Industries, Israel	03-025-1B
Penicillin/Streptomycin (Pen/Strep) Solution	5	Pen: 100 units/ml Strep: 100 µg/ml	Biological Industries, Israel	03-031-1B
RPMI 1640 Medium with L-glutamine and Phenol Red	475	-	Biological Industries, Israel	01-100-1A
TOTAL	500			

Table A.6. Leishmania Infection Medium

Ingredient	Volume (ml)	Final Concentration	Company	Cat No:
Heat Inactivated FBS	0.4	2 %	Biological Industries, Israel	04-127-1A
HEPES buffer 1M	0.4	20 mM	Biological Industries, Israel	03-025-1B
Penicillin/Streptomycin (Pen/Strep) Solution	0.2	Pen: 100 units/ml Strep: 100 µg/ml	Biological Industries, Israel	03-031-1B
RPMI 1640 Medium with L-glutamine and Phenol Red	19	-	Biological Industries, Israel	01-100-1A
TOTAL	20			

B. Recipes for Various Buffers and Solutions

1X NET Buffer

-10 mM Tris HCl (pH:8.0)

-10 mM EDTA(pH:8.0)

-100 mM NaCl

DNA Attachment Buffer, pH:8.0

-40 mM HEPES-Cl

-10 mM $MgCl_2$

ACK Lysis Buffer pH: ~7.3

-150 mM NH4Cl

-10 mM KHCO3

-0.1 mM Na_2EDTA

Electroporation Buffer pH: 7.5

-137 mM NaCl

-21 mM HEPES

-6 mM Glucose

-5 mM KCl

-0.7 mM Na_2HPO_4

Separating Gel for Gelatin Zymography (for 8 ml)

-2 ml 1.5M Tris pH 8.8

-2 ml 30% Acrylamide

-2 ml H_2O

-80 µl 10% SDS

-80 µl 10% APS

-10 µl TEMED

-2 ml Gelatin (4mg/ml)

Stacking Gel for Gelatin Zymography (for 5 ml)

-1.25 ml 0.5M Tris pH 6.8

-670 µl 30% Acrylamide

-3 ml H_2O

-50 µl 10% SDS

-50 µl 10% APS

-10 µl TEMED

5X non-reducing sample buffer for Gelatin Zymography

-4% SDS

-20% Glycerol

-0.01% Bromophenol Blue

-125 mM Tris-HCl, pH:6.8

Washing Buffer for Gelatin Zymography

-2.5% Triton X-100

-50 mM Tris-HCl, pH:7.5

-5 mM $CaCl_2$

-1 μM $ZnCl_2$

Incubation Buffer for Gelatin Zymography

-1% Triton X-100

-50 mM Tris-HCl, pH:7.5

-5 mM $CaCl_2$

-1 μM $ZnCl_2$

Staining Solution for Gelatin Zymography (for 100 ml)

-40 ml Methanol

-10 ml Acetic Acid

-50 ml H_2O

-0.5g Coomassie Blue

Destaining Solution for Gelatin Zymography (for 1 L)

-400 ml Methanol

-100 ml Acetic Acid

-500 ml H_2O

FACS Buffer (for 500 ml)

-500 ml 1X PBS

-5 g BSA

-125 mg Na-Azide

Coating Buffer for ELISA pH: 9.5 (for 1 L)

-8.4 g $NaHCO_3$

-3.56 g Na_2CO_3

Blocking Buffer for ELISA (for 500 ml)

-500 ml 1X PBS

-5 g BSA

-500 µl Tween-20

Wash Buffer for ELISA (for 10 L)

-1 L 1X PBS , 9 L dH_2O

-5 ml Tween-20

T-Cell Buffer for ELISA (for 500 ml)

-475 ml 1X PBS

-25 ml FBS

-250 µl Tween-20

C. Details of Custom pLEXSY-EGFP-LUC Plasmid and Proteomics Analysis

EGFP-LUC Sequence in FASTA Format

ATGGTGAGCAAGGGCGAGGAGCTGTTCACCGGGGTGGTGCCCATCCTGG
TCGAGCTGGACGGCGACGTAAACGGCCACAAGTTCAGCGTGTCCGGCGA
GGGCGAGGGCGATGCCACCTACGGCAAGCTGACCCTGAAGTTCATCTGC
ACCACCGGCAAGCTGCCCGTGCCCTGGCCCACCCTCGTGACCACCCTGAC
CTACGGCGTGCAGTGCTTCAGCCGCTACCCCGACCACATGAAGCAGCAC
GACTTCTTCAAGTCCGCCATGCCCGAAGGCTACGTCCAGGAGCGCACCA
TCTTCTTCAAGGACGACGGCAACTACAAGACCCGCGCCGAGGTGAAGTT
CGAGGGCGACACCCTGGTGAACCGCATCGAGCTGAAGGGCATCGACTTC
AAGGAGGACGGCAACATCCTGGGGCACAAGCTGGAGTACAACTACAAC
AGCCACAACGTCTATATCATGGCCGACAAGCAGAAGAACGGCATCAAGG
TGAACTTCAAGATCCGCCACAACATCGAGGACGGCAGCGTGCAGCTCGC
CGACCACTACCAGCAGAACACCCCCATCGGCGACGGCCCCGTGCTGCTG
CCCGACAACCACTACCTGAGCACCCAGTCCGCCCTGAGCAAAGACCCCA
ACGAGAAGCGCGATCACATGGTCCTGCTGGAGTTCGTGACCGCCGCCGG
GATCACTCTCGGCATGGACGAGCTGTACAAGTCCGGCCGGACTCAGATC
TCGAGCTCAAGCTTCGAATTCGAAGACGCCAAAAACATAAAGAAAGGCC
CGGCGCCATTCTATCCGCTGGAAGATGGAACCGCTGGAGAGCAACTGCA
TAAGGCTATGAAGAGATACGCCCTGGTTCCTGGAACAATTGCTTTTACAG
ATGCACATATCGAGGTGGACATCACTTACGCTGAGTACTTCGAAATGTCC
GTTCGGTTGGCAGAAGCTATGAAACGATATGGGCTGAATACAAATCACA
GAATCGTCGTATGCAGTGAAAACTCTCTTCAATTCTTTATGCCGGTGTTG
GGCGCGTTATTTATCGGAGTTGCAGTTGCGCCCGCGAACGACATTTATAA
TGAACGTGAATTGCTCAACAGTATGGGCATTTCGCAGCCTACCGTGGTGT
TCGTTTCCAAAAAGGGGTTGCAAAAAATTTTGAACGTGCAAAAAAAGCT
CCCAATCATCCAAAAAATTATTATCATGGATTCTAAAACGGATTACCAGG
GATTTCAGTCGATGTACACGTTCGTCACATCTCATCTACCTCCCGGTTTTA

187

ATGAATACGATTTTGTGCCAGAGTCCTTCGATAGGGACAAGACAATTGC
ACTGATCATGAACTCCTCTGGATCTACTGGTCTGCCTAAAGGTGTCGCTC
TGCCTCATAGAACTGCCTGCGTGAGATTCTCGCATGCCAGAGATCCTATT
TTTGGCAATCAAATCATTCCGGATACTGCGATTTTAAGTGTTGTTCCATTC
CATCACGGTTTTGGAATGTTTACTACACTCGGATATTTGATATGTGGATTT
CGAGTCGTCTTAATGTATAGATTTGAAGAAGAGCTGTTTCTGAGGAGCCT
TCAGGATTACAAGATTCAAAGTGCGCTGCTGGTGCCAACCCTATTCTCCT
TCTTCGCCAAAAGCACTCTGATTGACAAATACGATTTATCTAATTTACAC
GAAATTGCTTCTGGTGGCGCTCCCCTCTCTAAGGAAGTCGGGGAAGCGG
TTGCCAAGAGGTTCCATCTGCCAGGTATCAGGCAAGGATATGGGCTCAC
TGAGACTACATCAGCTATTCTGATTACACCCGAGGGGGATGATAAACCG
GGCGCGGTCGGTAAAGTTGTTCCATTTTTTGAAGCGAAGGTTGTGGATCT
GGATACCGGGAAAACGCTGGGCGTTAATCAAAGAGGCGAACTGTGTGTG
AGAGGTCCTATGATTATGTCCGGTTATGTAAACAATCCGGAAGCGACCA
ACGCCTTGATTGACAAGGATGGATGGCTACATTCTGGAGACATAGCTTA
CTGGGACGAAGACGAACACTTCTTCATCGTTGACCGCCTGAAGTCTCTGA
TTAAGTACAAAGGCTATCAGGTGGCTCCCGCTGAATTGGAATCCATCTTG
CTCCAACACCCCAACATCTTCGACGCAGGTGTCGCAGGTCTTCCCGACGA
TGACGCCGGTGAACTTCCCGCCGCCGTTGTTGTTTTGGAGCACGGAAAGA
CGATGACGGAAAAAGAGATCGTGGATTACGTCGCCAGTCAAGTAACAAC
CGCGAAAAAGTTGCGCGGAGGAGTTGTGTTTGTGGACGAAGTACCGAAA
GGTCTTACCGGAAAACTCGACGCAAGAAAAATCAGAGAGATCCTCATAA
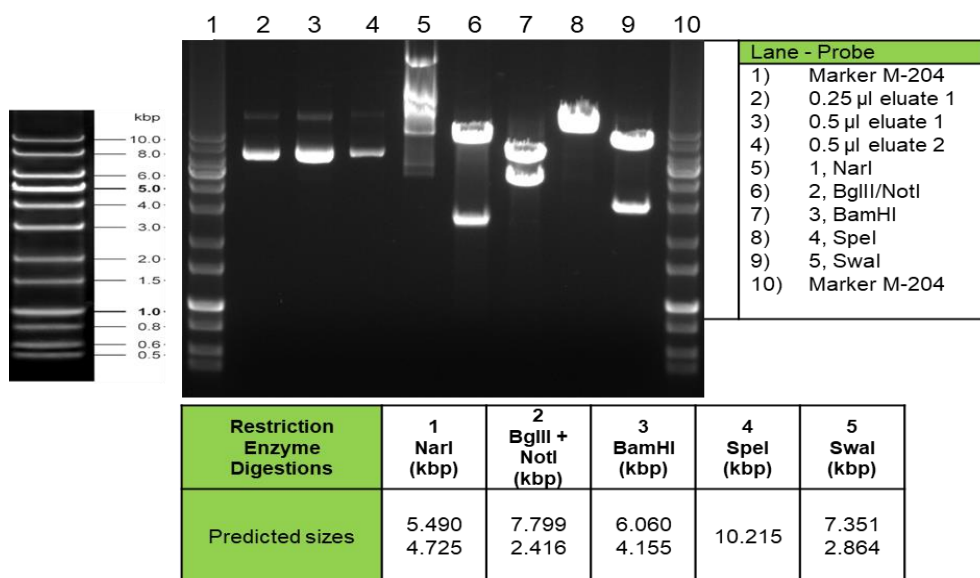AGGCCAAGAAGGGCGGAAAGATCGCCGTGTAA

Lane - Probe	
1)	Marker M-204
2)	0.25 µl eluate 1
3)	0.5 µl eluate 1
4)	0.5 µl eluate 2
5)	1, NarI
6)	2, BglII/NotI
7)	3, BamHI
8)	4, SpeI
9)	5, SwaI
10)	Marker M-204

Restriction Enzyme Digestions	1 NarI (kbp)	2 BglII + NotI (kbp)	3 BamHI (kbp)	4 SpeI (kbp)	5 SwaI (kbp)
Predicted sizes	5.490 4.725	7.799 2.416	6.060 4.155	10.215	7.351 2.864

Figure C.1. Quality Control Test for Custom Vector
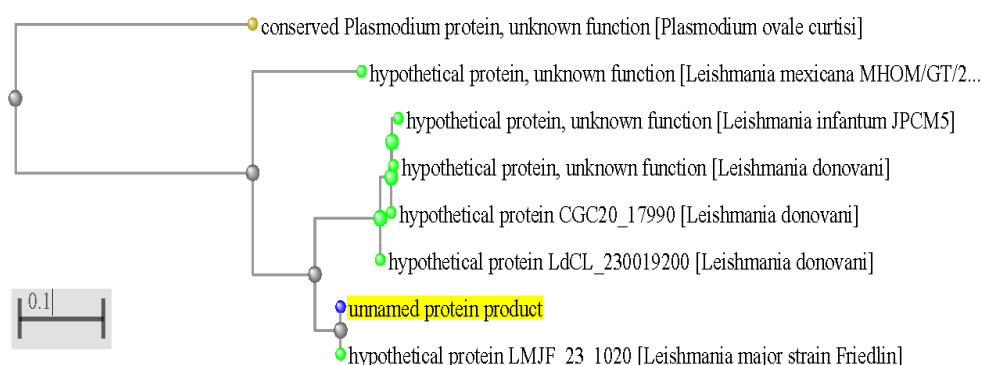

Figure C.2. Constructed Distance Tree Based on Pairwise Alignment of Hypothetical Protein (LmjF.23.1020) found in Leishmania Exosomes

Amino acid sequence of hypothetical protein (LmjF.23.1020) was ran on BLASTP to determine sequences producing significant alignments. Distance tree was constructed based on pairwise alignment of identified sequences

189

Table C.1. Full List of Identified Proteins (with a significant mascot score) in Purified Exosomes

Protein Description	Uniprot Acc. #
GP63, leishmanolysin OS=Leishmania major OX=5664 GN=GP63-2	Q4QHH1
Metallo-peptidase, Clan MA(E), Family M32 OS=Leishmania major OX=5664 GN=LMJF_33_2540	Q4Q3T3
Putative calpain-like cysteine peptidase OS=Leishmania major OX=5664 GN=SMP-1	Q5SDH5
Putative heat-shock protein hsp70 OS=Leishmania major OX=5664 GN=LMJF_28_2770	Q4Q7Y4
Heat shock protein 70-related protein OS=Leishmania major OX=5664 GN=HSP70.4	Q4Q970
Heat shock protein 83-1 OS=Leishmania major OX=5664 GN=HSP83-8 PE=3 SV=1	Q4Q4I0
Tubulin beta chain OS=Leishmania major OX=5664 GN=LMJF_33_0792 PE=3 SV=1	Q4Q4C4
Tubulin alpha chain OS=Leishmania major OX=5664 GN=LMJF_13_0280 PE=3 SV=1	Q4QGC5
Thiol specific antioxidant OS=Leishmania major OX=5664 GN=TRYP7 PE=2 SV=1	Q4QF68
Putative ATP-binding cassette protein subfamily A,member 8 OS=Leishmania major OX=5664 GN=ABCA8	E9AD74
Putative ras-related rab-4 OS=Leishmania major OX=5664 GN=LMJF_32_0490	Q4Q5N4
5-methyltetrahydropteroyltriglutamate-homocystein e S-methyltransferase OS=Leishmania major OX=5664 GN=LMJF_31_0010	Q4Q6R3
Nucleoside diphosphate kinase OS=Leishmania major OX=5664 GN=L1648.07	Q9U1E1
Threonylcarbamoyl-AMP synthase OS=Leishmania major OX=5664 GN=LMJF_28_2070	Q4Q859
Adenosylhomocysteinase OS=Leishmania major OX=5664 GN=LMJF_36_3910	Q4Q124
Glyceraldehyde-3-phosphate dehydrogenase OS=Leishmania major OX=5664 GN=LMJF_30_2980	Q4Q6Z4
Putative seryl-tRNA synthetase OS=Leishmania major OX=5664 GN=LMJF_11_0100	Q4QH70
Plasma membrane ATPase OS=Leishmania major OX=5664 GN=H1A-2	Q4QDN7
Activated protein kinase c receptor (LACK) OS=Leishmania major OX=5664 GN=LACK2	Q4Q7Y7
Enolase OS=Leishmania major OX=5664 GN=ENOL	Q4QFL8
Putative ribosomal protein L1a OS=Leishmania major OX=5664 GN=LMJF_29_1070	E9ADW5
Putative chaperonin TCP20 OS=Leishmania major OX=5664 GN=LMJF_13_1660	Q4QFY8
Putative IgE-dependent histamine-releasing factor OS=Leishmania major OX=5664 GN=LMJF_24_1500	Q4QAI0
Uncharacterized protein OS=Leishmania major OX=5664 GN=LMJF_23_1020	Q4QB61
Uncharacterized protein OS=Leishmania major OX=5664 GN=LMJF_27_1730	E9ADF0
Uncharacterized protein OS=Leishmania major OX=5664 GN=LMJF_18_0950	Q4QDU7
Uncharacterized protein OS=Leishmania major OX=5664 GN=LMJF_16_0490	Q4QEX1

OS: Organism Name, **OX:** Organism Identifier, **GN:** Gene Name

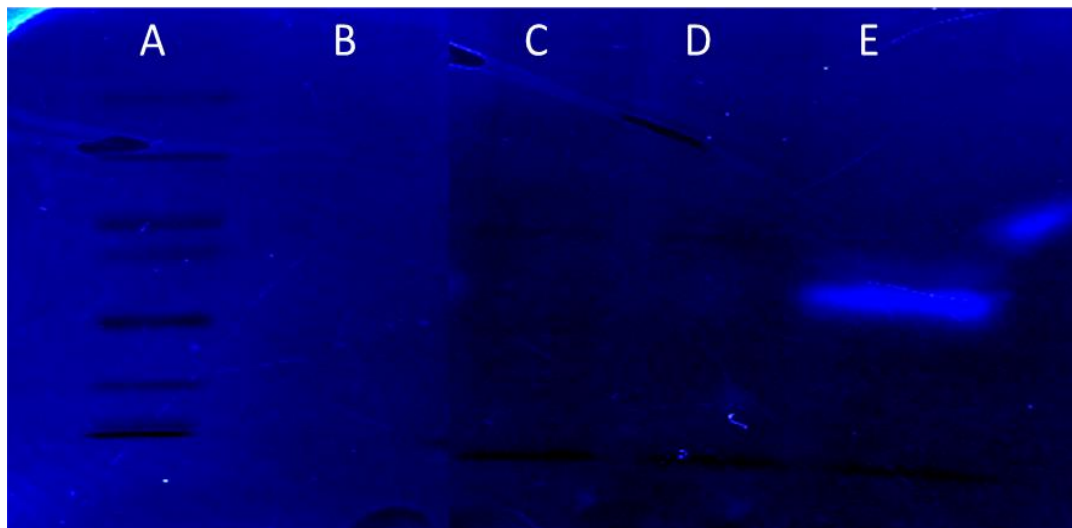## D. Assessment of gp63 Integrity and Activity Following Lyophilization

Figure D.1. Assessment of gp63 Inactivation Following Lyophilization by Gelatin Zymography

Lanes loaded as protein ladder (A), Ovalbumin as negative control (B), H_2O_2 treated non-lyophilized parasite lysates (C), H_2O_2 treated lyophilized parasite lysates (D), H_2O_2 untreated lyophilized parasite lysates (E).
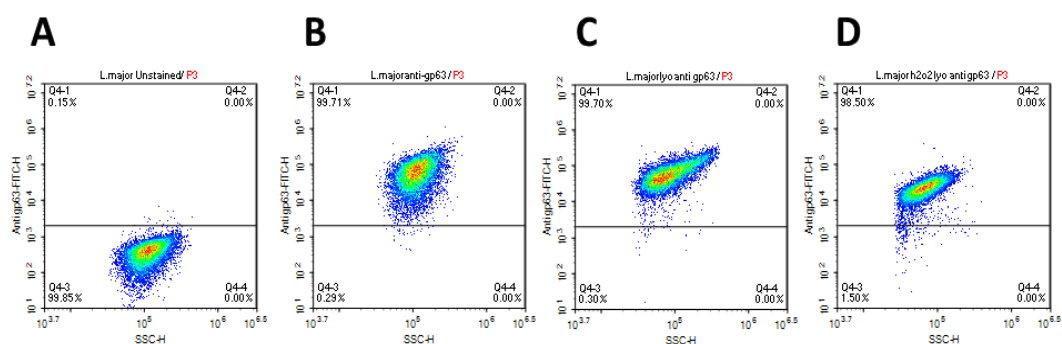

Figure D.2. Flow Cytometry Analysis of gp63 Integrity Following Lyophilization

Parasites grown in culture medium (late-log phase) were used as unstained control (A) and stained with anti-gp63-FITC without any treatment as positive control (B). H_2O_2 untreated (C) and H_2O_2 killed (D) parasites were stained with anti-gp63-FITC after lyophilization and hydration

CURRICULUM VITAE

PERSONAL INFORMATION

Surname, Name   : Ayanoğlu, İhsan Cihan
Nationality   : Turkish (TC)
Date and Place of Birth : 22 July 1987, Balıkesir
Phone   : +90 312 210 7627
E-mail   : ayanoglu@metu.edu.tr

EDUCATION

Degree	Institution	Year of Graduation
MS	METU Biology	2013
BS	METU Molecular Biology and Genetics	2010
High School	Edremit Anadolu High School, Balıkesir	2005

WORK EXPERIENCE

Year	Place	Enrollment
2010-Present	METU Biological Sciences	Research Assistant

FOREIGN LANGUAGES

Advanced English, Beginner German

PUBLICATIONS

1. Gul E., Sayar, E. H., Gungor, B., Eroglu, F. K., Surucu, N., Keles, S. Guner SN., Findik S., Alpdundar E., Ayanoglu IC., Kayaoglu B., Geckin B., Sanli HA., Kahraman T., Yakicier C., Muftuoglu M., Oguz B., Cagdas Ayvaz DN., Gursel I., Ozen S., Reisli I., Gursel, M. 2018. 'Type I IFN–related NETosis in ataxia telangiectasia and Artemis deficiency'. Journal of Allergy and Clinical Immunology, 142(1), 246–257. PMID: 29155101 DOI: 10.1016/j.jaci.2017.10.030